An improved stochastic modelling framework of biological networks: Case study modelling immunization in Alzheimer's disease

---

A thesis

submitted in partial fulfilment

of the requirements for the degree of

Doctor of Philosophy

In

Scientific Computing and Bioinformatics

at

Lincoln University

by

Ibrahim Altarawni

Lincoln University

2018

Abstract of a thesis submitted in partial fulfilment of the requirements for the degree of for the Doctor of Philosophy

Abstract

An improved stochastic modelling framework of biological networks: Case study modelling immunization in Alzheimer's disease

by

Ibrahim Altarawni

Alzheimer disease (AD) attacks the brain and is the most common cause of dementia worldwide and it is classified to be the main cause of cognitive impairment in elderly people. Beta-amyloids (Aβ) and tau are aggregated to produce respectively plaques and tangles that are classified to be prime suspects for cell deaths in Alzheimer's brain. Plaques target nerve cells to prevent their ability to contact each other in the correct way while tangles attack the transport system made of protein to be destroyed. However, the mechanisms that link Aβ and tau are still not fully understood. A recent proposed model (known immunization in AD model) not only examines pathways (DNA damage, p53 regulation, GSK3β activity, Aβ production and aggregation and tau dynamic and aggregation) involved in this relationship, but also how passive and active immunization against Aβ can indirectly reduce the level of tau pathologies.

In this research, we stochastically model immunization in AD for better understanding of the relationship between Aβ and tau since noise in biology is a rule rather than expectation. This modelling is done using a proposed approach that combines Mapping Reduction Method (MRM) and Gillespie Stochastic Simulation Algorithm (GSSA). This combination increases the performance of GSSA by accelerating a single run of GSSA and explicitly includes concurrency feature. To validate MRM/GSSA, we compare it with GSSA itself and the modified Tau leap method classified to be one of the fastest version of GSSA. MRM/GSSA is

not only faster than GSSA and comparable with the modified Tau-leap method, but also has more ability to represent stochastic feature and more reliable to be used for modelling any biochemical system than the modified tau leap method.

Local sensitivity analysis (LSA) is stochastically and deterministically performed using MRM/GSSA and ordinary differential equations (ODEs) to investigate the behaviour of the immunization in AD model when parameters are perturbed, one at a time. A finite difference approximation method (FDM) is used to deterministically to perform LSA while FDM in conjunction with the common random number (CRN) is used to stochastically perform LSA. LSA is performed to (1) determine the maximum and minimum ranges of each parameter, (2) classify the most important species that contribute to the overall behaviour of the system and (3) identify pathways that dramatically changed in response to parameter perturbation. LSA using ODEs and MRM/GSSA indicates that p53 regulation, DNA damage pathway and GSK3β activity are not contributing to the overall behaviour of the system. Aβ production and aggregation, Tau dynamic and aggregation and immunisation pathways (passive and active) are the most important pathways that dramatically contribute to the overall behaviour of the system. LSA also demonstrates that parameters specific to p53, Mdm2 and Aβ are the most important parameters that contribute most to the variation in the system.

Latin Hypercube Sampling and Partial Rank Correlation Coefficient (LHS/PRCC) are powerful tool employed with a minimum number of computer simulations in uncertainty analysis to monotonically relate the model outputs to the input parameters. We use LHS/PRCC to not only deterministically (ODEs), but also stochastically (MRM/GSSA) investigate the epistemic uncertainties of parameters of immunization in AD model. We explore at three different time points the effects of parameters on the key outputs of immunization in AD model (selected from the included pathways). This is to discover the most important parameters that uncertainties contribute to predication imprecision and rank these parameters by their importance in contributing to this imprecision. PRCC analysis using ODEs and MRM/GG demonstrates that binding relationship between p53 and Mdm2 and Mdm2 synthesis are the most important reactions that contribute to the behaviour of nearly all selected species in response to combination of LHS matrix. PRCC

analysis using MRM/GSSA indicates some other parameters such as kgenROSGila and kbinE2UB also have strong correlation with the key outputs.

Keywords: Alzheimer's disease, Gillespie stochastic simulation algorithm, Mapping reduction method, ordinary differential equations, Amyloid-β production, tau dynamic, p53 regulation, DNA damage, immunization in Alzheimer's disease, finite difference approximation method, LHS/PRCC.

Acknowledgements

بسم الله الرحمن الرحيم

(وَوَصَّيْنَا الْإِنسَانَ بِوَالِدَيْهِ إِحْسَانًا ۖ حَمَلَتْهُ أُمُّهُ كُرْهًا وَوَضَعَتْهُ كُرْهًا ۖ وَحَمْلُهُ وَفِصَالُهُ ثَلَاثُونَ شَهْرًا ۚ حَتَّىٰ إِذَا بَلَغَ أَشُدَّهُ وَبَلَغَ أَرْبَعِينَ سَنَةً قَالَ رَبِّ أَوْزِعْنِي أَنْ أَشْكُرَ نِعْمَتَكَ الَّتِي أَنْعَمْتَ عَلَيَّ وَعَلَىٰ وَالِدَيَّ وَأَنْ أَعْمَلَ صَالِحًا تَرْضَاهُ وَأَصْلِحْ لِي فِي ذُرِّيَّتِي ۖ إِنِّي تُبْتُ إِلَيْكَ وَإِنِّي مِنَ الْمُسْلِمِينَ) الآية 19 من سورة النمل

First of all, I would like to express my deepest gratitude to my supervisors, Professor Sandhya Samarasinghe and Professor Don Kulasiri for their constant encouragement and guidance. Without their supervision, this work would not be able to be achieved. A special thank for Professor Don Kulasiri for his insightful ideas and comments on my study, I'm truly grateful for all support he has provided me, which helped me to become an independent researcher.

I would like to thank my friends, Rahman Muhammad, Dr Mohammad Al-Tarawni who helped me to improve my biological background, Dr Mohammad Zeidan who did proofreading for me, Eyed Al-Hodiani and Mohammad Al-Shamaileh who helped me improve my coding ability in some stages since they have very good experience in programming.

I want to thank my mom, father, brothers, sisters, wife (Ebtehal) and my daughter (Gala) for unconditional love and support.

Table of Contents

List of Tables

List of Figures

Abbreviations

Terminology

AD	**Alzheimer's disease**
Aβ	**beta-amyloids**
GSSA	**Gillespie stochastic simulation algorithm**
ODEs	**Ordinary differential equations**
LSA	**Local sensitivity analysis**
OAT	**one-at-a-time**
GSA	**Global sensitivity analysis**
MRM	**Mapping Reduction method**
FDA	**finite difference approximation**
CRN	**common random number**
LHS	**Latin hypercube sampling**
PRCC	**partial rank correlation coefficient analysis**
PDF	**probability density function**
CME	**chemical master equation**
CDF	**cumulative distribution function**
ROS	**Reactive Oxygen Species**
PRV	**Poisson Random Variable**
CDF	**Cumulative distribution function**
MRM/GSSA	**Mapping Reduction Method/ Gillespie stochastic simulation algorithm**
MC	**Markov chain**
IRN	**Independent random number**
CRP	**Common Reaction Path**
CFD	**Coupled Finite difference**

Chapter 1

Introduction

1.1 Alzheimer's disease

Alzheimer's disease (AD) attacks the brain and is the most common cause of dementia worldwide. Dementia is the general term for a chronic or persistent disorder in mental processes caused by brain disease or injury that is enough to interfere with daily life. Alzheimer's disease patients slowly, but surely, lose their memory and their cognitive abilities; their personalities could also change dramatically (Mattson, 2004). These changes are a result of the dysfunction and death of the nerve cells that have the responsibility to store and process information in the brain.

1.1.1 History

Dr Alois Alzheimer was a German neurologist and psychiatrist. He discovered AD in 1906. He initially observed this disease in a 51-year-old woman named Auguste Deter. In 1901, her family noticed changes in her personality and behaviour so they brought her to him. After five years of looking after her, Dr Alzheimer noted many abnormal symptoms, including difficulty speaking, confusion and impaired comprehension (Khachaturian & Radebaugh, 1996). Later, Dr Alzheimer described her as a person with an aggressive form of dementia, language deficits and a malfunctioning memory. He did an autopsy after her death, in 1906, and found that there were not only fatty deposits in her blood vessels but also an intense shrinkage of the cerebral cortex. At that time, neurofibrillary tangles and senile plaques were discovered; these species have since become indicative of AD (Possin et al., 2013).

1.1.2 Biological Background

The reason for the cell deaths in Alzheimer's brain is not fully understood but scientists classify plaques and tangles prime suspects for these deaths (McCarter, 2014). Plaques are formed when protein pieces called beta-amyloids (Aβ) (BAY-TUH-AM-uh-loyeds) clump together and begin to build up between nerve cells

and prevent their ability to contact each other in the correct way. Figure 1.1 shows the difference between healthy cell and Alzheimer's cell.

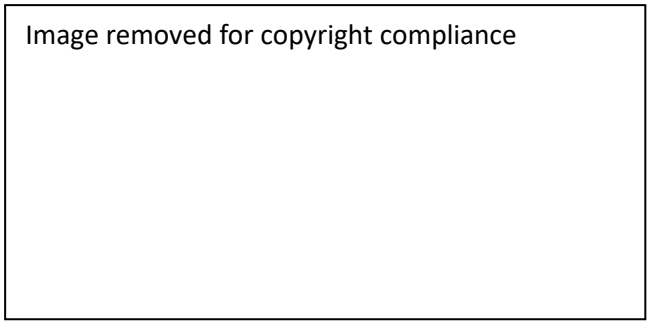

Figure 1.1: The difference between healthy cells and Alzheimer's cells. Plaques in Alzheimer's cells are clusters of Amelyod beta proteins that build up between nerve cells. Tangles cause death of nerve cells. Retrieved from https://www.alz.org/braintour/plaques.asp.

Tangles attack the transport system made of proteins to be destroyed. The transport system is used for food, cell parts and other materials to travel between nerve cells. As shown in Figure 1.2, in healthy cells, the tau proteins help this system to be organized into parallel strands. In Alzheimer's cells, these tracks can no longer be straight because tau collapses into twisted strands called tangles. Cells eventually die because the transport system is not able to transfer nutrients and other materials through the cell any more. As a result of the increasing number of tangles and plaques, healthy neurons start to function less effectively and are progressively unable to communicate and, eventually, they die (Theofilas et al., 2018).

Changes in the brain associated with AD commence years before any signs of the disease. This time period is referred to as preclinical AD. AD, itself, also progresses gradually and can last for decades (Yang, Mufson, & Herrup, 2003). Three different stages of AD have been discovered, each with its own symptoms and challenges (Goedert & Spillantini, 2006). These stages, as described in Table 1.1, are the mild-, moderate-, and severe-stages.

Image removed for copyright compliance

Figure 1.2: Transport system in healthy and Alzheimer cells. This system is used for food, cell parts and other materials to be travelled along the tracks. In healthy cells, tau helps this system to be organized in parallel strands. In Alzheimer's cells, the tracks can no longer be straight because tau collapses into twisted strands called tangles. Cells will not be able to survive since the transport system is no able any more to transfer nutrients and other materials through the cell. Retrieved from https://www.alz.org/braintour/plaques.asp.

Table 1.1: Stages of AD. Retrieved from www.emedicinehealth.com**.**

Mild-stage	Moderate-stage	Severe-stage
Lasts two to four years	lasts for many years	lasts for one to three years
# of tangles and plaques are small	# of tangles and plaques start to increase and tend to spread throughout the cortex.	# many plaques and tangles that are spread throughout the cortex
Patients have difficulties in - • Retaining new information • Solving problems • Making decisions • Managing finances	Patients have difficulties in - • Making progressively poor judgments • Achieving hard tasks • Remembering their personal history.	Patients have difficulties in • Communicating. • Personal care.
Image removed for copyright compliance	Image removed for copyright compliance	Image removed for copyright compliance

For more details about these stages see (Dubois et al., 2010; Jack Jr et al., 2011; Mangialasche, Solomon, Winblad, Mecocci, & Kivipelto, 2010).

For better understanding of AD whether how it is caused or treated, cellular mechanisms are involved to increase or decrease the level of plaques and tangles need to be investigated and analysed. Modelling approaches and sensitivity analysis techniques have been increasingly recognized as worthy tools to investigate and analyse the cellular mechanisms involved in ageing and age-related diseases (Proctor, Boche, Gray, & Nicoll, 2013). Different modelling approaches and sensitivity analysis techniques have been proposed to investigate and analyse the cellular mechanisms involved in AD. In the next section we briefly describe the most popular approaches and analysis techniques that have been used to investigate the cellular mechanisms. In Chapter 2, we provide a historical overview about the existing approaches and analysis methods that are used to investigate AD.

1.2 Modelling Approaches and Sensitivity Analysis methods

Four different types of mathematical modelling approaches are used to determine the overall behaviour of biochemical systems or cellular mechanisms. These approaches are: (1) discrete deterministic; (2) continuous deterministic; (3) stochastic; and (4) hybrid. They are used to investigate and understand system activities, such as regulators, oscillations and feedback loops. (Klipp, Liebermeister, Wierling, Kowald, & Herwig, 2016; Szallasi, Stelling, & Periwal, 2006). For more details about these approaches see (Herajy, Liu, Rohr, & Heiner, 2017; Thieme, 2018; Veliz-Cuba, Jarrah, & Laubenbacher, 2010; Wattis, 2006). The most popular approaches are continuous deterministic, based on ordinary differential equations (ODE) and stochastic models, using Gillespie stochastic simulation algorithm (GSSA) or one of its variants since they have been intensively used to model biochemical systems.

ODEs are used in a track the exact concentration of biological components through the continuous representation of system dynamics over time (Fuβ, Dubitzky, Downes, & Kurth, 2005). The ODEs are used to describe the reaction rates of interactions between species according to chemical kinetic theory (Cloez

et al., 2017; Fuβ et al., 2005; Heath & Kavraki, 2009; Tyson, Novak, Odell, Chen, & Thron, 1996). Recently, the use of ODEs has intensified significantly for biological systems, especially with the advent of experimental techniques, such as whole genome sequencing and high throughput flow cytometry that are capable of providing a wealth of new biological data. Stochastic models are frequently used to model biochemical systems, which are classified as small systems (<100 particles for each species in a given system). The denotational semantics of stochastic models define rules to describe how the system modelled moves from one state to another state. Therefore, stochastic models are used to quantitatively describe the states of the modelled system by determining the initial state, and the procedure to be applied, to give a new system state (Fisher & Henzinger, 2007). More relevant details about these two approaches are given in Chapter 2.

The behaviour of any biological model can be strongly dependent on its parameters. If some of these parameters are not precisely known, the uncertainty of these parameters is taken into the model output (Kitano, 2002). Therefore, using sensitivity analysis methods to address the lack of precise parameter values and incorporate the uncertainty of these parameters into the model helps to quantify the uncertainty in the output (Kiparissides, Kucherenko, Mantalaris, & Pistikopoulos, 2009; Kulasiri, Liang, He, & Samarasinghe, 2017).

Sensitivity analysis, in the context of biological systems, is defined as how much the behaviour of a biochemical system depends on the parametrization of the model (Kulasiri et al., 2017). A comprehensive set of predictions is generated by sensitivity analysis to indicate how model's output is affected quantitatively by changes in any of its parameters. This procedure is able to: (1) Identify predictions that could be consistent or inconsistent with the experiment data; (2) Validate the model; and (3) Reduce the model complexity by identifying pathways that are not dramatically affected when parameters are perturbed (Lee, Liu, Hwang, Knollmann, & Sobie, 2013).

Local sensitivity analysis (LSA) methods belong to the class of one-at-a-time (OAT) methods because in each run of the model just one parameter is given a new

value, while assuming that all other parameters remain at their baseline values. However, one-at-a-time methods could not only be of limited use, but also be outright misleading especially when the relative importance of uncertain factors needed to be assessed. To cope with this limitation, the influence of simultaneous changes in parameter values needs to be investigated (Saltelli, Ratto, Tarantola, & Campolongo, 2005).

Global sensitivity analysis (GSA) addresses the behaviour of a biochemical system over a wide range of parameter values. These ranges are not only based on a rough estimation of parameter values, but also the upper and lower bounds may be used to specify them. Statistical methods are always used to sample the values of these parameters within the specified domains of the parameter spaces (Saltelli et al., 2008). More relevant details about sensitivity analysis techniques are given in Chapter 2.

1.3 Immunisation in AD

In 2013, Proctor and his colleagues developed a mathematical model to study how a patient with AD could be immunized against plagues and tangles (Proctor et al., 2013). As shown in Figure 1.1, they used two different types of immunization systems, passive and active; using antibodies and Glia, respectively. The mechanisms which link Aβ and tau are still not fully known although many suggestions have been made by (Ittner et al., 2010; Rapoport, Dawson, Binder, Vitek, & Ferreira, 2002; Roberson et al., 2007; Small & Duff, 2008).

Proctor et al. (2013) examined not only some of the key pathways involved in the mechanisms link Aβ and tau, such as DNA damage, p53 regulation, GSK3β activity and Aβ production and aggregation, Tau dynamic and aggregation and immunisation pathways (passive and active), but also how immunization against Aβ can indirectly reduce the level of tau pathologies. Proctor et al., (2013) also included possible players, such as p53, GSK3β, and ROS, that have roles linking Aβ and tau, as shown in Figure 1.1. This system is the case study that has been used in this research. Therefore, this system is discussed in detail in Chapter 3.

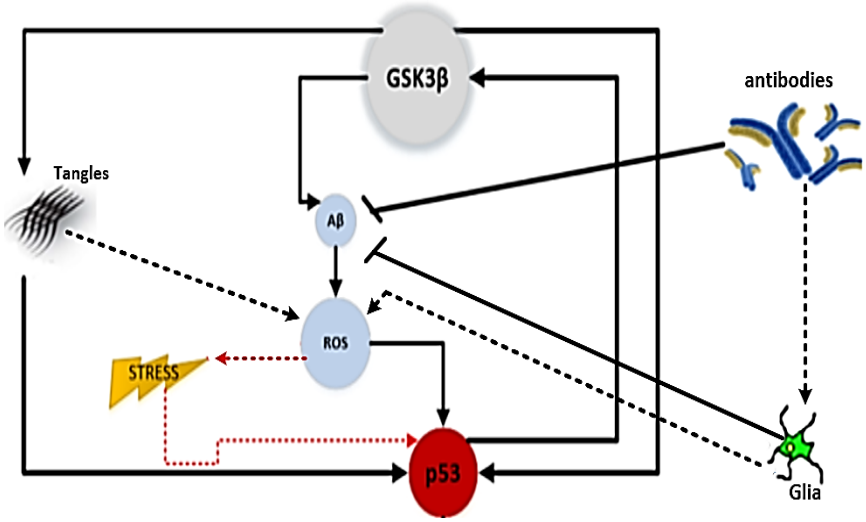

Figure 1.3: Immunization in AD. Passive and active Immunization using antibodies and Glia to reduce the number of Aβ that indirectly reduces the number of tangles.

1.4 Motivation and main research questions

The importance of stochasticity in biological systems has gained greater acceptance because it has become very clear that noise in biology is the rule rather than the exception (McAdams & Arkin, 1999). Therefore, stochastic approaches are the best way to investigate the behaviour of biochemical systems. GSSA described in Chapter 2 is the first stochastic algorithm that was introduced by D.T. Gillespie more than 40 years ago (Gillespie, 1976). However, the time required for executing GSSA, especially when the biochemical system under study have many reactions, is very high. Sequential running is also one of the main limitations of GSSA and its variants while concurrency is considered to be one of the main features of biochemical systems. Concurrency means that components of any biochemical systems have the ability to simultaneously collide each other. Different versions have been proposed to accelerate the GSSA, each version has its own advantages and disadvantages. These versions are described in Chapter 2. Therefore, the first question that we ask is:

1- How could a single run of GSSA be accelerated and how could GSSA be extended to include the concurrency feature?

To answer the two parts of this question, Mapping Reduction method (MRM) is selected to be modified and combined with GSSA itself to not only accelerate the GSSA but also indirectly to include the concurrency feature by advancing the system with several reactions. This combination is discussed in Chapter 4 (sections 4.1 and 4.2).

2- What are the main advantages of MRM/GSSA over not only GSSA, but also one of the fastest version of GSSA (modified Tau-leap method)?

To answer this question, immunization in AD is modelled by GSSA, MRM/GSSA and the modified Tau-leap method. These approaches are compared from different angles, results, CPU times and implementation. This comparison is discussed in Chapter 4 (section 4.5).

As previously mentioned, Proctor et al. (2013), include possible players, such as p53 and GSK3β, to investigate the link between Aβ and tau and how these players participate to reduce the level of tangles when a patient with AD is immunized against Aβ. Investigating the behaviour of these players in addition to other players in this system is a need to check how the system behaves in response parameters perturbation. Therefore, LSA and GSA using ODEs and MRM/GSSA are performed to achieve this purpose.

At the level of LSA analysis, we aim to answer six questions. These questions are:

1- What are maximum and minimum ranges of each parameter?
2- What are the most important species in the system?
3- What are the most important parameters that contribute most to the variation in the system?
4- What are the most important parameters that specifically contribute most to the variation on the level of plaques and tangles?
5- What are the most important pathways that are hugely affected when parameters are perturbed?
6- What time are species showing the maximum sensitivity in response to parameters perturbation?

To answer these question, LAS using ODEs and MRM/GSSA is performed and each parameter in this system is perturbed by two values (50% and 200%) of its basal values, one at a time. The main players of the system are selected to be checked against parameters perturbation. These players are p53 (from p53 regulation), ATMA (from DAN damage activity), p53_GSK3β (from GSK3β activity) Aβ & plaques (from Aβ production and aggregation), tangles (from Tau dynamic and aggregation) and GliaA (from immunisation pathways (passive and active)).

Each player is used to measure the sensitivity of its pathways against parameters perturbation to classify these pathways and reduce the complexity of the system by determining pathways that are not dramatically affected when parameters are perturbed. LSA identifies the most important parameters that contribute most to the variation and group the parameters that contribute to the behaviour of plaques and Tangles. Sensitivity is computed at each time step, the time step for the maximum sensitivity value of each species is determined.

The results of the LSA using ODEs and MRM/GSSA are discussed in Chapter 5.

At the level of GSA, using ODEs and MRM/GSSA, we aim to answer two questions.

1- How would changing a wide range of parameter values simultaneously drive the dynamic behaviour of the system?

This question is answered by checking the behaviour of the system in response to perturbing all parameters at the same time to explore the effects of the interactions between parameters. This helps to identify the key parameters that drive the dynamic behaviour of the system.

2- Is there any difference between the results of GSA using ODEs or MRM/GSSA?

Identifying the key parameters that drive the dynamic behaviour of the system using ODEs and MRM/GSSA separately helps to achieve this comparison.

1.5 Objectives

There are three major objectives in this study

(1) To not only accelerate a single run of GSSA but also to include the concurrency feature in order to increase its performance.

To achieve this objective, we modified MRM to be suitable to be combined with GSSA. The MRM method is a programming model that uses a parallel distributed algorithm on a cluster to run multiple processes simultaneously. The main benefit of the MPR is dividing the work across many processors and keeping as much data in memory as possible during processing. MRM employs k worker threads to execute the same task at the same time. Therefore, we use MRM to run GSSA for the same system k times (k is determined depending on the number of reactions that have the propensity function at greater than zero). The main two steps of this combination are election and selection. Each thread elects a reactions index, j, and a time step, τ. The k index is then analysed to select the eligible reactions. This combination not only allows us to accelerate GSSA, but also includes the concurrency feature by advancing the state of the system by several reactions within the calculated time step, τ. MRM and MRM/GSSA are described in detail in Chapter 4 (sections 4.1 and 4.2).

(2) To validate MRM/GSSA.

The model of immunization in AD is modelled by MRM/GSSA, GSSA and the modified Tau-leap method. To validate MRM/GSSA, these three methods are compared at three different levels; results, performance and implementing difficulties.

(3) To investigate the critical behaviour of main players in immunization in the AD model, LSA and GSA are performed not only using ODEs, but also MRM/GSSA.

- To perform LSA using ODE models, we use a finite difference approximation (FDA) that is the most popular and simplest way to perform LSA (Saltelli, Chan, & Scott, 2000). To perform LSA using the MRM/GSSA model, we use the common random number (CRN) method (Rathinam, Sheppard, & Khammash, 2010) for sensitivity estimation. Positive correlations are obtained by using the CRN method for nominal and perturbed parameters in conjunction with MRM/GSSA. The results of LAS are discussed in detail in Chapter 5.

- To perform GSA using ODEs and the MRM/GSSA model, we use Latin hypercube sampling (LHS) in combination with partial rank correlation coefficient analysis (PRCC) since it is shown to be efficient in assessing a model over a global parameter space (Saltelli et al., 2000). The PRCC method is a useful tool since it has the ability to monotonically relate the model outputs to the input parameters. Input-output scatter plots are used to examine the monotonic relationships between the inputs and outputs (Marino, Hogue, Ray, & Kirschner, 2008). The results of GSA are discussed in Chapter 6.

LSA and GSA allow us to:

- Quantify the uncertainty in the outputs by incorporating uncertainties into the modelling process.
- Reduce model output uncertainty since sensitivity analysis has the ability to determine the parameters that contribute most to the variation. Therefore, experimental effort should be focussed on refining those parameters.
- Identify the parameters that are most dominant with respect to the system output and suggest targets for intervention since it provides a method for systematically investigating the effects of perturbations.

1.6 Thesis structure

This thesis consists of seven chapters.

In the current chapter, Chapter 1, we briefly give an introduction about different topics: AD, modelling approaches, sensitivity analysis techniques and immunization in AD. We also discuss the motivations and objectives of this thesis.

Chapter 2 reviews in detail: (1) the deterministic and stochastic approaches; (2) the sensitivity analysis techniques (LAS and GSA); and (3) the existing computational approaches that have been used to investigate AD.

Chapter 3 discusses the case study (immunizations in AD).

Chapter 4 proposes MRM/GSSA for stochastically modelling biochemical systems. It also describes the LSA and GSA methods that are used to analyse the system.

We also validate the proposed method by comparing it with the GSSA and Tau-leap methods.

Chapter 5 discusses the results of LSA analysis using ODEs and MRM/GSSA and provides comparisons between them.

Chapter 6 presents the results of GSA analysis using ODEs and MRM/GSSA.

Chapter 7 summarizes the work and the contribution of this thesis and suggests future directions for this research.

Chapter 2

Literature Review

2.1 Background

Numerous molecular processes (pathways) contributing to AD have already been elucidated. However, these processes have a daunting complexity and it was challenging to understand their integrated functions and the dynamic crosstalk between them. This complexity arises from the large number of interactions and the non-linear character of these processes (Lloret-Villas et al., 2017). To cope with this challenge, different types of modelling approaches and sensitivity analysis techniques have been proposed to gain a better understanding of biological systems at the system level. Modelling approaches are developed to explicitly predict and test the dynamic behaviour of biochemical pathways as a whole instead of their individual components (Toh & Allen-Vercoe, 2015; Ullah, Schmidt, Cho, & Wolkenhauer, 2006). Sensitivity analysis techniques are used to address the lack of precise parameter values, and incorporating the uncertainty of these parameters into the model helps to quantify the uncertainty in the output (Kiparissides et al., 2009; Kulasiri et al., 2017). This chapter reviews the most popular approaches and techniques for modelling and analysing the biochemical pathways, as well as a comprehensive review of mathematical models of AD.

2.2 Modelling Approaches

Two popular approaches for modelling and simulating biochemical pathways are deterministic and stochastic approaches. The deterministic approach (mainly ODEs) constructs a set of equations to describe the reactions in a biochemical pathway (Mellman & Misteli, 2003). Stochastic approaches involve the formation of a set of chemical master equations with probabilities as variables (Van Kampen, 1992).

2.2.1 Deterministic modelling and simulation

The deterministic approach (mainly ODEs) ignores all fluctuation events and regards variables as continuous concentrations rather than actual particle or molecular numbers (Bluman & Anco, 2002). Therefore, at any particular instant,

the state of the system is observed as a list of concentrations of molecules, and changes in these concentrations are assumed to occur by deterministic processes (Wilkinson, 2009). To represent a biological system using ODE models, two assumptions are made: (1) the molecular number is very large; and (2) reactions are very frequent. ODEs are equations in the form:

$$\frac{\mathbf{d(y)}}{\mathbf{dt}} = \mathbf{f}\big(\mathbf{k}, \mathbf{Y(t)}\big), \mathbf{Y(0)} = \mathbf{Y^0} \qquad \mathbf{2.1}$$

Here $Y(t)$ is the vector of variables, k is the m-vector of system parameters, Y^0 are the initial values. ODEs have been widely studied for many years. Therefore, there are many accurate solvers available for analysing and numerically solving ODE models, such as one-step first-order methods (Euler method) (Shampine & Watts, 1969), multistage methods (fourth order Runge-kutta method) (Hu, Hussaini, & Manthey, 1996), multistep methods and the Richardson extrapolation (Deuflhard, Hairer, & Zugck, 1987). For more details about these methods see (Hairer, Lubich, & Roche, 2006; Székely, 2014; Xing & Stern, 2010).

Euler method (One step methods)

This method is classified as the simplest ODE solver and its solution at each time steps depends on the solution of the previous step. For example, the solution at step $m + 1$ depends only on the solution at step m:

$$Y_{m+1}^h = Y_m^h + hf(t_m, Y_m^h) \qquad 2.2$$

$\boldsymbol{Y}_m^h$ is the approximate solution to Eq 2.1 at time step m with step size h and $t_m = mh$. The Euler method takes only one step to get a single sample of the gradient of $\boldsymbol{f}$ for calculating the next step. Therefore, it is called a one-step, one-stage explicit solver. However, it is not often used because of its low accuracy. The local truncation error of this method, is the difference among the true solution and the numerical approximation of the Euler method:

$$\varepsilon((t_{m+1} - t_m), h) = Y(t_{m+1}) - Y_{m+1}^h = Y(t_{m+1}) - Y_m^h - hf(t_m, Y_m^h) \qquad 2.3$$

The method is considered to be consistent if and only if its local error tends to zero as the step-size is decreased,

$$\lim_{h\to 0}\big(\varepsilon((t_{m+1}-t_m),h)\big)=0 \qquad 2.4$$

Multistage and multistep methods

The Euler method is simple and fast but it is not always a good solver of ODE models because of its low accuracy. According to (Székely, 2014), a higher accuracy is achieved by sampling the function $\boldsymbol{Y}$, more times at each time step. Two methods are used to do this sampling but they differently deal with the evaluating the function $\boldsymbol{Y}$; these methods are one-step multistage and multistep methods. For example, to find $\boldsymbol{Y_{m+1}}$ one-step multistage method evaluates the function $\boldsymbol{Y}$ and its derivatives at several points between $\boldsymbol{Y_m}$ and $\boldsymbol{Y_{m+1}}$ (such as $\boldsymbol{Y_m}, \boldsymbol{Y_{m+h/2}}, \boldsymbol{Y_{m+h/4}}, \dots\dots\dots\dots\dots\dots\dots, \boldsymbol{etc}$), while multistep method uses the solutions and derivatives of previous steps such as $\boldsymbol{Y_{m-1}}, \boldsymbol{Y_{m-2}}$ …… ……..$\boldsymbol{etc}$

One-step multistage methods

These methods are used to achieve greater accuracy than the Euler method. As stated before, one-step multistage methods evaluate the function $\boldsymbol{Y}$ and its derivatives at several points between $\boldsymbol{Y_m}$ and $\boldsymbol{Y_{m+1}}$ (such as $\boldsymbol{Y_m}, \boldsymbol{Y_{m+h/2}}, \boldsymbol{Y_{m+h/4}}, \dots\dots\dots\dots\dots\dots\dots, \boldsymbol{etc}$) (Humphries & Stuart, 1998). In other words, additional samples within the step are taken to achieve higher accuracy. The simplest multistage method is called the midpoint method. The general form of the midpoint method is similar to one step method (Eq (2.2)) but sampling of the gradient needs to be done halfway between $\boldsymbol{t_m}$ and $\boldsymbol{t_{m+1}}$ at $\boldsymbol{t = t_m + \frac{h}{2}}$:

$$Y_{m+1}^h = Y_m^h + hf\left(t_m + \frac{h}{2},\ Y_m^h + \frac{h}{2} f\,(t_m, Y_m^h)\right) \qquad 2.5$$

Midpoint method is classified as the simplest member of the Runge-Kutta family of numerical solvers (Schwartz, 1996). This group is considered to be an important member of multistage methods for achieving higher accuracy as the members of this group use extra samples within the current step (Munthe-Kaas, 1999). In this family, the most frequently used method is called fourth order Runge-kutta

method. Runge-kutta 4th order method (RK4) solves first order differential equation of the form:

$$\frac{dy}{dt} = f(x,y), y(0) = y0 \qquad 2.6$$

In this algorithm, four function evaluations are made, two intermediate evaluations on the gradient at two points around the midpoint and two other gradient evaluations at the start and the end of the step, respectively.

$$Y_{i+1} = Y_i + \frac{1}{6}(k_1 + 2 * k_2 + 2 * k_3 + k_4) * h \qquad 2.7$$

where knowing the value $\boldsymbol{Y_i}$ at $\boldsymbol{x_i}$, the value of $\boldsymbol{Y_{i+1}}$ could be easily found at $\boldsymbol{x_{i+1}}$ and $h = \boldsymbol{x_{i+1}} - \boldsymbol{x_i}$ (step size). k_j is the gradient at the 4 points. RK4 algorithm performs well for different types of problems including non-smooth ones especially when it is combined with adaptive step size. It is fast to run, as well as being accurate and easy to code (Press, 2007).

To generate k_j for Equation 2.7, this equation is equated to the first five terms of Taylor series that is used to represent a function as an infinite sum of terms calculated from the values of the function's derivatives at a single point.

$$y_{i+1} = y_i + \frac{dy}{dx}|_{x_i,y_i}(x_{i+1} - x_i) + \frac{1}{2!}\frac{d^2y}{dx^2}|_{x_iy_i}(x_{i+1} - x_i)^2 + \frac{1}{3!}\frac{d^3y}{dx^3}|_{x_iy_i}(x_{i+1} - x_i)^3 + \frac{1}{4!}\frac{d^4y}{dx^4}|_{x_iy_i}(x_{i+1} - x_i)^4 \qquad 2.8$$

Knowing that $\boldsymbol{\frac{dy}{dx} = f(x,y)}$ and $h = \boldsymbol{x_{i+1}} - \boldsymbol{x_i}$

$$y_{i+1} = y_i + f(x,y)h + \frac{1}{2!}f(x,y)'h^2 + \frac{1}{3!}f(x,y)''h^3 + \frac{1}{4!}f(x,y)'''h^4 \qquad 2.9$$

Equating Equations (2.8) and (2.9), one of the most popular solutions used for Equation (2.7) is obtained, where:

$$k_1 = f(x_i, y_i) \qquad 2.10$$

$$k_2 = f(x_i + \tfrac{1}{2}h, y_i + \tfrac{1}{2}k_1h) \qquad 2.11$$

$$k_3 = f(x_i + \tfrac{1}{2}h, y_i + \tfrac{1}{2}k_2h) \qquad 2.12$$

$$k_4 = f(x_i + h, y_i + k_3h) \qquad 2.13$$

Discarding the evaluations carried out at all previous steps at the next step is considered to be the main drawback of one-step multistage methods (Akrivis, Crouzeix, & Makridakis, 1999).

(a) Multistep methods

Multisptep methods aruge that soultions to differential equations are more efficient if an algorithm stores the solutions that are already calculated at all previous steps and use these solutions in the next steps (Székely, 2014).

According to (Székely, 2014) multistep methods are not only face some problems when the step size is varied, but also they do not have stability properties as one-step methods.

(b) Richardson extrapolation

Richardson extrapolation is a technique that is proposed to improve the order of accuracy of deterministic numerical methods when the structure of the error is known (Székely, 2014). The main idea of Richardson extrapolation is to perform numerical calculations using various values of step size. This is used for numerical calculation whose accuracy depends on unknown analytic function of the step size h. The deterministic function $Y(t)$ resulting from numerical solution using the same solver with different stepsizes at a given time $T = nh$ is written as:

$$Y(T) = Y_T^h + \varepsilon(T, h) \qquad 2.14$$

$\boldsymbol{Y_T^h}$ is consdiered to be an estimattion to $Y(T)$ at time T using stepsize h and $\boldsymbol{\varepsilon(T, h)}$ is the (global) error of the approximate solution. $\boldsymbol{\varepsilon(T, h)}$ could be written in terms of powers of the stepsize h for general numerical solver as:

$$\varepsilon(T, h) = e_{k1}h^{k1} + e_{k2}h^{k2} + e_{k3}h^{k3} \qquad 2.15$$

The $\boldsymbol{e_{k1}}$ are constant vectors that depend on the final integration time T and $\boldsymbol{k_1 < k_2 < k_3}$ …… in Eq (2.15) are known as the global error expansions in this method. Constructing a higher-order approximation is the main reason for the existence of such an expansion. Fundamentally, Richardson extrapolation employes polynomial extrapolation of approximations $\boldsymbol{Y_T^{h_q}, q = 1, 2, \ldots\ldots}$ where $\boldsymbol{q}$ can be any integer and $\boldsymbol{h_1 > h_2 \ldots\ldots h_q}$ to estimate $\boldsymbol{Y_T^0}$.

Bulirsch-Stoer algorithm and Romberg integration are major practical applications of Richardson method. These methods are considered to be very powerful and accurate ODE solvers that rely on extrapolation within each step.

Bulirsh-Stoer algorithm (Bulirsch & Stoer, 1966) is an accurate method for numerical solutions of ODEs. This algorithm is based on three different ideas: (i) Richardson extrapolation, (ii) using rational function extrapolation in Richardson-type applications, (iii) using the modified midpoint method (MMP, Algorithm 2.1) to obtain high accuracy numerical soultions for ODE models with comparatively little computational effort.

Bulirsh-Stoer algorithm argues that rational functions as fitting functions are superior to polynomial functions in Richardson extrapolation in numerical integration (Monroe, 2002). This is because rational functions have the ability to estimate functions with poles whereas polynomial functions uses higher-power terms in the denominator to account for nearby poles (Chambers, Quintana, Duncan, & Lissauer, 2002). In a complex plan, a polynomial functions are able to produce worthy results when the nearest pole is rather far outside of the circle around the known data points, while rational functions can have notably accurate results even in the presence of nearby poles (Fang et al., 2011).

The modified midpoint method (MMP, Algorithm 2.1) is considered to be a second order method but the main advantage of MMP is requiring one derivative evaluation per subset (Gragg, 1965). The modified midpoint method subdivides each step size $\boldsymbol{h}$ into ($\widehat{\boldsymbol{m}}$) substeps of size $\widehat{\boldsymbol{h}}$ where $\widehat{\boldsymbol{h}}$= $\boldsymbol{h}/\widehat{\boldsymbol{m}}$ as shown in MMP Algorithm 2.1. The error expansion of the The modified midpoint method covers even powers only of $\hat{h}$. This results in fast convergence (Gragg, 1965). This makes MMP significantly useful to the Bulirsh-Stoer algorithm because the accuracy is increased by two different orders at a time step when the results of separate attempts cross the interval h with increasing numbers of substep sizes are combined (Bowers, Dror, & Shaw, 2006).

Algorithm 2.1: Modified midpoint method (MMP)

$\mathbf{f(t, Y(t)) = \frac{dY(t)}{dt}}$ **and** $\mathbf{Y(0) = y_0}$,

assuming the system is in state $\mathbf{y_m = Y(t_m)}$ **at time** $\mathbf{t_m}$**, and a substepsize** $\mathbf{\hat{h} = h/\hat{m}}$

1. **Set** $\mathbf{z_0 = y_m}$
2. **Calculate first intermediate stage** $\mathbf{z_1 = z_0 + \hat{h} f(t_m, z_0)}$.
3. **Evaluate next intermediate stages** $\mathbf{z_{l+1} = z_{l-1} + 2\hat{h} f(t_m + l\hat{h}, z_l), l = 1, \ldots\ldots\ldots\ldots\ldots\ldots \hat{m} - 1}$.
4. **Update** $\mathbf{y_{m+1} = \frac{1}{2}\left(z_{\hat{m}} + z_{\hat{m}-1} + \hat{h} f(t_m + h, z_{\hat{m}})\right)}$ **and** $\mathbf{t_{m+1} = t_m + h}$

The Bulirsch-Store algorithm has the ability to adapt its order step-size for maximising not only its accuracy, but also its computational efficiency (Székely, 2014).

Romberg integration estimates the value of the integral

$$\int_a^b f(t)dt \tag{2.16}$$

The composite trapezium rule is a common way to evaluate this integration with $P = \frac{b-a}{h}$ intervals. Then, the integral can be approximated as:

$$\int_a^b f(t)dt = h(\frac{f(a) + f(b)}{2} + \sum_{p=1}^{P-1} f(a + ph)) + O(h^2) \tag{2.17}$$

Romberg integration repeats this evaluation using $2P$ intervals, $4P$ intervals, etc, and then extrapolate them to get more successively accurate solutions.

However, ODE models are not able to address the role of noise, one of the major challenges in current biology, or the random switching between different states of the system as ODE models predict the average and continuous behaviour at the population level. Deterministic models argue that random events could be

averaged because, in many cases, these random events happen on a very small time scale while deterministic models focus on larger time scales (Proctor & Gray, 2008; Trewavas, 2006).

2.2.2 Stochastic modelling and simulation (Discrete stochastic methods)

It has become very clear that noise in biology is the rule rather than an exception (Sauer, 2012). Therefore, stochastic models have received a great deal of attention recently leading to many recent reviews (Burrage, Burrage, Leier, & Marquez-Lago, 2017; Češka, Šafránek, Dražan, & Brim, 2014; Gillespie, 2007; Pischel, Sundmacher, & Flassig, 2017; Raser & O'shea, 2005). Stochastic models are widely used to model biological systems and are classified as small systems (<100 molecules for each species in a given system). The denotational semantics of stochastic models are through the definition of rules to describe how the modelled system moves from one state to the next state. Therefore, stochastic models have been used to describe the states of the modelled system by determining the initial state and the procedure to be applied to give a new system state (Fisher & Henzinger, 2007). GSSA and its extensions are the most popular approaches that have been used to stochastically investigate biochemical systems.

The GSSA (a trajectory-based approach) is a technique used to generate individual realizations (Monte Carlo paths) from the full distribution given by the chemical master equation (CME) (Székely, 2014). The CME is an exact method that is used to enumerate all possible states for any stochastic system at any given time by tracking the behaviour of the system (Gillespie, 1992).

Using GSSA, a PDF (probability density function) can be obtained from an infinite number of simulations and this PDF is identical to the true distribution of the system, as given by the CME (Haugh, 2004). However, the identical PDF to the true distribution is never reached but an accurate PDF that depends on the system or type of application could be achieved using a high number of repeats of the GSSA (Gillespie, 2007). The GSSA is used to generate a step-by-step trajectory of the system instead of following the time evolution of the probabilities of the CME. In each time step, the GSSA uses the current state of the system and determines what reaction will occur next and when it will occur. In the literature, there are several

implementation strategies that have been proposed for the GSSA. They are: (1) the direct method (Gillespie, 1977); (2) the first reaction method (Gillespie, 1977); (3) the next reaction method (Gibson & Bruck, 2000); (4) the optimized direct method (Cao, Li, & Petzold, 2004); (5) the sorted direct method (McCollum, Peterson, Cox, Simpson, & Samatova, 2006); (6) the logarithmic direct method (Madani et al., 2006); and (7) the Tau-leap modified Poisson method (Cao, Gillespie, & Petzold, 2006).

Direct method

The direct method is a well-known technique that is used to stochastically model biochemical reactions and it is roughly equivalent to the CME. Assume a system involves N molecular species $(S_1, \dots\dots\dots\dots, S_N)$, species are represented by $X(t)$ $=\big(X_1(t), \dots\dots\dots\dots, X_N(t)\big)$ (the state vector), where $X_i(t)$ is the number of molecules of S_i at time t and M reactions channels $(R_1, \dots\dots\dots\dots, R_m)$. The GSSA steps along in time reaction-by-reaction, governed by the reaction probability (a_j) (propensity function) and by the state change vector $v_j = \big(v_{1j}, \dots., v_N\big)$. $a_j(x)dt$ gives the probability that one reaction will occur in the next time step. The steps of the direct method are summarized in Figure 2.1.

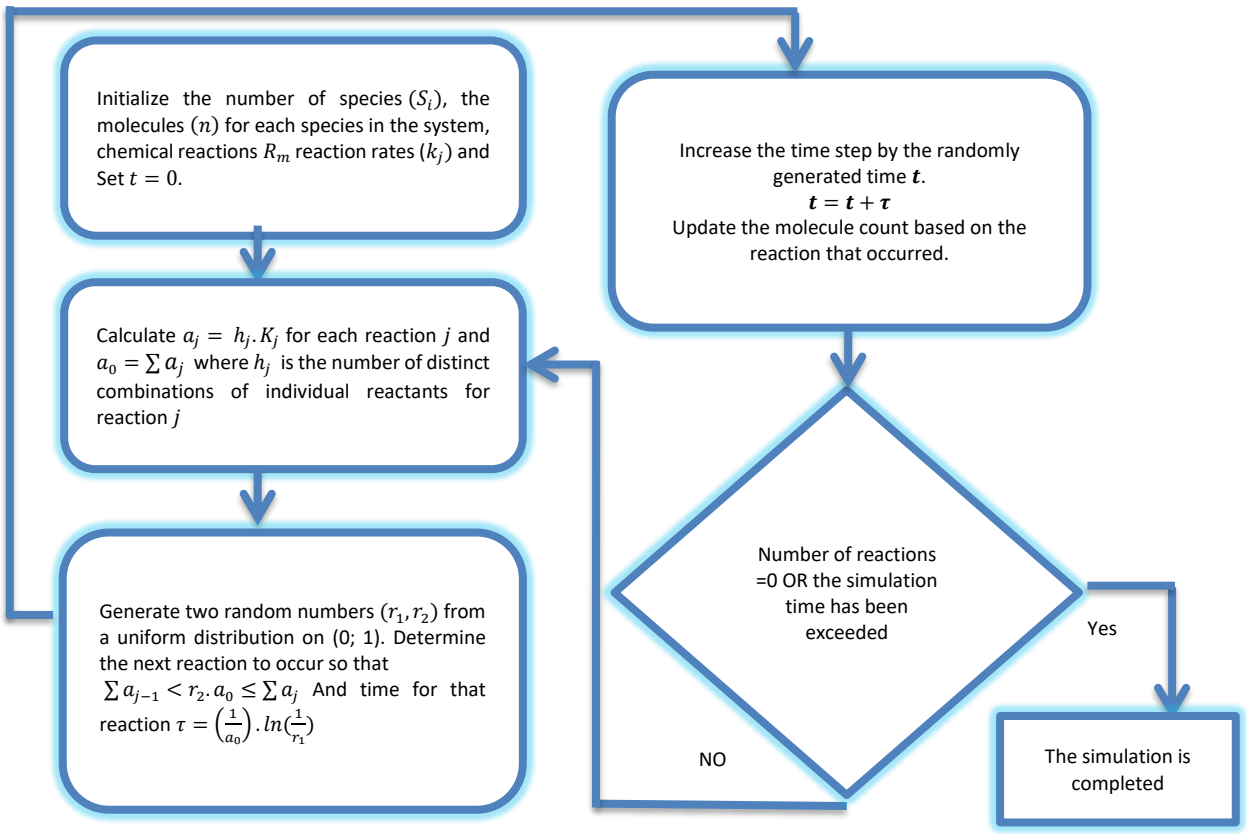

Figure 2.1: Schematic of the direct method

First reaction method

The first reaction method (Gillespie, 1977) is theoretically equivalent to the direct method since they select just one reaction to be run. The main difference between them is that the first reaction method is much less efficient than the direct method since M random numbers need to be generated to select just one reaction. Generating random numbers is computationally expensive (Cao & Samuels, 2009). The pseudo code of this method is given by Gillespie (1977).

Next Reaction method

In the next reaction method, remarkable progress has been made to the first reaction method to improve its efficiency. A dependent graph is used to record the influence of each reaction on the other reactions. This method employs a dependent graph to record the absolute time, $t + \tau_k$, as the expected firing time for the R_k reaction (the expected firing reaction). It aims to avoid unnecessary updates of the reactions that are not affected by the firing reactions in the current state (Cao & Samuels, 2009). The pseudo code for this method was given by Gibson

& Bruck (2000). According to Gibson and Bruck (2000), in the next reaction method, there are two different data structures that need to be created. These data structures are the dependency graph and the indexed priority queue.

- The dependency graph is used to precisely determine what a_j has to change once a reaction is executed. In this graph, reactions are symbolized as nodes and a directed edge connecting R_i and R_j if the execution of R_i affects the reactants in R_j. The graph recalculates the minimal number of propensity functions.
- The indexed priority queue (heap tree) is a data structure that is used to display ordered pairs in the form (i, τ_i), i is the reaction channel index and τ_i is the time for reaction, i. In the heap tree, each parent has a smaller τ than either of its leaves. Therefore, the minimum values stay at the top and the order is always vertical. Theoretically, for the m reaction, this procedure takes at most $ln(M)$ operations. In practice, there are usually a few reactions that occur frequently. Thus, the actual update takes fewer than $ln(M)$ operations.

The next reaction method and the direct method have the same efficiency. The only difference between these two methods is that the next reaction method needs only one random number to be generated while the direct method needs two. However, the direct method is much easier to be implemented since there is no need to deal with different types of data structures (Cao & Samuels, 2009).

Optimized Direct Method

The optimized direct method adopts a dependent graph that is used in the next reaction method to be able to efficiently index the reactions. The main idea behind this method is that the frequent reactions are always indexed before the less frequent ones (Cao et al., 2004). However, the re-indexing technique used by this method needs many sample runs of the GSSA to collect information, and this is not convenient in many applications (Cao & Samuels, 2009). More details about this method are given by Cao et al. (2004).

Sorted Direct Method

The sorted direct method involves a bubble up sorting method that is proposed in order to dynamically adjust the index of reactions. In the simulation, every time when one reaction occurs, its reaction index decreases by one so that in the next step it is found more quickly. It is a less efficient than the optimized direct method but it is mainly used to reduce the average search depth (McCollum et al., 2006).

Logarithmic direct method

The logarithmic direct method uses a binary search method to determine which reaction is due to fire next. The search is totally independent on the ordering of the propensity functions for reactions (Madani et al., 2006).

The modified Tau- leaping method

All versions of the GSSA need to create a state vector for all chemical reactions in any given chemical system at each time step. This process needs a long time because the effects of many reactions are computed at each time step. Therefore, the fastest version of the SSA is not fast enough especially when the system is large. In 2001, Gillespie proposed the Tau-leap method to speed up the stochastic simulation by leaping over many reactions at each time step by approximating the firing of each reaction as a Poisson random variable (Gillespie, 2001). However, the possibility that the population of some reactant species could be driven become negative is the main issue of this version since the Poisson random variable has the ability to have arbitrarily large sample values that cause one or more reactions to fire many times (Cao, Gillespie, & Petzold, 2005). A negative occurrence is avoided by replacing the Poisson random variable with a binomial random variable (Tian & Burrage, 2004). Cao et al. (2005) also proposed a modified procedure of Tau-leap to not only avoid negative population, but also be easier to implement than the binomial procedure. In the modified Poisson tau-leap method, reactions that have propensity functions of more than zero are divided into two groups, critical and non-critical reactions. Let L_j be the maximum number of permitted firings of R_j during τ. A reaction is classified as a critical reaction if it is currently in the state of exhausting any of its reactants and L_j is equal or less than some critical value, c_n.

The value assigned to c_n is discretionary but, typically, it should be between 2 and 20. The modified Poisson tau-leap method ensures that no more than one critical reaction can occur in each single τ leap to make sure it is impossible for any critical reactions to produce negative population counts. The steps of the modified Poisson tau-leap method are summarized in Figure 2.2. For more details about the modified Poisson tau-leap method see (Cao et al., 2005).

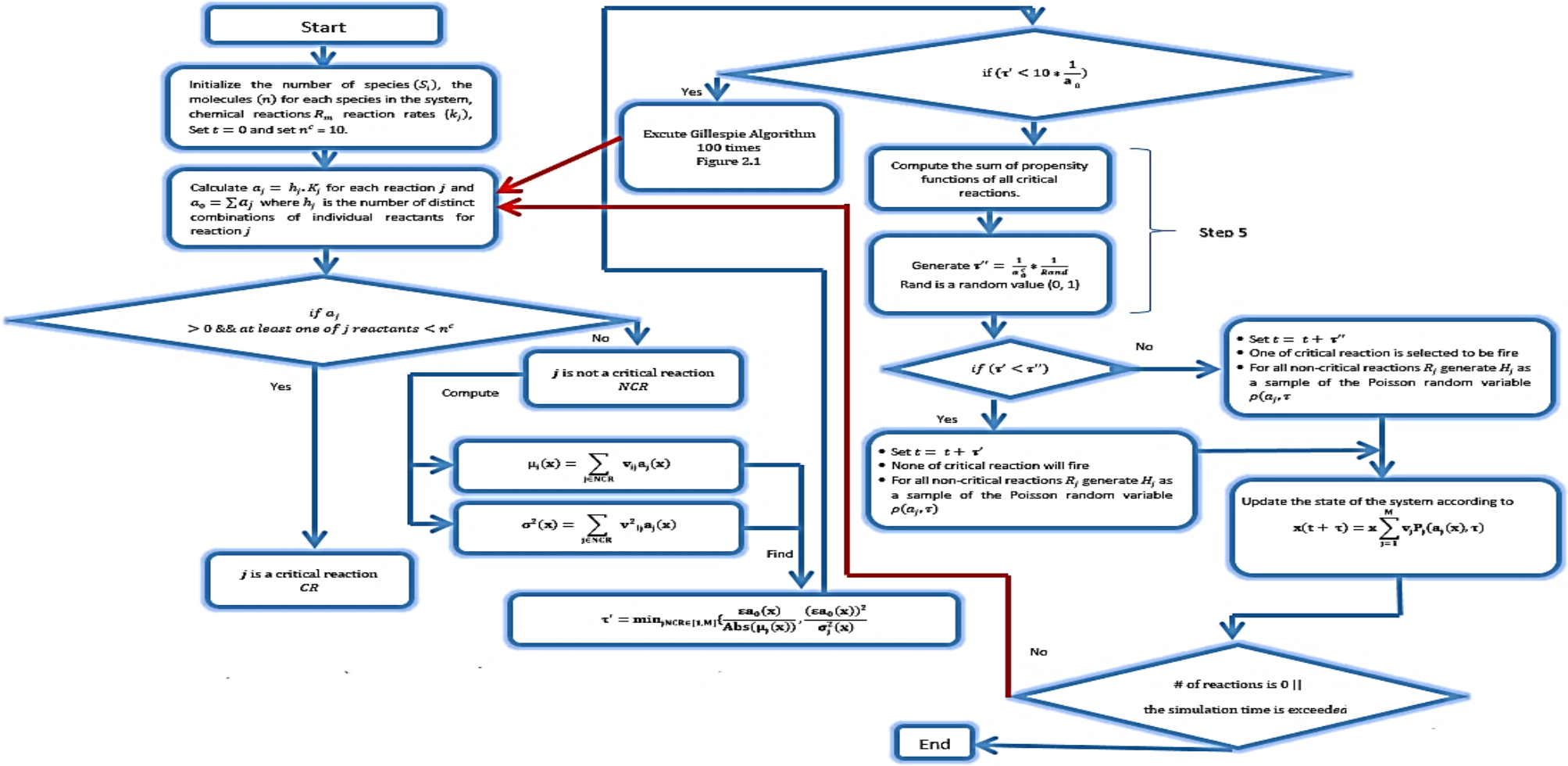

Figure 2.2: Schematic of the modified Poisson tau-leap method

2.3 Applications of sensitivity analysis (SA) in systems biology

Sensitivity analysis, as a term, has a different meanings in different disciplines (Nestorov, 1999), and was defined by Nestorov (1999) as:

> "The systematic investigation of the model responses to either perturbations of the model quantitative factors (e.g. inputs and/or parameters) or ii) variations in the model qualitative factors (e.g. structure, connectivity modules or sub models)."

The investigation of quantitative factors has received the most work in SA because in complex mathematical and computational models, values of some parameters are estimated and not precisely known. Therefore, uncertainty in the values of these parameters produces uncertainty in the outputs of the model. Using SA techniques to understand and quantify this uncertainty is an important part of the development and use of these models (Saltelli, Tarantola, Campolongo, & Ratto, 2004).

As mentioned in Chapter 1, there are two main classes of SA: LSA and GSA. LSA is specifically used to pay attention to a specific set of nominal parameter values. Studying the impact of small perturbations on the outputs of the model is used to simplify the analysis and interpretation of the results (Castillo, Hadi, Conejo, & Fernández-Canteli, 2004). GSA addresses the behaviour of a model over a wide range of parameter values simultaneously. These ranges are not only based on an approximation of parameter values, but also the upper and lower boundaries might be used to specify them. Statistical methods are always used to sample the values of these parameters within specified domains of the parameter spaces (Saltelli et al., 2008).

2.3.1 Local Sesntivity Analysis (LSA)

when undertaking LSA for a general ODE model (Eq 2.1), A Taylor series expansion is used to express the effect of a small parameter change.

$$\mathbf{x_i(t, k + \Delta k) = x_i(t, k) + \sum_{j=1}^{m} \frac{\partial x_i}{\partial k_j} \Delta k_j + \frac{1}{2} \sum_{l=1}^{m} \sum_{j=1}^{m} \frac{\partial^2 x_i}{\partial k_l \partial k_j} \Delta k_l \Delta k_j + \cdots} \qquad \mathbf{2.18}$$

The partial derivatives $\frac{\partial x_i}{\partial k_j}$ (known as the first-order local sensitivity coefficients) form the sensitivity matrix. A sensitivity matrix $S(t) = \frac{\partial x_i}{\partial k_j} * s_{ij}(t)$ is used to describe the effect of a small change in the j^{th} parameter around its nominal value on the i^{th} output at time, t. However, $S(t)$ at each time point is needed to be numerically calculated; therefore, numerical methods must be used to do this calculation (Van Griensven et al., 2006). Table 2.1 lists some of LSA techniques that have been used to numerically calculate the sensitivity matrix and their advantages and disadvantages.

Table 2.1: Advantages and disadvantages of some LSA techniques

LSA techniques	Advantages	Disadvantages
Indirect Method (De Pauw & Vanrolleghem, 2003).	• Simplest technique for calculating local sensitivities for a general ODE model. • No need any extra numerical machinery since it does not need more sophisticated methods to access to and modify of the model code, something that is not often desirable.	• Using the finite difference approximation method to mathematically formulate the partial derivative (subtraction of nearly equal numbers) • Selection of the step size Δk (Perturbation value of parameter k) is implemented as the nominal parameter value, k, that is multiplied by a user defined perturbation factor, ε. Once the perturbation factor is chosen to be very small it will result in numerical instabilities. The perturbation factor should not be also chosen to be too large because the nonlinearity of the model will start to play an important role in the sensitivity analysis.

Complex step Derivative approximation method (Martins, Sturdza, & Alonso, 2003)	• Easy to be implemented. • Avoiding the subtraction of nearly equal numbers and therefore does not exhibit the accuracy problems associated with small step-size. This is by using Taylor series expansion of a function in terms of complex variables.	• Only the first order derivative accessible using the imaginary part of Taylor series expansion, while the second derivatives needs to be evaluated by the real part of Taylor series expansion (Abreu, Stich, & Morales, 2013).
Feature Sensitivity Analysis (Saltelli et al., 2000)	• More interested in the sensitivity of aspects of the output of biological systems rather than the sensitivity of the output at a given time. This is likely to be the case when biologists wish to answer questions about features of the biological systems output such as how does the period of an oscillatory solution vary with the model parameters?	• In some cases, a feature that needs to be analysed might not be present in all runs (for example only certain parameter values may generate oscillations in the output) like what happened in (Ihekwaba et al., 2005) when they analysed of the $\mathrm{NF}-\kappa\mathrm{B}$ signalling pathway by using the feature sensitivity analysis.

However, these methods have a number of limitations. These limitations are summarised as follows.

- In biology the input values are always very uncertain and they cover large ranges that could not be investigated by local sensitivity methods (Marino et al., 2008).
- Local sensitivity techniques change one parameter at each time step while all other parameters should remain fixed at their nominal values. In biological systems, the interactions between parameters are very important.

Therefore, changes to more than one parameter at each time step should be also considered (van Riel, 2006).

Therefore, global sensitivity analysis methods are required to cope with these limitations.

2.3.2 Global Senstivity Analysis (GSA)

Recently, GSA methods have been applied to biological systems (Zielinski et al., 2017). In this section, we discuss the application of a number of global methods to model biological systems.

Sampling-based Methods

Monte-Carlo (MC) methods are used to explore the mapping between uncertain model inputs and outputs. A general sampling based approach for a model with N inputs, $x = (x_1, x_2, x_3 \dots \dots \dots \dots, x_N)$, involves five main steps (Saltelli et al., 2000) shown in Figure 2.3.

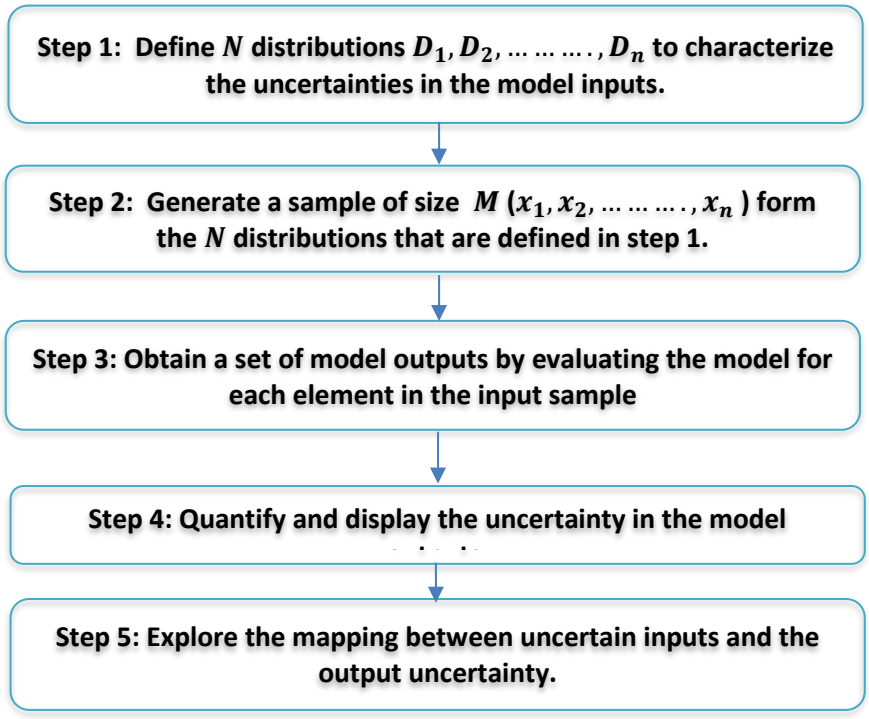

Figure 2.3: Five main steps that are involved by a general sampling approach to model a system with N inputs.

Saltelli et al (2000) state that the output of any MC method is extremely sensitive to distributions; therefore, those distributions are probably the most important part of the sampling-based method. The definition of these distributions depends

not only on the purpose of the analysis, but also on the available knowledge about the input values. When there is enough information, specific distributions could be assigned for each input whether by using parametric fitting to known distributions or by using non-parametric density estimation techniques. With limited data on a particular parameter the minimum and maximum values of that parameter could be identified. The natural choice with the limitation of data is to assume a uniform distribution across this range. Uniform distributions are always used in biological modelling since the lack of information is always encountered.

Random sampling is considered to be the simplest way to generate samples from the input distributions. However, computational cost is the main issue for random sampling since a large number of samples is required to be generated to ensure that the entire range of each input is sampled appropriately (Sumner, 2010).

Latin hypercube sampling (LHS) was introduced by Mckay et al. in 1979 (McKay, Beckman, & Conover, 1979). LHS is a sampling procedure shown to be more efficient than random sampling. In LHS, the range of each input is split into n intervals that have equal probability; then, one value from these intervals is selected randomly. These random values are combined in a random manner to generate n samples (Kulasiri et al., 2017; Marino et al., 2008; Segovia-Juarez, Ganguli, & Kirschner, 2004). When the n samples are generated, evaluating the model for each set of inputs and storing the results of each run is the next step of LHS. If the model outputs are scalar, assessing the overall uncertainty in the model output is performed by the mean values and variance. Plotting the probability density function (PDF) or cumulative distribution function (CDF) is used to obtain more information about the uncertainty in the model output. For time dependent model outputs, Helton and Davis (2000) suggest that the picture of the output uncertainty is obtained by plotting together the point-wise mean with some appropriate point-wise percentiles. Finally, exploring the effects of individual parameters on the model output is performed by examining scatter plots of the output against parameter values for each parameter (Kulasiri et al., 2017). The main steps of LHS are:

1. Start out with a mathematical model of interest.

2. List all parameters in the model $(\mathrm{i.e.\ M\ parameters})$.
3. Identify the uncertain parameters in the parameter list.
4. Decide the sample size for the model analysis. The sample size is determined by the number of simulations that are intended to be run. Assume we decided to do N simulations. Also, assume there are L uncertain parameters. Then the parameter space for the uncertain parameters is defined by L dimensions. The choice for N should be at least $\mathrm{k}+1$ (Marino et al., 2008), where K is the number of parameters.
5. Each of the L dimensions corresponds to an uncertain parameter and the length of each dimension is determined by the number of runs, N. Each of the N input values is selected or determined by the LHS sampling method for each uncertain parameter.
6. For each uncertain parameter, the LHS sampling method is implemented by specifying a probability density function (PDF). The variability in the probability density function could be used as a direct measure of the variability of the uncertain parameter. Each specified PDF is used not only to describe a range of possible values, but also the probability of occurrence of any specific value for the parameter.
7. Sampling values for each parameter is achieved by dividing the probability density function into N non-overlapping equiprobable intervals. This sampling is used to reflect the shape of the particular PDF.
8. Each interval of each parameter is then randomly sampled. The frequency of the selection of possible values of each parameter is determined by the probability of occurrence in the PDF. Each parameter is sampled independently.

Once step 8 is completed, each uncertain parameter will have N values. These values should be stored in a $N * L$ matrix. The values for each column in this matrix are random and they are not arranged in any particular order. Each column of this matrix has entry (r_j, v_i), where$1 \leq i \leq k, 1 \leq j \leq N$. Therefore, each row in this matrix comprises K random values that each correspond to a specific LHS parameter.

LHS, in combination with Partial rank correlation coefficient analysis (PRCC) (LHS/PRCC), has been shown as a very useful procedure to perform a sensitivity analysis over a global parameter space with a minimum number of computer simulations. PRCC is a robust sensitivity method that is used to indicate not only nonlinear, but also the monotonic relationships between the LHS parameters (inputs), $\boldsymbol{x_i}$ and outcomes (outputs), $\boldsymbol{y}$ as long as little to no correlation exists between the inputs (Hamby, 1994). This is used to measure the strength of the relationship between two variables while controlling the effect of the other variables.

LHS/PRCC is used to precisely indicate the degree of monotonicity between a specific input and the corresponding output variable to measure the strength of a relationship between two variables while controlling the effect of the other variables. Therefore, only outcome measure having a monotonic relationship with the input variables should be chosen for this type of sensitivity analysis (De La Fuente, Bing, Hoeschele, & Mendes, 2004).

Once the LHS parameter ranges are adjusted and generate a final version of sample LHS matrix, the k values in each row of the sample matrix are used as input values for the numerical simulation of the model. Then, a frequency histogram and descriptive statistics, such as minimum, maximum, mean and variance, could be calculated for the outcome measures (Kulasiri et al., 2017). PRCC is performed by:

1- Rank the LHS matrix
2- Rank the matrix for the outcome measure

} Using a sort routine

3- For each parameter in the LHS matrix and each outcome measure, there are two linear regression models are used
    - The first linear model is used to represent a ranked parameter in the sampled LHS matrix in terms of the other ranked parameters
    - The second linear model is used to represent the ranked outcome measures in terms of the other ranked parameter values.
4- The PRCC value for that specific parameter is given by a Pearson correlation coefficient for the residuals from those two regression models.

Variance Based Methods

Variance-based methods are considered to be free model since they are not dependent on any assumption about the relationships between model inputs and outputs (Saltelli et al., 2000). These methods are used to identify the amount of variation that is explained by the uncertainty in the parameters by partitioning the total output variance. These methods are used not only to quantify the relative importance of parameters that have the ability to drive system the output, but also to investigate the effects on the interactions between parameters.

Two approaches are commonly used to calculate the variance-based sensitivity indices. These approaches are the Fourier amplitude sensitivity test (FAST) (Cukier, Levine, & Shuler, 1978) and its extended version (eFAST) (Saltelli, Tarantola, & Chan, 1999). These approaches are used to explore the uncertain parameters in the frequency space. eFAST was previously classified as the most efficient method that has been used to determine the main parameters in the model and their total effects. This was used by Marino et al. (2008) for applying global sensitivity analysis in systems biology (Marino et al., 2008). See (Sumner, 2010) for full description about variance based methods.

Sobol's method is an alternative variance-based approach (Zi, 2011). This method is based on the decomposition of the variance of the output or system into terms that can be attributed to inputs. For example, if a system has two inputs and one output, one might find that 60% of the output variance is caused by the variance in the first input, 25% by the variance in the second input and 15% of the output variance because of interactions between these two inputs. These percentages are directly used as measures of sensitivity. See (Sobol, (1993), ((2001); Sumner (2010)) for more details about Sobol's method.

Screening Methods

Screening methods are a class of sensitivity analysis approaches used with models containing large numbers of input factors. The main advantage of screen methods is their economy since they require a fewer number of runs than other methods (Yue, Brown, He, Jia, & Kell, 2008). However, they have the ability to provide only a

qualitative measure of importance; they can rank the parameters in order of their importance but the differences in importance are not quantified. There are different screening methods that have been proposed (Saltelli et al., 1999). Morris' method (Cropp & Braddock, 2002) is classified in the literature as the most robust and effective screening method.

By using the Morris method, an approximate global importance measure is provided by using the average and standard deviation of a number of local sensitivity measures. The Morris method is considered to be an efficient way to select the input points that are used to not only optimise coverage of the space, but also to minimise the number of evaluations required to calculate the elementary effects (Van Griensven et al., 2006).

The low computational cost makes the Morris method an appropriate technique that has the ability to study complicated biological systems involving large number of parameters. The Morris method was used to study a model of circadian rhythm in a type of mould, $Neurospra$ (Jin, Peng, Liang, & Ma, 2008). It was also used to analyse the $NF-kB$ pathway that already been analysed by local methods (Yue et al., 2006). Yue et al., (2008) found that the Morris method has the ability to identify additional important parameters whose interaction effects were not really captured by local sensitivity analysis methods (Yue et al., 2008).

2.3.3 Sensitivity analysis of discrete stochastic chemical reaction networks

With stochastic models, the quantification of the parameter sensitivities is a challenging task since each simulation has the ability to generate a different result. Therefore, if a parameter is modified and a change in behaviour is observed, it could not be known whether this change is from the parameter alteration or from the inherent randomness (Gunawan, Cao, Petzold, & Doyle, 2005). In the stochastic setting, computing a finite difference via Monte Carlo simulations is considered to be the simplest and commonest method for finite perturbation systems (Rathinam et al., 2010). Several estimators using a finite difference approximation have been proposed: Independent random number (IRN) (Ethier & Kurtz); Common random number (CRN) (Glynn & Iglehart, 1988); Common Reaction Path (CRP) (Rathinam et al., 2010) and Coupled Finite difference (CFD) (Anderson, 2012).

CRN in conjunction with MRM/GSSA is used for parametric sensitivity of immunization in AD model. CRN is the easiest and most common method to achieve variance reduction. Implementation of CRN is achieved by using the same stream of uniform random numbers. CRN in conjunction with MRM/GSSA is described in detail in Chapter 4 (Methodology chapter).

2.4 Alzheimer's disease models

Molecular processes involved in Alzheimer's is constructed in a comprehensive interaction map that was published in (Mizuno et al., 2012). Due to the complexity, this map is not able to provide a clear view of Alzheimer's disease according to Mizuno et al. (2012) as it includes around 1347 molecules, 1070 reactions and about 129 phenotypes. Mizuno et al. (2012) collected this information from 100 review articles on Alzheimer's disease. However, the map is used to provide an overview of Alzheimer's pathways overlaid with canonical pathway annotations, as shown in Figure 2.4.

For better visualisation, a comprehensive interaction map for neurodegenerative diseases (including Alzheimer's and Parkinson's disease) was published in (Lloret-Villas et al., 2017). Only the important mechanisms involved in these diseases are shown in this map.

From the literature, we collected 31 mathematical models. These models are listed in Table 1 the Appendix A. These models have been developed over the last two decades to describe different aspects of Alzheimer's disease. There are 14 different aspects (or pathways) described by these models. These pathways are listed in Table 2.2.

Some of the models as shown in Table 2.3 are exclusive models (models devoted to a single pathway), while others are shared models (models involving multiple pathways). APP breakdown, fibril organization and synaptic transmission are the most exclusively modelled systems.

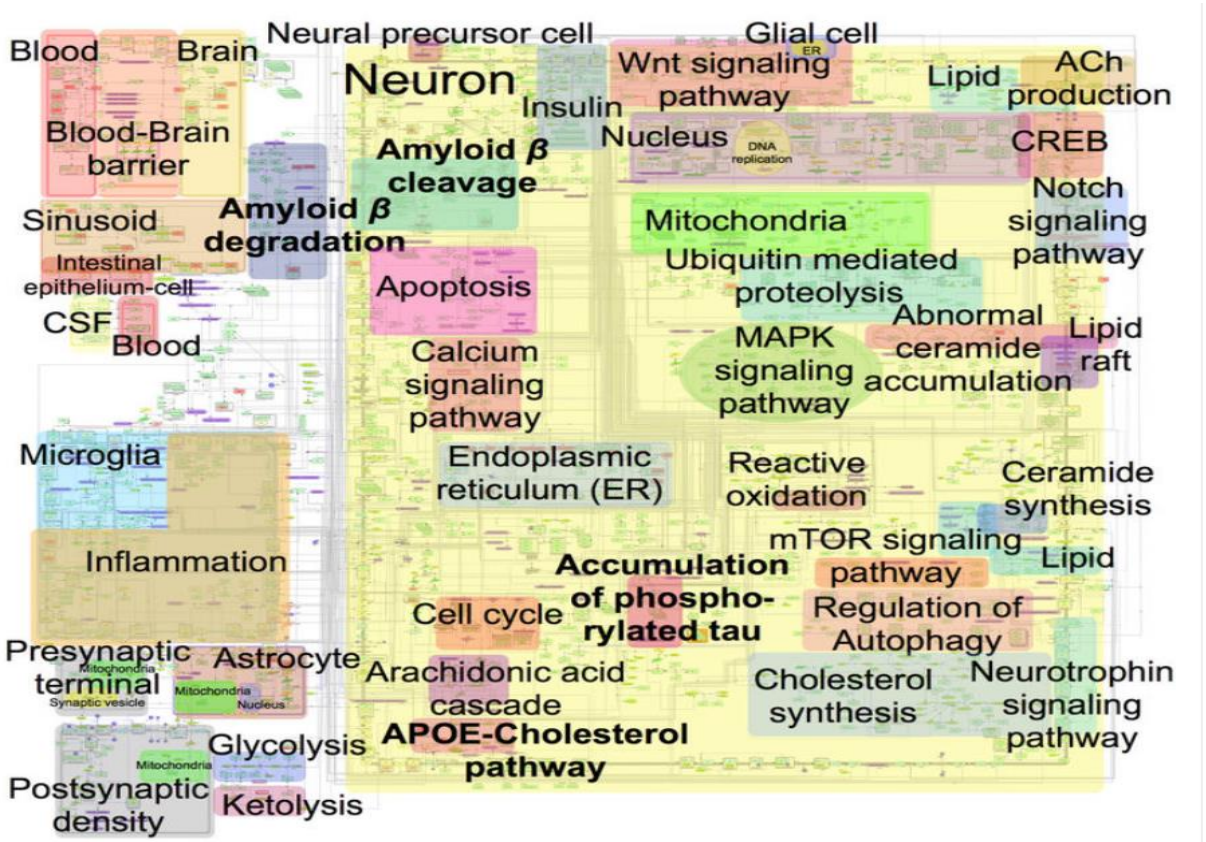

Figure 2.4: Overview of Alzheimer's pathways overlaid with canonical pathway annotations for an explanation of the Alzheimer's interaction map by Minzuno et al (2012). These pathways include 1347 molecules, 1070 reactions and 129 phenotypes (Acknowledgement: This figure is Figure 1 in (Mizuno et al., 2012)).

Table 2.2: Functional modules in AD.

1	**Intercellular signalling**	**8**	**Blood–brain barrier transport (BBB-transport)**
2	**Energy metabolism**	**9**	**Protein degradation**
3	**Oxidative metabolism**	**10**	**Fibril organization**
4	**Inflammatory response**	**11**	**Tauopathy**
5	**Apoptosis**	**12**	**APP breakdown**
6	**Ion homoeostasis**	**13**	**Microtubule-based transport**
7	**Synaptic transmission**	**14**	**genetics**

This might be because they are specifically aberrant in Alzheimer's disease so they receive specific attention to be understandable (Lloret-Villas et al., 2017). Empirical data from human cells are used by most of the models that have had their fibril organization aspects investigated. These models are relatively simple and small because the fibrillation mechanism in Alzheimer's disease involves only a few

molecules (Lloret-Villas et al., 2017). By analysing the shared models, we observed that there are varying degrees of association among the different pathways. For example, fibril organization has frequent associations with protein degradation and oxidative stress while other pathways, such as microtubule-based transport, are less studied in association with other pathways.

Table 2.3: Number of models according to the shared pathways they represent.

Alzheimer's pathways	Intercellular signalling	Energy metabolism	Oxidative metabolism	Inflammatory	Apoptosis	Ion homoeostasis	Synaptic transmission	BBB transport	Protein degradation	Fibril organization	Tauopathy	APP breakdown	Microtubule-based	Genetics
Intercellular signalling	2			2	2					1		1		1
Energy metabolism		2		1		1	1	1		1		1		
Oxidative metabolism			3	2	3				1	3	2			
Inflammatory response	2	1	1	6	3		1	1		3	1	2		1
Apoptosis	2		1	3	3					2	1	1		1
Ion homoeostasis		1				3	1			1	1			
Synaptic transmission		1		1		1	7	1		1		3		
BBB transport		1		1			1	4		3		3		
Protein degradation			1						1	1	1			
Fibril organization	1	1	3	3	2	1	1	3	1	11	2	4		1
Tauopathy			2	1	1				1	2	5			
APP breakdown	1	1		3	1		3	3		3		12		1
Microtubule-based transport											1		1	
Genetics	1			1						1		1		3

Our model collection includes models for Alzheimer's pathways from 1996 to 2016. In Figure 2.5, we investigate the evolution of these models. Most of models were developed between 2012 and 2016 as there were 16 mathematical models to investigate Alzheimer's processes. The periods from 2000 to 2003 and 2008 to 2011 have six models each while the periods from 2004 to 2007 and 1996 to 1999 have one and two models, respectively.

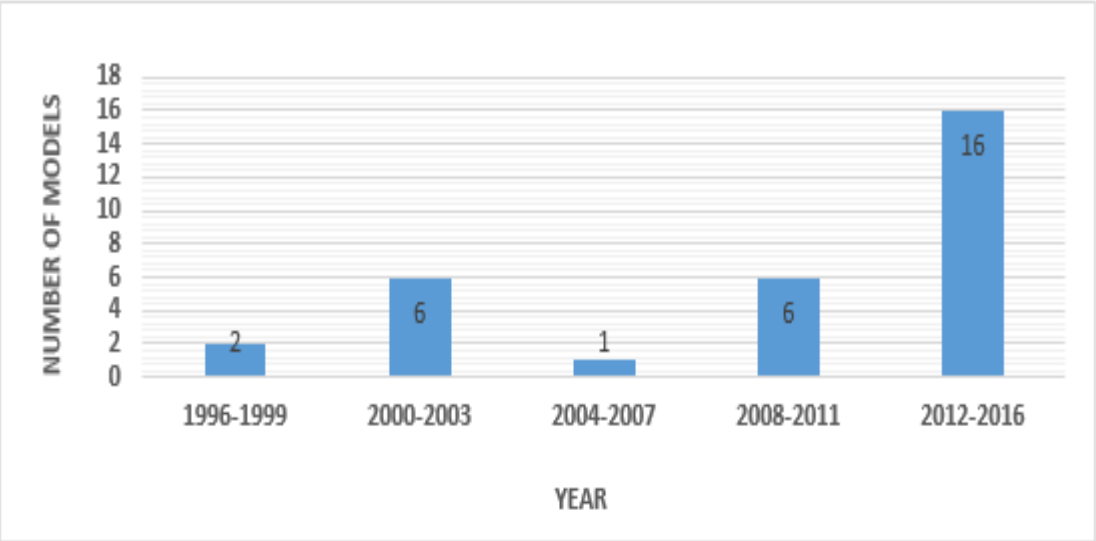

Figure 2.5: Evolution of Alzheimer's models. This graph shows evolution of mathematical models that have been used to describe Alzheimer's processes over 20 years in four-year increments. Most of models in the collection were proposed after 2012.

Alzheimer's pathways in our collection of models use different approaches, as shown in Table 2.3. Some pathways are modelled by using multiple approaches (hybrid models). Table 2.4 lists all approaches and their frequency in our collection of models.

Table 2.4: Modelling approaches and their frequency in the collection of models.

#	Modelling Type	Frequency
1	Ordinary Differential Equations	15
2	Hybrid models	7
3	Partial Differential Equations	3
4	Algebraic Equations	3
5	Stochastic Models	2
6	Rule-based Models	1
	Total	31

ODEs were the predominant technique used in the collection of models because ODEs not only were used in 15 models, but also were nearly a part of all hybrid approaches.

2.5 Summary

This chapter is divided into three main sections.

The first section focuses on deterministic and stochastic approaches that have been widely used to investigate, understand and model biochemical systems. It has been found that the deterministic approaches are used to describe the dominant physical processes and give the average behaviour of a given system. Deterministic models deterministically track the exact concentration of biological components through continuous representation of system dynamics over time. Stochastic approaches look at biological systems differentially from the deterministic approaches. The denotational semantics of stochastic models is by defining rules to describe how the modelled system moves from one state to another state. Stochastic approaches focus on the importance of the randomness and they have been used mainly to model small biological systems.

In the second section we describe the most popular sensitivity analysis methods (LSA and GSA) that have been used to investigate the behaviour of biochemical system in response to parameters perturbation, one at a time, using LSA and over the space of parameters using GSA.

Third part covers a historical review of mathematical models that are used to investigate aspects of Alzheimer's disease over the last two decades. A collection of models include 31 models for Alzheimer's pathways.

Chapter 3

Case study- Immunisation in Alzheimer's disease

3.1 Overview

Alzheimer's disease (AD) is mainly characterized by the presence of two proteins and their aggregation relationship. These proteins are amyloid-beta (Aβ) and micro-tubular binding protein (tau) accompanied by glial cell activation, together with synaptic and neuronal losses (Proctor et al., 2013). It has been found that there is no effective treatment that could target the underlying neurodegeneration in AD in spite of many interventions tested. For instance, a phase 11a clinical trial of PBT2 (an experimental drug candidate) according to (Lannfelt et al., 2008) shows preliminary promising results though larger trails are needed. Also, based on promising experimental results and the amyloid cascade hypothesis (Schenk, Barbour, Dunn, & Gordon, 1999).

Aβ immunotherapy in some clinical trials for animals shows that cognitive function deterioration has slowed down or deteriorating slowly (Hock et al., 2003); however, septic meningoencephalitis was developed in a small part of subjects that were treated with the first Aβ immunotherapy agent (AN1792) (Bayer et al., 2005). Therefore, the trial had to be halted. Different side effects that were unexpected by the pre-clinical animal models are classified to be the main problem. This demonstrates that animal models of Alzheimer's disease would not be able to replicate the complexity of the human disease (Jucker, 2010). In human clinical trials, unforeseen side effects are also considered to be the main reason to slow development of therapeutic interventions of AD (Nicoll et al., 2003).

Neuropathological studies of patients with AD have shown that a decrease in Aβ-plaques occurs if patients are immunised against Aβ (Boche, Denham, Holmes, & Nicoll, 2010). This observation has been subsequently confirmed in vivo by amyloid imaging (Rinne et al., 2010). The techniques of how immunisation is used to clear Aβ are not fully understood but it seems that phagocytosis of Aβ by microglia and the solubilisation of Aβ by antibody binding are involved (Boche et

al., 2010; Maarouf et al., 2010; Nicoll et al., 2006; Nicoll et al., 2003; Zotova et al., 2011).

Due to these relapses, new approaches are highlighted as needed for pre-clinical testing of possible interventions. Modelling approaches and computer simulation are considered to be new approaches in the medical fields and their potential is being progressively recognised as a valuable complementary tool to gain better understanding of Alzheimer's disease (Proctor et al., 2013).

Therefore, the system developed by Proctor et al. (2013) and described in this chapter is used to examine how plaques and tangles formation could be affected by immunising an AD patient against Aβ. Two sub-systems for immunisation against Aβ are included in this system (passive and active). Passive and active immunisation systems use antibodies and glia, respectively, to immunise against Aβ. An overview of the system is shown in Figure 3.1.

Hint, all figures in this chapter are created using Visio 2016 tool.

3.2 Reactions

The system developed by Proctor et al (2013) has 112 reactions. The reactions and ODEs are listed in Tables 1 and 2 in the Appendices (B).

3.3 Species

The system developed by Proctor et al (2013) contains 69 species. Five species are set to be constant as they are not able to be changed by any reaction. The numbers of antibodies are initially zero but change to 50 on day 4. These species and their initial values are listed in Table 3 in the Appendices (B).

3.4 Parameters

The system developed by Proctor et al (2013) contains 73 global parameters. These parameters and their values are listed in Table 4 in the Appendices (B).

3.5 Events

Each event in the model is initiated when its trigger condition switches from false to true. A delay function then postpones the effects of an event to a later time point. In This system, antibodies is initially zero and when the time reach 345600 seconds (day #4), antibodies are added to the system and the value of antibodies is changed suddenly from 0 to 50.

Trigger condition	$t \geq 345600$ (day #4)
Assignment	antibodies $= 50$

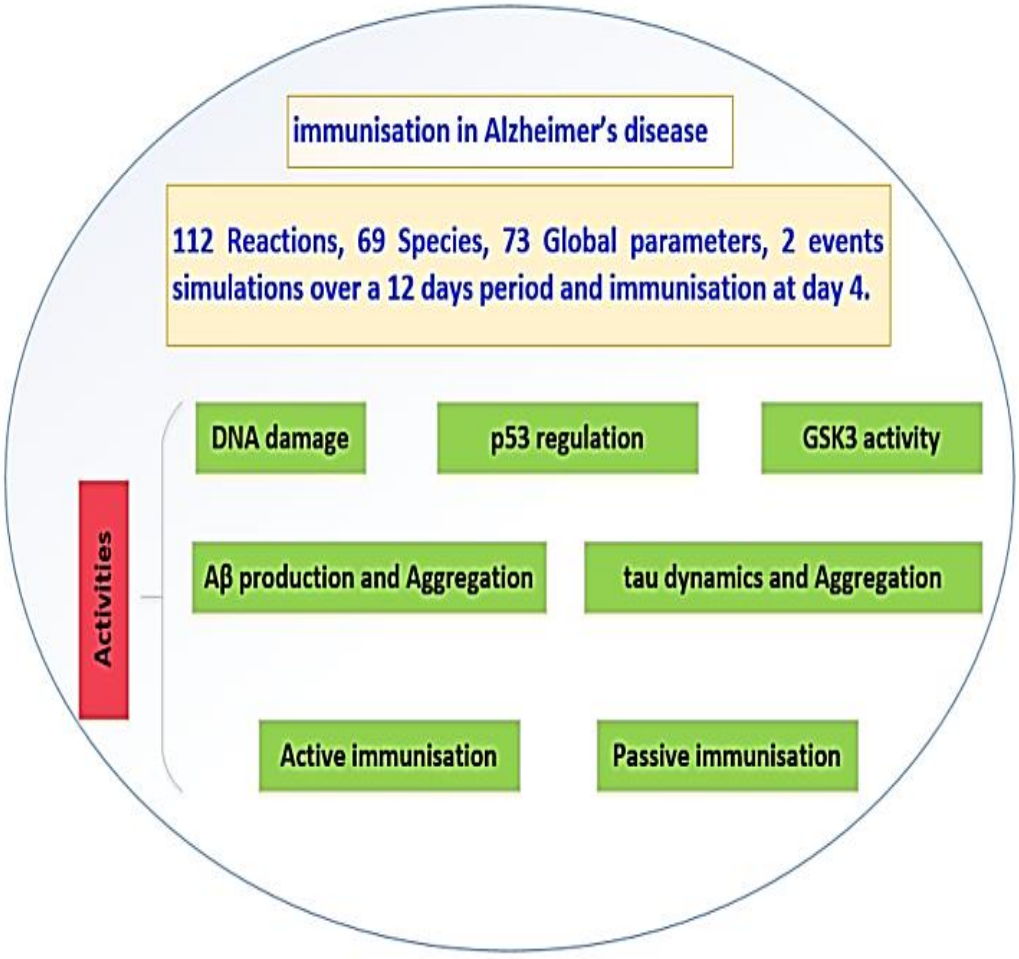

Figure 3.1: Overview of immunization in AD. The system includes 112 reactions, 69 species, 73 global parameters, simulation over a 12-day period and immunisation at day 4. It has seven main activities that are included in this system (DNA damage, p53 regulation, Gsk3 activity, Aβ production and aggregation, tau dynamics and aggregation, and active and passive immunisation).

3.6 Sub-systems (activities)

The model proposed by Proctor et al (2013) includes six main activities (or pathways). These pathways are DNA damage, p53 regulation, GSK3 activity, Aβ production and aggregation, tau dynamics and aggregation, and active and passive immunisation. Some assumptions are made by Proctor et al. (2013) when they built this model because the pathways involved in Aβ immunization are complex and many of the mechanisms are not fully known. These assumptions, below, are also shown in Figure 3.2:

A. Aβ could cause harmful effects by motivating the production of Reactive Oxygen Species (ROS) that lead to further DNA damage.
B. ROS increases DNA damage that results in increasing the production of p53, which leads to increased activity of GSK3β.
C. Aβ can directly enhance the production of p53.
D. Soluble Aβ has the ability to inhibit the proteasome that has detrimental effects on cells.
E. The pool of soluble Aβ is decreased by plaques.

However, these assumptions may not be in agreement with other points of view because there is controversy over the different mechanisms used to investigate Aβ immunisation.

Figure 3.3 shows the activity of DNA damage pathway and GSK3b activity. DNA damage is the first initiator of the system. When stress happens, the system responds by increasing the activity of ATM that phosphorylates p53 and Mmd2 to break the binding relationships between them. When the level of p53 is elevated, binding relationship is established between p53 and GSK3β to increase the activity of both proteins; this leads to more phosphorylation of tau and Aβ to form tangles and plaques. p53 regulation is displayed in Figure 1 in the Appendices (B).

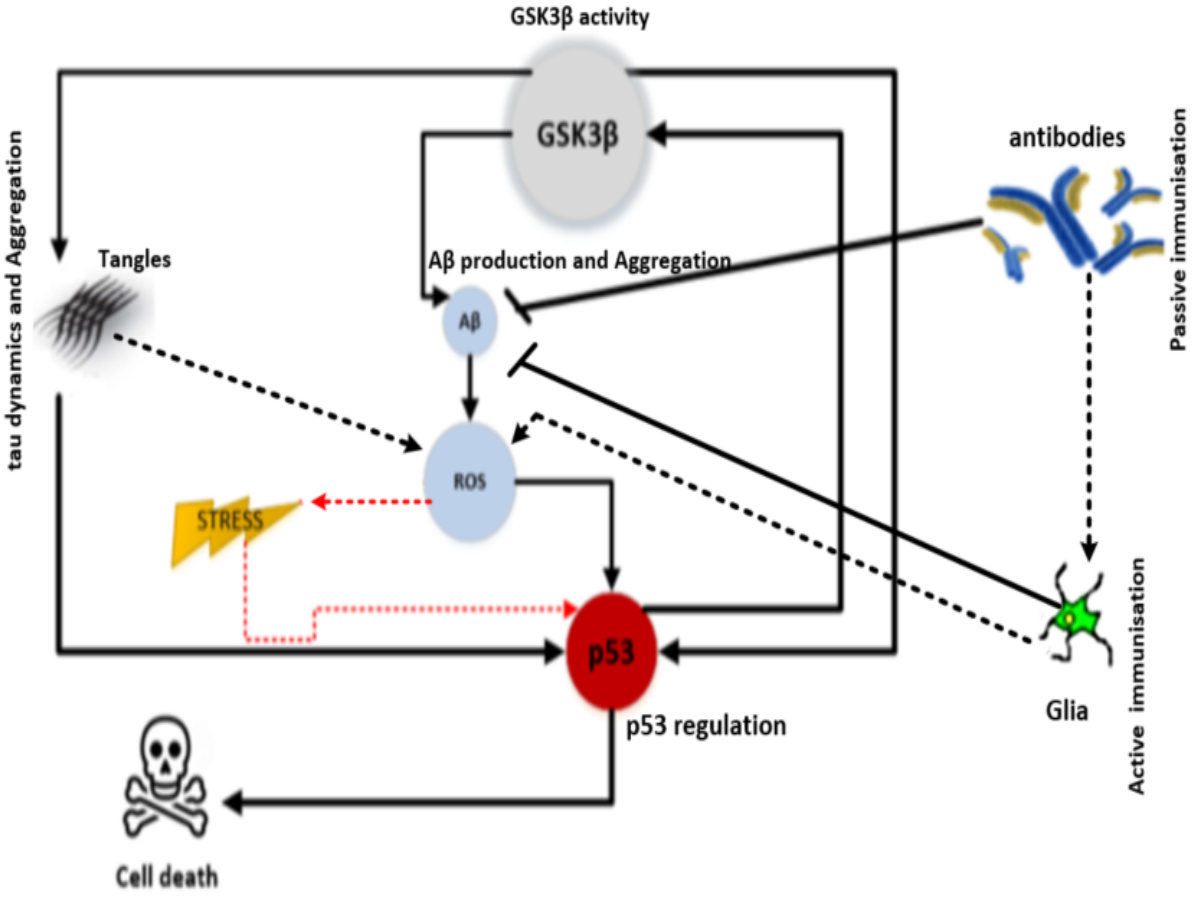

Figure 3.2: System activities. The DNA damage signal activates p53, and this causes phosphorylation of p53 and Mdm2 to prevent their binding, so p53 is no longer degraded. When the level of p53 is elevated, a binding relationship is established between p53 and GSK3β to increase the activity of both proteins. Tau then starts to aggregate and the production of Aβ is increased. In passive immunisation, antibodies reduce the levels of soluble Aβ and plaques. The active immunisation (microglia cells) used not only reduces the levels of plaques but also makes sure that antibodies are continually produced. However, microglia cells might also increases the production of ROS as shown in Figure 3.6.

Figure 3.4 shows how phosphorylated and non-phosphorylated p53_GSK3β increase the activity of Aβ (known as Abeta). Aβ increases the production of an Abeta_Dimer that is used to increase the production of plaques. Aβ directly increases the production of p53_mRNA. Therefore, it can easily be seen that there is an indirect positive feedback relationship between p53 and Aβ since both of them indirectly increase the production of each other through other species. Table 3.1 lists all reactions to achieve this activity.

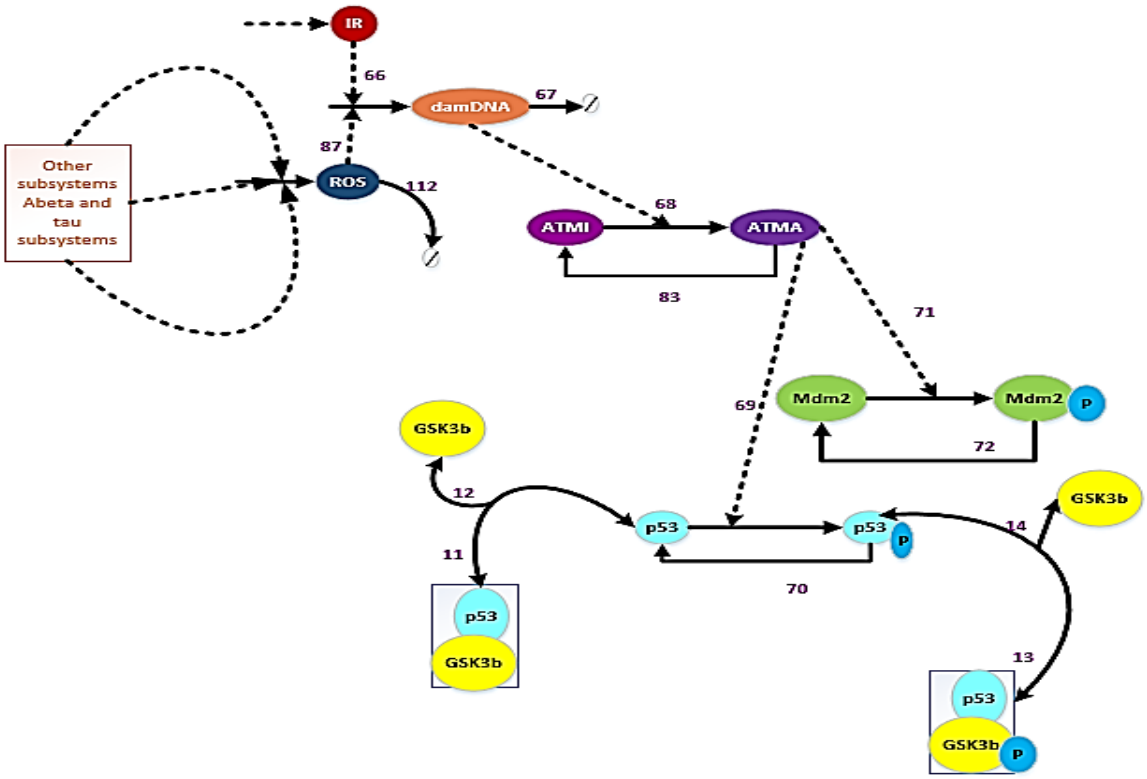

Figure 3.3: DNA damage and GSK3 activity. It displays that DNA damage through ATM activities of p53 and Mdm2 and breaks the binding relationship to elevate the level of p53. Unbound p53 establishes a binding relationship with GSK3β to increase its activity and that leads to more phosphorylation of tau and Aβ. Dashed lines from a species indicates the species is a modifier of the reaction.

Table 3.1: Reactions for DNA damage pathway and GSK3b activity. Reaction numbers correspond to the numbers in the reaction table of the whole system (Table 1 in the Appendices (B)).

#	Reaction name	Reaction Equation
11	GSK3_p53 Binding	$\mathrm{GSK3b} + \mathrm{p53} \xrightarrow{\mathrm{kbinGSK3bp53}} \mathrm{GSK3b\_p53}$
12	GSK3_p53 Release	$\mathrm{GSK3b\_p53} \xrightarrow{\mathrm{krelGSK3bp53}} \mathrm{GSK3b} + \mathrm{p53}$
13	GSK3_p53_P Binding	$\mathrm{GSK3b} + \mathrm{p53\_P} \xrightarrow{\mathrm{kbinGSK3bp53}} \mathrm{GSK3b\_p53\_P}$
14	GSK3_p53_P Release	$\mathrm{GSK3b\_p53\_P} \xrightarrow{\mathrm{kbinGSK3bp53}} \mathrm{GSK3b} + \mathrm{p53\_P}$
66	DNA damage	$\mathrm{IR} \xrightarrow{\mathrm{kdam}} \mathrm{IR} + \mathrm{damDNA}$
67	DNA repair	$\mathrm{damDNA} \xrightarrow{\mathrm{krepair}} \mathrm{Sink}$
68	ATM activation	$\mathrm{damDNA} + \mathrm{ATMI} \xrightarrow{\mathrm{kactATM}} \mathrm{damDNA} + \mathrm{ATMA}$
69	p53 phosphorylation	$\mathrm{p53} + \mathrm{ATMA} \xrightarrow{\mathrm{kphosp53}} \mathrm{p53\_P} + \mathrm{ATMA}$
70	p53 dephosphorylation	$\mathrm{p53\_P} \xrightarrow{\mathrm{kdephosp53}} \mathrm{p53}$
71	Mdm2 phosphorylation	$\mathrm{Mdm2} + \mathrm{ATMA} \xrightarrow{\mathrm{kphosMdm2}} \mathrm{Mdm2\_P} + \mathrm{ATMA}$
72	Mdm2 dephosphorylation	$\mathrm{Mdm2\_P} \xrightarrow{\mathrm{kdephosMdm2}} \mathrm{Mdm2}$
73	Mdm2_P Ubiquitination	$\mathrm{Mdm2\_P} + \mathrm{E2\_Ub} \xrightarrow{\mathrm{kMdm2PUb}} \mathrm{Mdm2\_P\_Ub} + \mathrm{E2}$
87	ROS DNA damage	$\mathrm{ROS} \xrightarrow{\mathrm{kdamROS}} \mathrm{ROS} + \mathrm{damDNA}$
112	ROS removal	$\mathrm{ROS} \xrightarrow{\mathrm{kremROS}} \mathrm{Sink}$

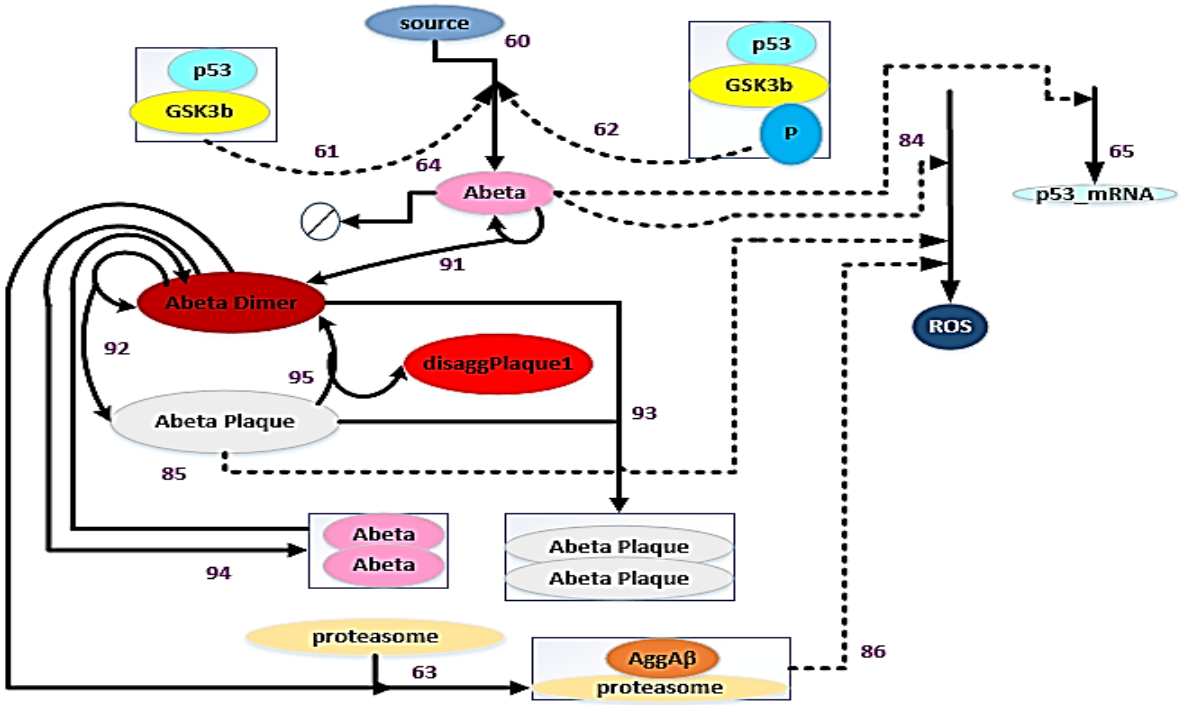

Figure 3.4: Activity of Aβ (Abeta in the figure) production and aggregation. It shows that p53_GSK3β in the phosphorylated and non-phosphorylated form is used to increase the activity of Abeta that not only increases the activity of Aβ _Dimer to increase the activity of plaques, but also directly increases the activity of p53_mRNA. Dashed lines from a species indicate the species is a modifier of the reaction.

Table 3.2: Reactions of Aβ (Abeta in in the Table) production and aggregation. Reaction numbers correspond to the numbers in the reaction table of the whole system (Table 1 in the Appendices (B)).

#	Reaction name	Reaction Equation
60	Abeta production1	$\text{Source} \xrightarrow{\text{kprodAbeta}} \text{Abeta}$
61	Abeta production2	$\text{GSK3b\_p53} \xrightarrow{\text{kprodAbeta2}} \text{Abeta} + \text{GSK3b\_p53}$
62	Abeta production3	$\text{GSK3b\_p53\_P} \xrightarrow{\text{kprodAbeta2}} \text{Abeta} + \text{GSK3b\_p53\_P}$
63	Proteasome Inhibition Abeta	$\text{AbetaDimer} + \text{Proteasome} \xrightarrow{\text{kinhibprot}} \text{AggAbeta\_Proteasome}$
64	Abeta Degradation	$\text{Abeta} \xrightarrow{\text{kdegAbeta}} \text{Sink}$
65	p53 transcription Via Abeta	$\text{Abeta} \xrightarrow{\text{ksynp53mRNAAbeta}} \text{p53\_mRNA} + \text{Abeta}$
84	Abeta ROS production1	$\text{Abeta} \xrightarrow{\text{kgenROSAbeta}} \text{Abeta} + \text{ROS}$
85	Plaque ROS production	$\text{AbetaPlaque} \xrightarrow{\text{kgenROSPlaque}} \text{AbetaPlaque} + \text{ROS}$
86	Agg Abeta ROS production2	$\text{AggAbeta\_Proteasome} \xrightarrow{\text{kgenROSAbeta}} \text{AggAbeta\_Proteasome} + \text{ROS}$
91	Abeta Aggregation1	$2 * \text{Abeta} \xrightarrow{\text{kaggAbeta}} \text{AbetaDimer}$
92	Abeta Plaque Formation1	$2 * \text{AbetaDimer} \xrightarrow{\text{kpf}} \text{AbetaPlaque}$
93	Abeta Plaque Growth	$\text{AbetaDimer} + \text{AbetaPlaque} \xrightarrow{\text{kpf,kpghalf}} 2 * \text{AbetaPlaque}$
94	Abeta Disaggregation1	$\text{AbetaDimer} \xrightarrow{\text{kdisaggAbeta}} 2 * \text{Abeta}$
95	Abeta Disaggregation3	$\text{AbetaPlaque} \xrightarrow{\text{kdisaggAbeta1}} \text{AbetaDimer} + \text{disaggPlaque1}$

Figure 3.5 shows the dynamics and aggregation of tau and how phosphorylated and non-phosphorylated p53_GSK3β increases the phosphorylation process of tau be continuously aggregated to produce tangles (NFT in Figure 3.5). Table 3.3 lists all reaction to achieve tau dynamic and aggregation.

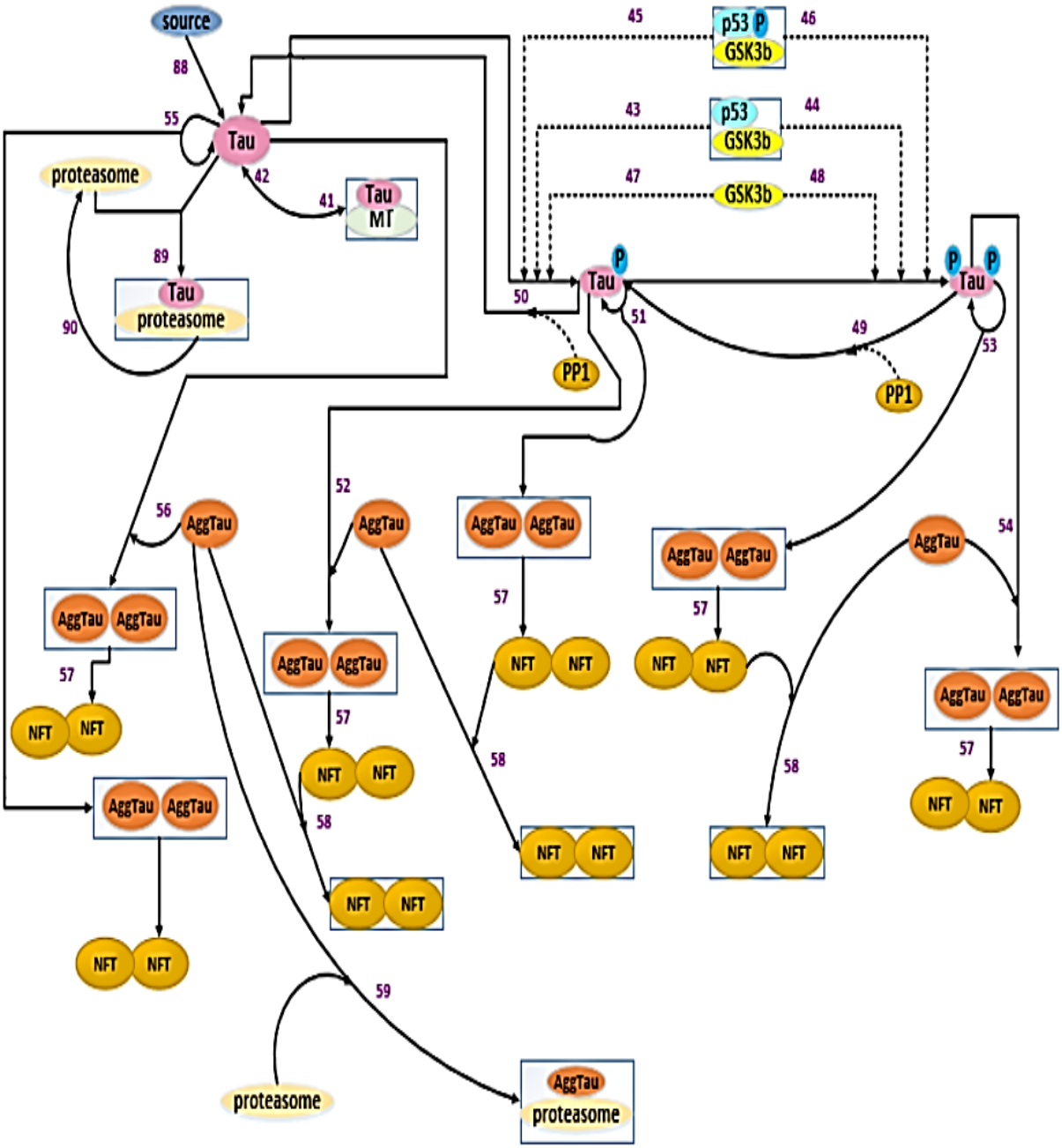

Figure 3.5: Tau dynamics and aggregation. It shows how all forms of GSK3β have the ability to increase the double phosphorylation process of tau to be aggregated to increase the production of tangles (NFT). Dashed lines from a species indicate the species is a modifier of the reaction.

Table 3.3: Reactions of tau dynamic and aggregation. Reaction numbers correspond to the numbers in the reaction table of the whole system (Table 1 in the appendices (B)).

#	Reaction name	Reaction Equation
41	Tau_MT binding	$\mathbf{Tau} \xrightarrow{\mathbf{kbinMTTau}} \mathbf{MT\_Tau}$
42	Tau_MT release	$\mathbf{MT\_Tau} \xrightarrow{\mathbf{krelMTTau}} \mathbf{Tau}$
43	Tau phosphorylation1	$\mathbf{GSK3b\_p53} + \mathbf{Tau} \xrightarrow{\mathbf{kphospTauGSK3bp53}} \mathbf{GSK3b\_p53} + \mathbf{Tau\_P1}$
44	Tau phosphorylation2	$\mathbf{GSK3b\_p53} + \mathbf{Tau\_P1} \xrightarrow{\mathbf{kphospTauGSK3bp53}} \mathbf{GSK3b\_p53} + \mathbf{Tau\_P2}$
45	Tau phosphorylation3	$\mathbf{GSK3b\_p53\_P} + \mathbf{Tau} \xrightarrow{\mathbf{kphospTauGSK3bp53}} \mathbf{GSK3b\_p53\_P} + \mathbf{Tau\_P1}$
46	Tau phosphorylation4	$\mathbf{GSK3b\_p53\_P} + \mathbf{Tau\_P1} \xrightarrow{\mathbf{kphospTauGSK3bp53}} \mathbf{GSK3b\_p53\_P} + \mathbf{Tau\_P2}$
47	Tau phosphorylation5	$\mathbf{GSK3b} + \mathbf{Tau} \xrightarrow{\mathbf{kphospTauGSK3b}} \mathbf{GSK3b} + \mathbf{Tau\_P1}$
48	Tau phosphorylation6	$\mathbf{GSK3b} + \mathbf{Tau\_P1} \xrightarrow{\mathbf{kphospTauGSK3b}} \mathbf{GSK3b} + \mathbf{Tau\_P2}$
49	Tau dephosphorylation1	$\mathbf{Tau\_P2} + \mathbf{PP1} \xrightarrow{\mathbf{kdephospTau}} \mathbf{Tau\_P1} + \mathbf{PP1}$
50	Tau dephosphorylation2	$\mathbf{Tau\_P1} + \mathbf{PP1} \xrightarrow{\mathbf{kdephospTau}} \mathbf{Tau} + \mathbf{PP1}$
51	Tau_P1 Aggregation1	$2 * \mathbf{Tau\_P1} \xrightarrow{\mathbf{kaggTauP1}} 2 * \mathbf{AggTau}$
52	Tau_P1 Aggregation2	$\mathbf{Tau\_P1} + \mathbf{AggTau} \xrightarrow{\mathbf{kaggTauP1}} 2 * \mathbf{AggTau}$
53	Tau_P2 Aggregation1	$2 * \mathbf{Tau\_P2} \xrightarrow{\mathbf{kaggTauP2}} 2 * \mathbf{AggTau}$
54	Tau_P2 Aggregation2	$\mathbf{Tau\_P2} + \mathbf{AggTau} \xrightarrow{\mathbf{kaggTauP2}} 2 * \mathbf{AggTau}$
55	Tau Aggregation1	$2 * \mathbf{Tau} \xrightarrow{\mathbf{kaggTau}} 2 * \mathbf{AggTau}$
56	Tau Aggregation2	$\mathbf{Tau} + \mathbf{AggTau} \xrightarrow{\mathbf{kaggTau}} 2 * \mathbf{AggTau}$
57	Tangle Formation1	$2 * \mathbf{AggTau} \xrightarrow{\mathbf{ktangfor}} 2 * \mathbf{NFT}$
58	Tangle Formation2	$\mathbf{NFT} + \mathbf{AggTau} \xrightarrow{\mathbf{ktangfor}} 2 * \mathbf{NFT}$
59	Proteasome Inhibition Agg Tau	$\mathbf{Proteasome} + \mathbf{AggTau} \xrightarrow{\mathbf{kinhibprot}} \mathbf{AggTau\_Proteasome}$
88	Tau Synthesis	$\mathbf{Source} \xrightarrow{\mathbf{ksynTau}} \mathbf{Tau}$
89	Tau Proteasome Binding	$\mathbf{Tau} + \mathbf{Proteasome} \xrightarrow{\mathbf{kbinTauProt}} \mathbf{Tau\_Proteasome}$
90	Tau 20SProteasome Degradation	$\mathbf{Tau\_Proteasome} \xrightarrow{\mathbf{kdegTau20SProt}} \mathbf{Proteasome}$

Glia is found in three different forms, inactive form (GliaI), partially active form (GliaM1 and GliaM2), or fully active form (GliaA). Initially, all glia are inactive. They are partially activated by immunotherapy and fully activated by antibodies. The fully active form of glia have the ability to bind to plaques for degradation. However, this binding relationship could generate ROS that increases DNA damage.

Figures 3.6 and 3.7 show their active and passive immunisation activities, respectively, and the reactions needed. Figure 3.6 shows how glia species need three different reactions and one modifier to be changed to be fully active and how they targets plaques to be degraded. This shows how antibodies (antiAb in the 3.6) take a part in the activation process of glia. Figure 3.7 displays how antibodies target not only soluble Aβ and the Aβ dimer for degradation, but also the plaques to be disaggregated and then target them to be degraded. It also shows that antibodies could be degraded to mimic diffusion from the cells.

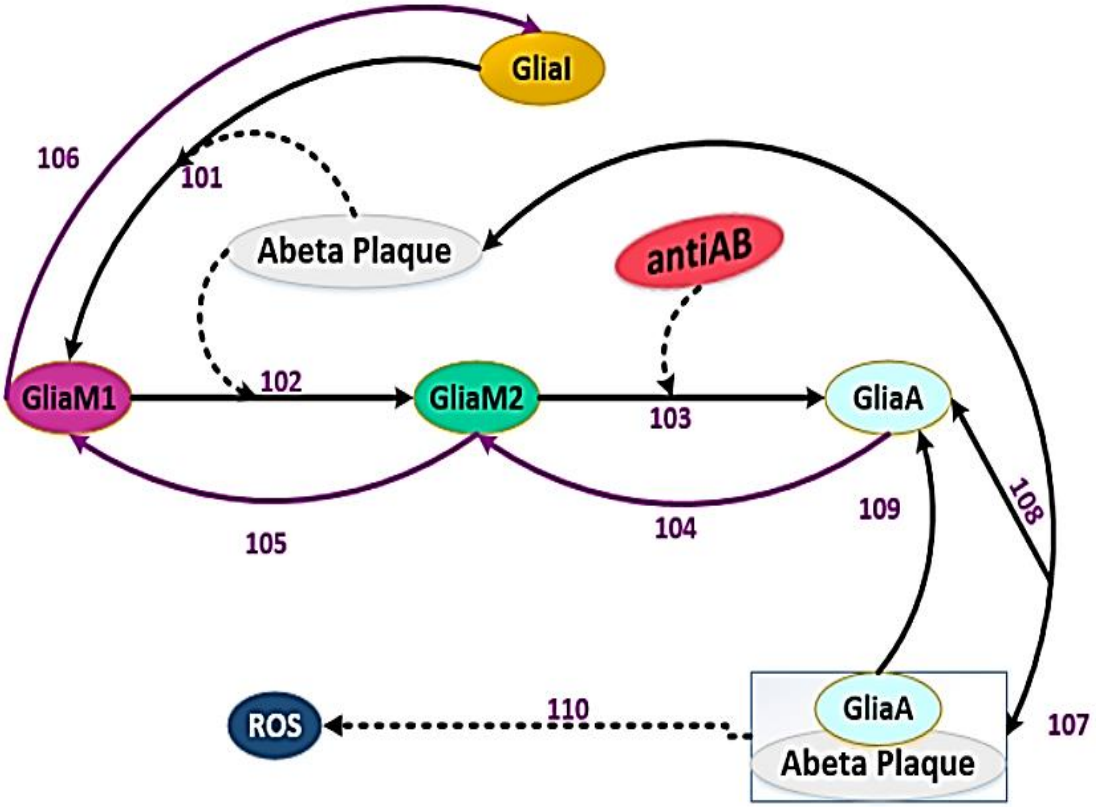

Figure 3.6: Active immunisation. It shows how the status of the glia is changed to be fully active through three different reactions and one modifier to target plaques to be degraded. Dashed lines from a species indicate the species is a modifier of the reaction.

Table 3.4: Reactions of active immunisation. Reaction numbers correspond to the numbers in the reaction table of the whole system (Table 1 in the appendices (B)).

#	Reaction name	Reaction Equation
101	Glia Activation Step1	$\mathbf{GliaI + AbetaPlaque \xrightarrow{kactglia1} GliaM1 + AbetaPlaque}$
102	Glia Activation Step2	$\mathbf{GliaM1 + AbetaPlaque \xrightarrow{kactglia1} GliaM2 + AbetaPlaque}$
103	Glia Activation Step3	$\mathbf{GliaM2 + antiAb \xrightarrow{kactglia2} GliaA + antiAb}$
104	Glia Inactivation Step1	$\mathbf{GliaA \xrightarrow{kactglia2} GliaM2}$
105	Glia Inactivation Step2	$\mathbf{GliaM2 \xrightarrow{kactglia2} GliaM1}$
106	Glia Inactivation Step3	$\mathbf{GliaM1 \xrightarrow{kactglia2} GliaI}$
107	Abeta Binding To Glia	$\mathbf{AbetaPlaqu + GliaA \xrightarrow{kbinAbetaGlia} AbetaPlaqu\_GliaA}$
108	Abeta Release From Glia	$\mathbf{AbetaPlaqu\_GliaA \xrightarrow{krelAbetaGlia} AbetaPlaqu + GliaA}$
109	Abeta Plaque Clearance By Glia	$\mathbf{AbetaPlaqu\_GliaA \xrightarrow{kdegAbetaGlia} GliaA + degAbetaGlia}$
110	ROS generation By Glia	$\mathbf{betaPlaqu\_GliaA \xrightarrow{kgenROSGlia} AbetaPlaqu\_GliaA + ROS}$

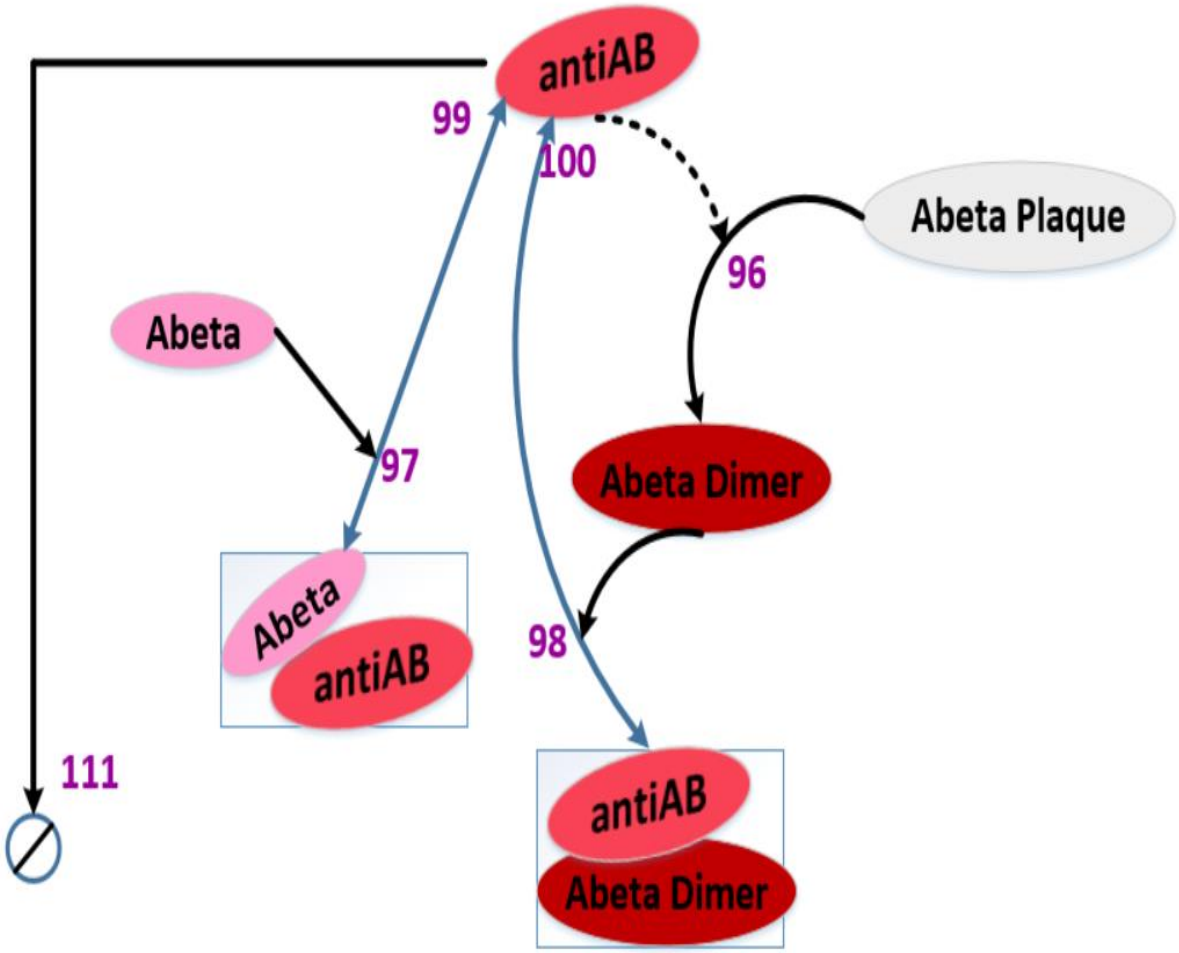

Figure 3.7: Passive immunisation. Antibodies (antiAb) are added to the system at day 4 and they are considered to be a species that has the ability to have reactions with other species. Antibodies target Aβ and Aβ_dimers (Abeta Dimer in the Figure) to be degraded and plaques to be disaggregated and then degraded. Antibodies also could be degraded to mimic diffusion from the cell. Dashed lines from a species indicates the species is a modifier of the reaction.

Table 3.5: Reactions for passive immunisation. Reaction numbers correspond to the numbers in the reaction table of the whole system (Table 1 in the Appendices (B)).

#	Reaction name	Reaction Equation
96	Abeta Disaggregation4	$\mathbf{AbetaPlaque + antiAb \xrightarrow{kdisaggAbeta2} AbetaDimer + antiAb + disaggPlaque2}$
97	Abeta_antiAb Binding	$\mathbf{Abeta + antiAb \xrightarrow{kbinAbantiAb} Abeta\_antiAb}$
98	AbetaDimer_antiAb Binding	$\mathbf{AbetaDimer + antiAb \xrightarrow{kbinAbantiAb} AbetaDimer\_antiAb}$
99	Abeta_antiAb Degradation	$\mathbf{Abeta\_antiAb \xrightarrow{kdegAbeta} antiAb}$
100	AbetaDimer antiAb Degradation	$\mathbf{AbetaDimer\_antiAb \xrightarrow{kdegAbeta} antiAb}$
111	antiAb Removal	$\mathbf{antiAb \xrightarrow{kdegAntiAb} Sink}$
110	ROS generation By Glia	$\mathbf{AbetaPlaqu\_GliaA \xrightarrow{kgenROSGlia} AbetaPlaqu\_GliaA + ROS}$

3.7 Summary

This chapter covers immunization in AD model (case study in this research). It describes all pathways that are involved to examine the relationship between Aβ and tau. Six biochemical pathways form this system. These pathways as described previously are DNA damage, p53 regulation, GSK3β activity, Aβ production and aggregation, tau dynamics and aggregation, and active and passive immunisation. The first four pathways are involved in the examination process while active and passive immunization pathways show how antibodies reduce the activity of Aβ and p53- GSK3β by reducing the level of ROS.

In response to immunization at day #4, the model predicts that: (1) the level of plaques is inhabited only at day # 4 while it starts to increase again from day # 5 to the end of the simulation, (2) the pool of soluble Aβ is reduced only by a small amount during day # 4 and then one day after immunization, Aβ starts to rise again, (3) the activity of p53-GSK3β reduced since antibodies target ROS to be reduced which results decreasing in the level of p53 and prevent its binding with GSK3β and (4) the levels of phospho-tau is instantly reduced after the addition of antibodies and, thereafter, remained at the appropriate constant levels. This is because the level of ROS is reduced after the clearance of plaques. The reduction in the level of phospho-tau agrees with neuropathological data.

It has been found that it is more appropriate to use a stochastic approach to model this system because:

1- Many of the mechanisms involved in protein aggregation are inherently random. For example, Proctor et al. (2013) mentioned that the fully active form of glia has the ability to bind to plaques for degradation and they said that the binding relationship might result in more ROS.
2- The number of molecules involved in many of reactions in this systems are small. Therefore, stochastic approaches are more appropriate to deal with a small number of molecules.

Chapter 4

Methods and Algorithms

This chapter covers all methods and algorithms that are used to stochastically model and investigate immunisation in AD.

4.1 Mapping Reduction Method (MRM)

MRM is an implementation tool that is used to process large data sets on a single multi-processor computer (using threads or processors) (Dean & Ghemawat, 2008), a cluster (Barroso, Dean, & Holzle, 2003), or a grid (Bent, Thain, Arpaci-Dusseau, Arpaci-Dusseau, & Livny, 2004). The MRM is also defined as a framework that is used for parallel problems to be processed across large datasets using a large number of nodes that work together and are seen as a single system. Each node performs the same task and is controlled and scheduled by software (Dean & Ghemawat, 2008; Lämmel, 2008).

A single multi-processor computer is able to employ multiple threads or processors to work in a parallel manner on the same machine (Dean & Ghemawat, 2010). A computer cluster is composed of a set of loosely, or tightly, connected computers on the same local network and using the same hardware. A computer grid is also a set of connected computers but these computers are not only shared over geographically distributed systems, but also use heterogeneous hardware (Mann, Trasatti, Carlozzi, Ywoskus, & McGrath, 2003).

Implementing MRM using a single machine is less complex than using a cluster or a grid because the input data is split only among worker threads that all reside on the same machine and typically use the same data store (Lattanzi, Moseley, Suri, & Vassilvitskii, 2011).

Additional complexity is added into the process when multiple computers are used to run MRM because the input data have to be split among all computers within the cluster using a master node (McKenna et al., 2010). Another challenge for using a cluster is that different physical memories on different machines have to be used

to save data from the reduction method (Lv et al., 2010). In other words, more routing needs to be done to get all reduction results to reside on one physical machine. A cluster is needed to implement MRM especially when the input and output data are too large to fit into the memory of a single computer (Ferreira Cordeiro et al., 2011).

Many programming platforms support thread-safe objects that are easily used to produce mapping reduction style programs (Guzev, 2008). Visual Studio (mainly C# paradigm) has a good ability to support this process since there are many features and classes used to successfully achieve mapping reduction processing (Groot & Kitsuregawa, 2010).

In a computer system, a thread pool is a software pattern used to achieve concurrency of execution in a computer program (Sturm, 2011). Multiple threads are maintained by the thread pool to complete different tasks in a concurrently executed manner (Benton, Cardelli, & Fournet, 2002). Maintaining a pool of threads not only increases the performance of the whole system, but also avoids latency in its execution. The size of a thread pool depends on the number of tasks needing to be completed in a concurrent manner. The main advantage of creating a thread pool over creating a thread for each task is that thread creation and destruction overheads are restricted to the initial creation of the pool. This may increase the performance level since creating and terminating threads is an expensive process in terms of time (Loidl, 2012). MRM is combined with GSSA to increase the performance of GSSA for generating a single realization by selecting multiple reactions at each time step.

4.2 MRM with GSSA

The GSSA and its variants have the ability to advance the state of the system under study by executing one reaction at a time. In cases where the system under study involves a large number of reactions, the simulation of this system becomes prohibitively expensive. Also, the GSSA and its variants totally ignore the concurrency feature that needs to be taken into consideration in modelling biochemical systems. The computational intractability of the GSSA has been

addressed in different ways (Cao et al., 2006; Gibson & Bruck, 2000; Gillespie, 1977; Madani et al., 2006; McCollum et al., 2006) , as described in Chapter 2.

Here, we propose a novel variant of the GSSA to not only address its computational intractability, but also include a concurrency feature by using MRM on a single multiprocessor computer to advance the system by several reactions. Here, we are not accelerating GSSA using a collection of threads to be executed synchronously to generate multiple independent trajectories, instead, we target a single run to be accelerated by advancing the system through several reactions at each time step. MRM/GSSA is divided into four steps. These steps are initialization, election (mapping), selection (reduction), and updating the system. These steps are summarized as follow.

Initialization step

1- Create a thread pool that contains T numbers of threads,

$$\mathbf{T = The\ number\ of\ reactions\ in\ the\ system}$$

The number of threads in the thread pool is set to be equal to the number of reactions for two reasons.

- All reactions in the system might have the ability to run together.
- Creating and terminating threads as needed is considered to be an expensive process in terms of time.

2- Initialize the biochemical system -

- The number of species (S_i)
- The molecules (n) for each species in the system
- Chemical reactions R_m
- Reaction rates (k_j)
- Set $t = 0$.
- Calculate the propensity function for each reaction $\mathrm{a_j = h_j . K_j}$

3- Create Election_index_array and Election_time_step_array to store the indexes and time steps, respectively that return from threads.

4- Create Selection_index_array and Selection_time_step_array to store the indexes and time steps, respectively, after the selection step.

Election step

1- Elect M threads to run GSSA

$$\mathbf{M = The\ number\ of\ reactions\ that\ have\ propensity\ fucntions > 0}$$

2- Each thread returns an index and a time step.

3- Store the index of the next M reactions to occur in the Election_index_array and M time steps in the Election_time_step_array.

Selection step

1- Test the eligibility of each reaction as follows:

- If all reaction indexes in the Election_index_array are different, all reactions are eligible for the selection step.
  A. Transfer the next M reactions from the Election_index_array to the Selection_index_array
  B. Transfer M time steps from the Election_time_step_array to the Selection_time_step_array
- If some reaction indexes are the same (for example, L threads return the same index, j).
  - ❖ Transfer all the different indexes $(M - L)$ next reactions to occur from the Election_index_array to the Selection_index_array
  - ❖ Transfer time steps for all different indexes from the Election_time_step_array to the Selection_time_step_array
  - Check the number of molecules for each species in reaction j
  - If the number of molecules for each participant species in reaction j is enough to run reaction j L times, reaction j is eligible for the selection step L times. So,
    - ❖ Transfer the L reaction j from the Election_index_array to the Selection_index_array
    - ❖ Transfer the L time steps for reaction j from Election_time_step_array to the Selection_time_step_array
  - Else

- ✓ Set x= the number of molecules for a species in reaction j that has the smallest number of molecules.
- ✓ Number j of eligible for the selection step = $x - L$
- ✓ Select indexes of j that have a large time step.
- ✓ Update the Selection_index_array.
- ✓ Update the Selection_time_step_array.

Updating the system

1- Update the number of molecules

❖ Update the molecules in the number of species in all the next reactions to occur in the Selection_index_array

2- Update the time of the system

❖ If Selection_time_step_array. length =1

- ✓ $\mathbf{t} = \mathbf{t} + \mathbf{Selection\_time\_step\_array}[\mathbf{0}]$

❖ If Selection_time_step_array. length =2

- ✓ $\mathbf{t} = \mathbf{t} + \mathbf{Selection\_time\_step\_array}[\mathbf{0}] + \mathbf{Selection\_time\_step\_array}[\mathbf{1}]$

❖ If Selection_time_step_array. length > 2

- ✓ $\mathbf{t} = \mathbf{t} + \mathbf{The\ largest\ three\ time\ steps\ in\ the\ Selection\_time\_step\_array}$

Figure 4.2 provides an illustration of the proposed method (MRM/GSSA). Algorithm 4.1 provides the pseudo code of MRM/GSSA.

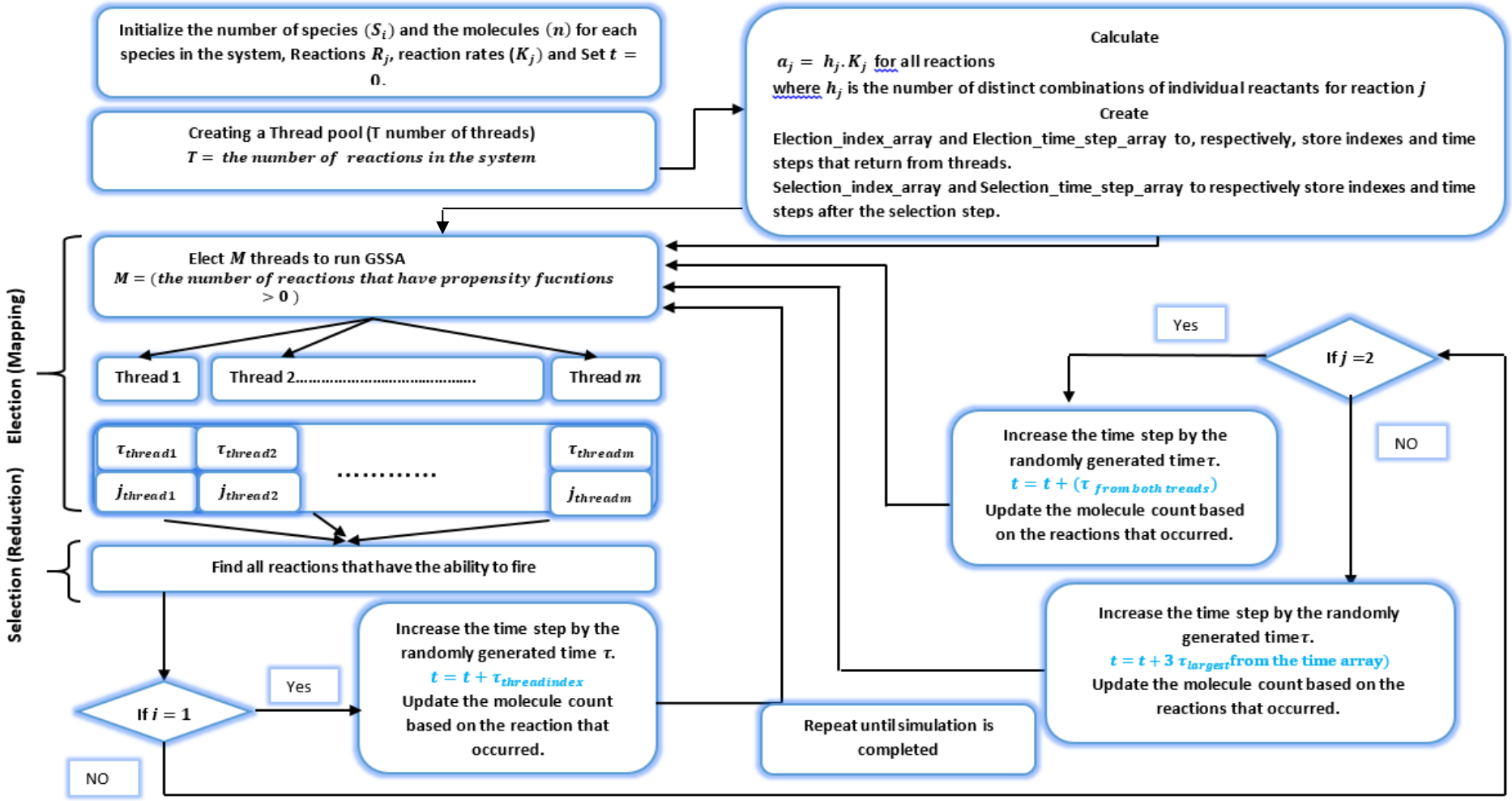

Figure 4.1: Schematic of MRM/GSSA.

Algorithm 4.1: MRM/GSSA

DEF initialization step (TP, S_i, n, R_j, K_j, t, τ, a_j,Va_j EIA,ETA,SIA,STA)

- **TP**: **Threads pool** (**T threads**)
- S_i: **Species in the system** [**array of double**]
- **n**: **Number of llmoelcues of each species**[**array of double**]
- R_j: **Reactions in the system** [**array of double** [**T**]]
- K_j: **Reactions rates** [**array of double**]
- **t**: **time of the system initially is equal to zero**
- **τ**: **time step initially is equal to zero**
- a_j: **propensity function** [**array of double**]
- Va_j: **propensity function** > 0 [**array of double**]
- **EIA**: **Election_Index_array** [**array of double**[Va_j]]
- **ETA**: **Election_time_step_array**[**array of double**[[Va_j]]
- **SIA**: **Slection_Index_array** [**array of double**]
- **STA**: **Slection_time_step_array**[**array of double**]

DEF Election (Mapping) step (*ET*)

- **ET**: **Elected threads to run GSSA** [**array of double**[[Va_j]]
- **for** (**int i** $=$ **0**; **i** $<$ Va_j; **i** $++$)
- {
- **Election_Index_array** $=$ **reactin index from thread_i**
- **Election_time_step_array** $=$ **time step from thread_i**
- }

DEF Selection (Reduction) step

- **for**(**int w** $=$ **0**; **w** $<$ **Election_Index_array**; **w** $++$)
- {
- **if**(**all index in the Election_Index_array are equal**) **then**
- {
- **Slection_Index_array**[**w**] $=$ **Election_Index_array**[**w**];
- **Slection_time_step_array** $=$ **Election_time_step_array**[**w**];
- }
- **else**
- {
- **List_index_forsame_index**;
- **List_index_fordifferent_index**;
- **List_Time_forsame_index**;
- **List_Time_fordifferent_index**;
- **for**(**int check** $=$ **0**; **check** $<$ **Election_Index_array**; **check** $++$)
- {
- **Check reaction_index** $=$ **Election_Index_array**[**check**];
- **for**(**int w1** $=$ **0**; **w1** $<$ **Election_Index_array**; **w1** $++$)
- {
- **if** (**Check reaction_index** $=$ **Election_Index_array**[**w1**];
- {
- **add**(**Election_Index_array**[**w1**]);

- List_Time_forsame_index. add(Election_time_step_array[w1]);
- }
- Else
- {
- List_index_for different_index. add(Election_Index_array[w1]);
- List_Time_for different_index. add(Election_time_step_array[w1]);
- all reactions in the List_index_ for different_index move to the Slection_Index_array;
- all time steps in the List_Time_ fordifferent_index move to the Slection_time_step_array;
- }}}
- Set x = the number of molecules for a species in reaction j that has
- the smallest number of molecules in the system
- if(x >= the number of indexes in List_index_for same_index)
- {
- all reactions in the List_index_forsame_index move to the Slection_Index_array;
- all time steps in the List_Time_forsame_index move to the Slection_time_step_array;
- }
- else
- {
- Select indexes of j that have large time step;
- Update the Selection_index_array;
- Update the Selection_time_step_array;
- }

DEF Updating the system

- Update number of species of molecules in all of the next reactions to occur inthe Selection_index_array
- If Selection_time_step_array. length =1
- t = t + Selection_time_step_array[0]
- If Selection_time_step_array. length =2
- t = t + Selection_time_step_array[0] + Selection_time_step_array[1]
- If Selection_time_step_array.length > 2
- t = t + The largest three time steps in the Selection_time_step_array

4.2.1 Test and validation of MRM/GSSA

In order to not only test, but also verify the quality of MRM/GSSA, it is used to model the immunisation in AD model that is described in Chapter 3. It has been found that MRM/GSSA is a useful way to model biochemical systems when number of reactions with propensity functions greater than zero are quite large. This allows MRM/GSSA to employ large numbers of threads to run GSSA. Therefore, the chance for multiple reactions to be eligible for the selection step is high. MRM/GSSA is compared with GSSA and the modified tau-leap method from different angles, results in term of stochasticity, and performance in term of CPU time and implementation difficulties. The result of this comparison is discussed in section 4.5. MRM/GSSA is used with LSA and GSA to stochastically investigate the behaviour of the immunisation in AD model in response to parameters perturbation. LSA and GSA discussed in Chapter 5 and 6.

4.3 LSA

In this research, LSA is performed to deterministically and stochastically investigate the behaviour of the most important players in the system (immunization in AD) against parameter perturbations, one-at-a time, using ODEs and MRM/GSSA.

The finite difference approximation method is used to compute the sensitivity analysis of the ODE and MRM/GSSA models, these methods are shown in Figures 4.3 and 4.4, respectively, and the result of the LSA using the ODE and MRM/GSSA models is discussed in Chapter 5.

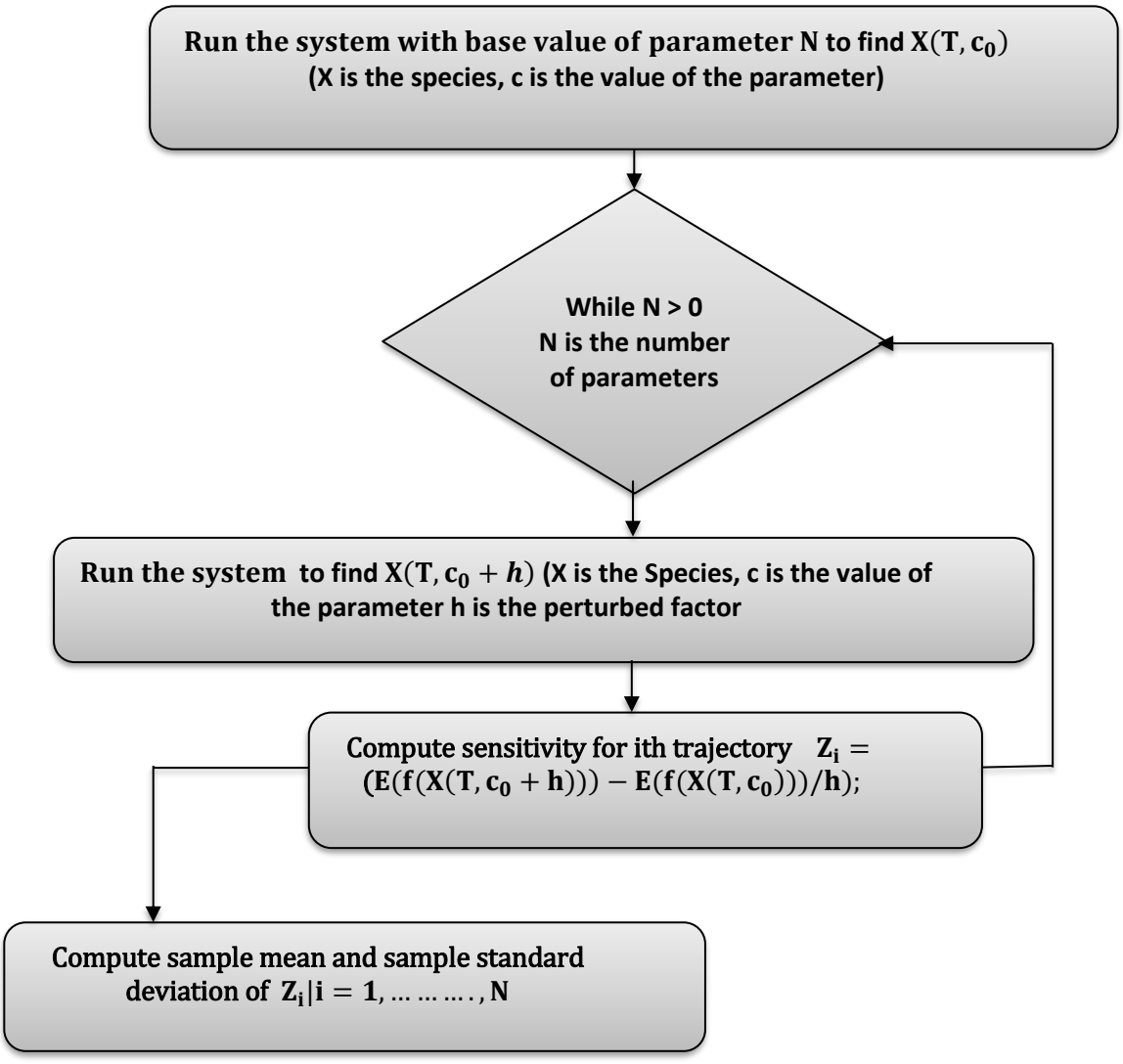

Figure 4.2: Steps of the finite difference method for calculating LSA using ODE models

In Figure 4.3 we show how the finite difference method is stochastically used to estimate the sensitivity of the parameters using MRM/GSSA in conjunction with the Common Random Number (CRN). The implementation of CRN to compute the

sensitivity with MRM/GSSA is achieved by using the same stream of uniform random numbers that need to be generated for selecting the next reaction and time step from each thread at each step. CRN in conjunction with MRM/GSSA reseeds the random number generator prior to computing $X(T, c_0 + h)$ with the same initial seed used to simulate $X(T, c_0)$ at each time step.

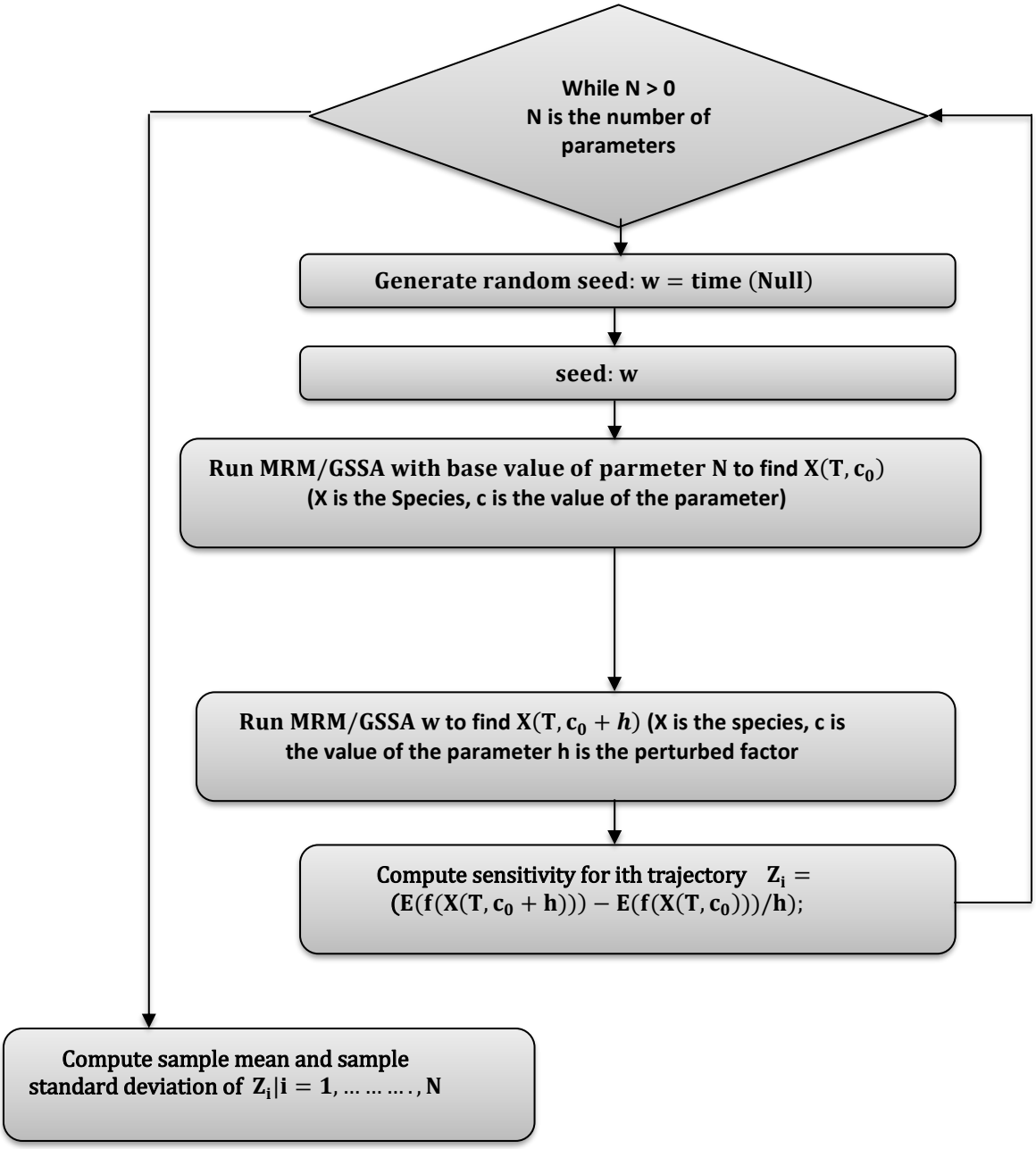

Figure 4.3: Steps of the finite difference method for calculating LSA using MRM/GSSA

The seed function is employed to ensure that the random numbers used when parameters are not perturbed are also used when parameters perturbed are (Rathinam et al., 2010).

4.4 GSA (LHS/PRCC)

LHS/PRCC is used in this research to assess not only the ODEs model of immunisation in AD, but also the MRM/GSSA over a global parameter space. See Chapter 2 for more details about LHS/PRCC. Several functions are implemented to perform GSA and interpret the results with LHS/PRCC. Figure 4.5 shows all these functions and how these functions are connected to each other. Table 4.1 shows the function names and their descriptions.

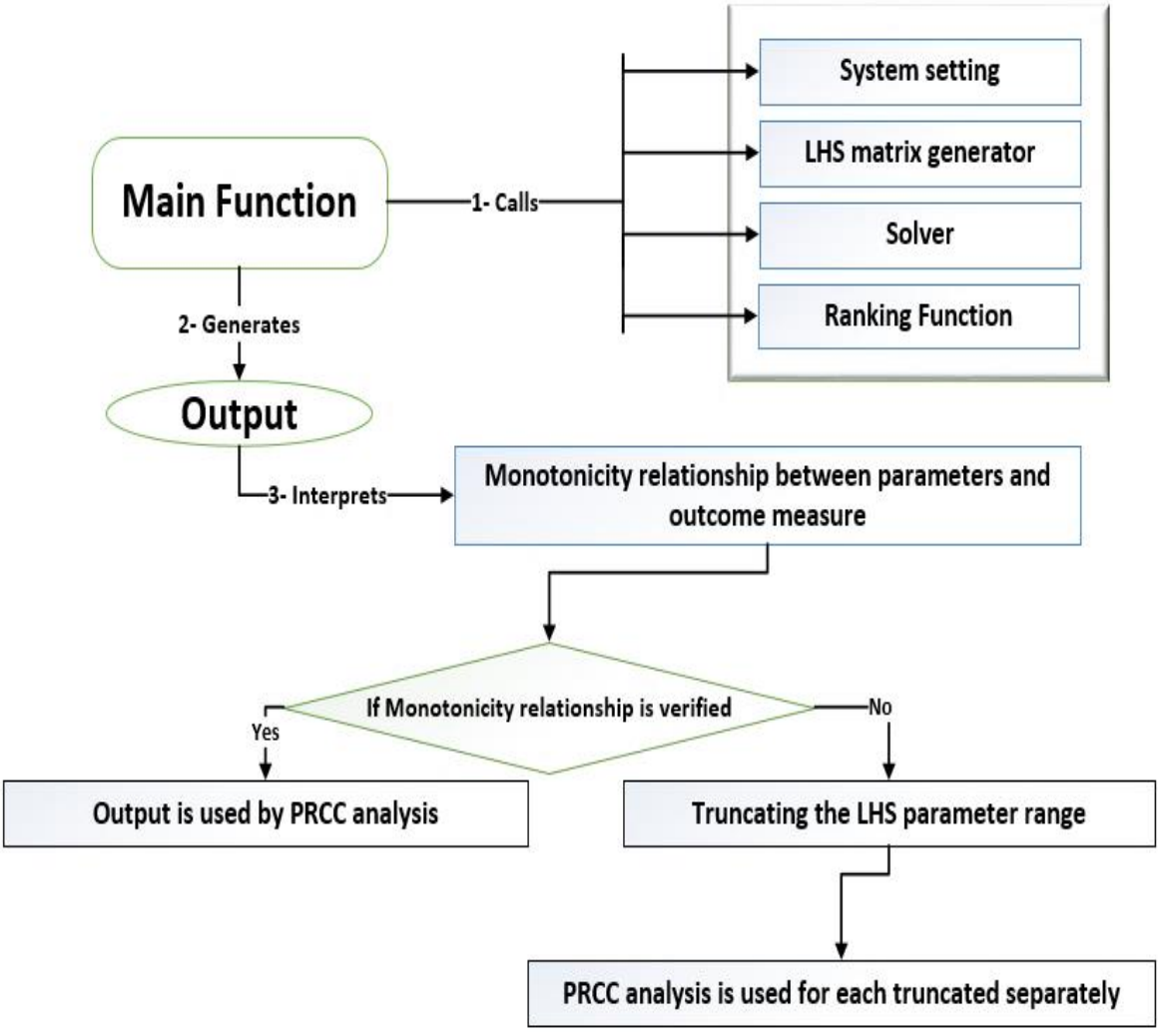

Figure 4.4: LHS/PRCC diagram.

To investigate the behaviour of a biochemical system using LHS/PRCC tool, as shown in Figure 4.4, there are different functions needed to be performed.

The main function calls four different sub functions to generate output to be used by PRCC analysis. System setting is used to define: (1) species and their initial values; (2) parameters and their baseline values; (3) time span of the simulation; (4) events; and (5) minimum and maximum values of each parameter for generating the LHS matrix. LHS matrix generator is used to generate the LHS parameters using the minimum and maximum values of each parameter. Assume a system includes M parameters. A probability distribution is assigned to each parameter. Each distribution is divided into N equiprobable regions, where N the required number of samples, and these regions are then sampled with no replacement. Thus the parameter space for the LHS parameters has a dimension of length M with each dimension specifying an uncertain parameter vector of length N. Solver runs the simulation using the LHS parameters combination. Ranking function is used to rank the LHS matrix and then the matrix for the outcome measure using a sort routine.

The monotonic relationship between the outcome measure and the LHS parameters is verified by picking separately each parameter's row form the LHS matrix and run simulations using its values from that row and the baseline values for all other parameters. This results in M simulations for this monotonicity test for each parameter.

If the monotonic relationship is verified, output is used by PRCC analysis to measure the strength of the relationship between the LHS parameters and outcomes. PRCC is used to classify the most important parameters that contribute most uncertainty to model predications. If non-monotonic regions exist over the whole interval for any of the LHS parameters, we consider truncating the range and looking at each truncated separately.

These steps are described using an example form immunization in AD model in Chapter 6. Results of LHS/PRCC for immunization in AD are also shown in Chapter 6.

4.5 An Analogy for MRM/GSSA and the Modified Tau-leap Method

In this research, immunization in AD model is modelled using four different approaches. These approaches are ODEs, GSSA, MRM/GSSA and the modified tau-leap method. The purpose of using ODEs is to be used with LSA and GSA (the results are presented in Chapters 5 and 6, respectively).

To validate MRM/GSSA, it is compared with GSSA and the modified tau-leap method. The main difference between GSSA and the other two approaches is that GSSA advances the state of the system by executing one reaction at a time while MRM/GSSA and the modified tau-leap method advance the system state by several reactions within a calculated time step, τ. Therefore, these two methods are mainly used to accelerate a single run of GSSA and explicitly include the concurrency feature.

However, MRM/GSSA and the modified tau-leap are different not only from assumptions that allow the system state to be advanced by several reactions, but also from the way of calculating the time step, τ. These two approaches are compared in this section from different angles, with the results in term of stochasticity depending on the GSSA results, performance in term of CPU time, reliability and implementation difficulties.

4.5.1 Results

Noise (known stochasticity or randomness) is one of the main biochemical systems features needed to be represented when these systems are stochastically modelled for better understanding of the behaviour of biochemical systems. Thus, when MRM/GSSA is developed, the stochastic feature is taken into consideration to be represented even we advance the system by several reaction at calculated time step, τ. In this research we verified that MRM/GSSA has more ability to represent the stochasticity feature than the modified tau leap method by comparing their results with GSSA.

Figure 4.5 (A) shows the average behaviour of p53 from 200 runs from GSSA (red line), MRM/GSSA (blue line) and the modified tau-leap method, where n is chosen to be 10, (black line). The value of n is an integer, but it might be anywhere

between 2 and 20. The value of n is used to determine the number of reactions that classified to be critical reactions.

At day # 4 (vertical line in Figure 4.5), the values of mean for p53 from MRM/GSSA, GSSA and the modified tau-leap method are 124.5423, 117.0693 and 111.8416, respectively. To check how each approach represents the stochasticity, the standard deviation (σ) is calculated at day #4 to measure how other values are spread around the mean μ for all approaches. It has been found that GSSA is more able to represent stochasticity feature than MRM/GSSA and the modified tau-leap method. MRM/GSSA shows that the values of the data set of p53 at day #4 are more widely spread than the modified tau-leap method since MRM/GSSA demonstrates larger standard deviation than the modified tau-leap as shown in Table 4.1.

Table 4.1: The mean and the standard deviation from MRM/GSSA, GSSA and the modified tau leap method for p53 at day #4.

	MRM/GSSA	GSSA	The modified tau-leap method
Mean (μ)	124.5	117.0	111.8
standard deviation (σ)	53.8	58.0	31.5

Table 4.1 shows that MRM/GSSA has the ability to represent more variance than the modified tau-leap method since the standard deviation of the mean at day # 4 is 53.8 while it is 31.5 from the modified tau-leap method. Figure 4.6 shows mean and (+/- 1 S.D.) of 200 run at day # 4 for p53 from all MRM/GSSA, GSSA and the modified tau-leap method

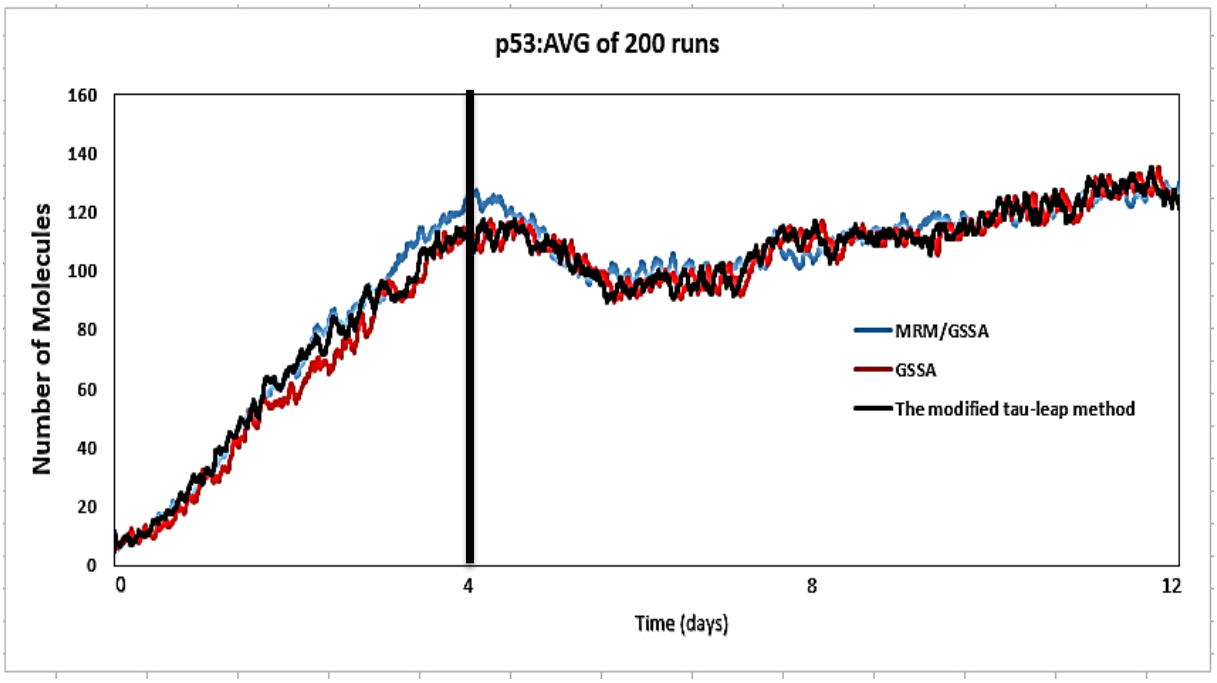

Figure 4.5: Average of 200 runs for p53 from MRM/GSSA, GSSA and the modified tau-leap method. GSSA advances the system by only one reaction at each time step while MRM/GSSA and the modified tau-leap method advance the system by several reactions. MRM/GSSA and the modified tau leap method show good representation of the behaviour of p53 comparing to GSSA even they advance the system by several reactions. At day # 4, vertical line, we compare between MRM/GSSA and the modified tau leap method in term of stochasticity depending the GSSA result. Results shown in Table 4.1.

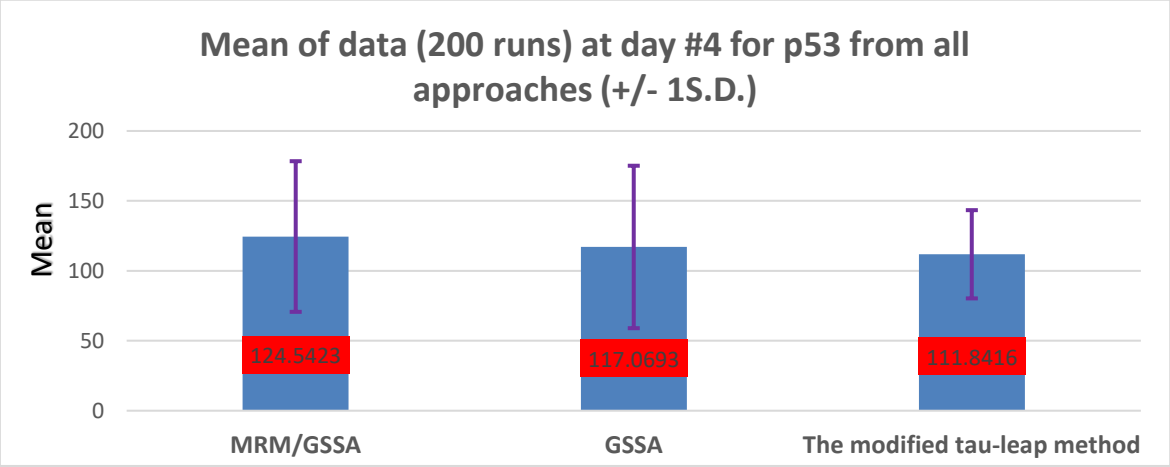

Figure 4.6: Mean of data (200 runs) at day #4 for p53 from MRM/GSSA, GSSA and the modified tau-leap method. Approaches name are labelled under columns, values of mean are shown in the red rectangle in each column. It could be clearly seen that MRM/GSSA shows better representing of variance than the modified tau-leap method depending on the result of GSSA.

4.5.2 Performance and Reliability

In MRM/GSSA, all reaction channels R_j for which $a_j(x) > 0$ that are eligible for the selected step are saved in a list. The system state is advanced by executing all these reactions where each reaction is executed just once.

In the modified tau-leap method, reaction channels, R_j, for which $a_j(x) > 0$ are classified into two different types, critical and non-critical reactions. Critical reactions: namely, those reaction channels for which $L_j \leq n$ (L_j is the maximum number of permitted firings of R_j and n is an integer value, but it might be anywhere between 2 and 20). The system state is advanced by executing a maximum of one reaction channel from the critical reactions list and all reaction channels from non-critical reactions' list. Each reaction channel in the non-critical reaction is executed k times (k is a sample of the Poisson random variable).

We use GSSA, MRM/GSSA and the modified tau-leap method to run the immunization in AD model to produce just one realization of the system for 10 times. The value of n in the modified tau-leap method is chosen to be 2, 10 and 20 respectively.

As shown in Table 4.2 (excluding rows 6 and 9) MRM/GSSA and the modified tau-leap method are much faster than GSSA at all the 10 times. It could be clearly seen that both of them need less than half of the time required by GSSA. Therefore, MRM/GSSA and the modified tau-leap method show good performance in term of time comparing to GSSA.

The modified tau-leap method shows better performance than MRM/GSSA but they still comparable in terms of time since it has been found that the modified tau-leap method only needs around 92% of the time required by MRM/GSSA.

Reliability is also another measure that needs to be taken into consideration for using the modified tau-leap method and MRM/GSSA. As shown in Table 4.2 (rows 6 and 9), when the modified tau-leap method assigns 2 for n, it went through a deadlock situation. The deadlock situation here means that the simulation went through an infinite loop. It happened because at each iteration, at least one

reaction should be located in the critical reaction list to avoid dividing by zero (step 5 in Figure 2.2 Chapter 2, compulsory step).

Therefore, the reliability of the modified tau-leap method is less MRM/GSSA because there is no way to determine the value of n, the value of n is arbitrary chosen between 2 and 20. To avoid a deadlock situation that could happened, the system under study should be manually analysed before modelling to determine n that suites the system. This results more time needed to produce results for the modified tau-leap method. Also, the modified tau leap method has no way to dynamically changing the value of n depending on the state of the system, n sets to the constant over the whole simulation time (Cazzaniga, Pescini, Besozzi, & Mauri, 2006).

Table 4.2: CPU time. GSSA, MRM/GSSA and the modified tau-leap method (n=2, 10 and 20). The average CPU time for MRM/GSSA and the modified tau-leap method is less than half of that for the GSSA.

#	GSSA	MRM/GSSA	The modified Tau-leap method		
			n		
			2	10	20
1	11m.23s.233ms	4m.55s.22ms	3m.41s.123ms	3m.23s.234ms	3m.41s.231ms
2	10m.55s.723ms	5m.01s.766ms	3m.52s.231ms	4m.17s.119ms	3m.17s.111ms
3	12m.42s.341ms	4m.22s.211ms	4m.12s.564ms	3m.55s.861ms	3m.51s.389ms
4	11m.45s.22ms	5m.14s.2ms	3m.23s.333ms	2m.13s.345ms	3m.37s.258ms
5	9m.59s.721ms	4m.57s.123ms	4m.01s.786ms	3m.22s.12ms	3m.58s.121ms
6	12m.1s.113ms	3m.59s.704ms	Deadlock	3m.56s.312ms	4m.01s.456ms
7	12m.15s.517ms	5m.44s.1ms	3m.22s.129ms	4m.12s.763ms	3m.49s.721ms
8	11m.12s.122ms	3m.59s.517ms	3m.45s.342ms	3m.11s.179ms	3m.23s.345ms
9	11m.51s.21ms	4m.52s.311ms	Deadlock	4m.02s.812ms	3m.55s.765ms
10	10m.56s.221ms	5m.10s.221ms	3m.55s.12ms	3m.29s.119ms	3m.39s.234ms
AVG	11m.36s.303ms	4m.38s.288ms	3m.35s.417ms	3m.49s.378ms	3m.27s.512ms

4.5.3 Implementation

Visual Studio (C# 2017) is used to implement all approaches used in this research to model immunization in AD. The structure of the code for GSSA, MRM/GSSA and the modified tau leap method is divided into three parts, as shown in Figure 4.7.

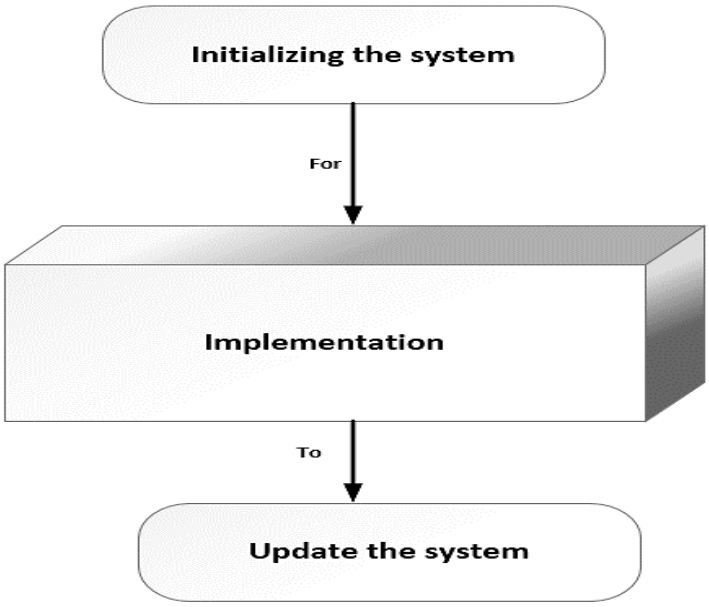

Figure 4.7: General structure of coding an algorithm. The system needs to be initialized before the implementation step updates the system

Initializing and updating the system in both algorithms are the same since both are used to model the system. During the implementation, it is found that MRM/GSSA is much easier to implement than the modified tau-leap method for different reasons.

1- Only three steps are needed to be implemented in MRM/GSSA (election, selection and calculating the time step). In the modified tau-leap method, eight steps are needed to be implemented. These steps are shown in Figure 2.2.
2- Only one summation mathematical equation needs to be calculated to compute time step, τ, while the modified tau-leap method needs three mathematical equations and a logical expression to calculate the final value of τ. The complexity of the code is increased when there are many mathematical equations.

3- Dividing reactions into critical and non-critical is like dealing with a black box because at each iteration, the status of these reactions could be changed from critical to non-critical or vice versa depending on the state of the system. This increases the complexity of the code because each reaction needs to be checked at each iteration.
4- Reject, accept and undo are used in the modified tau-leap method, these concepts are not particularly easy to implement.
5- The whole structure of MRM/GSSA is undertaken by coding 3313 lines in C# while 10338 lines are needed to implement the whole structure of the modified tau-leap method.

4.6 Specifications

The basic information about the computer that has been used to run all approaches and algorithms is listed in Table 4.3.

Table 4.3: Computer specifications.

Windows edition	10
Processor	Intel(R) Core(TM) i5-6300U CPU@2.40GHz 2.50 GHz
Installed memory (RAM)	8.00 GB
System type	64-bit Operating System, x64-based processor
Programming language	.Net (C# 2017)

4.7 Summary

This chapter covers the MRM/GSSA that is used to model immunization in AD model. It also described algorithms that are used to stochastically and deterministically perform LSA. The finite approximation method is used to deterministically perform LSA using ODEs and stochastically using MRM/GSSA in conjunction with CRN.

LHS/PRCC is described in this chapter since it is used to stochastically and deterministically investigate the behaviour of the model in response to parameters perturbation one-at-a time and over the space of the parameters, respectively.

Results of LSA and GSA are discussed in Chapters 5 and 6, respectively.

This chapter also describes how MRM is combined with GSSA to accelerate a single run of GSSA by advancing the system with several reactions at each time step and explicitly include the concurrency feature. The combination of MRM with GSSA is validated by comparing it with not only GSSA, but also the modified tau leap method (one of the fastest version of GSSA).

Chapter 5

Local Sensitivity Analysis of Immunization in an AD model

5.1 Overview

In order to examine the behaviour of immunisation in AD model against parameter perturbation, LSA is performed using not only ODEs, but also MRM/GSSA. In other words, the behaviour of the system is deterministically and stochastically investigated in response to parameters perturbation. All parameters in this system are perturbed to 50% and 200% of their basal values, one at a time to:

1- Determine the maximum and minimum ranges for each parameter.
2- Identify the most important parameters that contribute most of the variation.
3- Categorize the most important parameters that target the level of plaques and tangles to be changed since these species highly contribute to AD.
4- Identifying pathways that are not dramatically affected when parameters are perturbed.
5- Classify the most sensitive species in the system. LSA focuses on the main species in the system to be classified since this system has 69 species and it is hard to track the behaviour of all these species in response to parameter perturbations. The main species that are selected and their pathways are listed in Table 5.1.
6- Determine when a species is more sensitive to a parameter's perturbation.

The minimum value of parameters perturbation is chosen to be 50% of their basal value because parameters value are going to be very small if they are taken less than 50%. Table 5.2 lists all parameters in the system, their description, their basal values, and minimum and maximum values perturbation values.

Table 5.1: Selected species and their pathways.

Species	Pathway
p53	p53 regulation
ATMA	DAN damage pathway
p53_GSK3β	GSK3β activity
Aβ	Aβ production and aggregation
plaques	Aβ production and aggregation
tangles	tau dynamics and aggregation
GliaA	immunisation pathway

The species in Table 5.1 are selected to be investigated in response to parameters perturbation for different reasons. Firstly, Aβ, plaques and tangles are selected since they are considered to be the most important species that contribute AD. Secondly, Proctor et al., (2013) classified p53, ATMA and p53_GSK3β to be the main species respectively in p53 regulation, DAN damage pathway and GSK3β activity. p53 regulation, DAN damage pathway and GSK3β activity are classified to be the key pathways involved in the mechanisms that link Aβ and tau. GliaA is the main species that is used in the immunization pathway. Also, it has been found that these species take a prat of 52 reactions (around half reactions of the system), therefore, they have the most contribution of the behaviour of the system.

Table 5.2: parameters of the system, description, base values, minimum and maximum values.

Index	Rate constant ($\mathbf{k_s}$)	Description	Base value	Minimum value	Maximum value
1	kactATM	ATMactivation	0.0001	5.00E-05	0.0002
2	kactDUBMdm2	p53Deubiquitination3	1.00E-07	5.00E-08	2.00E-07
3	kactDUBp53	Mdm2PDeubiquitination4	1.00E-07	5.00E-08	2.00E-07
4	kactDUBProtp53		0.0001	5.00E-05	0.0002
5	kactglia1	GliaActivationStep1	6.00E-07	3.00E-07	1.20E-06
6	kactglia2	GliaActivationStep3	6.00E-07	3.00E-07	1.20E-06
7	kaggAbeta	Abetaaggregation1	3.00E-06	1.50E-06	6.00E-06
8	kaggTau	Tauaggregation1	1.00E-08	5.00E-09	2.00E-08
9	kaggTauP1	TauP1Aggregation1	1.00E-08	5.00E-09	2.00E-08
10	kaggTauP2	TauP2Aggregation1	1.00E-07	5.00E-08	2.00E-07
11	kbinAbantiAb	Abeta_antiAbBinding	1.00E-06	5.00E-07	2.00E-06

12	kbinAbetaGlia	AbetaBindingToGlia	1.00E-05	5.00E-06	2.00E-05
13	kbinE1Ub	E1UbBinding	0.0002	0.0001	0.0004
14	kbinE2Ub	E2UbBinding	0.001	0.0005	0.002
15	kbinGSK3bp53	GSK3p53Binding	2.00E-06	1.00E-06	4.00E-06
16	kbinMdm2p53	p53Mdm2Binding	0.001155	0.000578	0.00231
17	kbinMTTau	TauMTbinding	0.1	0.05	0.2
18	kbinProt	Mdm2ProteasomeBinding1	2.00E-06	1.00E-06	4.00E-06
19	kbinTauProt	TauProteasomeBinding	1.93E-07	9.63E-08	3.85E-07
20	kdam	DNAdamage	0.08	0.04	0.16
21	kdamROS	ROSDNAdamage	1.00E-05	5.00E-06	2.00E-05
22	kdegAbeta	AbetaDegredation	1.50E-05	7.50E-06	3.00E-05
23	kdegAbetaGlia	Abeta_antiAbDegredation	0.005	0.0025	0.01
24	kdegAntiAb	antiAbRemoval	2.75E-06	1.38E-06	5.50E-06
25	kdegMdm2	Mdm2Degradation	0.01	0.005	0.02
26	kdegMdm2mRNA	Mdm2mRNADegradation	0.0005	0.00025	0.001
27	kdegp53	p53Degradation	0.005	0.0025	0.01
28	kdegp53mRNA	p53mRNADegradation	0.0001	5.00E-05	0.0002
29	kdegTau20SProt	Tau20SProteasomeDegradation	0.01	0.005	0.02
30	kdephosMdm2	Mdm2dephosphorylation	0.5	0.25	1
31	kdephosp53	p53dephosphorylation	0.5	0.25	1
32	kdephospTau	Taudephosphorylation2	0.01	0.005	0.02
33	kdisaggAbeta	AbetaDisaggregation1	1.00E-06	5.00E-07	2.00E-06
34	kdisaggAbeta1	AbetaDisaggregation3	0.0002	0.0001	0.0004
35	kdisaggAbeta2	AbetaDisaggregation4	1.00E-06	5.00E-07	2.00E-06
36	kgenROSAbeta	AggAbetaROSproduction2	2.00E-05	1.00E-05	4.00E-05
37	kgenROSGlia	ROSgenerationByGlia	1.00E-05	5.00E-06	2.00E-05
38	kgenROSPlaque	PlaqueROSproduction	1.00E-05	5.00E-06	2.00E-05
39	kinactATM	ATMinactivation	0.0005	0.00025	0.001
40	kinactglia1	GliaInactivationStep1	5.00E-06	2.50E-06	1.00E-05
41	kinactglia2	GliaInactivationStep3	5.00E-06	2.50E-06	1.00E-05
42	kinhibprot	ProteasomeInhibitionAggTau	1.00E-07	5.00E-08	2.00E-07
43	kMdm2PolyUb	p53Polyubiquitination	0.00456	0.00228	0.00912
44	kMdm2PUb	Mdm2PUbiquitination	6.84E-06	3.42E-06	1.37E-05
45	kMdm2Ub	Mdm2Ubiquitination	4.56E-06	2.28E-06	9.12E-06
46	kp53PolyUb	Mdm2polyUbiquitination1	0.01	0.005	0.02
47	kp53Ub	p53Monoubiquitination	5.00E-05	2.50E-05	0.0001
48	kpf	AbetaPlaqueFormation	0.2	0.1	0.4
49	kpg	AbetaPlaqueGrowth	0.15	0.075	0.3
50	kpghalf	AbetaPlaqueGrowth1	10	5	20
51	kphosMdm2	Mdm2phosphorylation	2	1	4
52	kphosMdm2GSK3b	Mdm2GSK3phosphorylation1	0.005	0.0025	0.01
53	kphosMdm2GSK3bp53	Mdm2GSK3phosphorylation2	0.5	0.25	1
54	kphosp53	p53phosphorylation	0.0002	0.0001	0.0004
55	kphosTauGSK3b	Tauphosphorylation6	0.0002	0.0001	0.0004
56	kphospTauGSK3bp53	Tauphosphorylation4	0.1	0.05	0.2
57	kprodAbeta	Abetaproduction1	1.86E-05	9.30E-06	3.72E-05
58	kprodAbeta2	Abetaproduction2	1.86E-05	9.30E-06	3.72E-05
59	kproteff	Extra parameter is used in different degradation reactions	1	0.5	2
60	krelAbPGlia	AbetaReleaseFromGlia	5.00E-05	2.50E-05	0.0001
61	krelGSK3bp53	p53GSK3bRelease	0.002	0.001	0.004
62	krelMdm2p53	p53Mdm2Release	1.16E-05	5.78E-06	2.31E-05
63	krelMTTau	TauMTrelease	0.0001	5.00E-05	0.0002
64	kremROS	ROSremoval	7.00E-05	3.50E-05	0.00014
65	krepair	DNArepair	2.00E-05	1.00E-05	4.00E-05
66	ksynMdm2	Mdm2Synthesis	0.000495	0.000248	0.000595
67	ksynMdm2mRNA	Mdm2mRNASynthesis1	0.0005	0.00025	0.001

68	**ksynMdm2mRNAGSK3bp53**	**Mdm2mRNASynthesis3**	**0.0007**	**0.00035**	**0.0014**
69	**ksynp53**	**p53Synthesis**	**0.007**	**0.0035**	**0.014**
70	**ksynp53mRNA**	**p53mRNASynthesis**	**0.001**	**0.0005**	**0.002**
71	**ksynp53mRNAAbeta**	**p53transcriptionViaAbeta**	**1.00E-05**	**5.00E-06**	**2.00E-05**
72	**ksynTau**	**TauSynthesis**	**8.00E-05**	**4.00E-05**	**0.00016**
73	**ktangfor**	**TangleFormation1**	**0.001**	**0.0005**	**0.002**

5.2 ODEs and MRM/GSSA Results for the Selected Species

According to Proctor et al., (2013), the behaviour of this model is supported by neuropathological observations in Alzheimer patients immunised against Aβ. Figures 5.1 A and B show, respectively, the behaviour of the selected species from ODEs and MRM/GSSA when the parameters are not perturbed. Part B shows the average behaviour of 200 realizations produced by MRM/GSSA for all selected species.

To assume a species is highly sensitive to a parameter's perturbation, a dramatic change should happen in its behaviour by increasing or decreasing to an unpredictable level. Levels of all the selected species are tracked when parameters are perturbed (one at a time) to examine how these species contribute to the overall behaviour of the system.

A-ODEs results

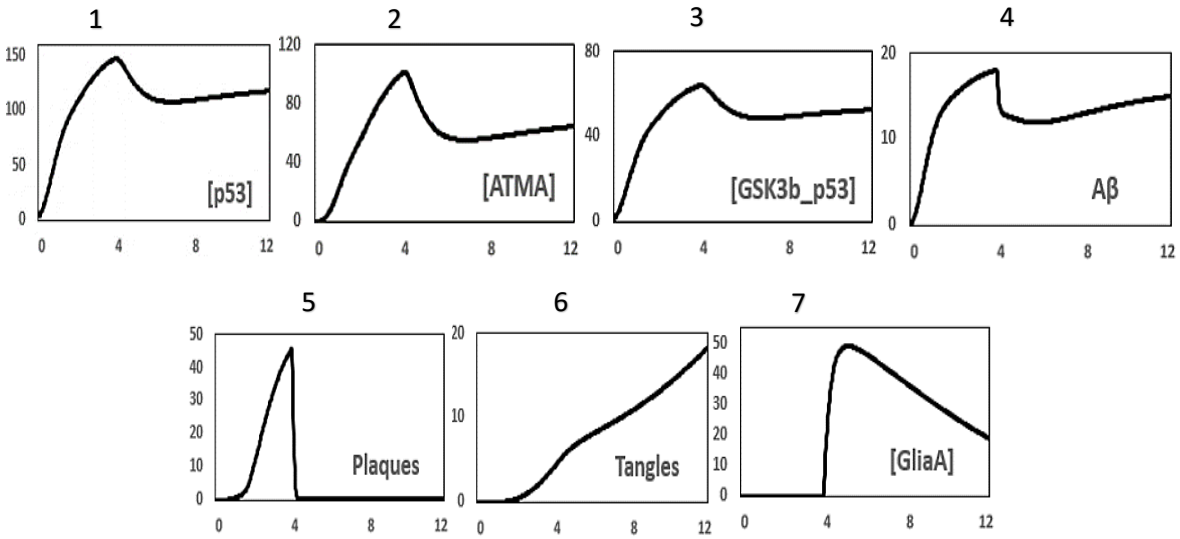

B-MRM/GSSA results (Average of 200 realizations)

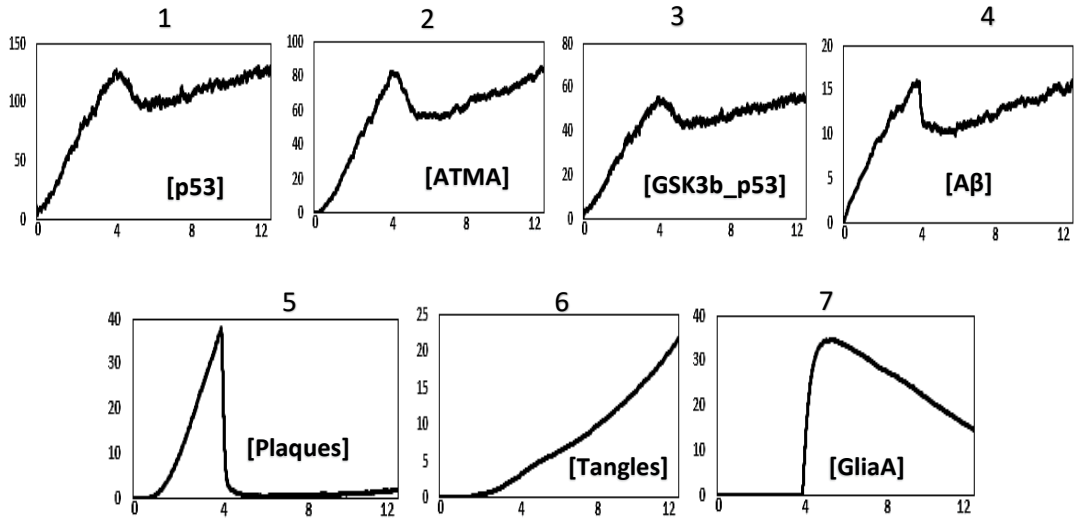

Figure 5.1: Behaviour of selected species from ODEs (A) and average of 200 realizations using MRM/GSSA (B). ODEs and MRM/GSSA show that the level ATAM (2 in A and B) increases in response to DNA damage. ATMA phosphorylates p53 (1 in A and B) to prevent its binding with Mdm2, and p53 is no longer degraded. p53 is elevated and binds to GSK3β to increase the level of p53_ GSK3β (3 in A and B). p53_GSK3β continuously phosphorylates Aβ (4 in A and B) and tau, which results in more production of plaques (5 in A and B) and tangles (6 in A and B), respectively. At day #4, the system is immunized by adding antibodies, which results in a dramatic increase in the level of GliaA (7 in A and B) and a slight decrease in the level of p53, ATMA, p53_ GSK3β, Aβ, totally cleared plaques and a small inhibition in the level of tangles.

5.3 LSA Results

To deterministically and stochastically perform LSA, we use the algorithms shown in Figures 4.3 and 4.4 to quantify the influence each parameter's perturbation had on the selected species. The sensitivity of each of the selected species in response to each parameter perturbation is computed at each time step. Assume that N time steps is needed to run the simulation. Therefore, N sensitivity values (SV) are produced for each species in response to any parameter perturbation over the time series of the system. Therefore, a list contains N sensitivity values, $SV_{list} = (SV_1, SV_2, SV_3, \dots\dots\dots\dots\dots SV_N)$.We use this list to generate three different values. These values are average (μ), standard deviation σ and Max.

1- $\mu = \sum_{i=1}^{N} SV_i/N$. It is used to display the average sensitivity on the behaviour of any of the selected species in response to any parameter perturbation.

2- $\sigma = \sqrt{\frac{1}{N}\sum_{i=1}^{N}(SV_i - \mu)^2}$. It is used to quantify how much the members of SV_{list} differ from μ.

3- $\mathrm{Max} = \mathrm{MAX}(SV_1, SV_2, SV_3, \dots\dots\dots\dots\dots SV_N)$. It is used to identify the maximum member of SV_{list} (the minus sign indicates a decreasing status). We also find the exact time (Time days) for Max to determine exactly when the maximum sensitivity of a species in response to a parameter happened. We use Max and (Time days) to determine the good time for observing a species in response to a parameter perturbation.

Parameters are divided into three groups (A, B and C). Group A includes all parameters that have no effect on the behaviour of a selected species when parameters are perturbed. Group B consists of parameters that have minor effect on the behaviour of a selected species when parameters are perturbed. Group C lists all parameters that dramatically change the behaviour of the selected species when parameters are perturbed.

Results of LSA using ODEs and MRM/GSSA are generated using visual studio (C# 2017). All 3D figures that are used to show the maximum sensitivity of the selected species are drawn using a statistical package produced and distributed

by NCSS. Figures that are used to show μ and σ of SV_{list} are created using Excel tool 2016.

μ, σ, Max, $\mathrm{and\ Time\,(second)}$ for each species in response to all parameters using ODEs and MRM/GSSA are listed in Tables 1 and 2 in the Appendices C.

5.3.1 Results of LSA for p53, ATMA, p53_ GSK3β and Aβ

LSA using ODEs and MRM/GSSA demonstrates that the behaviour of p53, ATMA, p53_GSK3β and Aβ are not dramatically changed when parameters are perturbed to 50% and 200% of their basal values, one at a time.

Using ODEs to perform LSA shows that p53, ATMA and p53_ GSK3β are slightly changed in response to 28 parameters while Aβ is altered in response to only 24 parameters. Performing LSA using MRM/GSSA demonstrate that the behaviour of p53 is altered in response to 66 parameters when the parameters are perturbed to 50% of their basal values while 71 parameters change its behaviour when they perturbed to 200% of their basal values. Therefore, p53 is more sensitive for increasing the rates of parameters. Whereas, ATMA, p53_ GSK3β and Aβ are sensitive to 71 parameters when the list of parameters in the system adjusted to 50% and 200% of their basal values.

Thus, LSA using ODEs and MRM/GSSA demonstrates that p53, ATMA, p53_ GSK3β and Aβ are not highly contributing to the overall behaviour of the system in response to parameters perturbation. Therefore, minimum and maximum ranges of parameters for these species could be less and greater than 50% and 200% of their basal values, respectively. The results of LSA using ODEs and MRM/GSSS for p53, ATMA, p53_ GSK3β and Aβ are summarized in Table 5.3.

LSA using ODEs indicates that days # 4 and 5 of the simulation time are the most important days to observe the behaviour of p53, ATMA, p53_ GSK3β and Aβ because the maximum sensitivity of these species in response to parameters perturbation is recoded in these two days.

Using MRM/GSSA to perform LSA shows that the maximum sensitivity of p53, ATMA, p53_ GSK3β and Aβ is recorded over the whole period of the system. The

maximum sensitivity of these species is recorded over the whole period of the system because these species are targeted to be altered to more parameters specific to different pathways that are activated at different times. Therefore, observing the maximum changed on the behaviour of these species when LSA uses MRM/GSSA should be done over the whole period of the system.

For simplicity we just show figures for p53 and Aβ to display how the maximum sensitivity is demonstrated using ODEs and MRM/GSSA. Figures 5.2 (A and B) and 5.3 (A and B) show $\mathrm{Max\ and\ Time\ (days)}$ of p53 in response to parameters perturbation when parameters are perturbed to 50% and 200% of their basal values using ODEs and MRM/GSSA, respectively while Figures 5.4 (A and B) and 5.5 (A and B) show same for Aβ.

Because p53, ATMA and p53_GSK3β are not hugely contribute to the whole system since they are not dramatically changed in response to parameters perturbation, we conclude that also pathways included these species are not hugely affect the behaviour of the whole the system. Therefore, we identify that p53 regulation, DNA damage pathway and GSK3β activity are not dramatically changed in response to parameters perturbation. Aβ has no ability to contribute the overall behaviour of the system since minor changes happened to its behaviour in response to parameters perturbation but its pathway is identified as an important pathway in the system because plaques are dramatically changed in response to parameters perturbation. The results LSA for plaques are described in the next section.

Table 5.3: Summary of LSA results using ODEs and MRM/GSSA for p53, ATMA, p53_ GSK3β and Aβ. Groups A, B and C, respectively, contain parameters that have no effect, minor effects and major effects on the behaviour of these species.

Parameters are perturbed to 50% of their basal values.	**LSA Using ODEs**			**LSA Using MRM/GSSA**		
Is p53 very sensitive to parameters perturbations?	**NO**			**NO**		
Number of parameters in each group	**Group A**	**Group B**	**Group C**	**Group A**	**Group B**	**Group C**
	45	**28**	**0**	**7**	**66**	**0**
Is ATMA very sensitive to parameters perturbations?	**NO**			**NO**		
Number of parameters in each group	**Group A**	**Group B**	**Group C**	**Group A**	**Group B**	**Group C**
	45	**28**	**0**	**2**	**71**	**0**
Is p53_GSK3β very sensitive to parameters perturbations??	**NO**			**NO**		
Number of parameters in each group	**Group A**	**Group B**	**Group C**	**Group A**	**Group B**	**Group C**
	45	**28**	**0**	**2**	**71**	**0**
Is Aβ very sensitive to parameters perturbations?	**NO**			**NO**		
Number of parameters in each group	**Group A**	**Group B**	**Group C**	**Group A**	**Group B**	**Group C**
	45	**28**	**0**	**2**	**71**	**0**
Minimum ranges of parameters	**50% or less**			**50% or less**		
Parameters are perturbed to 200% of their basal values.	**LSA Using ODEs**			**LSA Using MRM/GSSA**		
Is p53 very sensitive to parameters perturbations?	**NO**			**NO**		
Number of parameters in each group	**Group A**	**Group B**	**Group C**	**Group A**	**Group B**	**Group C**
	45	**28**	**0**	**2**	**71**	**0**
Is ATMA very sensitive to parameters perturbations?	**NO**			**NO**		
Number of parameters in each group	**Group A**	**Group B**	**Group C**	**Group A**	**Group B**	**Group C**
	45	**28**	**0**	**2**	**71**	**0**
Is p53_GSK3β very sensitive to parameters perturbations??	**NO**			**NO**		
Number of parameters in each group	**Group A**	**Group B**	**Group C**	**Group A**	**Group B**	**Group C**
	45	**28**		**2**	**71**	**0**
Is Aβ very sensitive to parameters perturbations?	**NO**			**NO**		
Number of parameters in each group	**Group A**	**Group B**	**Group C**	**Group A**	**Group B**	**Group C**
	45	**28**		**2**	**71**	**0**
Maximum ranges of parameters	**200% or more**			**200% or more**		

(A) Maxiumum senstivity of p53 and its time in resposne to paramater pertubation using ODEs when parameters are pertubed to 50% basal values.

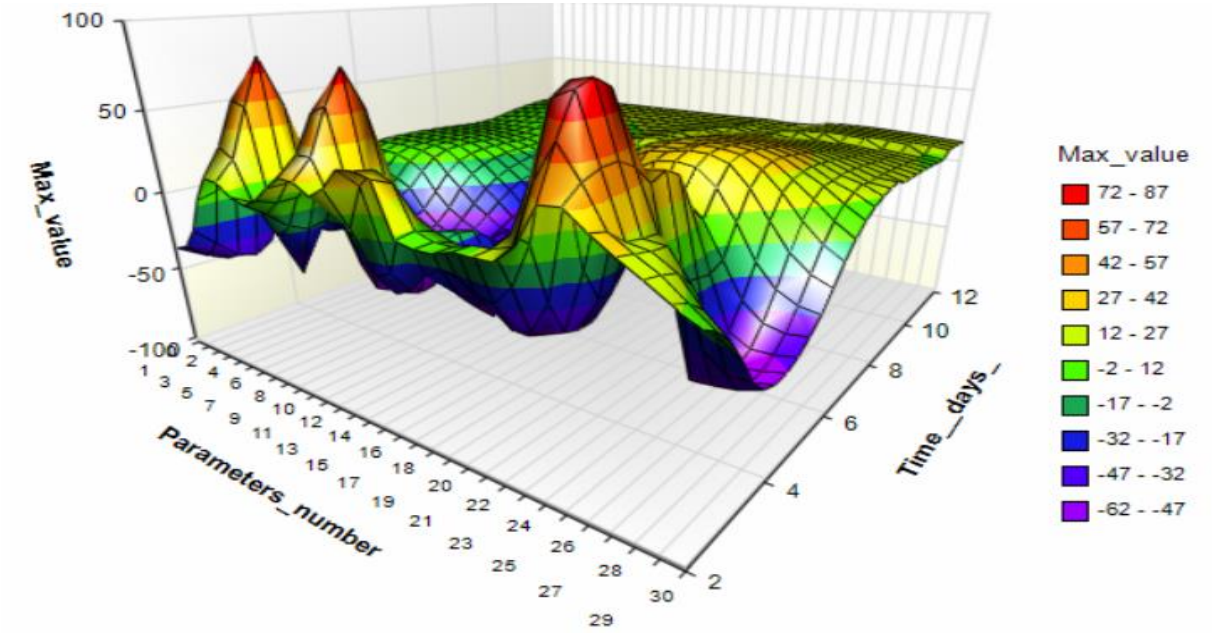

(B) Maxiumum senstivity of p53 and its time in resposne to paramater pertubation using MRM/GSSA when parameters are pertubed to 50% basal values.

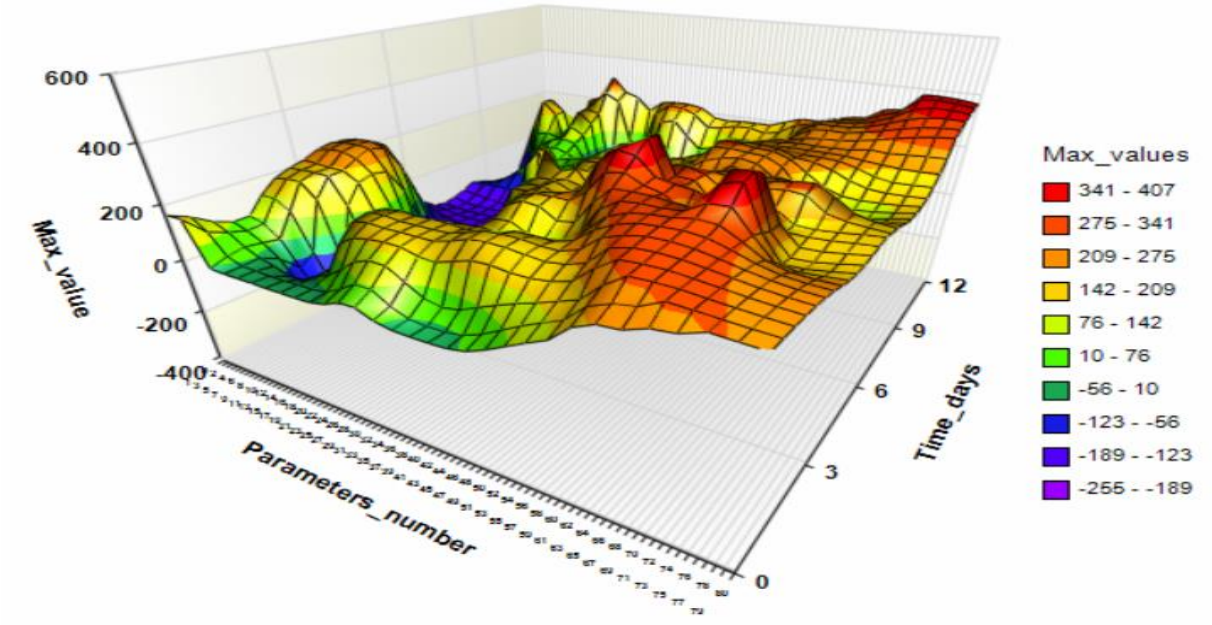

Figure 5.2: Maximum sensitivity and it's time for p53 when parameters are adjusted to 50% of their basal values using ODEs (A) and MRM/GSSA (B), respectively. A shows that p53 using ODEs to perform LSA recodes its maximum sensitivity in response to parameters perturbation in the early stage of the system, mainly from day #4 to day #6. B shows that p53 records its maximum sensitivity over the whole period of the system when MRM/GSSA is used in response to parameters perturbation.

A. Maxiumum senstivity of p53 and its time in resposne to paramater pertubation using ODEs when parameters are pertubed to 200% basal values.

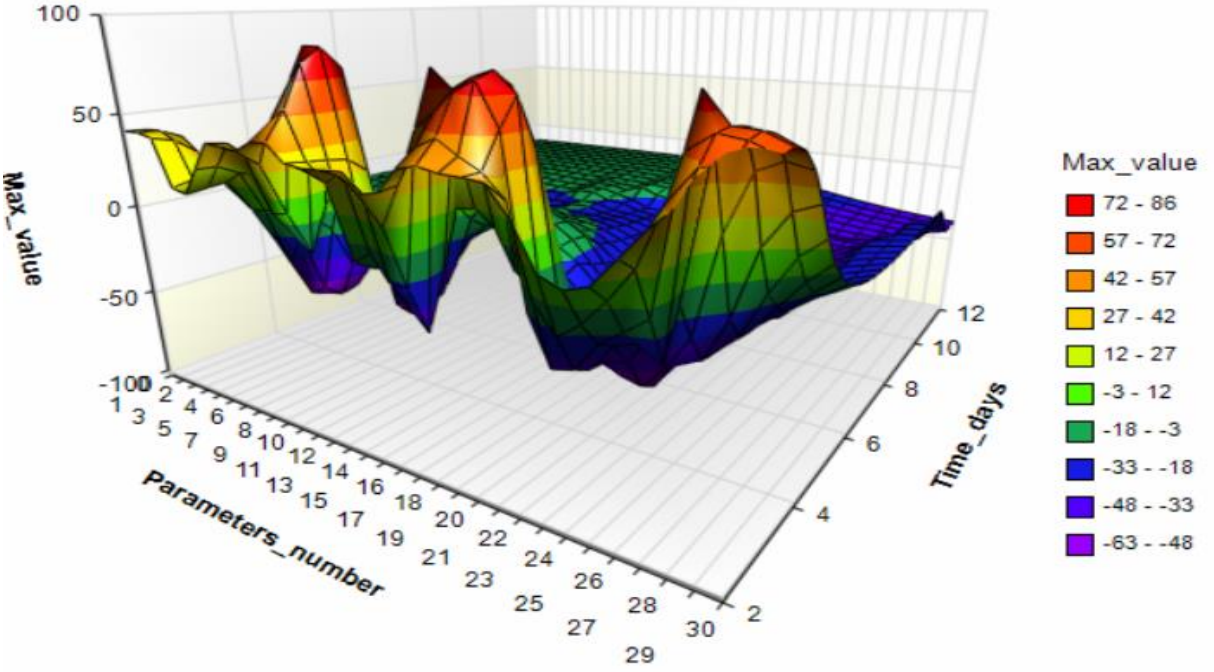

B. Maxiumum senstivity of p53 and its time in resposne to paramater pertubation using MRM/GSSA when parameters are pertubed to 200% basal values.

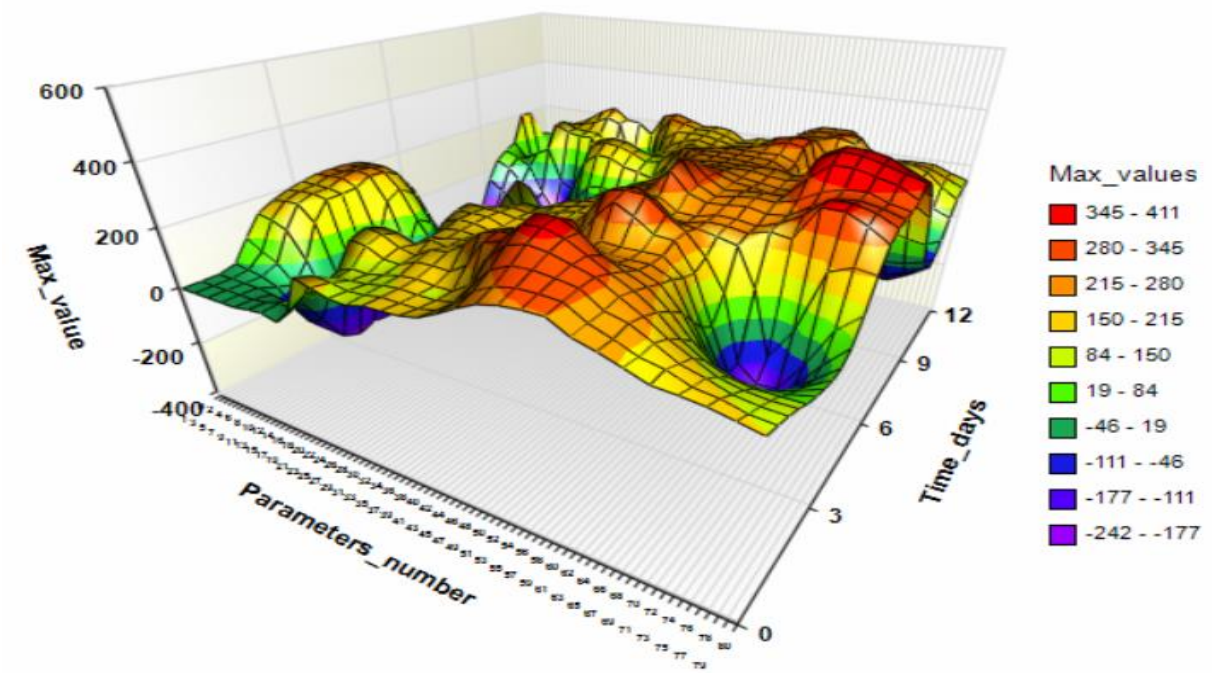

Figure 5.3: Maximum sensitivity and it's time for p53 when parameters are adjusted to 200% of their basal values using ODEs (A) and MRM/GSSA (B), respectively. A shows that p53 using ODEs to perform LSA recodes its maximum sensitivity in response to parameters perturbation in the early stage of the system, mainly from day #4 to day #6. B shows that p53 records its maximum sensitivity over the whole period of the system when MRM/GSSA is used in response to parameters perturbation.

A. Maxiumum senstivity of Aβ and its time in resposne to paramater pertubation using ODEs when parameters are pertubed to 50% basal values.

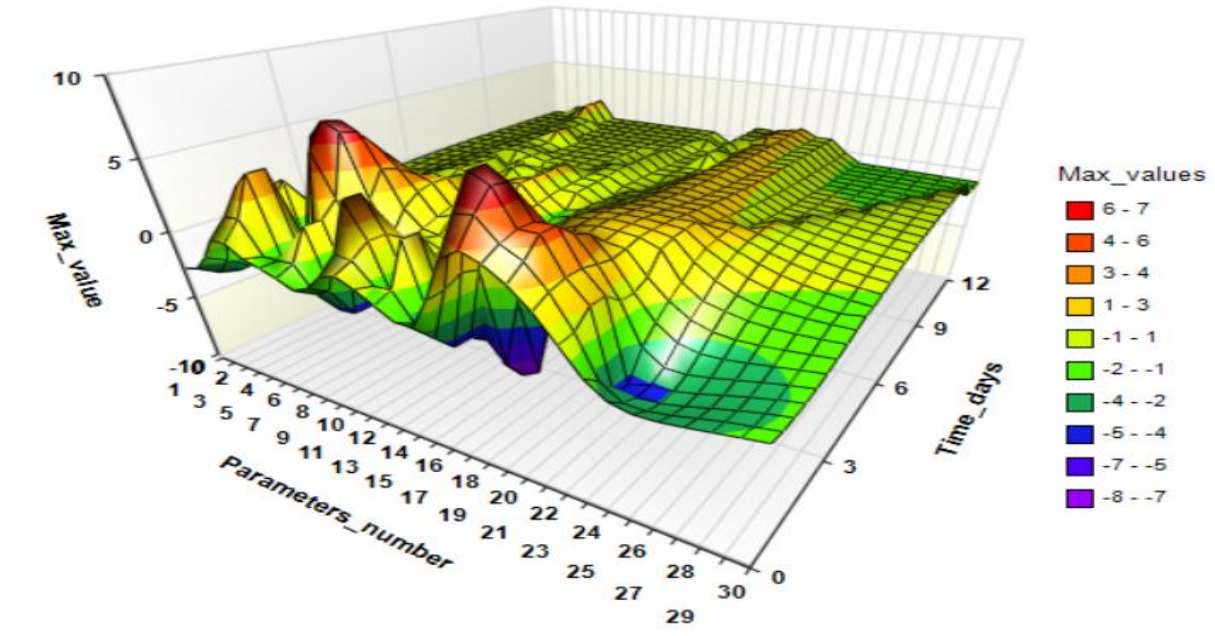

B. Maxiumum senstivity of Aβ and its time in resposne to paramater pertubation using MRM/GSSA when parameters are pertubed to 50% basal values.

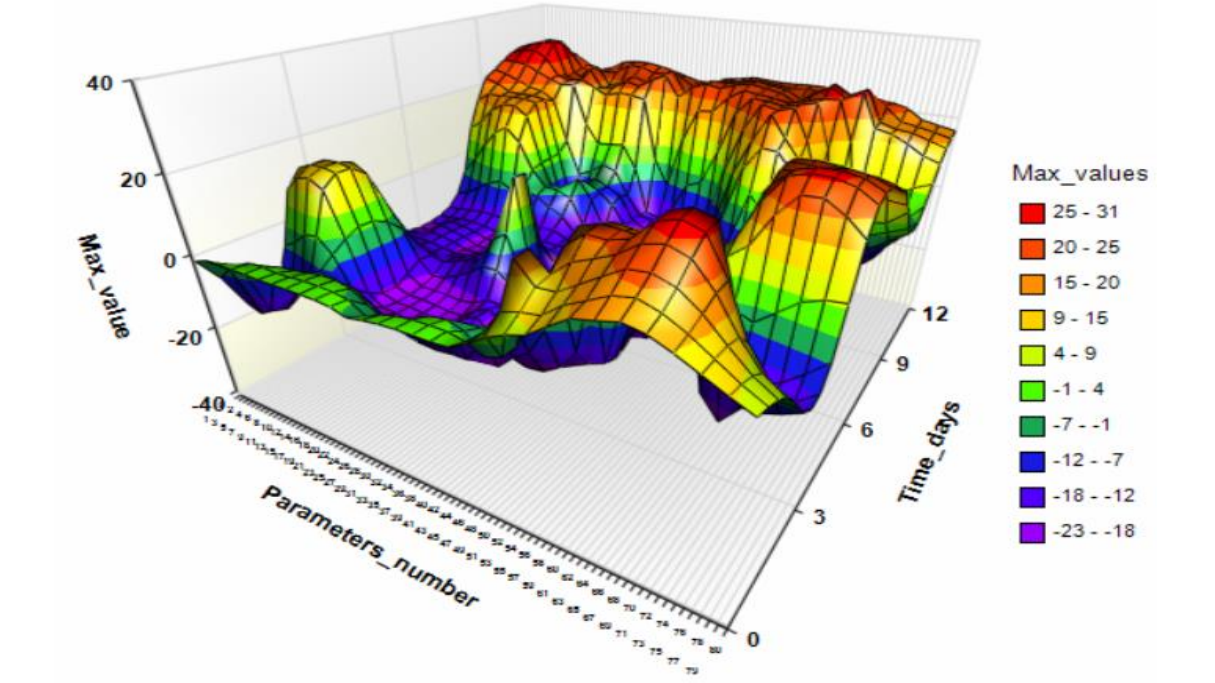

Figure 5.4: Maximum sensitivity and it's time for Aβ when parameters are adjusted to 50% of their basal values using ODEs (A) and MRM/GSSA (B), respectively. A shows that Aβ using ODEs to perform LSA recodes its maximum sensitivity in response to parameters perturbation in the early stage of the system, mainly from day #4 to day #6. B shows that p53 records its maximum sensitivity over the whole period of the system when MRM/GSSA is used in response to parameters perturbation.

A. Maxiumum senstivity of Aβ and its time in resposne to paramater pertubation using ODEs when parameters are pertubed to 200% basal values.

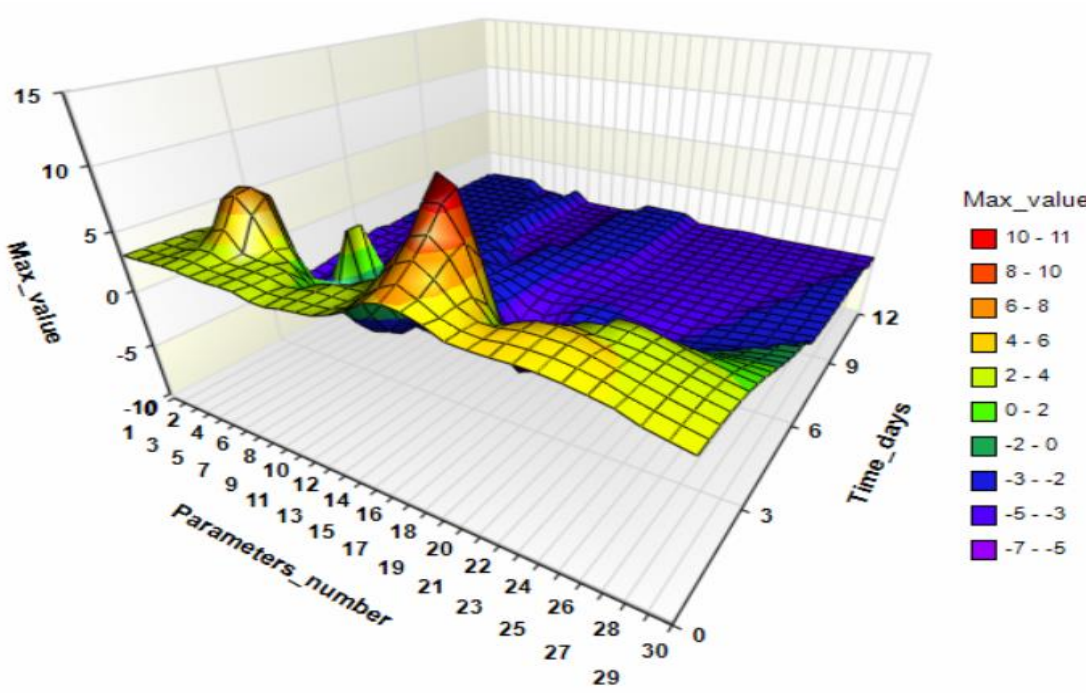

B. Maxiumum senstivity of Aβ and its time in resposne to paramater pertubation using MRM/GSSA when parameters are pertubed to 200% basal values.

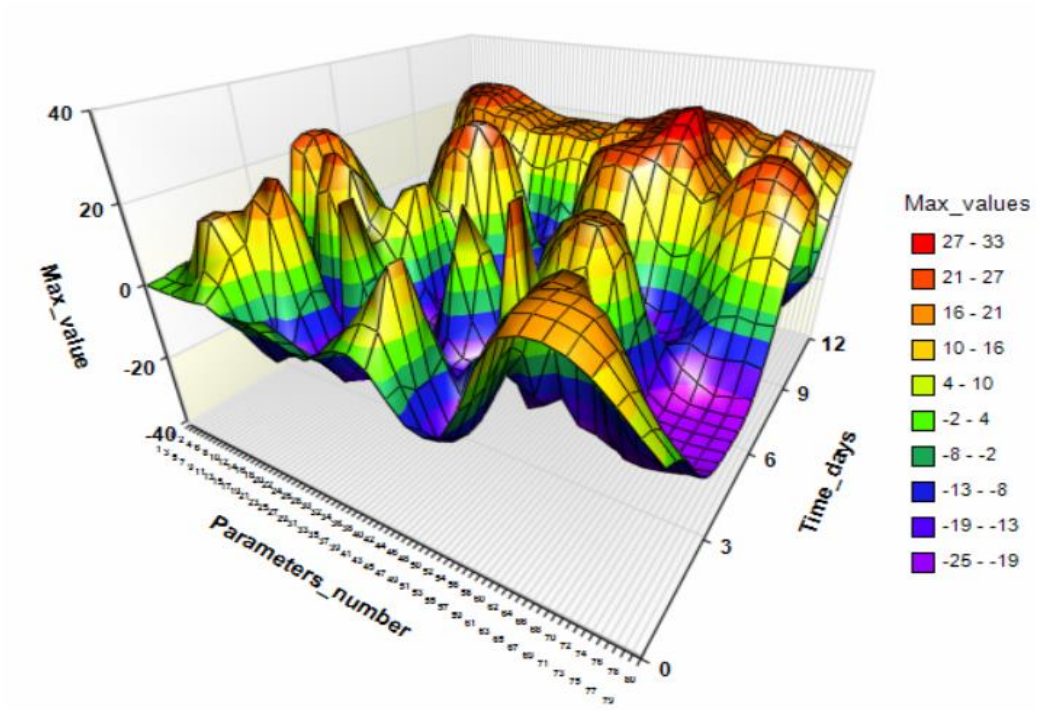

Figure 5.5: Maximum sensitivity and it's time for Aβ when parameters are adjusted to 200% of their basal values using ODEs (A) and MRM/GSSA (B), respectively. A shows that Aβ using ODEs to perform LSA recodes its maximum sensitivity in response to parameters perturbation in the early stage of the system, mainly from day #4 to day #6. B shows that p53 records its maximum sensitivity over the whole period of the system when MRM/GSSA is used in response to parameters perturbation.

Figures 5.6 (A and B) and 5.7 (A and B) show μ and σ of SV_{list} for p53 in response to parameters perturbation when parameters are perturbed to 50% and 200% of their basal values using ODEs and MRM/GSSA respectively.

B. μ and σ of SV_{list} for p53 in response to parameters perturbation using ODEs when parameters are perturbed to 50% of their basal values.

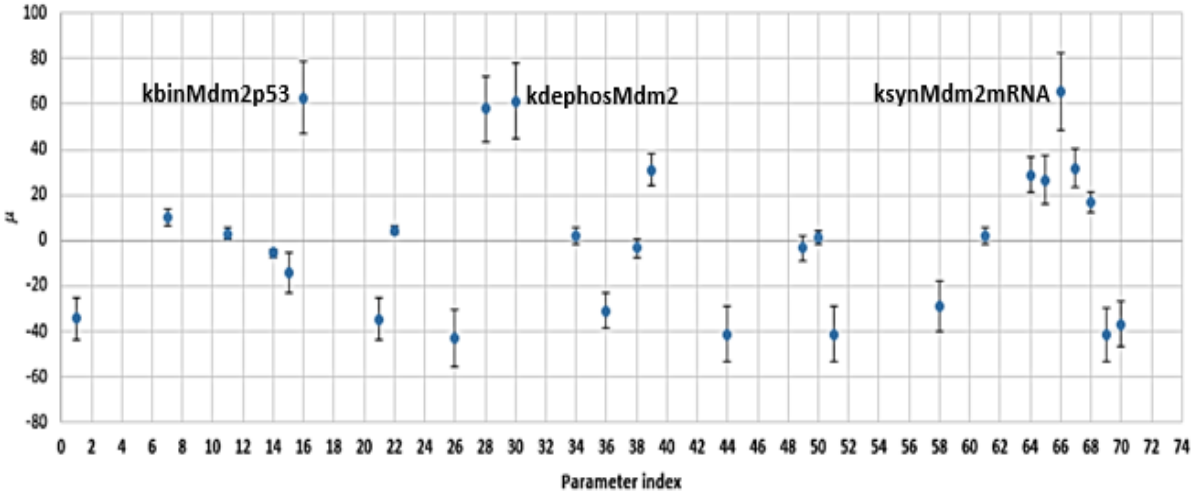

B. μ and σ of SV_{list} for p53 in response to parameters perturbation using ODEs when parameters are perturbed to 200% of their basal values.

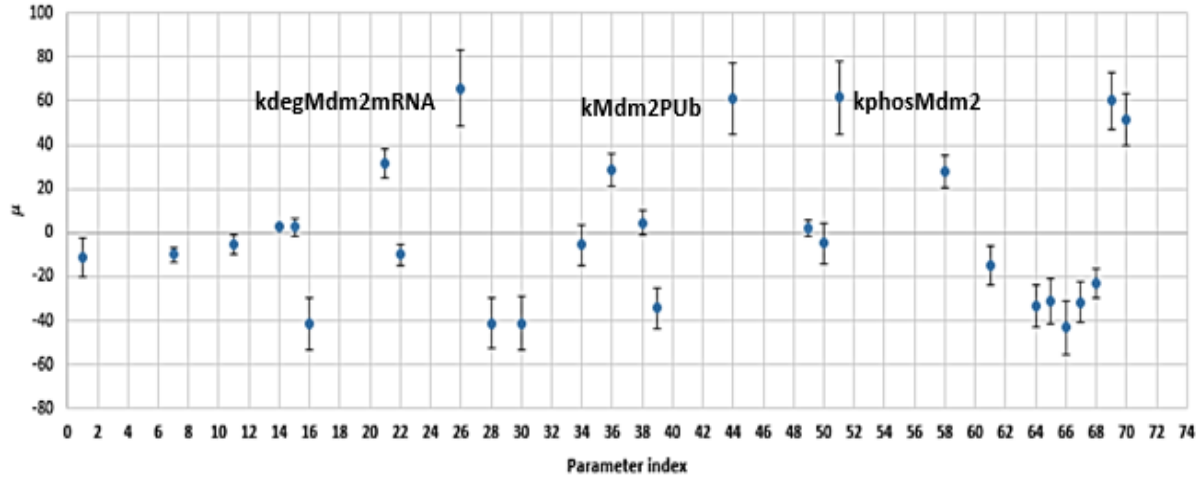

Figure 5.6: μ and σ of SV_{list} for p53 in response to parameters perturbation using ODEs when parameters are perturbed to 50% (A) and 200% (B) of their basal values. The parameter indexes correspond to the indexes in Table 5.1. All parameters have minor effects on the behaviour of p53. When parameters are perturbed to 50% (A), 13 parameters decrease the level of p53 while 16 parameters decrease its level when parameters are perturbed to 200%. In A when parameters are perturbed to 50% of their basal value, parameters 16 and 30 (indicated in A) have the same effect on the level of p53 while parameter 67 (indicated in A) has the major effect on the behaviour of p53. B shows that 44 and 51 (indicated in B) have the same effect on the level of p53. Parameters 26 (indicated in B) has the major effect on the behaviour of p53. Therefore, it could be clearly seen that parameters specific to Mdm2 are the most important parameters that affect p53 when LSA uses ODEs.

A. μ and σ of SV_{list} for p53 in response to parameters perturbation using MRM/GSSA when parameters are perturbed to 50% of their basal values.

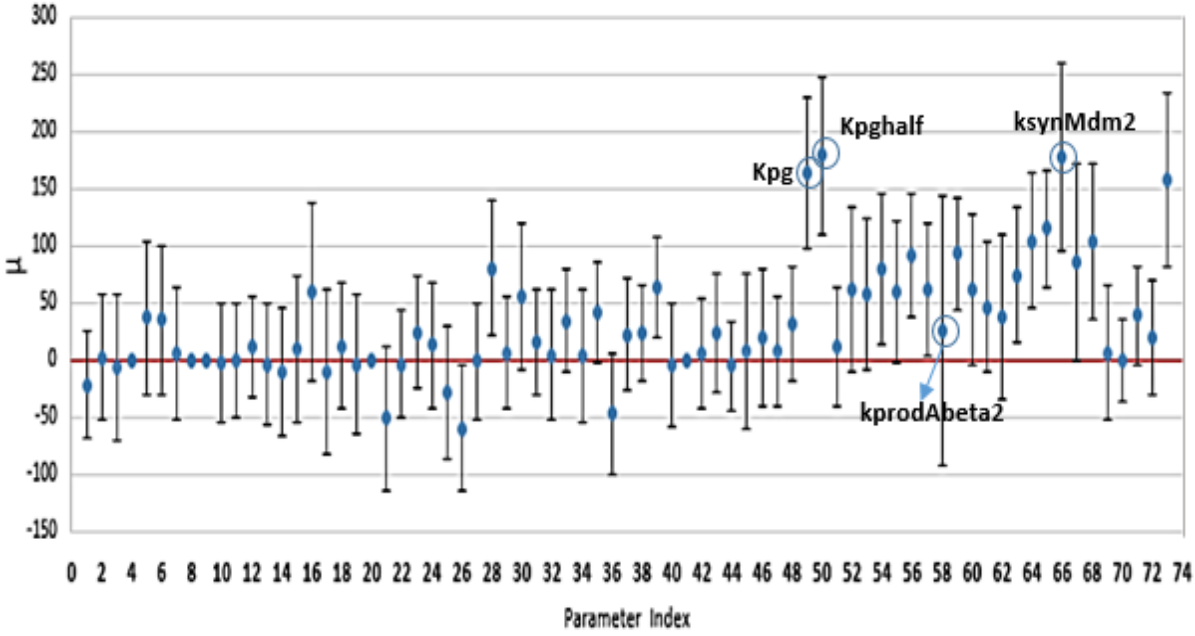

B. μ and σ of SV_{list} for p53 in response to parameters perturbation using MRM/GSSA when parameters are perturbed to 200% of their basal values.

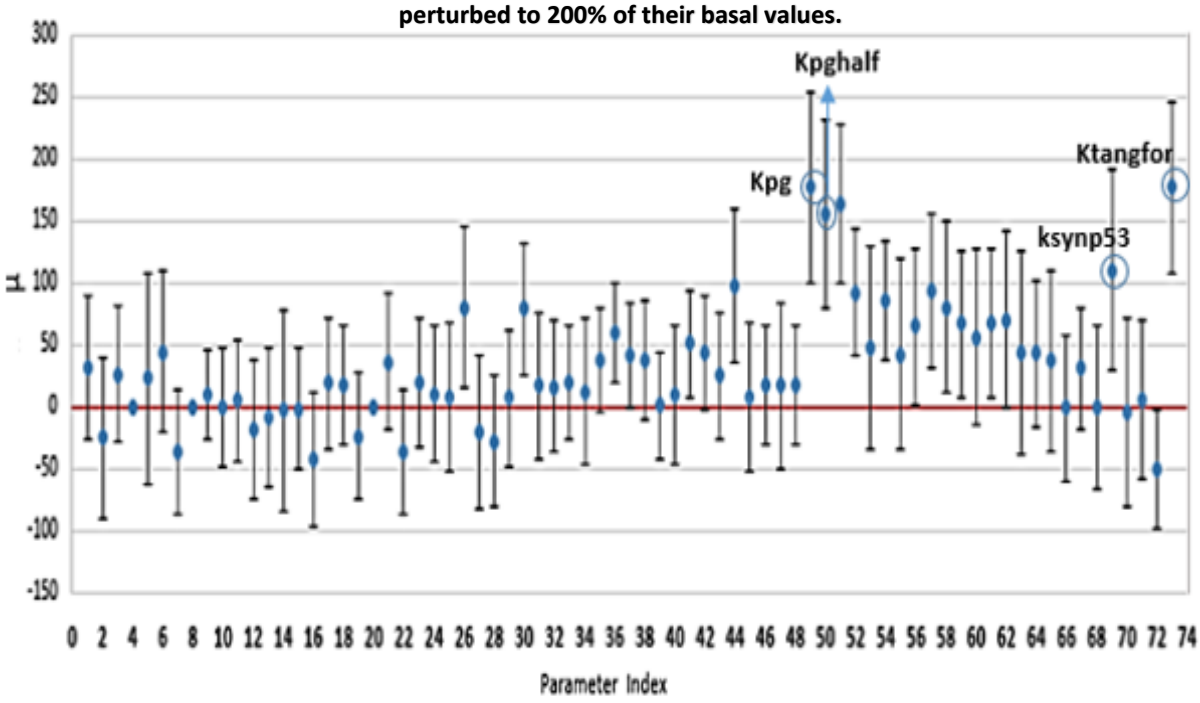

Figure 5.7: μ and σ of SV_{list} for p53 in response to parameters perturbation using MRM/GSSA when parameters are perturbed to 50% (A) and 200% (B) of their basal values. The parameter indexes correspond to the indexes in Table 5.1. All parameters have minor effects on the behaviour of p53. In A, it is clearly seen that parameters # 49, 50, 58 and 66 (indicated in A) have the major effects on the behaviour of p53 when parameters are perturbed to 50% of their basal value. Parameters # 49, 50, 69 and 74 (indicated in A) have the major effects on the behaviour of p53 when parameters are perturbed to 50% of their basal value. When parameters are perturbed to 50% and 200% of their basal values, p53 is more sensitive to parameter specific to Aβ.

It has been found that ATMA and p53_GSK3β are more sensitive to KinactATM (1 in Table 5.2) when LSA uses ODEs and parameters are perturbed to 50% and 200%. LSA using MRM/GSSA demonstrates that ATMA and p53_GSK3β are more sensitive parameters specific to p53 and Mdm2 such as ksynp53, kbinE2Ub, ksynMdm2 (69, 14 and 66 in Table 5.2) when parameters are perturbed to 50% of their basal values. Parameter specific to Aβ such as kpg and KprodAbeta2 and Kpghalf (49, 50 and 58 in Table 5.2) have more effects than others on the behaviour of ATMA and p53_GSK3β when parameters are perturbed to 200%.

Aβ is more sensitive to KrelGSK3bp53 specific p53_GSK3b (61 in Table 5.2) using ODEs and MRM/GSSA when parameters are perturbed to 50% of their basal values. KprodAbeta2 specific to Aβ (58 in Table 5.2) is the more effectiveness parameter on the behaviour of Aβ using ODEs and MRM/GSSA when parameters are perturbed to 200% of their basal values. Figures 5.8 (A, and B), 5.9 (A and B) show μ and σ of SV_{list} for Aβ in response to parameters perturbation when parameters respectively are perturbed to 50% and 200% of their basal values using ODEs and MRM/GSSA, respectively

It is really interesting to find that KrelGSK3bp53 and KprodAbeta2 is the most effective parameter on the behaviour of Aβ using respectively ODEs and MRM/GSSA when parameters are perturbed to 50% and 200% of their basal values, respectively.

A. μ and σ of SV_{list} for Aβ in response to parameters perturbation using ODEs when parameters are perturbed to 50% of their basal values.

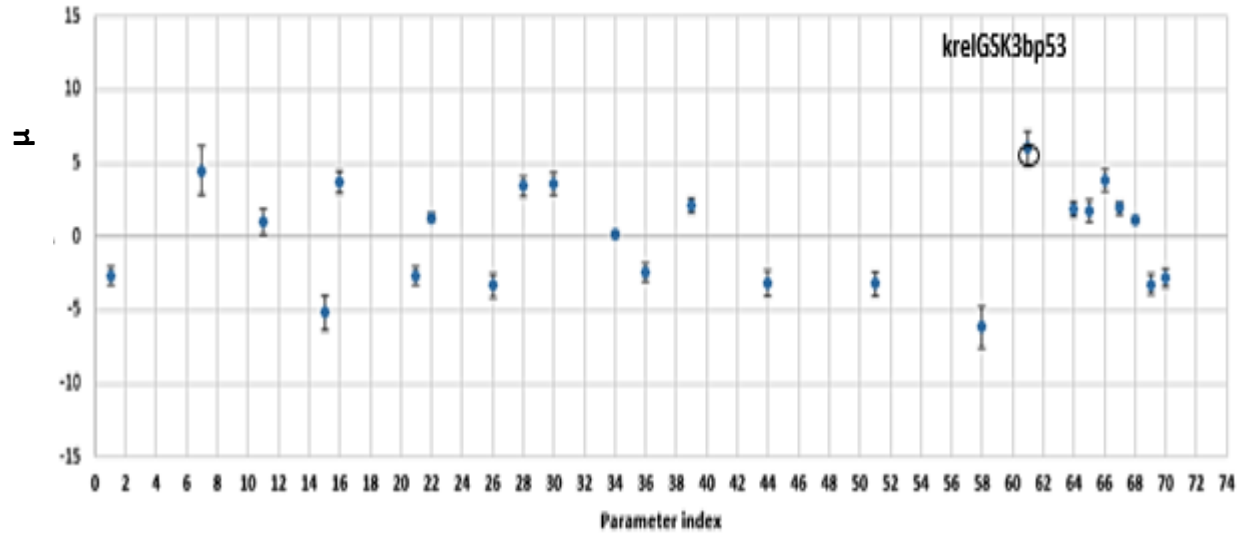

B. μ and σ of SV_{list} for Aβ in response to parameters perturbation using ODEs when parameters are perturbed to 200% of their basal values.

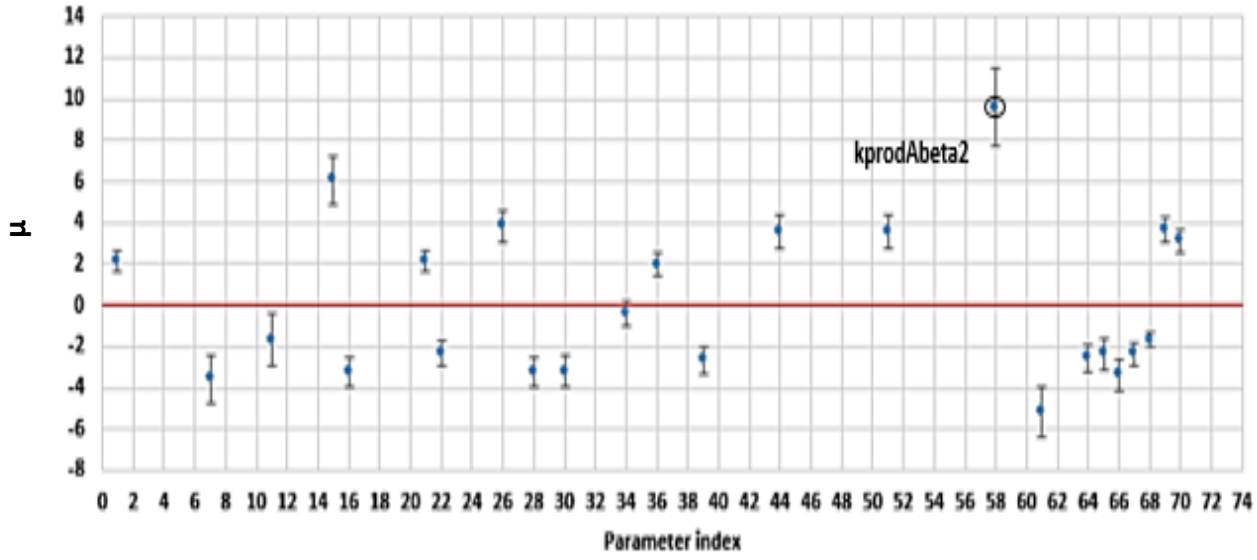

Figure 5.8: μ and σ of SV_{list} for Aβ in response to parameters perturbation using ODEs when parameters are perturbed to 50% (A) and 200% (B) of their basal values. The parameter indexes correspond to the indexes in Table 5.1. All parameters have minor effects on the behaviour of p53. KrelGSK3bp53 (61 in Table 5.1) is the most effectives parameter on the behaviour of Aβ when parameters are perturbed to 50% of their basal values using ODEs. KprodAbeat2 has the largest effects on the behaviour of Aβ using ODEs when parameters are perturbed to 200% of their basal values.

A. μ and σ of SV_{list} for Aβ in response to parameters perturbation using MRM/GSSA when parameters are perturbed to 200% of their basal values.

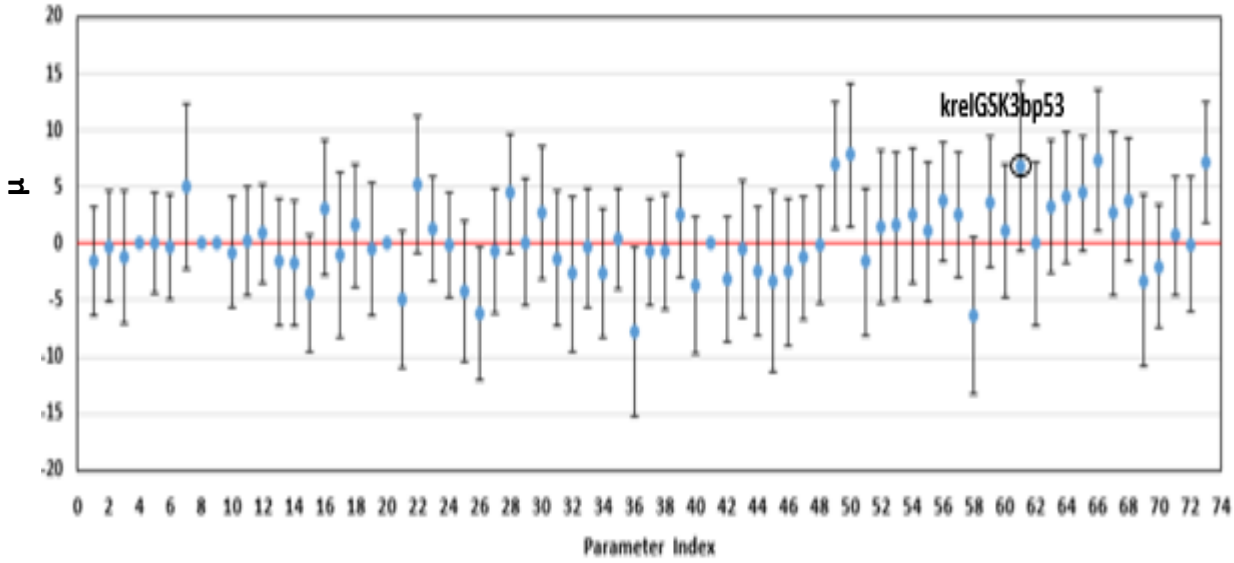

B. μ and σ of SV_{list} for Aβ in response to parameters perturbation using MRM/GSSA when parameters are perturbed to 200% of their basal values.

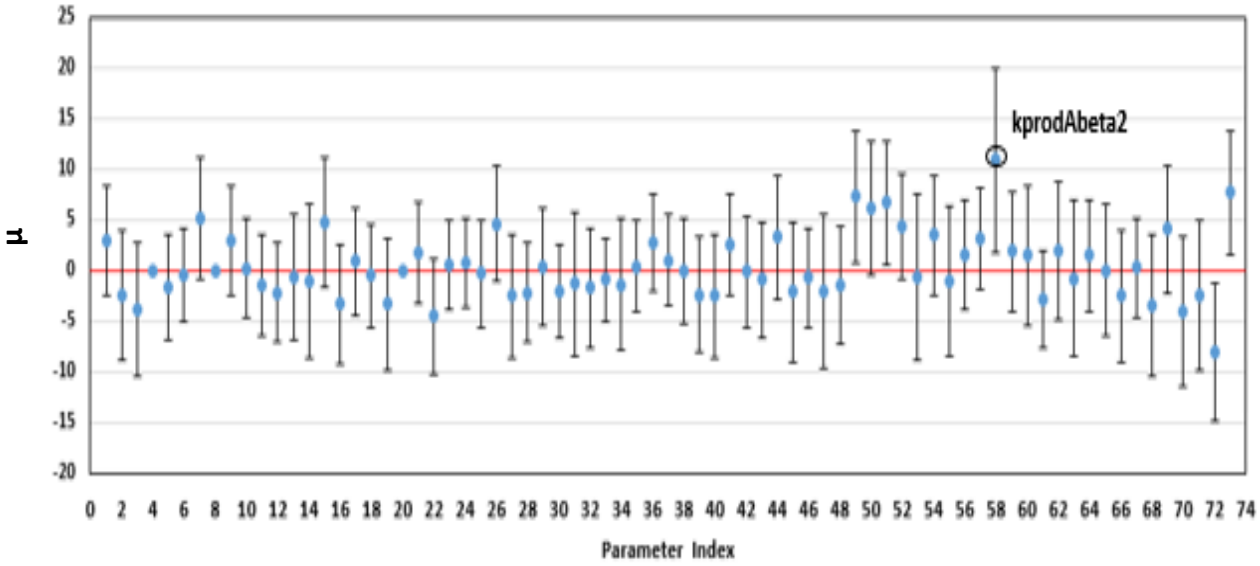

Figure 5.9: μ and σ of SV_{list} for Aβ in response to parameters perturbation using MRM/GSSA when parameters are perturbed to 50% (A) and 200% (B) of their basal values. The parameter indexes correspond to the indexes in Table 5.1. All parameters have minor effects on the behaviour of p53. KrelGSK3bp53 (61 in Table 5.1) is the most effectives parameter on the behaviour of Aβ when parameters are perturbed to 50% of their basal values using MRM/GSSA. KprodAbeat2 has the largest effects on the behaviour of Aβ using MRM/GSSA when parameters are perturbed to 200% of their basal values.

5.3.2 Results of LSA for plaques

LSA using ODEs shows that the behaviour of plaques is changed in response to 26 parameters when the list of parameters are perturbed to 50% and 200% of their basal values. When MRM/GSSA is used to perform LSA, plaques are sensitive to 71 parameters. Day #4 is the day that the species of plaques shows it maximum sensitivity using ODEs as shown in Figures 5.10 (A and B). From day # 4 to the end of the simulation, plaques show their maximum sensitivity in response to parameter perturbation when MRM/GSSA is used to perform LSA as shown in Figure 5.11 (A and B).

Plaques are classified to be one of the most important species of the system since it is dramatically changed in response to parameters perturbation using ODEs and MRM/GSSA.

LSA using ODEs shows that plaques are hugely affected by parameters specific p53_GSK3β and Aβ when parameters are perturbed to 50% and 200% of their basal values as shown in Table 5.4. LSA using MRM/GSSA shows that the behaviour of plaques could be dramatically changed in response to more parameters than ODEs do and these parameters are specific to different species in the system as shown in Table 5.5.

Therefore, plaques are classified to be very important species that contribute to the overall behaviour of the system and all parameters listed in Tables 5.4 and 5.5 are identified to be the most important parameters that contribute most to the variation of plaques.

Here we just show μ and σ of SV_{list} for plaques in response to parameters perturbation when parameters are perturbed to 50% and 200% of their basal values respectively using ODEs as shown in Figures 5.12 (A and B). Parameters in Tables 5.4 are indicated in Figure5.12. Parameters listed in Table 5.5 contribute most to the variation of plaques when LSA uses MRM/GSSA.

B. Maxiumum senstivity of plaques and its time in resposne to paramater pertubation using ODEs when parameters are pertubed to 50% basal values.

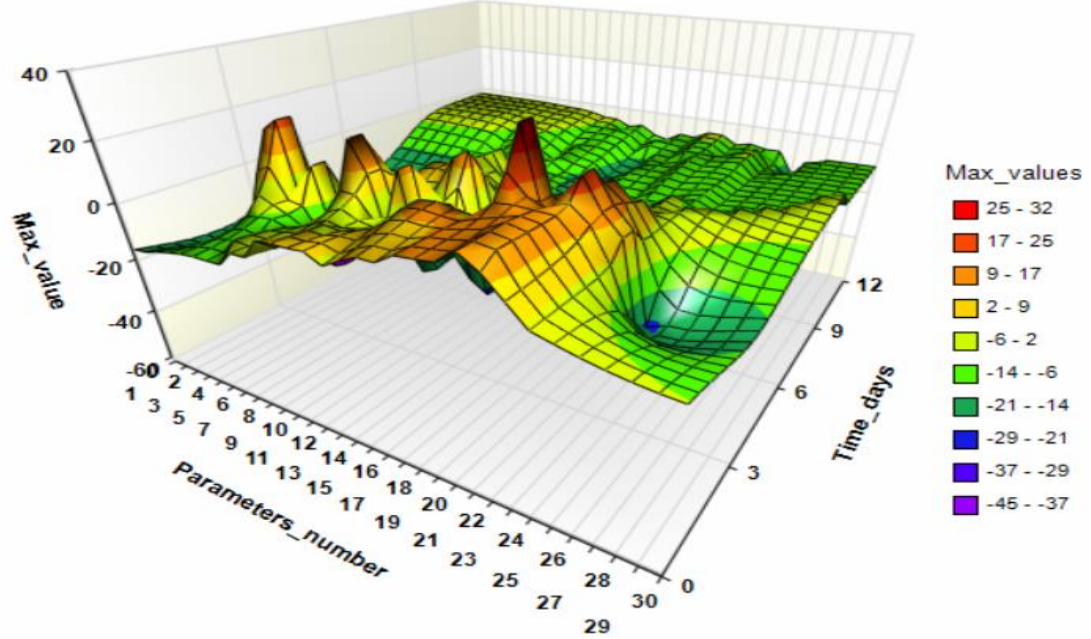

A. Maxiumum senstivity of plaques and its time in resposne to paramater pertubation using ODEs when parameters are pertubed to 200% basal values.

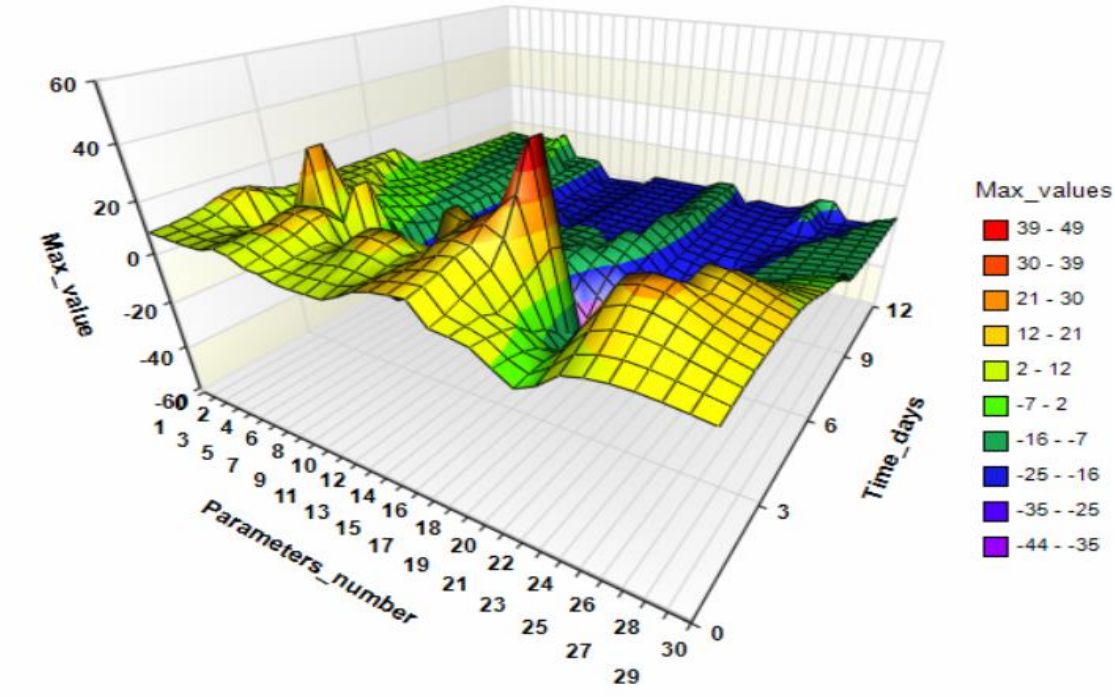

Figure 5.10: Maximum sensitivity and it's time for plaques when parameters are altered to 50% (A) and 200% (B) of their basal values using ODEs, respectively. A and B show that plaques using ODEs to perform LSA recode their maximum sensitivity in response to parameters perturbation at Day #4. Therefore, LSA using ODEs demonstrates that plaques should be observed only at day #4 in response to parameters perturbation.

A. Maxiumum senstivity of plaques and its time in resposne to paramater pertubation using MRM/GSSA when parameters are pertubed to 50% basal values.

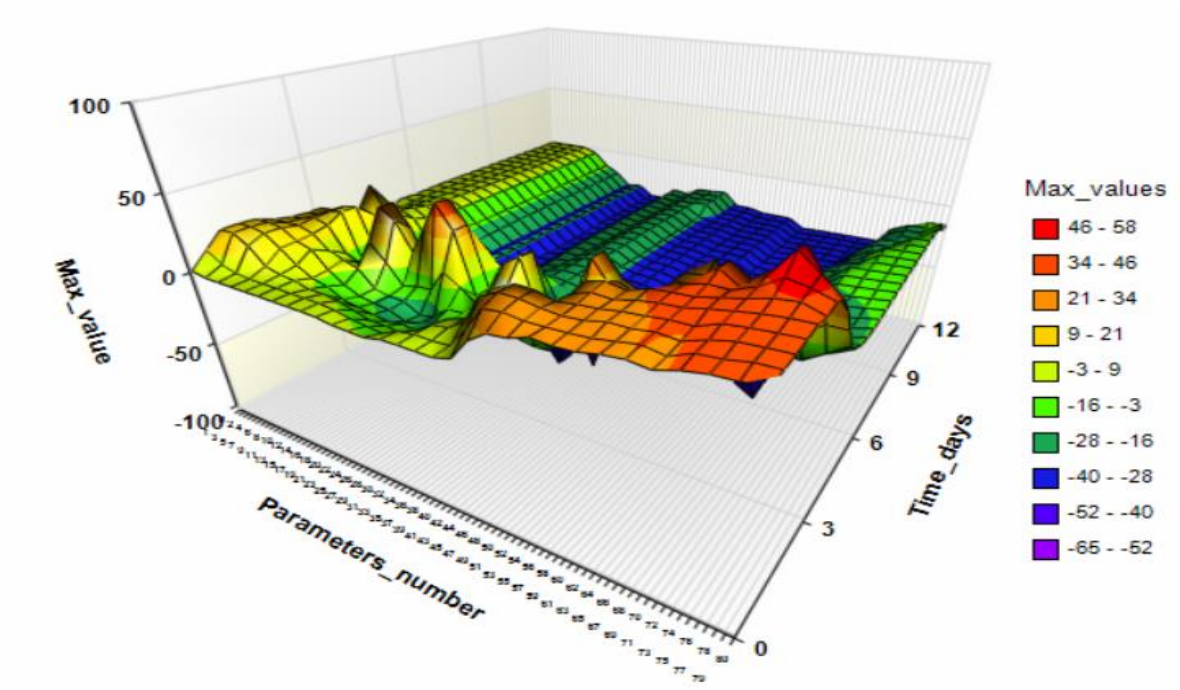

B. Maxiumum senstivity of plaques and its time in resposne to paramater pertubation using MRM/GSSA when parameters are pertubed to 200% basal values.

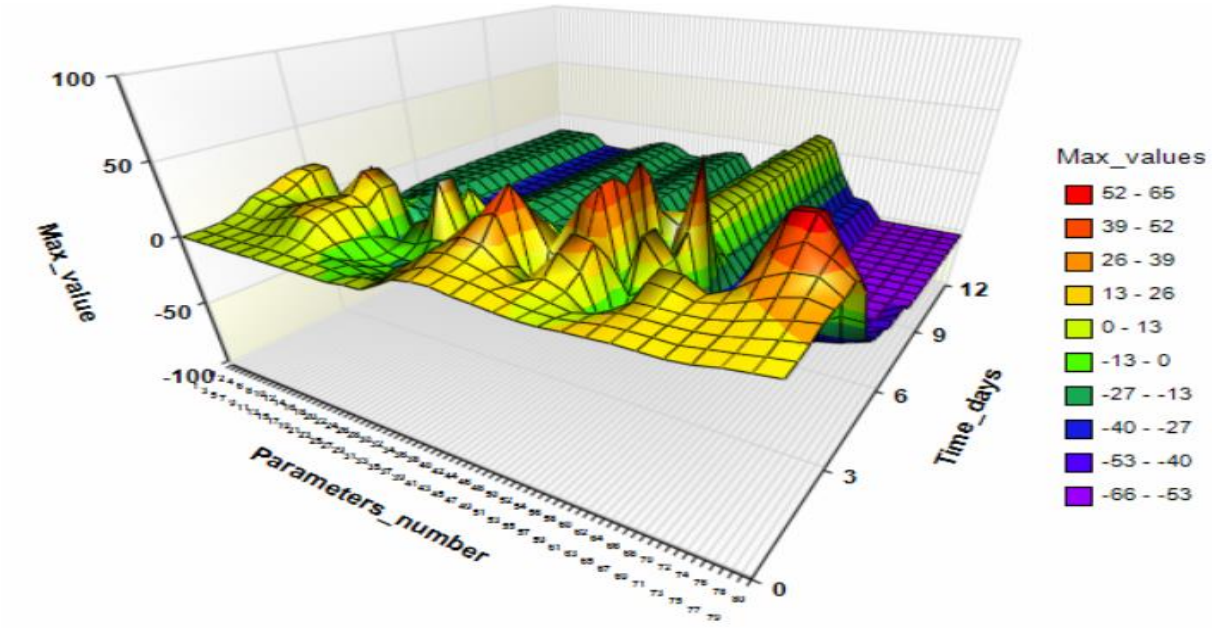

Figure 5.11: Maximum sensitivity and it's time for plaques when parameters are altered to 50% (A) and 200% (B) of their basal values using MRM/GSSA, respectively. A and B show that plaques using MRM/GSSA to perform LSA recode their maximum sensitivity in response to parameters perturbation from Day #4 to the end of the simulation.

Table 5.4: Parameters hugely affected the behaviour of plaques. LSA uses ODEs

50%			200%		
Index	Name	Status	Index	Name	Status
15	kbinGSK3bp53	↓	15	kbinGSK3bp53	↕
58	kprodAbeta2	↓	34	kdisaggAbeta1	↓
61	krelGSK3bp53	↑	50	kpghalf	↓
			58	kprodAbeta2	↕
			61	krelGSK3bp53	↓

Table 5.5: Parameters hugely affected the behaviour of plaques. LSA uses MRM/GSSA

50%			200%		
Index	Name	Status	Index	Name	Status
15	kbinGSK3bp53	↓	14	kbinE2Ub	↓
25	kdegMdm2	↓	32	kdephospTau	↓
26	kdegMdm2mRNA	↓	34	kdisaggAbeta1	↓
36	kgenROSAbeta	↓	47	kp53Ub	↓
45	kMdm2Ub	↓	49	kpg	↑
50	kpghalf	↕	50	kpghalf	↕
69	ksynp53	↓	51	kphosMdm2	↕
73	ktangfor	↑	53	kphosMdm2GSK3bp53	↓
			55	kphospTauGSK3b	↓
			63	krelMTTau	↓
			68	ksynMdm2mRNAGSK3bp53	↓
			70	ksynp53mRNA	↓
			71	ksynp53mRNAAbeta	↓

Tables 5.4 and 5.5 show that plaques are more sensitive for increasing the rates of parameters using both approaches since more parameters affect the behaviour of plaques when parameters are perturbed to 200% of their basal values.

Parameters are specific to p53_GSK3β and Aβ are the most effectiveness parameters on the behaviour of plaques when LSA uses ODEs while parameters that are specific different species in the system dramatically affect the behaviour of plaques when LSA uses MRM/GSSA as shown Table 5.5.

The results of LSA for plaques using ODEs and MRM/GSSA are summarized in Table 5.6.

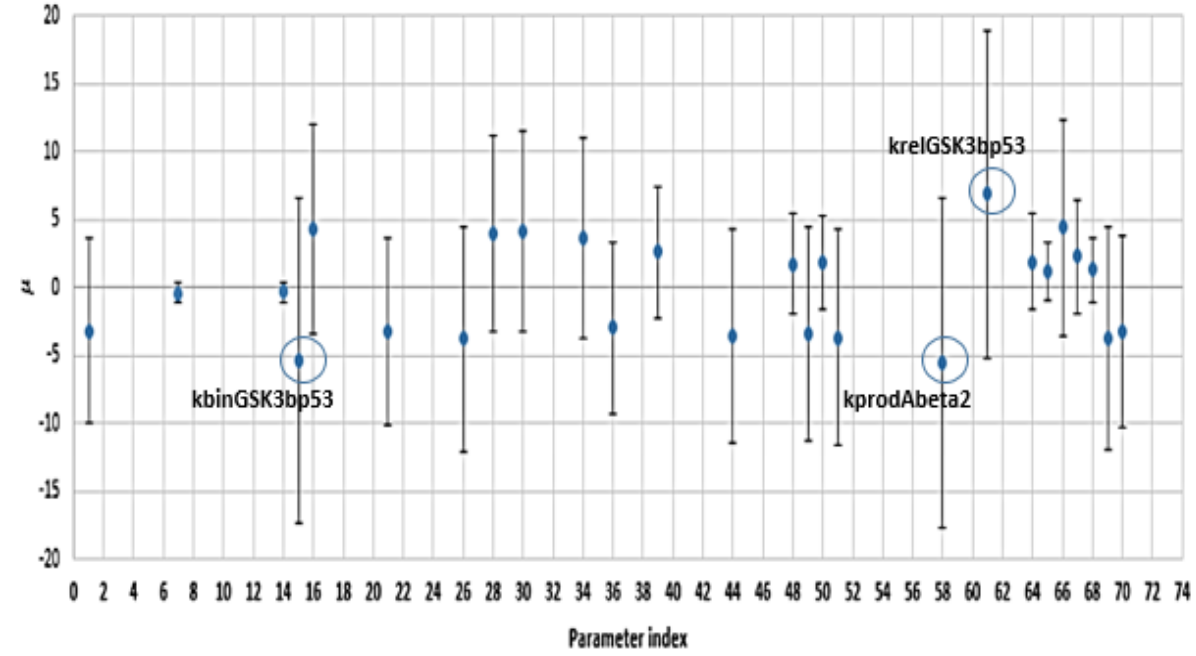

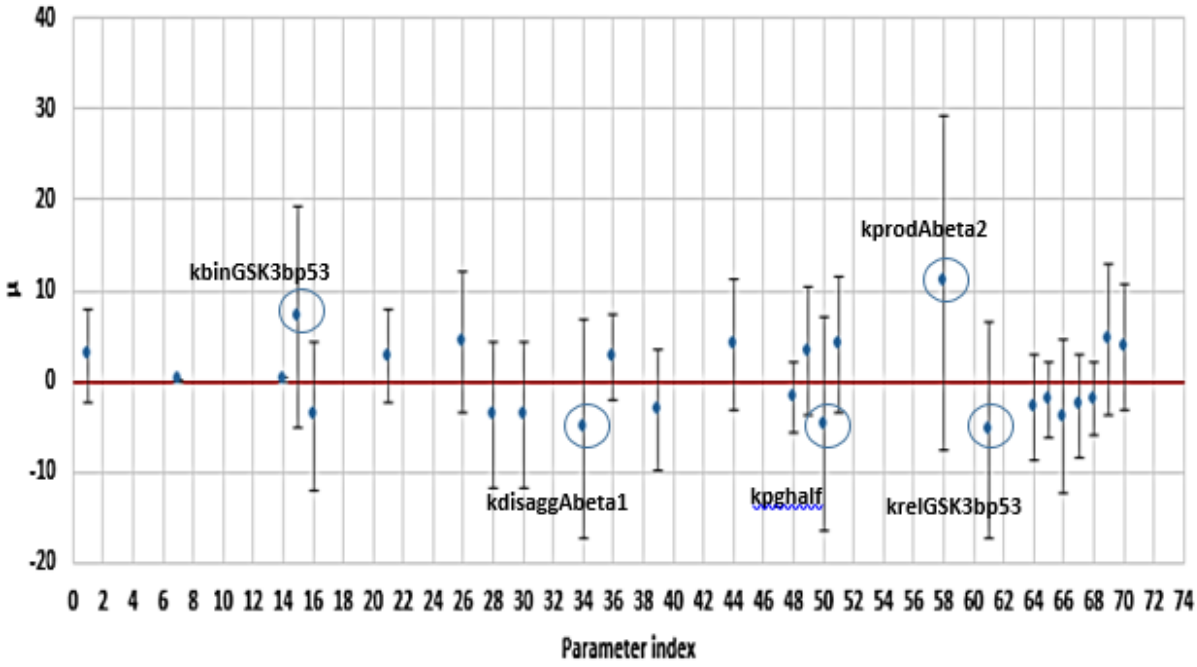

Figure 5.12: μ and σ of SV_{list} for plaques in response to parameters perturbation using ODEs when parameters are perturbed to 50% (A) and 200% (B) respectively of their basal values. The parameter indexes correspond to the indexes in Table 5.2. Parameters indicated in A and B are majorly affected the behaviour of plaques while others have only minor effect on the behaviour of plaques. KbinGSK3bp53, kprodAbeta2 and krelGSK3bp53 (15, 58 and 61 in Table 5.2) are the most important parameter that affect the behaviour of plaques using ODEs.

Table 5.6: Summary of LSA results using ODEs and MRM/GSSA for plaques. Groups A, B and C, respectively, contain parameters that have no effect, minor effects and major effects on the behaviour of these species.

Parameters are perturbed to 50% of their basal values.	**LSA Using ODEs**			**LSA Using MRM/GSSA**		
Are plaques very sensitive to perturbations?	**YES**			**YES**		
Number of parameters in each group affecting plaques	**Group A**	**Group B**	**Group C**	**Group A**	**Group B**	**Group C**
	45	**25**	**3**	**2**	**63**	**8**
Are plaques production and aggregation contributing highly to the overall system?	**YES**			**YES**		
Minimum ranges	**Group A**	**Group B**	**Group C**	**Group A**	**Group B**	**Group C**
	<= 50%		**> 50%**	**<= 50%**		**> 50%**
Parameters are perturbed to 200% of their basal values.	**LSA Using ODEs**			**LSA Using MRM/GSSA**		
Are plaques very sensitive to perturbations?	**YES**			**YES**		
Number of parameters in each group affecting plaques	**Group A**	**Group B**	**Group C**	**Group A**	**Group B**	**Group C**
	45	**23**	**5**	**2**	**57**	**14**
Are plaques production and aggregation contributing highly to the overall system?	**YES**			**YES**		
Maximum ranges	**Group A**	**Group B**	**Group C**	**Group A**	**Group B**	**Group C**
	>=200%		**< 200%**	**>=200%**		**< 200%**

LSA using ODEs and MRM/GSSA demonstrates that plaques are more sensitive to increase the rates of parameters as shown in Table 5.6. Three parameters dramatically change the behaviour of plaques when LSA uses ODEs and parameters are perturbed to 50% of their basal values while 8 parameters affect the plaques level when ODEs are used to perform LSA and parameters are perturbed to 200% of their basal values. Five and 14 parameters dramatically changed the behaviour of plaques when LSA uses MRM/GSSA and parameters are perturbed to 50% and 200% of their basal values.

5.3.3 LSA for Tangles

We select tangles from the pathway of tau dynamics and aggregation as the main species since they highly contribute to AD. The level of tangles according to Proctor et al., (2013) is initially zero and increases slightly until it reaches around 18 molecules at the end of the simulation. Proctor et al., (2013) predicts that immunisation results in small inhibitions to the level of tangles. In this section we show how parameter perturbations using ODEs and MRM/GSSA could change its

behaviour and determine the most important parameters that affect behaviour of tangles.

1- Tangles are sensitive to 28 parameters when LSA uses ODEs and 71 parameters affect the behaviour of tangles when LSA uses MRM/GSSA.
2- The last day for observing immunization in AD (day #12) recodes the maximum sensitivity on the level of tangles in ODE and MRM/GSSA when the parameters are perturbed to 50% and 200% of their basal values, as shown in Figures 5.12(A and B) and 5.13 (A and B).

Therefore, observing the behaviour of tangles in response to parameters perturbation should be done on the last day of the system using ODEs and MRM/GSSA.

Parameters that dramatically change the behaviour of tangles using ODEs and MRM/GSSA are listed in Tables 5.7 and 5.8. Tables 5.7 shows that tangles are more sensitive to decrease the rate of parameters when ODEs are used to perform LSA while same number of parameters affects the behaviour of tangles when parameters are perturbed to 50% and 200% of their basal values using MRM/GSSA as shown in Table 5.8. Table 5.8 shows that tangles are sensitive to more parameters when LSA uses MRM/GSSA.

Results of LSA using ODEs for tangles in response to parameter perturbation demonstrates that tangles are hugely affected by parameters that are specific to Mdm2. Parameters specific to different species dramatically change the behaviour of tangles when LSA uses MRM/GSSA.

Results of LSA for tangles are summarized in Table 5.9.

A. Maxiumum senstivity of tangles and its time in resposne to paramater pertubation using ODEs when parameters are pertubed to 50% basal values.

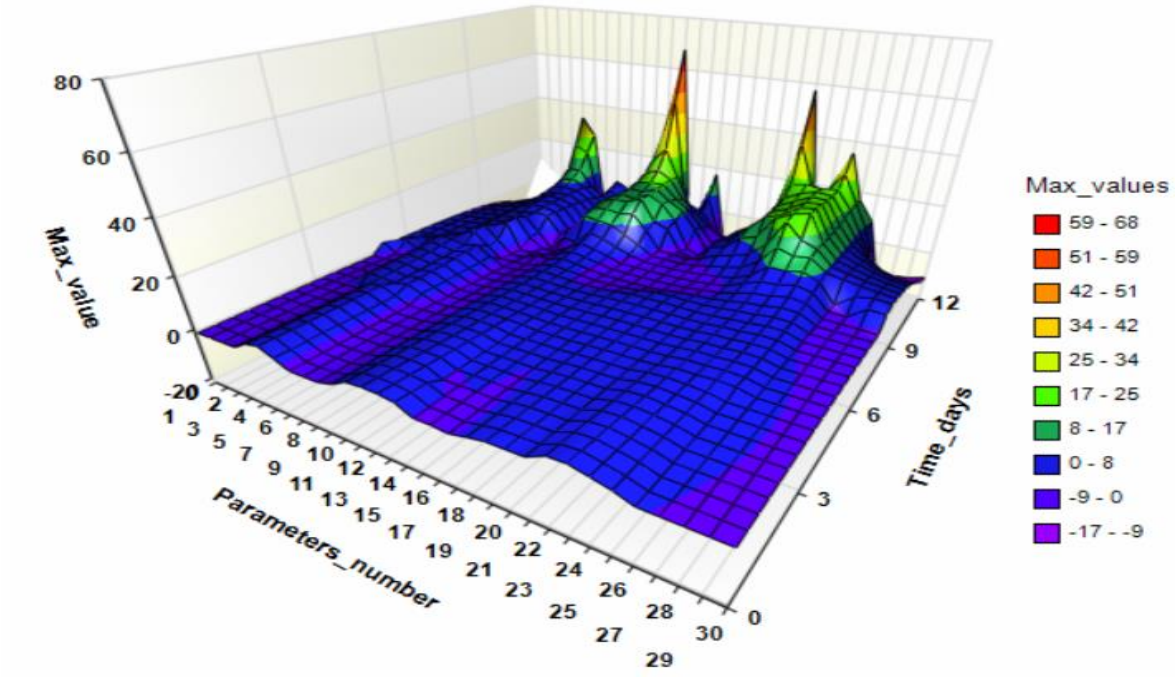

B. Maxiumum senstivity of tangles and its time in resposne to paramater pertubation using ODEs when parameters are pertubed to 50% basal values.

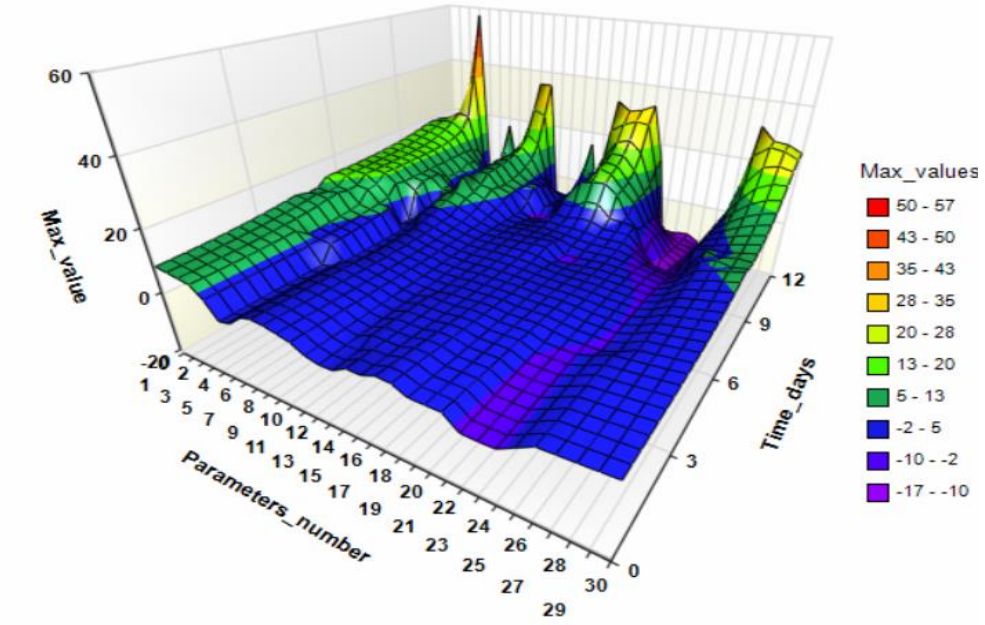

Figure 5.12: Maximum sensitivity and it's time for plaques when parameters are altered to 50% (A) and 200% (B) of their basal values using ODEs. A and B show that tangles using ODEs to perform LSA recode their maximum sensitivity in response to parameters perturbation at Day #12. Therefore, ODEs demonstrates that tangles should be observed only at the last day of the in response to parameters perturbation.

A. Maxiumum senstivity of tangles and its time in resposne to paramater pertubation using MRM/GSSA when parameters are pertubed to 50% basal values.

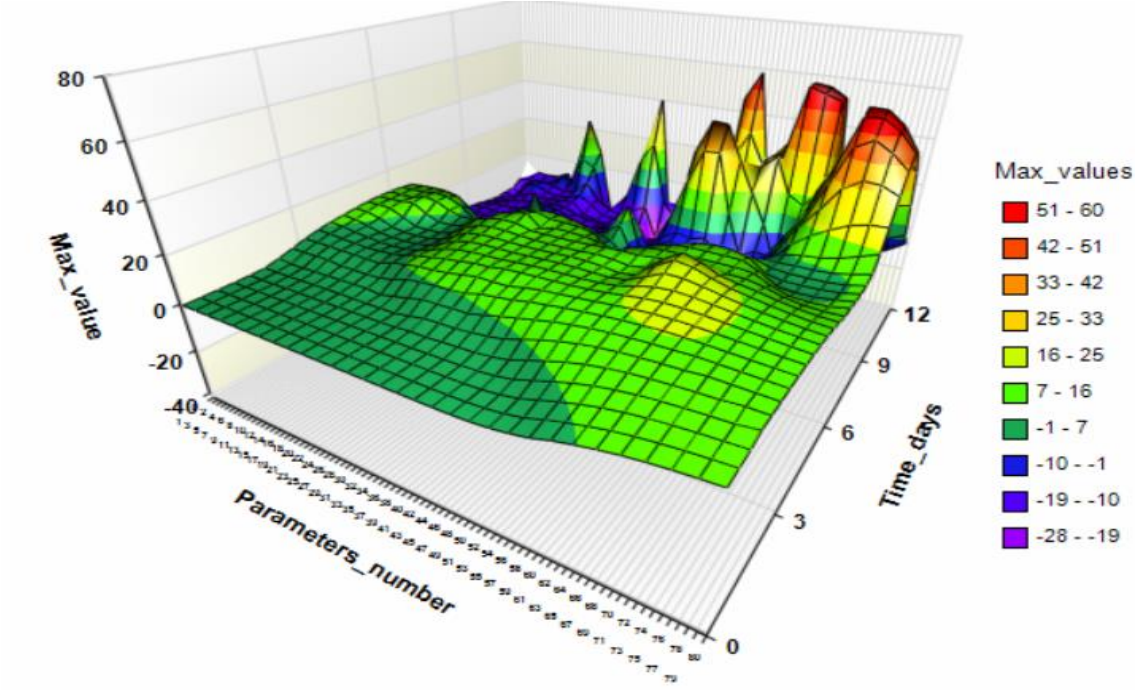

B. Maxiumum senstivity of tangles and its time in resposne to paramater pertubation using MRM/GSSA when parameters are pertubed to 200% basal values.

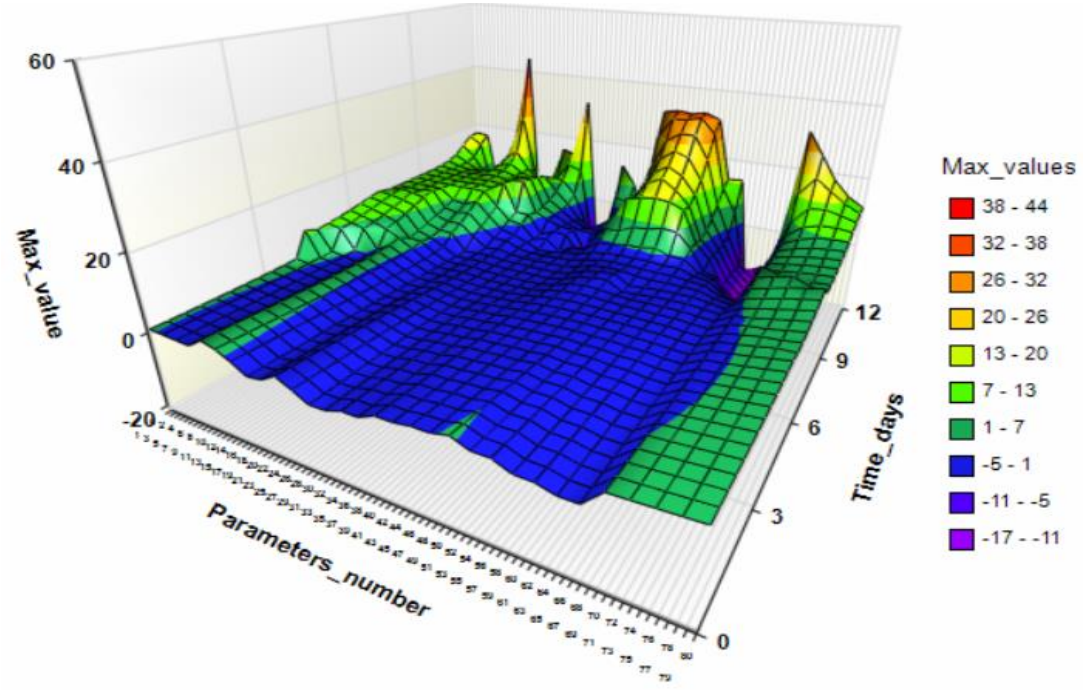

Figure 5.13: Maximum sensitivity and it's time for plaques when parameters are altered to 50% (A) and 200% (B) of their basal values using MRM/GSSA. A and B show that tangles using MRM/GSSA to perform LSA recode their maximum sensitivity in response to parameters perturbation at Day #12.

Table 5.7: Parameters are hugely affected by the behaviour of tangles. LSA uses ODEs

50%			200%		
Index	Name	Status	Index	Name	Status
15	kbinGSK3bp53	↓	15	kbinGSK3bp53	↑
16	kbinMdm2p53	↑	26	kdegMdm2mRNA	↑
17	kbinMTTau	↑	44	kMdm2PUb	↑
26	kdegMdm2mRNA	↓	51	kphosMdm2	↑
28	kdegp53mRNA	↑	69	ksynp53	↑
30	kdephosMdm2	↑	70	ksynp53mRNA	↑
32	kdephospTau	↑			
44	kMdm2PUb	↓			
51	kphosMdm2	↓			
61	krelGSK3bp53	↑			
66	ksynMdm2	↑			

Table 5.8: Parameters are hugely affected the behaviour of plaques. LSA uses MRM/GSSA

50%			200%		
Index	Name	Status	Index	Name	Status
15	kbinGSK3bp53	↓	15	kbinGSK3bp53	↑
21	kdamROS	↓	26	kdegMdm2mRNA	↑
25	kdegMdm2	↓	44	kMdm2PUb	↑
26	kdegMdm2mRNA	↓	49	kpg	↑
32	kdephospTau	↑	50	kpghalf	↑
36	kgenROSAbeta	↓	51	kphosMdm2	↑
40	kinactglia1	↓	56	kphospTauGSK3bp53	↑
44	kMdm2PUb	↓	57	kprodAbeta	↑
49	kpg	↑	58	kprodAbeta2	↑
50	kpghalf	↑	61	krelGSK3bp53	↑
61	krelGSK3bp53	↑	62	krelMdm2p53	↑
66	ksynMdm2	↑	63	krelMTTau	↑
70	ksynp53mRNA	↓	69	ksynp53	↑
73	ktangfor	↑	73	ktangfor	↑

Therefore, tangles are classified as a very important species that contribute to the overall behaviour of the system and all parameters listed in Tables 5.7 and 5.8 are identified to be the most important parameters that contribute most to the variation.

Table 5.9: Summary of LSA results for tangles using ODEs and MRM/GSSA. Groups A, B and C contain parameters, respectively, that have no effect, minor effects and major effects on the behaviour of the tangles.

Parameters are perturbed to 50% of their basal values.	**LSA Using ODEs**			**LSA Using MRM/GSSA**		
Are tangles very sensitive to perturbations?	**YES**			**YES**		
Number of parameters in each group affecting tangles	**Group A**	**Group B**	**Group C**	**Group A**	**Group B**	**Group C**
	44	**17**	**11**	**2**	**57**	**14**
Are tangles production and aggregation contributing highly to the overall system?	**YES**			**YES**		
Minimum ranges	**Group A**	**Group B**	**Group C**	**Group A**	**Group B**	**Group C**
	<= 50%		**> 50%**	**<= 50%**		**> 50%**
Parameters are perturbed to 200% of their basal values.	**LSA Using ODEs**			**LSA Using MRM/GSSA**		
Are tangles very sensitive to perturbations?	**YES**			**YES**		
Number of parameters in each group affecting tangles	**Group A**	**Group B**	**Group C**	**Group A**	**Group B**	**Group C**
	44	**22**	**6**	**2**	**57**	**14**
Are tangles production and aggregation contributing highly to the overall system?	**YES**			**YES**		
Maximum ranges	**Group A**	**Group B**	**Group C**	**Group A**	**Group B**	**Group C**
	>=200%		**< 200%**	**>=200%**		**< 200%**

5.3.4 LSA for GliaA

According to Proctor et al., (2013), glia are activated by adding antibodies to the system. GliaA is selected to be the main species in the immunization pathway because it targets the plaques to be degraded.

GliaA is sensitive to 28 parameters when LSA uses ODEs and 71 parameters to affect the behaviour of GliaA when LSA uses MRM/GSSA. GliaA as shown in Figures 5.14 (A and B) and 5.15 (A and B) records its maximum sensitivity from day # 4 until the end of the simulation using ODEs and MRM/GSSA when parameters are perturbed to 50% and 200% of their basal values.

A. Maxiumum senstivity of GliaA and its time in resposne to paramater pertubation using ODEs when parameters are pertubed to 50% basal values.

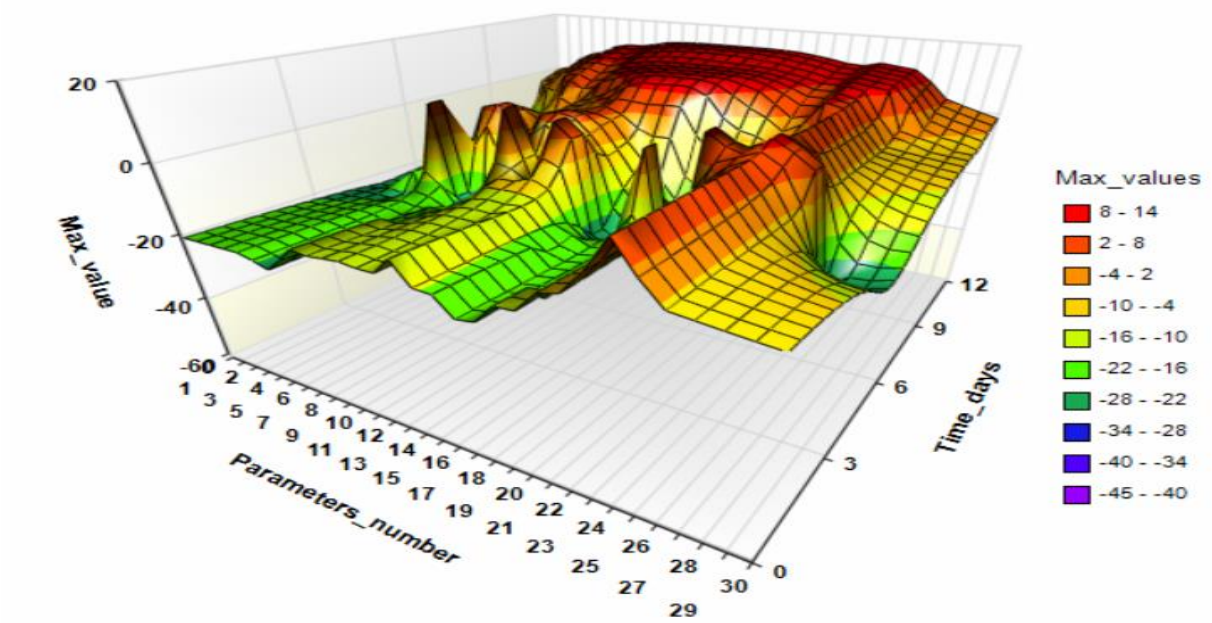

B. Maxiumum senstivity of GliaA and its time in resposne to paramater pertubation using ODEs when parameters are pertubed to 50% basal values.

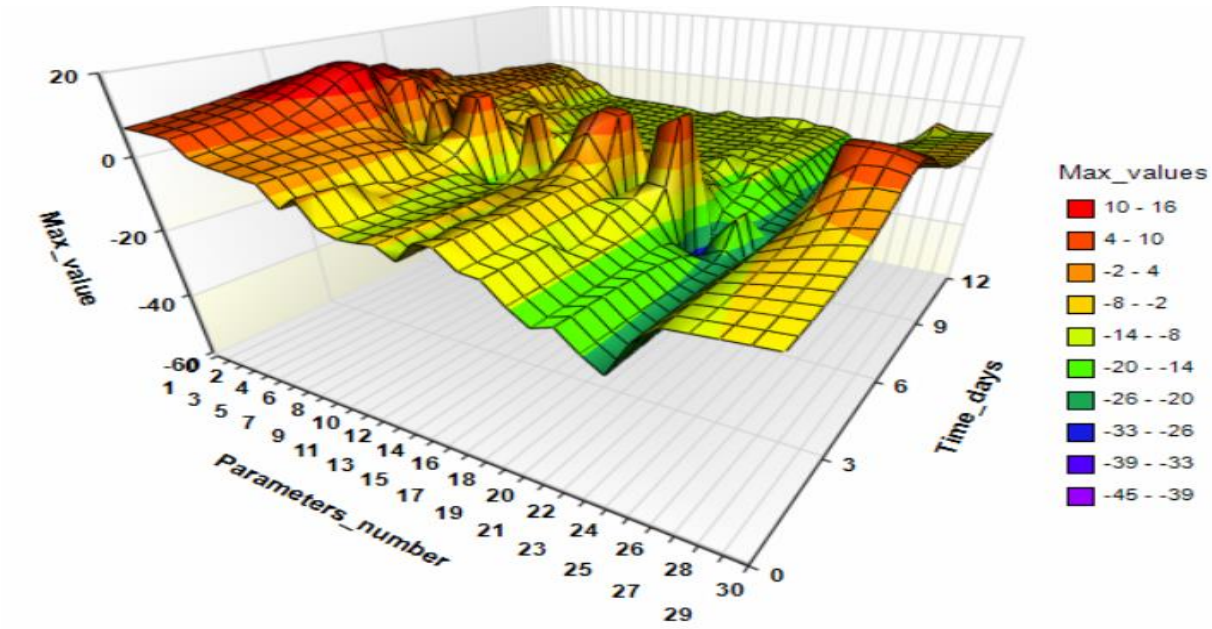

Figure 5.14: Maximum sensitivity and it's time for GliaA when parameters are altered to 50% (A) and 200% (B) of their basal values using ODEs. A and B show that GliaA using ODEs to perform LSA recodes its maximum sensitivity in response to parameters perturbation from day #4 to the end of the simulation.

A. Maxiumum senstivity of GliaA and its time in resposne to paramater pertubation using MRM/GSSA when parameters are pertubed to 50% basal values.

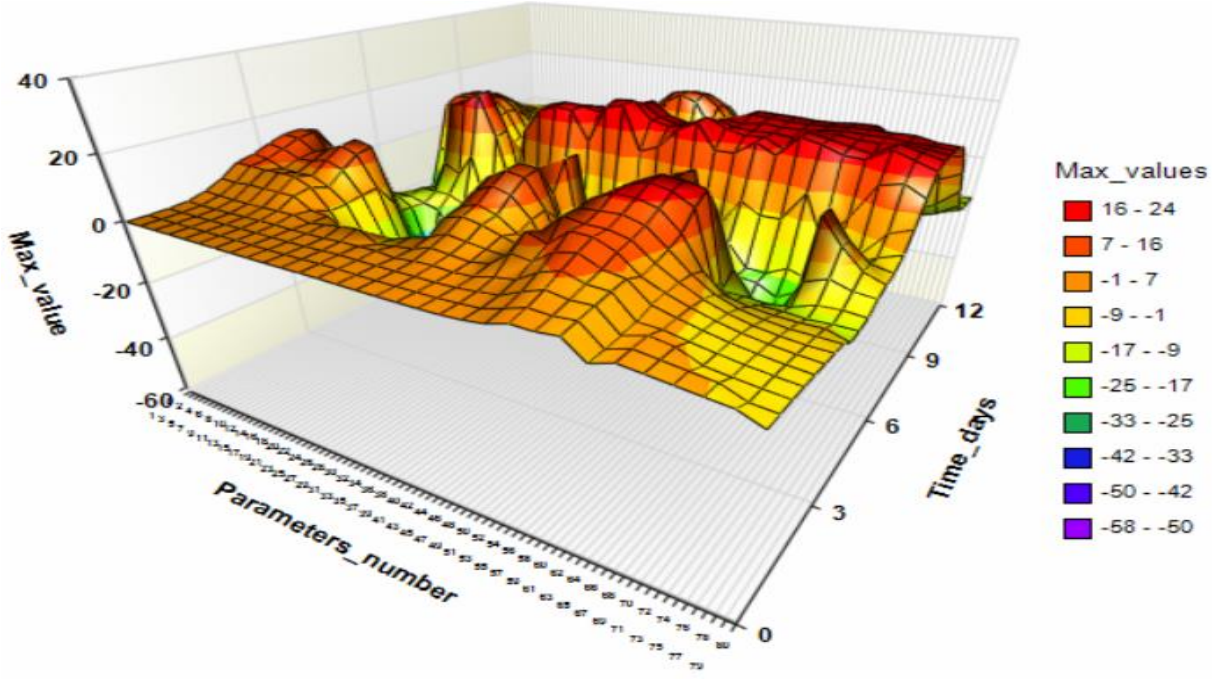

B. Maxiumum senstivity of GliaA and its time in resposne to paramater pertubation using MRM/GSSA when parameters are pertubed to 200% basal values.

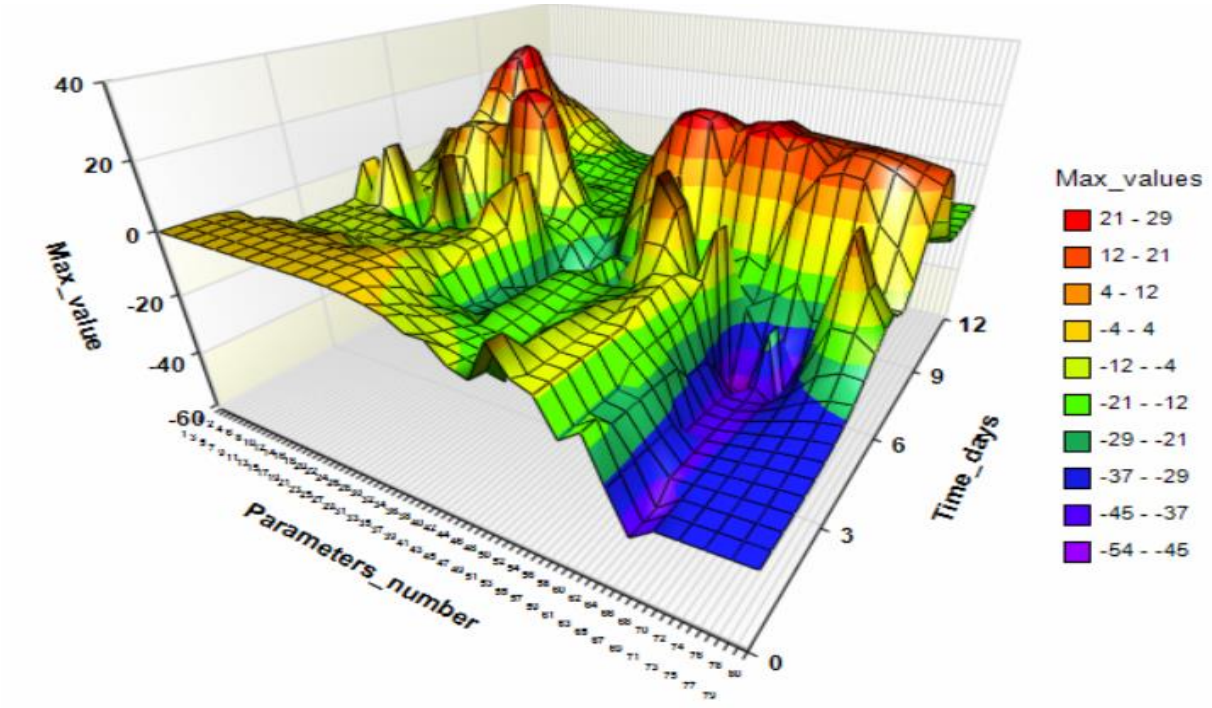

Figure 5.15: Maximum sensitivity and it's time for GliaA when parameters are altered to 50% (A) and 200% (B) of their basal values using MRM/GSSA. A and B show that GliaA using MRM/GSSA to perform LSA recodes its maximum sensitivity in response to parameters perturbation from day #4 to the end of the simulation.

When parameters are perturbed to 50% of their basal values, LSA using ODEs shows that that only two parameters significantly change the behaviour of GliaA. These parameters are kbinGSK3bp53 and kprodAbeta2 (15 and 58 in Table 5.2). These two parameters kept the level of GliaA at nearly zero for the whole time of the system. Whereas, GliaA is dramatically decreased in response to 6 parameters listed in Table 5.10 when LSA uses MRM/GSSA.

When parameters are perturbed to 200% of their basal values, LSA using ODEs shows that 6 parameters shown in Table 5.11 significantly change the behaviour of GliaA. These parameters also kept the level of GliaA is nearly zero for the whole time of the system. Whereas, 13 parameters are kept the level GliaA is zero listed in Table 5.12 when LSA uses MRM/GSSA.

Table 5.10: Parameters decreased the level of GliaA to around zero when LSA uses MRM/GSSA and parameters are perturbed to 50% of their basal value.

Parameter index	Parameter name
21	kdamROS
25	kdegMdm2
26	kdegMdm2mRNA
36	kgenROSAbeta
45	kMdm2Ub
69	ksynp53

Table 5.11: Parameters dramatically decrease the level of GliaA when LSA uses ODEs and parameters are perturbed to 200% of their basal value

Parameter	Parameter name	Parameter	Parameter name
16	kbinMdm2p53	34	kdisaggAbeta1
28	kdegp53mRNA	50	kpghalf
30	kdephosMdm2	61	krelGSK3bp53

Table 5.12: Parameters dramatically decrease the level of GliaA when LSA uses MRM/GSSA and parameters are perturbed to 200% of their basal value

Parameter index	Parameter name
3	kactDUBp53
14	kbinE2Ub
19	kbinTauProt
32	kdephospTau
34	kdisaggAbeta1
45	kMdm2Ub
47	kp53Ub
53	kphosMdm2GSK3bp53
55	kphospTauGSK3b
63	krelMTTau
68	ksynMdm2mRNAGSK3bp53
70	ksynp53mRNA
71	ksynp53mRNAAbeta

It has been found that GliaA is more sensitive for increasing the rate of parameters since more parameters affects its behaviour when parameters are perturbed to 200% of their basal values. Parameters specific to p53 and Mdm2 are more affected than others on the behaviour of GliaA when LSA uses ODEs and MRM/GSSA.

Table 5.13: Summary of LSA results for tangles using ODEs and MRM/GSSA. Groups A, B and C contain parameters, respectively, that have no effect, minor effects and major effects on the behaviour of GliaA.

Parameters are perturbed to 50% of their basal values.	**LSA Using ODEs**			**LSA Using MRM/GSSA**		
Is GliaA very sensitive to perturbations?	**YES**			**YES**		
Number of parameters in each group affecting tangles	**Group A**	**Group B**	**Group C**	**Group A**	**Group B**	**Group C**
	44	**26**	**2**	**2**	**65**	**6**
Is GliaA production and aggregation contributing highly to the overall system?	**YES**			**YES**		
Minimum ranges	**Group A**	**Group B**	**Group C**	**Group A**	**Group B**	**Group C**
	<= 50%		**> 50%**	**<= 50%**		**> 50%**
Parameters are perturbed to 200% of their basal values.	**LSA Using ODEs**			**LSA Using MRM/GSSA**		
Is GliaA very sensitive to perturbations?	**YES**			**YES**		
Number of parameters in each group affecting tangles	**Group A**	**Group B**	**Group C**	**Group A**	**Group B**	**Group C**
	44	**22**	**6**	**2**	**58**	**13**
Is GliaA production and aggregation contributing highly to the overall system?	**YES**			**YES**		
Maximum ranges	**Group A**	**Group B**	**Group C**	**Group A**	**Group B**	**Group C**
	>=200%		**< 200%**	**>=200%**		**< 200%**

Therefore, LSA using ODEs and MRM/GSSA demonstrates that GliaA is one of the most important species that contributes to the overall behaviour of the system when parameters are perturbed to 50% and 200% of their basal values. KbinGSK3bp53 and kprodAbeta2 and parameters listed in Tables 5.10, 5.11 and 5.12 are identified to be the most important parameters that contribute most to the variation.

5.4 Summary

LSA using ODEs and MRM/GSSA classifies that:

1- The behaviour of p53, ATMA and p53_GSK3β are not dramatically changed in response to parameter perturbations whether parameters are perturbed to 50% or 200% of their basal values. As a result of this classification, we identify that p53 regulation, the DNA damage pathway and GSK3β activity have no effect on the overall behaviour of the system.
2- The differences between ODEs and MRM/GSSA are the number of parameters that affect the behaviour of these species and time for the maximum sensitivity of these species.
3- LSA using ODEs shows that p53 is more sensitive to parameters that are specific to Mdm2 while when LSA uses MRM/GSS, parameters specific to Aβ are more effectiveness on the behaviour of p53. ATMA and p53_GSK3β are more sensitive to KinactATM (1 in Table 5.1) when LSA uses ODEs and parameters are perturbed to 50% and 200%.
4- LSA using MRM/GSSA demonstrates that ATMA and p53_GSK3β are more sensitive parameters specific to p53 and Mdm2 such as ksynp53, kbinE2Ub, ksynMdm2 (69, 14 and 66 in Table 5.1) when parameters are perturbed to 50% of their basal values. Parameter specific to Aβ such as kpg and KprodAbeta2 and Kpghalf (49, 50 and 58 in Table 5.1) have more effects than others on the behaviour of ATMA and p53_GSK3β when parameters are perturbed to 200%.
5- Aβ is also not dramatically changed in response to parameters perturbation and it doesn't contribute to the overall behaviour of the system. However, Aβ production and aggregation is classified as an important pathway since

plaques are dramatically changed in response to parameters perturbation using ODEs and MRM/GSSA. It was really interesting to find that KrelGSK3bp53 and KprodAbeta2 is the most effectiveness parameter on the behaviour of Aβ using respectively ODEs and MRM/GSSA when parameters are perturbed to 50% and 200% of their basal values, respectively.

6- LSA using ODEs and MRM/GSSA classifies that the behaviour of plaques, tangles and GliaA are not dramatically changed in response to parameter perturbations weather parameters are perturbed to 50% or 200% of their basal values. As a result of this classification, we identify that Aβ production and aggregation, tau dynamics and aggregation, and the immunisation pathway hugely affect the overall behaviour of the system. The only difference between ODEs and MRM/GSSA is that the number of parameters that affect the behaviour of plaques, tangles and GliaA.

7- Parameters are specific to p53_GSK3β and Aβ are the most effectiveness parameters on the behaviour of plaques when LSA uses ODEs while parameters that are specific different species in the system dramatically affect the behaviour of plaques when LSA uses MRM/GSSA. LSA using ODEs for tangles in response to parameter perturbation demonstrates that tangles are hugely affected by parameters that are specific to Mdm2 when parameters are perturbed to 50% of their basal value. In general, tangles are hugely affected by parameters that are specific to Mdm2, p53, Aβ tau and p53_GSK3β. GliaA is affected by parameters specific to different species in the system.

Chapter 6
Latin Hypercube Sampling and Partial Rank Correlation Coefficient (LHS/PRCC) Analysis Applied to Immunization in an AD Model

6.1 Overview

Chapter 5 discussed the results of LSA using ODEs and MRM/GSSA. However, LSA only considers changes to one parameter at a time while all the other parameters remain fixed at their base values. LSA methods do not accurately assess uncertainty and sensitivity in biochemical systems. GSA techniques, therefore, are needed to demonstrate how a multi-dimensional parameter space can be studied to accurately assess uncertainty and sensitivity in biochemical systems.

The combination of LHS and PRCC makes a powerful tool that employs a minimum number of computer simulations for uncertainty analysis to explore the entire parameter space of a model. The main goal of this tool is to identify key parameters whose uncertainties contribute to prediction imprecision and rank these parameters by their importance in contributing to the imprecision. Specifically, LHS/PRCC provides a measure of monotonicity between the LHS parameters and the outcomes measured after the removal of the linear effect of the LHS parameters (inputs), x_i, and the output measure (outputs), y.

Therefore, this tool is used to deterministically and stochastically using ODEs and MRM/GSSA to: (1) explore the entire parameter space of immunization in the AD model and measure the monotonicity between model's parameters and the outcome; and (2) rank all parameters in this model.

Here, we assess the effect of uncertainty and sensitivity on the behaviour of the main players used in Chapter 5 (p53, ATMA, p53_GSK3β, plaques, tangles and GliaA) using LHS/PRCC at three different time points (days #4, #8 and # 12). These time points are chosen because we want to assess how the system behaves in response to perturbations on the day of immunization and after immunization.

The LHS matrix and simulation results for the selected species in response to a combination of the LHS parameters are generated for both approaches (ODEs and

MRM/GSSA) using visual studio (C# platform). Ranking the LHS matrix and the results of the selected species are achieved by developing a C# program. Data produced after the ranking process was statistically analysed using the IBM SPSS statistics tool.

6.2 Performing the LHS

For immunization in the AD model, 73 LHS parameters, as shown in Table 5.1, are identified. Probability distributions are assigned to the parameters, the intervals in the distribution are divided into 100 equiprobable regions, and these intervals are then sampled without replacement. Thus, the parameter space for the LHS parameters has a dimension of length 73 with each dimension specifying an uncertain parameter vector of length 100. Fifty per cent and 200% are determined to be minimum and maximum values for each of the 73 parameters.

A sample LHS matrix/table for parameter immunization in the AD model is illustrated in Figure 6.1. Note that for this matrix, each column has an entry (P_i, S_j) and the jth sampled random value of the ith parameter, where $1 \leq j \leq k, 1 \leq i \leq N$. Each row in the table contains k samples corresponding to a specific LHS parameter.

		S_1	S_2	S_3	S_4	S_5	S_6	S_7	.....
kactATM	P_1	0.000101	5.23E-08	1.30E-07	0.000156	6.26E-07	7.75E-07	5.17E-06	.....
kactDUBMdm2	P_2	0.000192	6.44E-08	8.63E-08	8.59E-05	3.46E-07	7.02E-07	4.44E-06	.....
kactDUBp53	P_3	0.000138	7.95E-08	1.50E-07	5.91E-05	6.83E-07	9.84E-07	4.95E-06	.....
kactDUBProtp53	P_4	0.000179	1.91E-07	1.09E-07	8.48E-05	4.71E-07	3.73E-07	3.41E-06	.....
kactglia1	P_5	7.47E-05	1.48E-07	1.23E-07	7.93E-05	7.75E-07	5.15E-07	3.11E-06	.....
Kactglia2	P_6	6.46E-05	6.74E-08	1.04E-07	0.000104	9.24E-07	7.99E-07	4.67E-06	.....
kaggAbeta	P_7	0.000169	1.93E-07	1.72E-07	0.000146	4.10E-07	7.10E-07	1.94E-06	.....
kaggTau	P_8	0.000142	8.31E-08	1.00E-07	0.000144	1.18E-06	6.58E-07	2.96E-06	.....
.	.	.	.	.	.	.	.	.	.....
.	.	.	.	.	.	.	.	.	.....

Figure 6.1: Sample LHS matrix/table

6.3 Interpreting the Monotonicity Plots

As discussed in Chapters 2 and 3, PRCC measures the strength of the relationship between two variables while the effect of the other variables is controlled. This is achieved by indicating the degree of monotonicity between a specific input variable and outputs. Only output measures having a monotonic relationship with the input variables should be chosen for this LHS/RPCC.

Consequently, we verify that there is a monotonic relationship between the values of the selected species and the LHS parameters at the level of ODEs and MRM/GSSA. To investigate the level of monotonicity for the LHS test parameter, kactATM (P_1) in Figure 1 and p53; as an example, we pick its row from the LHS matrix and run simulations using its values from that row and the baseline values for all other parameters. This results in M simulations for this monotonicity test. Figure 6.2 (A and B) shows that monotonicity exists between kactATM and p53 using ODEs and MRM/GSSA.

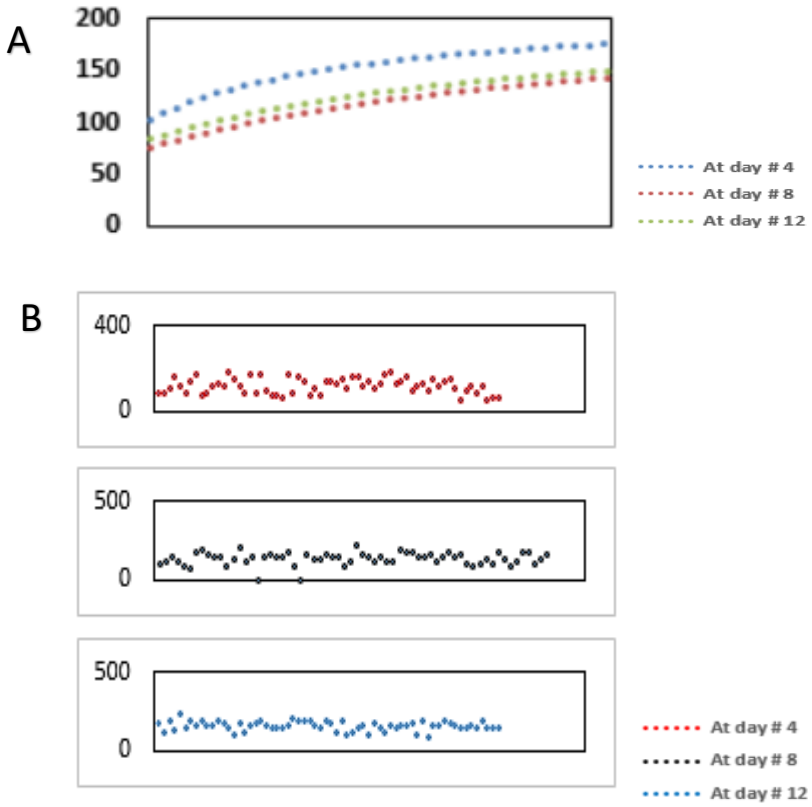

Figure 6.2: Sample monotonicity plot of kactATM for p53 using ODEs (A) and MRM/GSSA (B) at days #4, #8 and #12.

Monotonicity plots of each parameter in the LHS for each of the selected species are shown in the next sections. Note, PRCC values and p-values for all parameters for each species are shown in Appendix D. Here we just show the PRCC values for parameters that have the strongest correlation with the selected species.

6.4 Handling the PRCC steps

Once the LHS parameter ranges are adjusted and the final version of the LHS matrix is generated, PRCC analysis is able to be used. All the k values in each column in the LHS matrix are used as input values for the numerical simulation of the model. The non-parametric partial rank correlation coefficients are then used to determine the most sensitive parameters. How parameter values are selected per run is demonstrated in Figure 6.3.

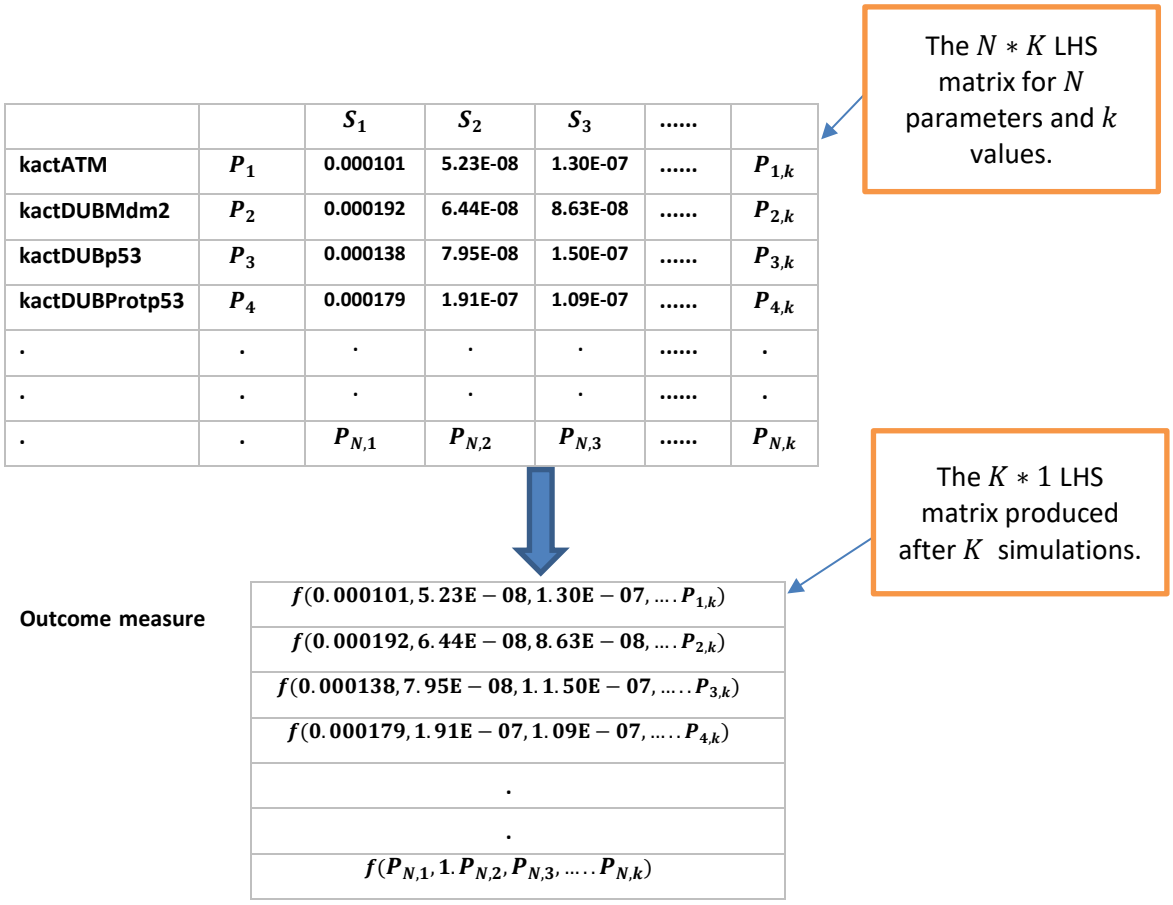

Figure 6.3: How parameter values are selected per run

PRCC is used to answer the question about which parameters contribute most uncertainty to model predications. A parametric procedure is applied to the rank the data instead of the data themselves. The ranking is undertaken simply by arranging the values of our data in order and then assigning the largest values to be 1 and the next largest value to be 2, etc. The transformation usually results in uniform residuals for the transformed variables.

Hence, to perform PRCC, we first rank the LHS matrix and then the matrix for the outcome measure using a sort routine. For each parameter and each outcome measure, two linear regression models are found, the first representing the ranked parameter in terms of the other ranked parameter values, and the second, representing the ranked outcome measures in terms of the other ranked parameter values. A Pearson correlation coefficient (PCC) for the residuals from those two regression models gives the PRCC value for that specific parameter (see Equations (1) and (2) in (Marino et al., 2008)). The PRCC steps using kbinGSK3bp53 as a parameter of interest, and p53 at day #8 as an example, are illustrated in Figure 6.3.

A Pearson correlation coefficient for the residuals from those two regression models gives the PRCC value for that specific parameter. To assess the level of uncertainty the LHS parameter contributes to the model, a partial rank correlation analysis equips us with PRCC and the corresponding p-values. Parameters with a large PRCC (<-0.5 or >0.5) with correspondingly small p-values are the most important parameters that contribute uncertainty to the model.

The next seven sections show the level of uncertainty from the LHS parameters on the behaviour of the selected species (p53, ATMA, GSK3β, Aβ, plaques, tangles and GliaA).

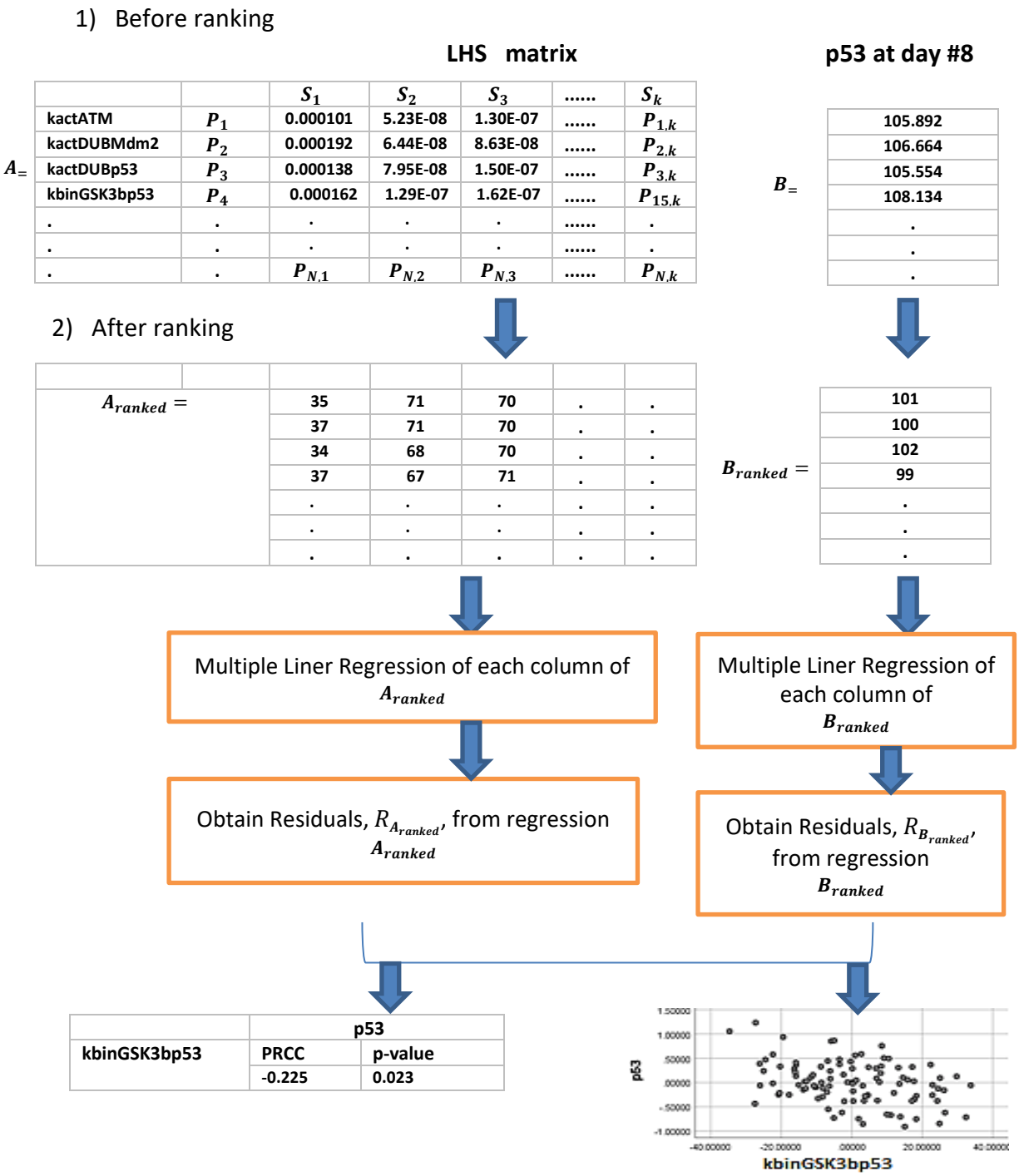

Figure 6.4: An Illustration of the PRCC steps. KbinGSK3bp53 is the parameter of interest and p53 at day #8 is an example. LHS and the outcome matrix are ranked, then multiple linear regressions on each of the ranked columns in each matrix are performed. Residuals from the regressions are used to find the PRCC value and the p-value and to plot the results.

6.5 Results of LHS/PRCC for p53

The plots in Figure 6.5 show the behaviour of p53 over 12 days corresponding to the parameter combinations of the LHS scheme using ODEs (A) and MRM/GSSA (B). Vertical lines (red lines in the plots) indicate the time points where we calculate the level of uncertainty from the LHS parameters (days #4, #8 and #12).

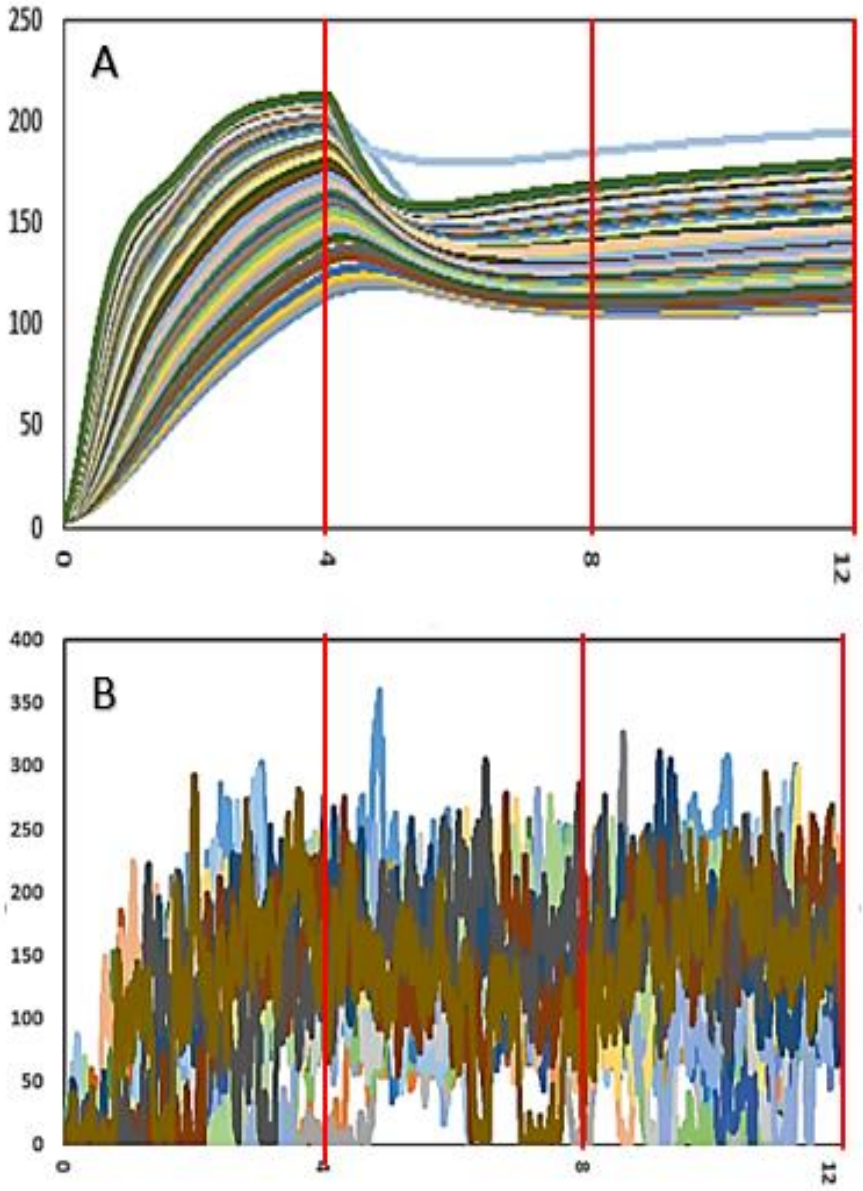

Figure 6.5: Behaviour of p53 over 12 days corresponding to the parameter combinations of the LHS scheme using ODEs (A) and MRM/GSSA (B). Days 4, 8 and 12, indicated by the vertical lines (red lines), are used as time points to compute the level of uncertainty from the LHS parameters on the behaviour of p53. The behaviour of p53 is not dramatically changed in response to the combination of LHS parameters using ODEs and MRM/GSSA.

To measure the strength of the relationship between p53 and each parameter in the LHS matrix, we first verify that a monotonic relationship exists between p53 and the LHS parameters. Figures 6.6 and 6.7 verify that a monotonic relationship exists between p53 and the LHS parameters using ODEs and MRM/GSSA, respectively.

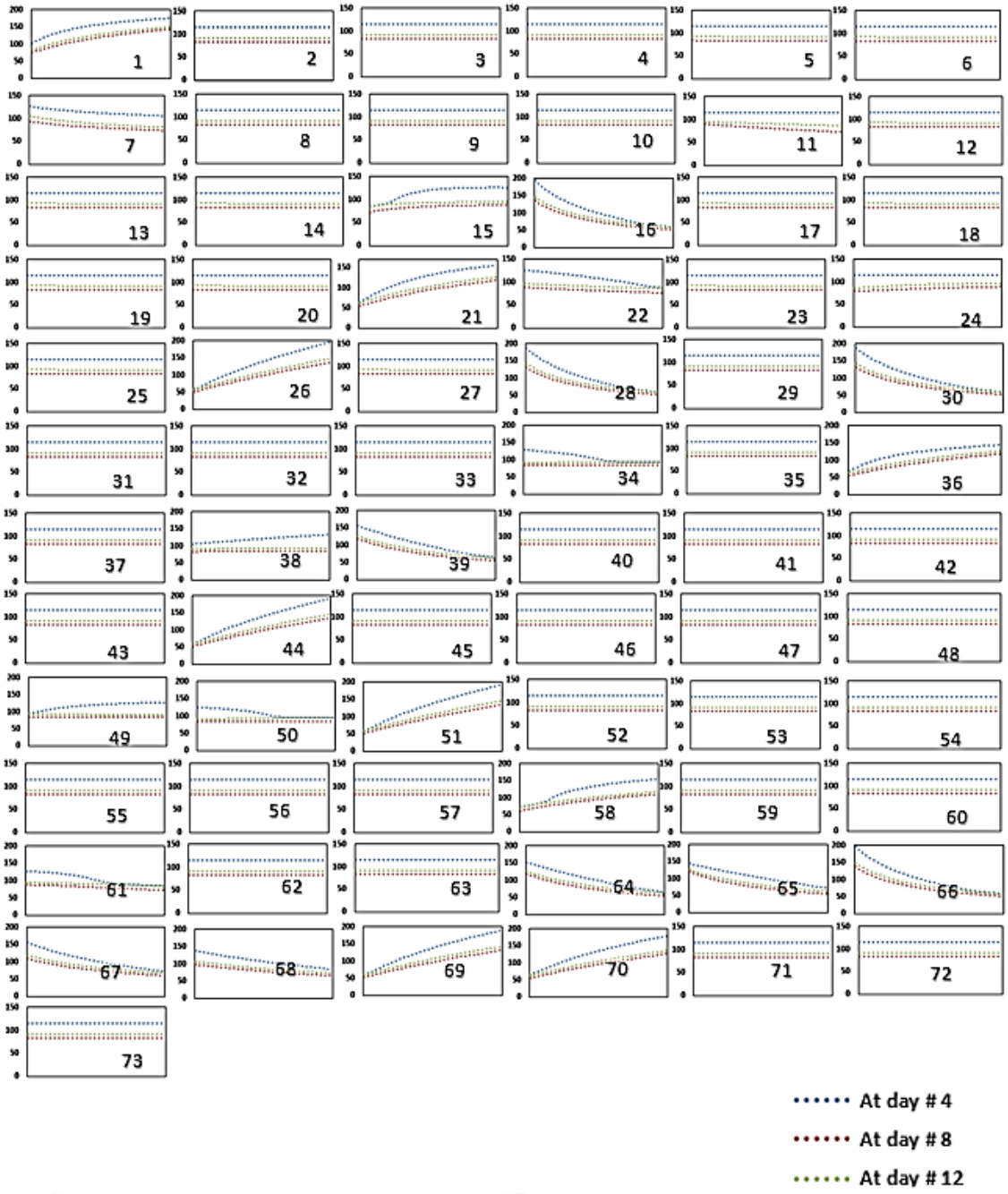

Figure 6.6: Monotonicity plots of all parameters in the LHS matrix for p53 using ODEs at times t = 4, 8 and 12 (days). Numbers shown in the plots correspond to the parameter indexes in Table 5.2.

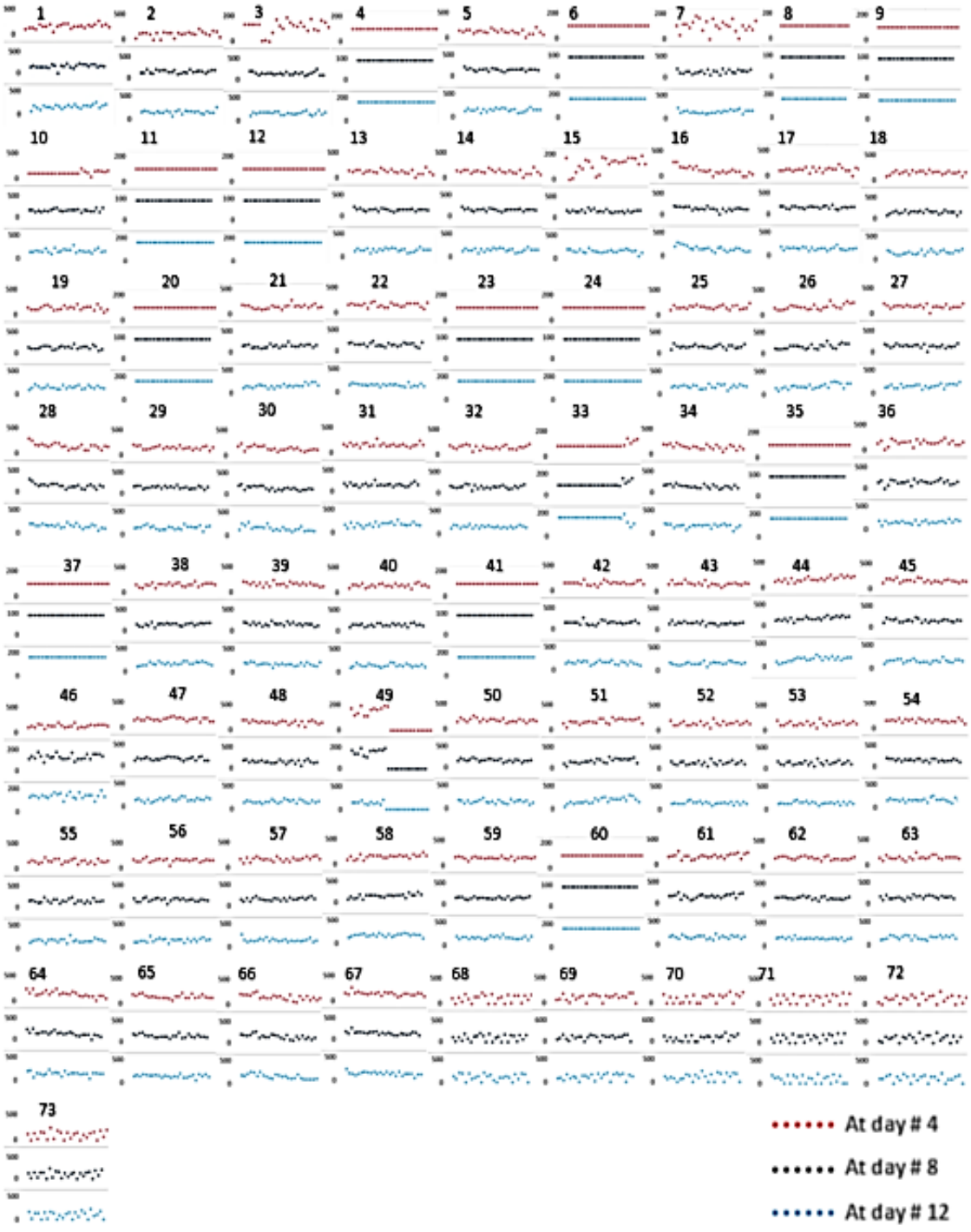

Figure 6.7: Monotonicity plots of all parameters in the LHS matrix for p53 using MRM/GSSA at times t = 4, 8 and 12 (days). Numbers shown above the figures correspond to the parameter indexes in Table 5.2.

PRCC analysis using ODEs and MRM/GSSA shows that none of the parameters in the LHS matrix has a strong correlation with p53 at all time points. Tables 6.1 and 6.2 list the sub-sets of parameters from ODEs and MRM/GSSA that have the largest correlation with p53. The output from PRCC analysis for all parameters is listed in Table 1 in Appendix D.

Table 6.1: Output from PRCC analysis for p53 using ODEs

Index	Parameter name	At day # 4
		PRCC
21	kdamROS	0.204
39	kinactATM	0.210
Index	Parameter name	At day # 8
		PRCC
15	kbinGSK3bp53	-0.305
35	kdisaggAbeta2	0.277
Index	Parameter name	At day # 12
		PRCC
16	kbinMdm2p53	-0.387
14	kbinE2Ub	0.226

Table 6.2: Output from PRCC analysis for p53 using MRM/GSSA

Index	Parameter name	At day # 4
		PRCC
16	kbinMdm2p53	-0.411
64	kremROS	0.230
Index	Parameter name	At day # 8
		PRCC
11	kbinAbantiAb	0.407
71	ksynp53mRNAAbeta	0.219
Index	Parameter name	At day # 12
		PRCC
36	kgenROSAbeta	-0.247
16	kbinMdm2p53	-0.371

Figure 6.8 (A and B) shows the PRCC output for three test parameters from each method. In A, we show the PRCC output for kinactATM, kbinGSK3bp53 and kbinMdm2p53 when PRCC uses ODEs. In B, we show the PRCC output when it uses MRM/GSSA for kbinMdm2p53, kbinAbantiAb and kbinMdm2p53. Note that

in the plots, the y-axis corresponds to the regression coefficients for p53 while the x-axis represents regression coefficients parameters.

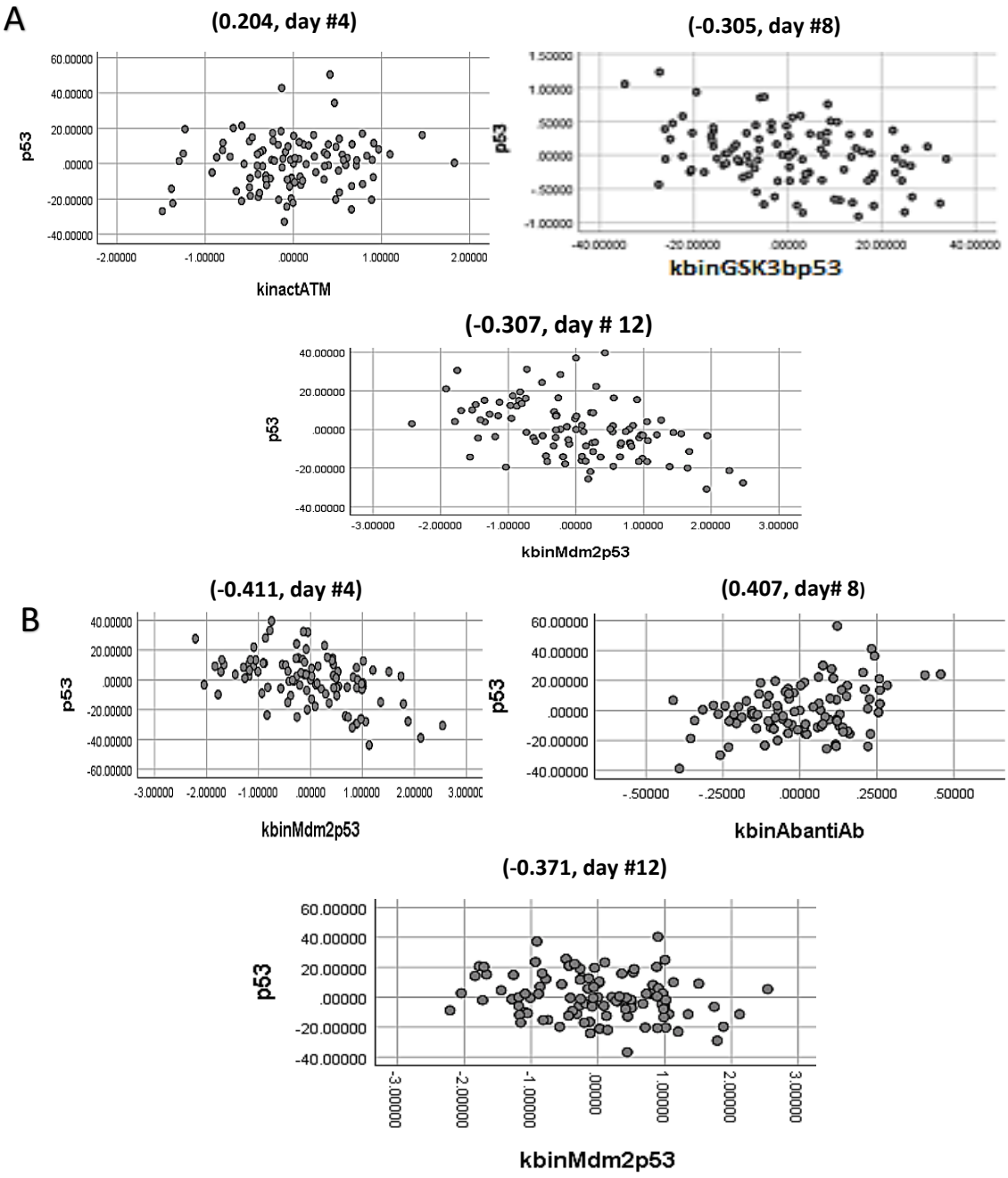

Figure 6.8: PRCC plots for p53 using ODEs (A) and MRM/GSSA (B). A and B show the plots of the parameters that have the largest correlation with p53 using ODEs and MRM/GSSA. The values of PRCC and their time points are shown in brackets above the plots. PRCC analysis using ODEs demonstrates that kbinMdm2p53 (16 in Table 5.2) is the most important parameter that affects the behaviour of p53. In addition to kbinMdm2p53, PRCC illustrates that kbinAbantiAb (11 in Table 5.2) is also important for p53 at day #8 using MRM/GSSA.

6.6 Results of LHS/PRCC for ATMA

ATMA is the second species that we are interested in checking its behaviour over the parameter space of the mode. Figure 6.9 A and B shows the behaviour of ATMA using the 100 values in the LHS matrix from ODEs and MRM/GSSA respectively, over 12 days.

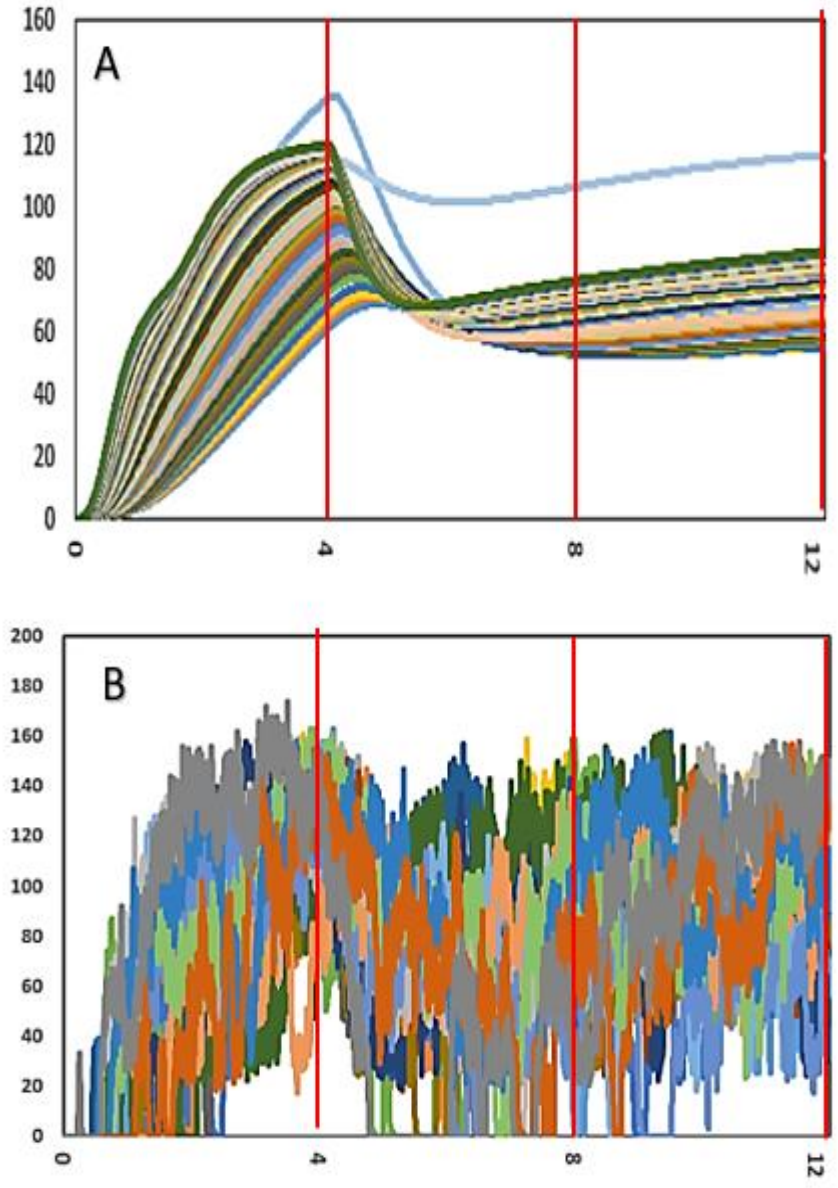

Figure 6.9: Behaviour of ATMA over 12 days corresponding to the parameter combinations of the LHS scheme using ODEs (A) and MRM/GSSA (B). Days 4, 8 and 12 are indicated by the vertical lines (red lines) used as time points to compute the level of uncertainty from the LHS parameters on the behaviour of ATMA. The behaviour of ATMA does not change very much in response to the combination of the LHS parameters using ODEs and MRM/GSSA.

In Figure 6.10 we verify that there is a monotonic relationship between ATMA and all parameters in the LHS matrix when PRCC uses ODEs, while Figure 6.11 verifies that a monotonic relationship exists between ATMA and all parameters when RPCC uses MRM/GSSA.

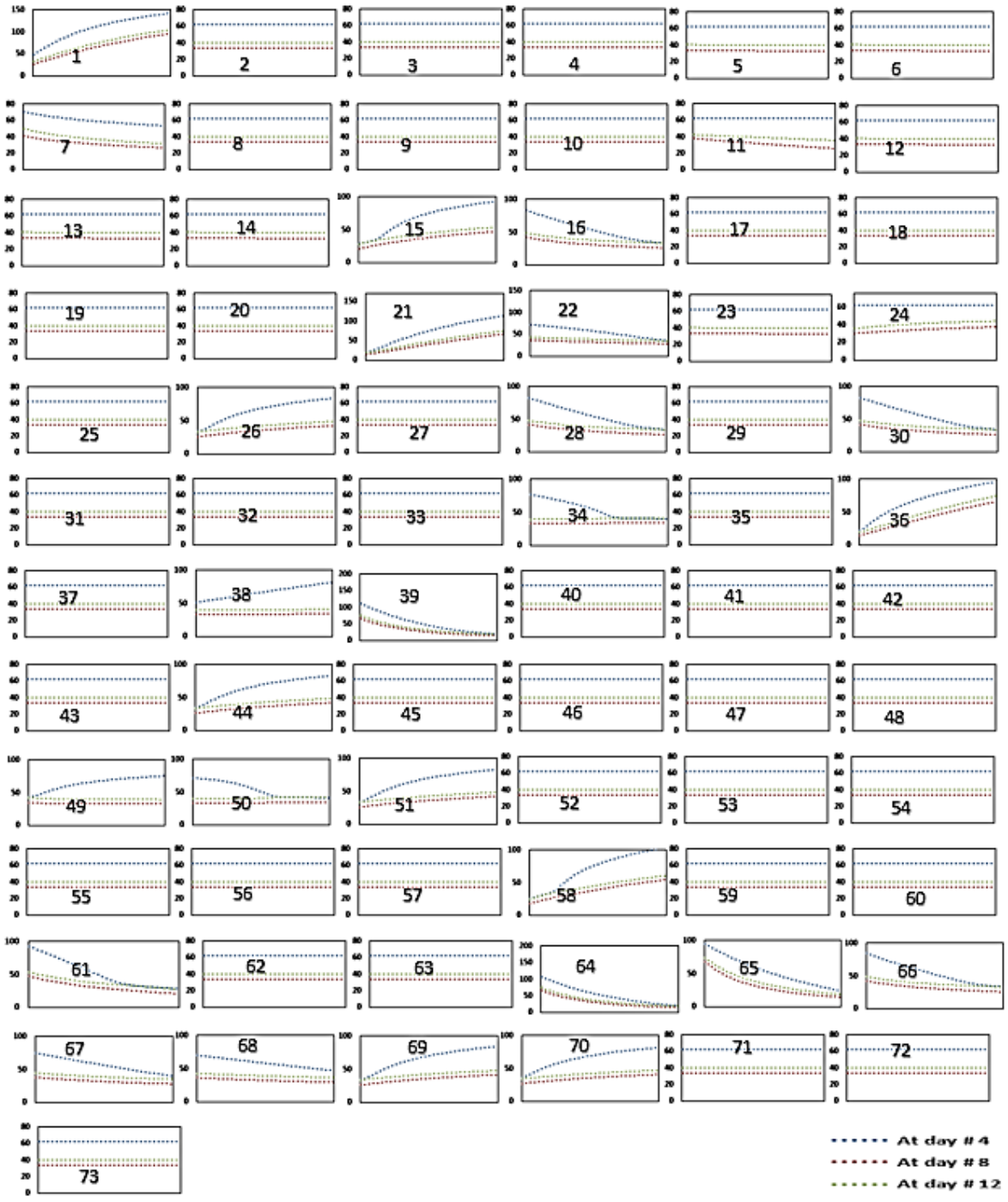

Figure 6.10: Monotonicity plots of all parameters in the LHS matrix for ATMA using ODEs at times t = 4, 8 and 12 (days). Numbers shown in the figures correspond to the parameter indexes in Table 5.2.

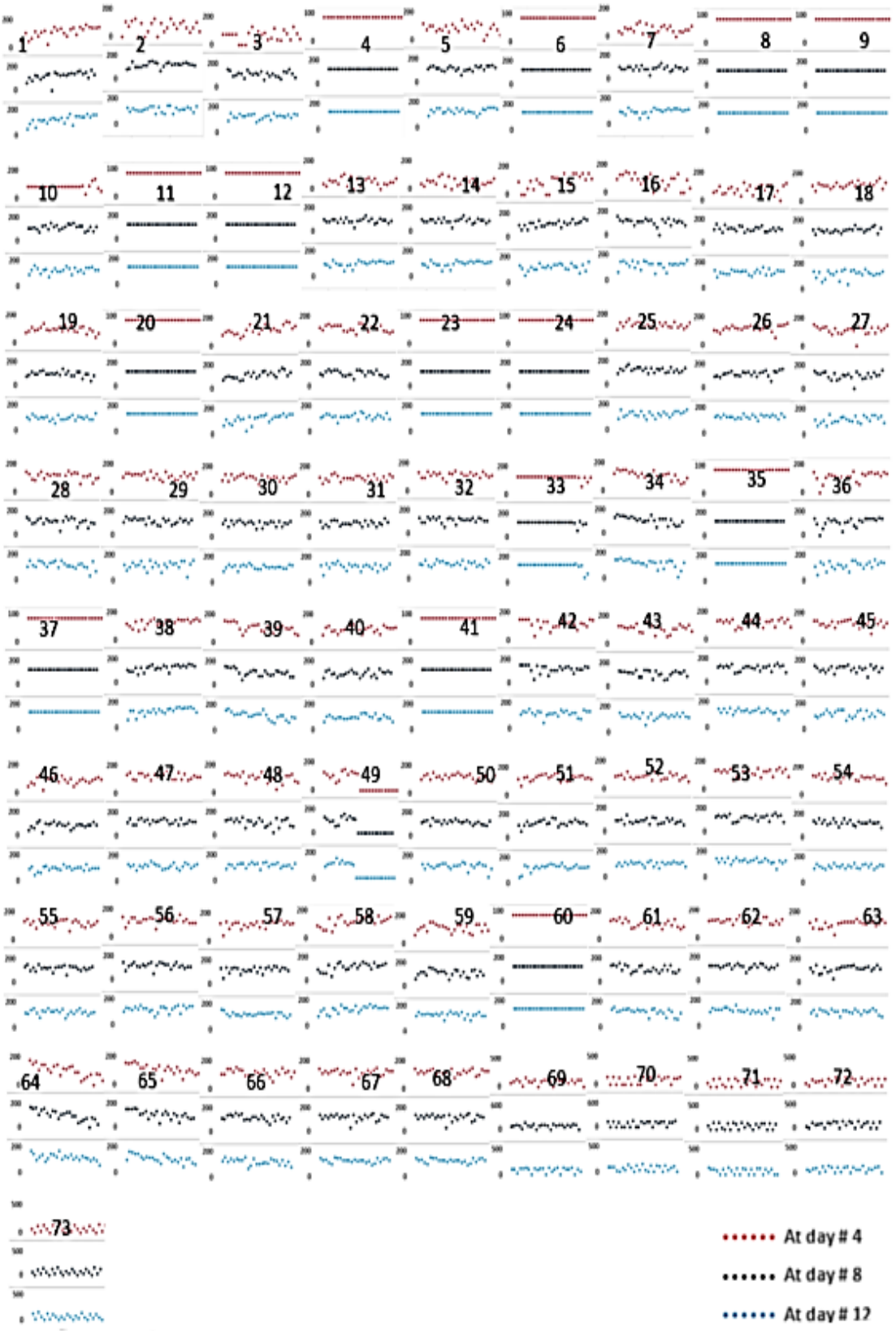

Figure 6.11: Monotonicity plots of all parameters in the LHS matrix for ATMA using MRM/GSSA at times t = 4, 8 and 12 (days). Numbers shown above the figures correspond to the parameter indexes in Table 6.1.

The results of PRCC analysis using ODEs shows that only kbinMdm2p53 (16 in Table 5.2) has a strong correlation with ATMA at all the time points selected, while ksynp53mRNAAbeta (71 in Table 5.2) shows a strong correlation with ATMA at day #12 when PRCC uses MRM/GSSA. Tables 6.1 and 6.2 show the two most effective parameters at each time point on the behaviour of ATMA using ODEs and MRM/GSSA, respectively.

Table 6.3: Output from PRCC analysis for ATM using ODEs

Index	Parameter name	At day # 4
		PRCC
16	kbinMdm2p53	-0.501
13	kbinE1Ub	0.228
Index	Parameter name	At day # 8
		PRCC
16	kbinMdm2p53	-0.508
13	kbinE1Ub	0.218
Index	Parameter name	At day # 12
		PRCC
16	kbinMdm2p53	-0.560
13	kbinE1Ub	0.223

Table 6.4: Output from PRCC analysis for ATM using MRM/GSSA

Index	Parameter name	At day # 4
		PRCC
5	Kactglia1	-0.231
29	KdegTau20Port	0.221
Index	Parameter name	At day # 8
		PRCC
45	KMdm2Ub	-0.293
72	ksynTau	0.219
Index	Parameter name	At day # 12
		PRCC
36	Kdegp53mRNA	0.402
71	Ksynp53mRNAAbeta	0.502

Using ODEs, kbinMdm2p53 is the strongest parameter that affects the behaviour of ATMA over the whole period of the system, while Ksynp53mRNAAbeta is the only parameter that strongly affects the behaviour of ATMA when PRCC uses MRM/GSSA.

Figure 6.12 (A and B) shows the PRCC outputs from ODEs and MRM/GSSA. In A, we show the PRCC output only for kbinMdm2p53 at days #4 and #12 because this is the only parameter that has a strong correlation with ATMA. In B, we show the PRCC output for Kactglia1 at day #4, KMdm2Ub at day #8, and Ksynp53mRNAAbeta at day #12.

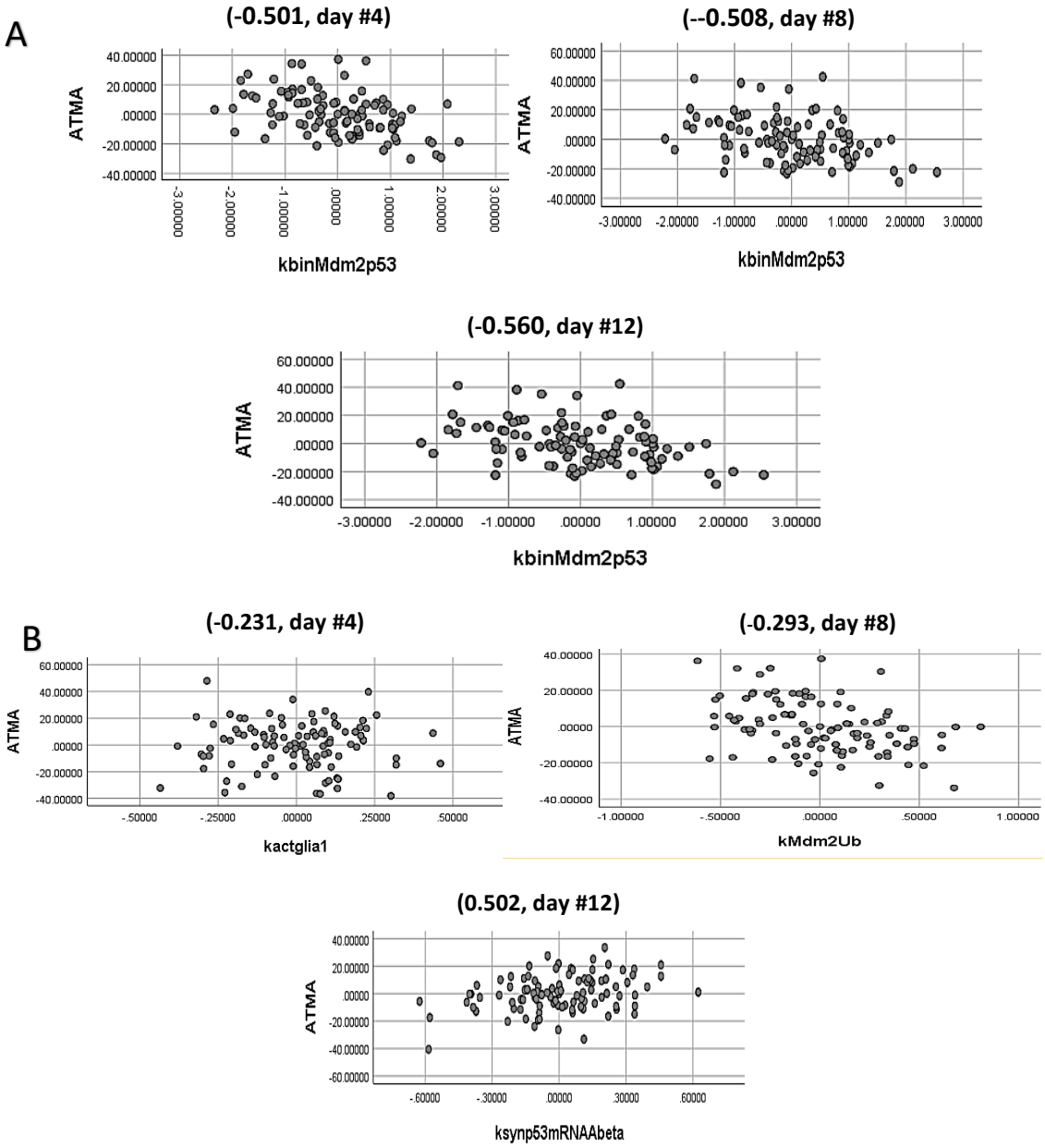

Figure 6.12: PRCC plots for ATMA using ODEs (A) and MRM/GSSA (B). (A) Shows plots of kbinMdm2p53 at days #4, #8 and #12 since it has the strongest correlation with ATAM. (B) Shows the plots of kactglia, kMdm2Ub and Ksynp53mRNAAbeta (5, 45 and 71 in Table 5.1). RPCC using MRM/GSSA shows that ATMA is only affected by Ksynp53mRNAAbeta while kactglia and kMdm2Ub have minor effects the behaviour of ATMA. The values of PRCC and time point are shown in brackets above the plots.

6.7 Results of LHS/PRCC for p53_GSK3β

p53_GSK3β is the main player in GSK3β activity and is considered to be one of the most important species in the system since it activates not only the activity of Aβ production and aggregation but also tau dynamics and aggregation, as shown in Figure 3.2. Therefore, it has been chosen to be analysed using LHS/PRCC. Figure 6.13 (A and B) shows the behaviour of p53_GSK3β using the 100 values in the LHS matrix from ODEs and MRM/GSSA, respectively, over 12 days.

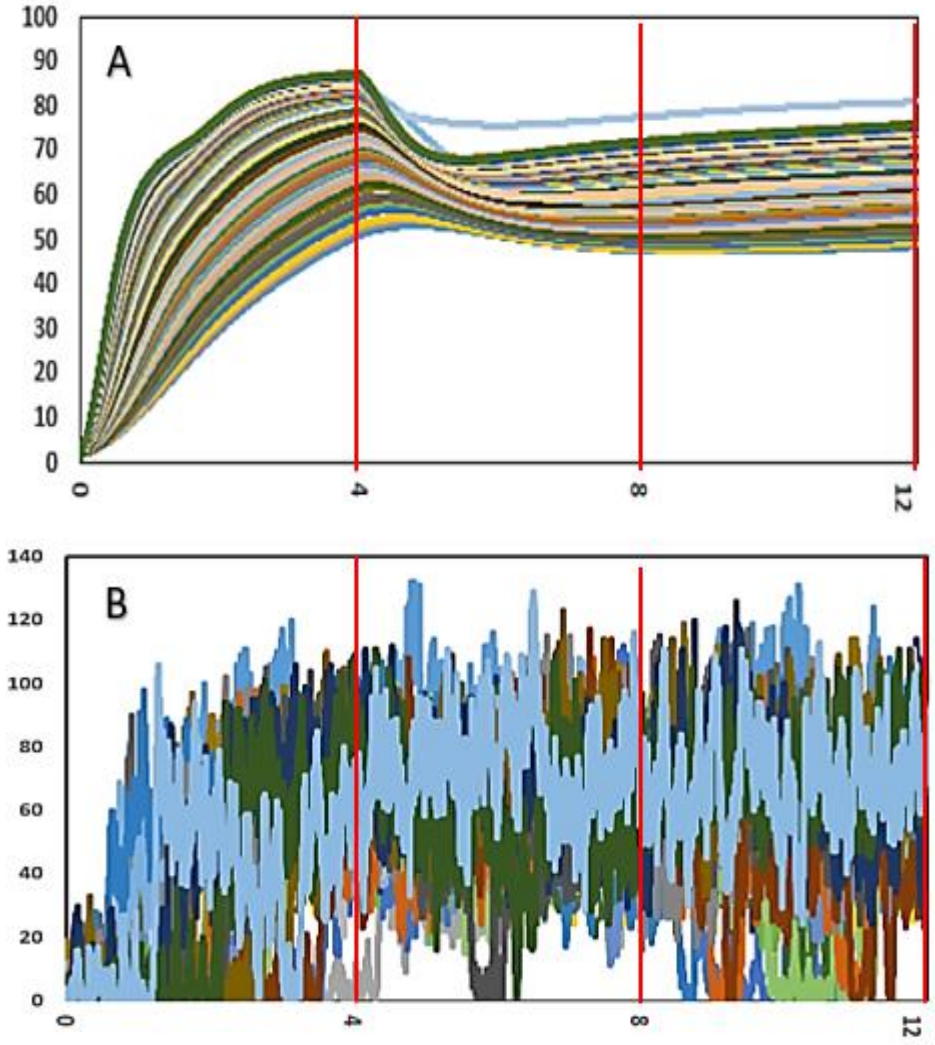

Figure 6.13: Behaviour of p53_GSK3β over 12 days corresponding to the parameter combinations of the LHS scheme using ODEs (A) and MRM/GSSA (B). Days 4, 8 and 12, indicated by the vertical lines (red lines), are used as time points to compute the level of uncertainty from the LHS parameters on the behaviour of p53_GSK3β. ODEs illustrate that the level of p53_GSK3β decreases when the rates of the parameters in the LHS matrix decrease while its level increases in response to the increasing rates of these parameters. MRM/GSSA shows a different time point for p53_GSK3β to start increasing in response to the parameter combinations in the LHS matrix.

The monotonic relationship between p53_GSK3β and the parameters in the LHS matrix is verified using ODEs and MRM/GSSA. Figures 6.14 and 6.15 show the monotonicity plots of all LHS parameters and p53_GSK3β at days #4, #8 and #12.

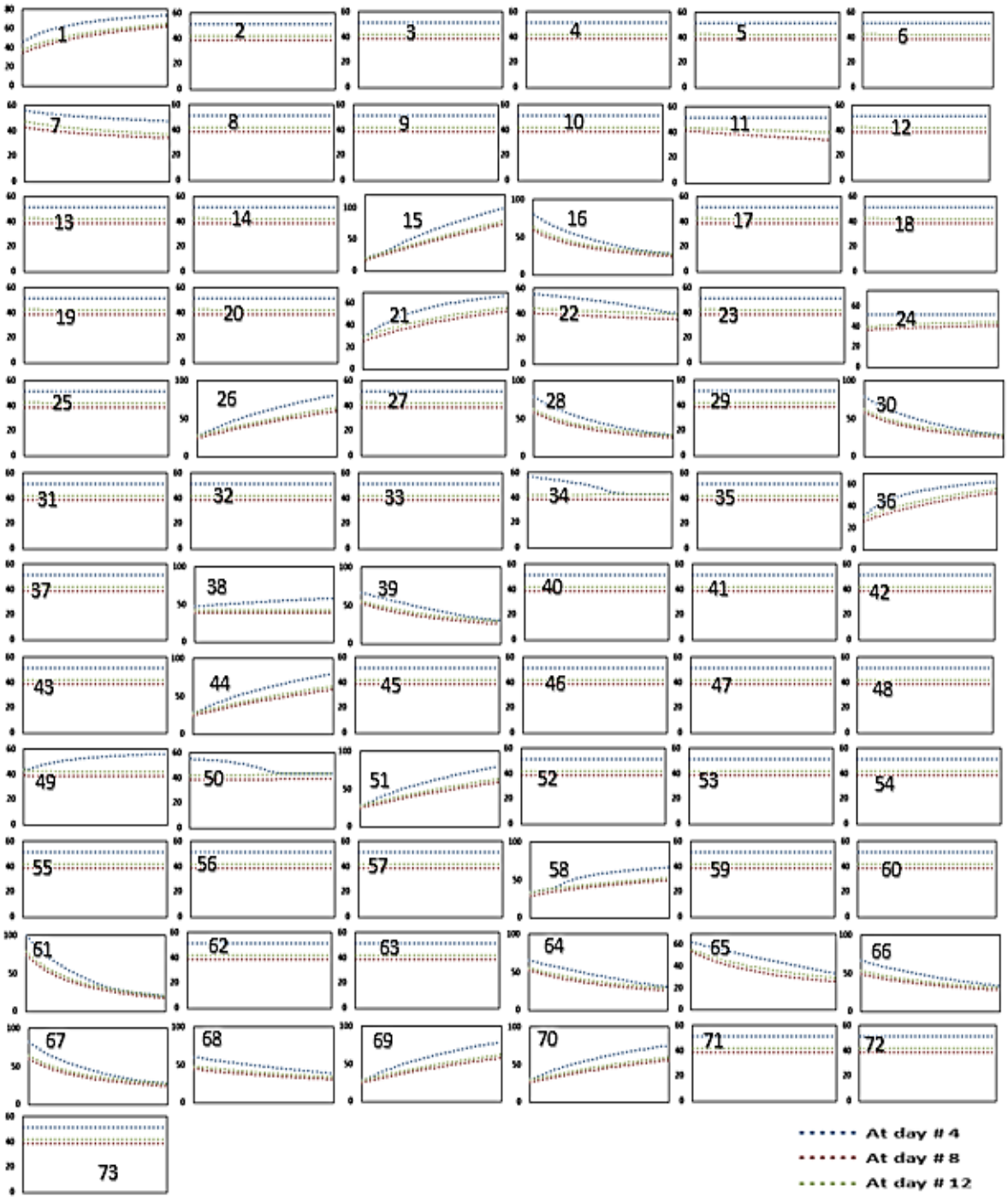

Figure 6.14: Monotonicity plots of all parameters in the LHS matrix for p53_GSK3β using ODEs at times t = 4, 8 and 12 (days). The plots show that there is a monotonic relationship between the LHS parameters and p53_GSK3β. Numbers shown in the figures correspond to the parameter indexes in Table 5.2.

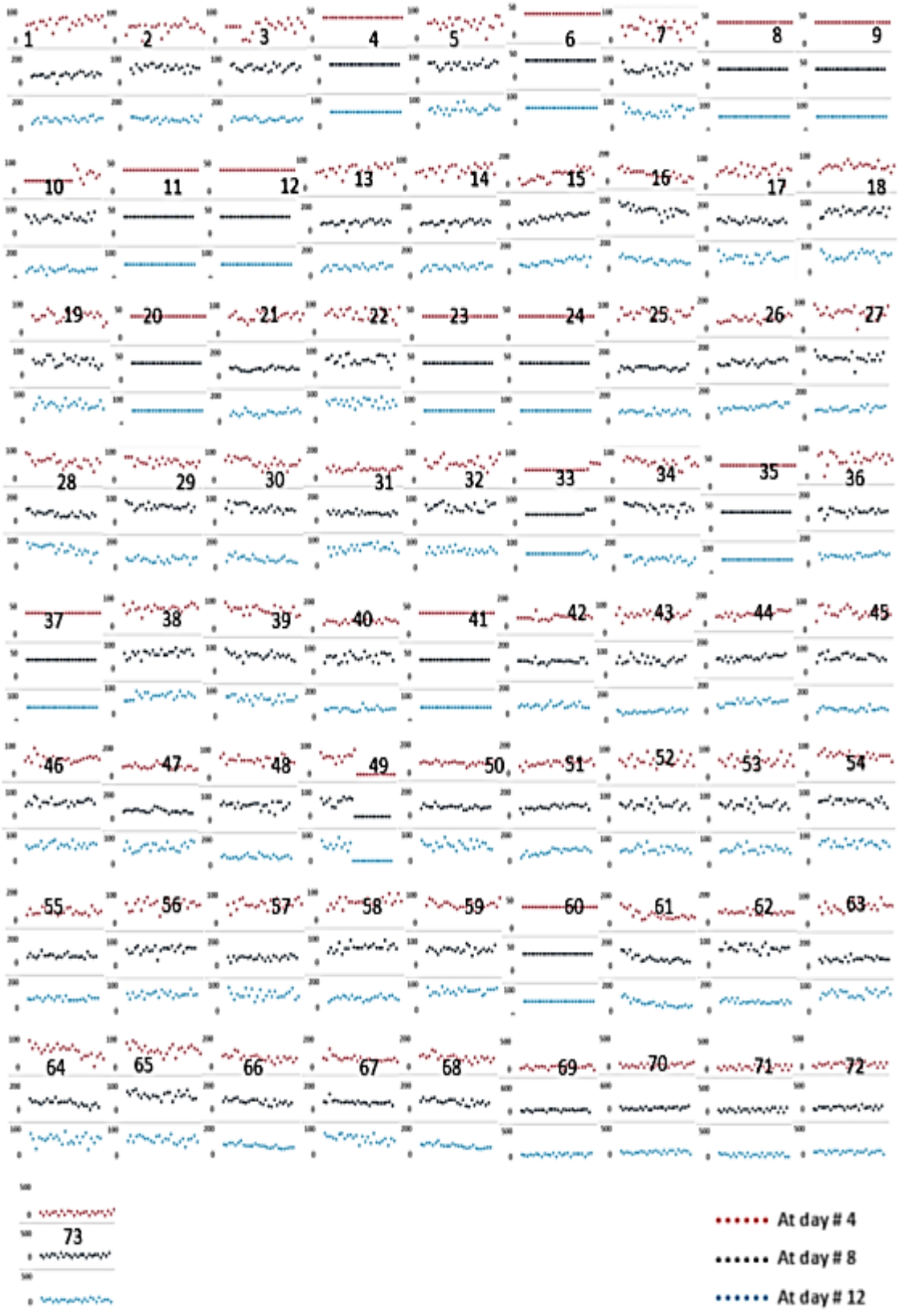

Figure 6.15: Monotonicity plots of all parameters in the LHS matrix for p53_GSK3β using MRM/GSSA at times t = 4, 8 and 12 (days). Numbers shown above the figures correspond to the parameter indexes in Table 5.2. The plots show that there is a monotonic relationship between the LHS parameters and p53_GSK3β.

PRCC analysis using ODEs shows that there are three parameters that have a strong correlation with p53_GSK3β and all these parameters have this strong correlation at day #4. These parameters are kbindMdam2p53, KbinGSk3p53 and KbinE2Ub (16, 15 and 14 in Table 5.2). The PRCC values and p-values for these parameters are shown in Table 6.5.

Table 6.5: Sub-set of parameters for which PRCC>0.5 and p<0.05 against p53_GSk3β at day #4 when PRCC uses ODEs

Index	Parameter name	PRCC	p-value
16	kbinMdm2p53	-0.592	0.00112
15	kbinGSK3bp53	0.671	4.2E-05
14	kbinE2Ub	0.620	0.0016705

Figure 6.16 shows the PRCC plots for p53_GSK3β using ODEs. KbinMdm2p53, KbinGSk3bp53 and KbinE2Ub have an important influence on the behaviour of p53_GSK3β.

PRCC analysis using MRM/GSSA demonstrates that only two parameters have an important influence on the behaviour of p53_GSK3β at day #4. These parameters are KbinMdm2p53 and KsynMdm2 (16 and 66 in Table 5.2). PRCC using ODEs and MRM/GSSA illustrates that KbinMdm2p53 is the most important parameter that influences the behaviour of p53_GSK3β. The PRCC values and p-values for kbinMdm2p53 and KsynMdm2 are listed in Table 6.6. Figure 6.17 shows PRCC plots for p53_GSK3β using MRM/GSSA.

Table 6.6: Sub-set of parameters for which PRCC>0.5 and p<0.05 against p53_GSk3β at day #4 when PRCC uses MRM/GSSA

Index	Parameter name	PRCC	p-value
16	kbinMdm2p53	-0.588	0.001032
66	KsynMdm2	0.504	0.00424

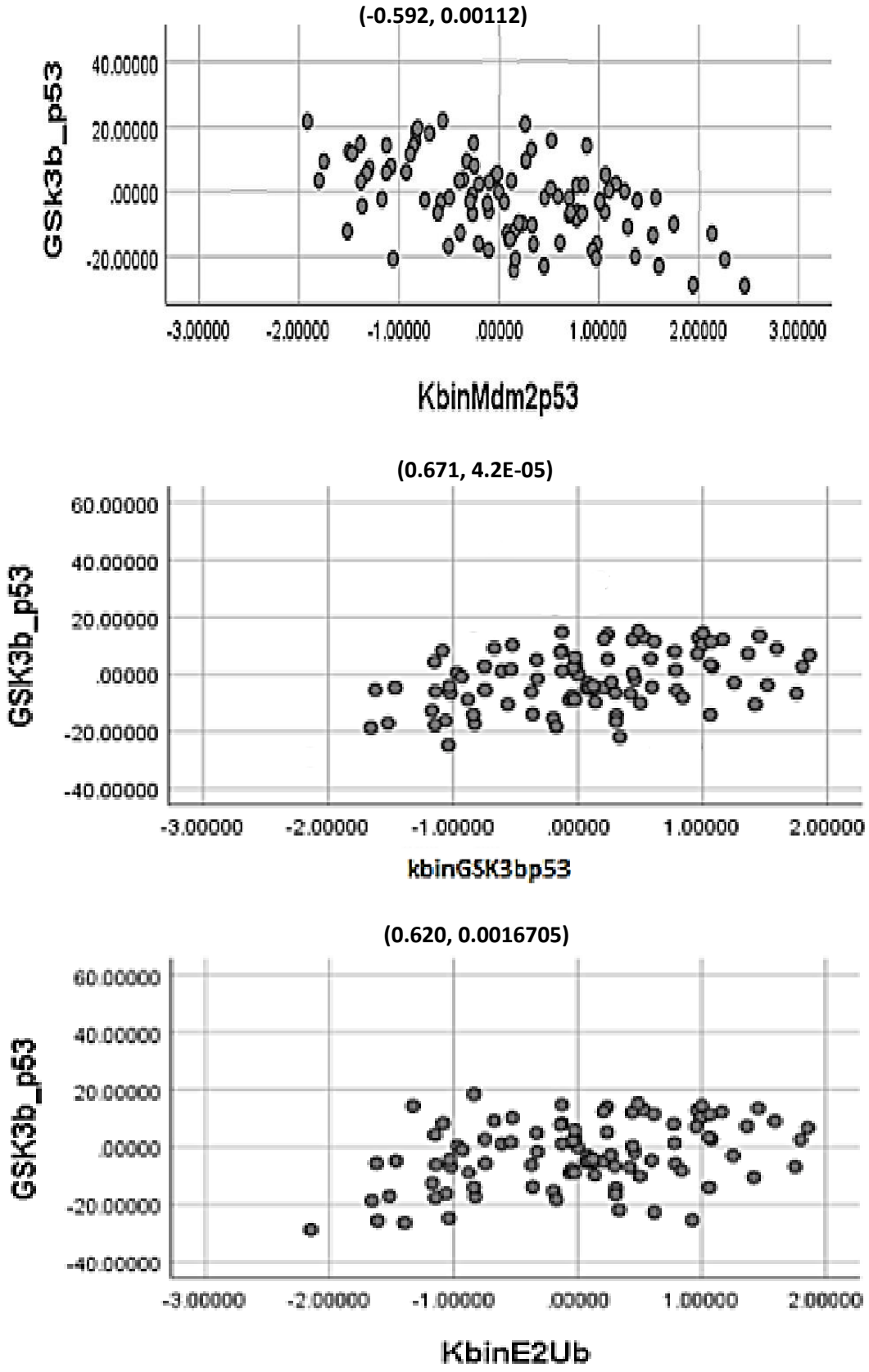

Figure 6.16: PRCC Plots for p53_GSK3β using ODEs. KbinMdm2p53, KbinGSk3bp53 and KbinE2Ub have an important influence on the behaviour of p53_GSK3β. PRCC values and p-values are shown in brackets above the plots. The y-axis corresponds to the regression coefficients for p53_GSK3β while the x-axis represents the regression coefficient parameters.

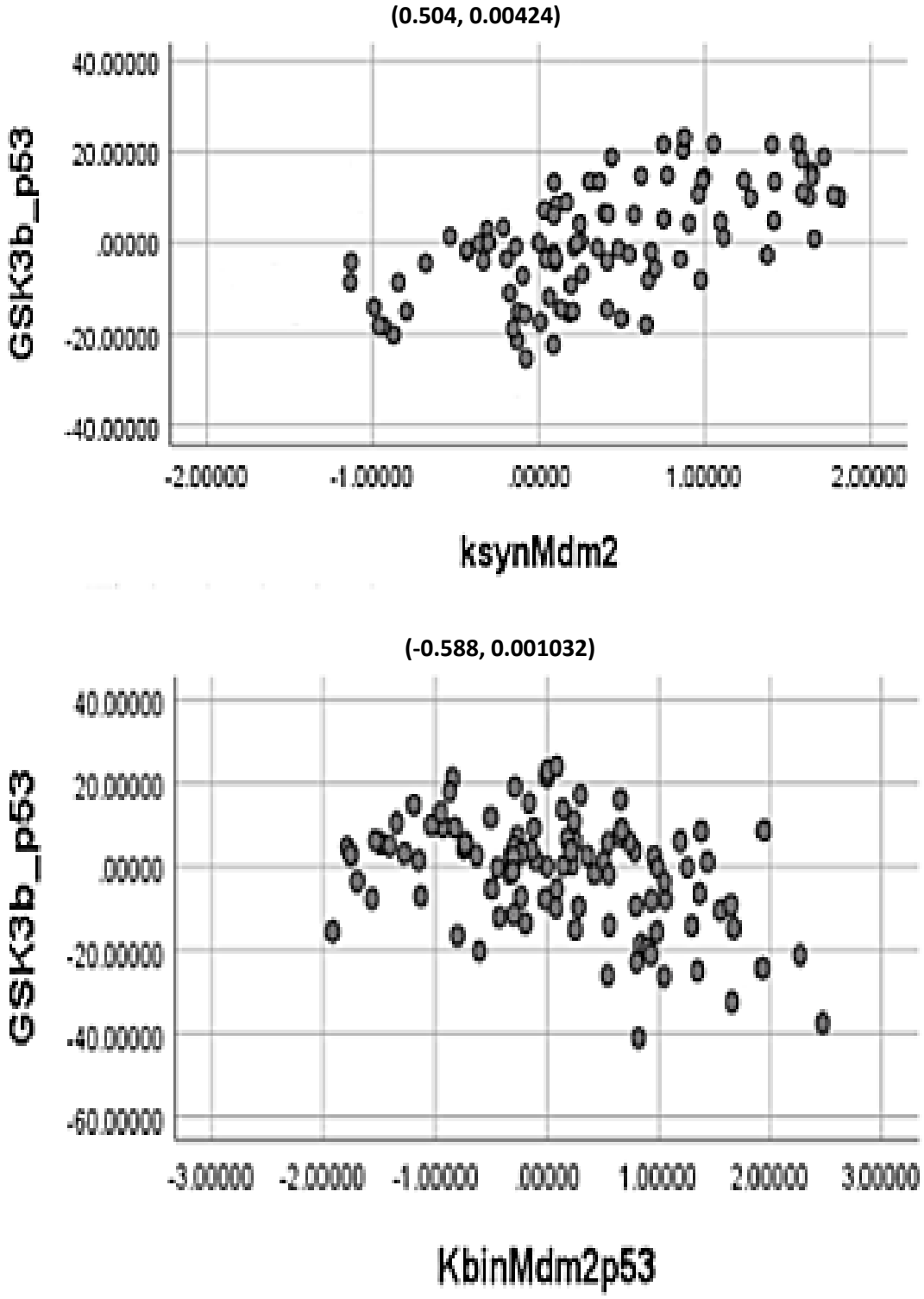

Figure 6.17: PRCC plots for p53_GSK3β using MRM/GSSA for ksynMdm2 and KbinMdm2p53. The y-axis corresponds to the regression coefficients for p53_GSK3β while the x-axis represents regression coefficients parameters. PRCC values and p-values are shown in brackets above the plots. The y-axis corresponds to the regression coefficients for p53_GSK3β while the x-axis represents the regression coefficient parameters.

6.8 Results of LHS/PRCC for Aβ

Aβ is selected to investigate the space of the parameters in the model because of its importance as it is one of the most important species that contributes to AD, as described in Chapter 2. Figure 6.18 (A and B) shows the behaviour of Aβ in response to parameter combinations in the LHS matrix using ODEs and MRM/GSSA.

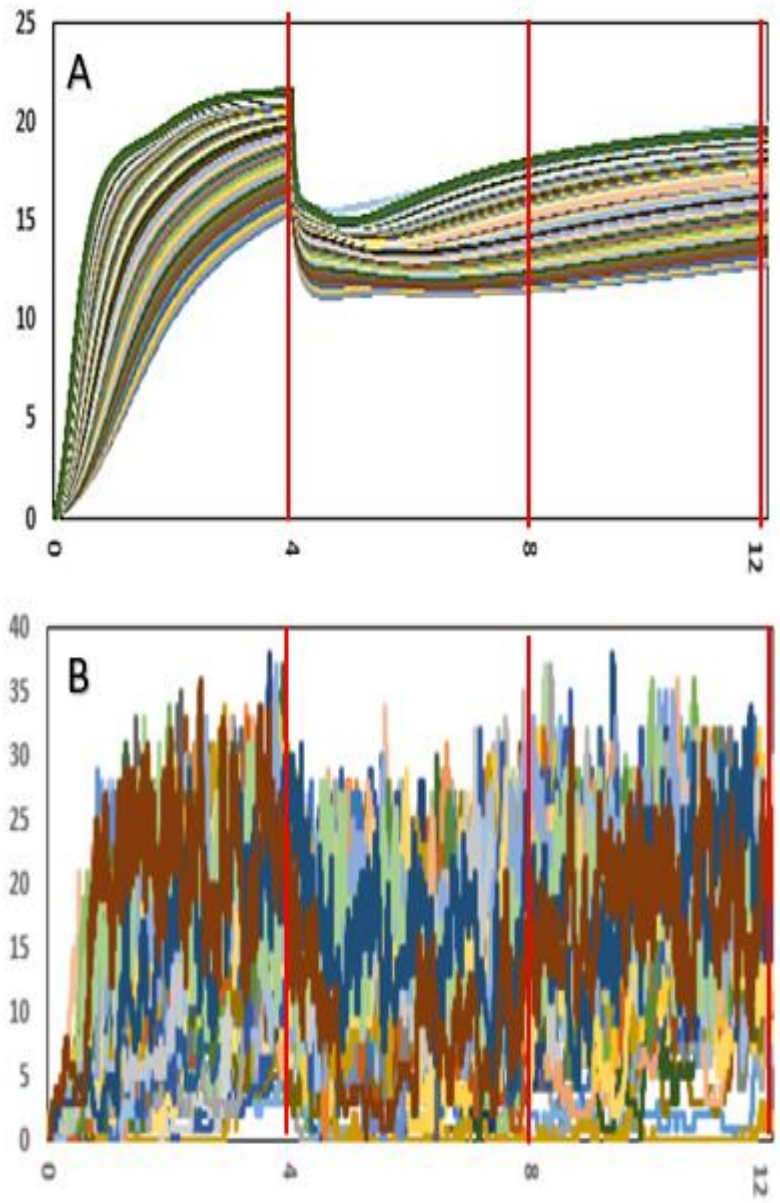

Figure 6.18: Behaviour of Aβ over 12 days corresponding to the parameter combinations of the LHS scheme using ODEs (A) and MRM/GSSA (B). Days 4, 8 and 12, indicated by the vertical lines (red lines), are used as time points to compute the level of uncertainty from the LHS parameters on the behaviour of Aβ. More variance is shown in the behaviour of Aβ when MRM/GSSA is used, as shown in B while ODEs in A shows that Aβ has the same pattern in response to parameters in the LHS matrix

Before using PRCC analysis we verify that a monotonic relationship exists between Aβ and all parameters in the matrix using ODEs and MRM/GSSA at all-time points (days #4, #8 and #12). Figures 6.19 and 6.20 show that a monotonic relationship exists between Aβ and all LHS parameters when ODEs and MRM/GSSA are used, respectively.

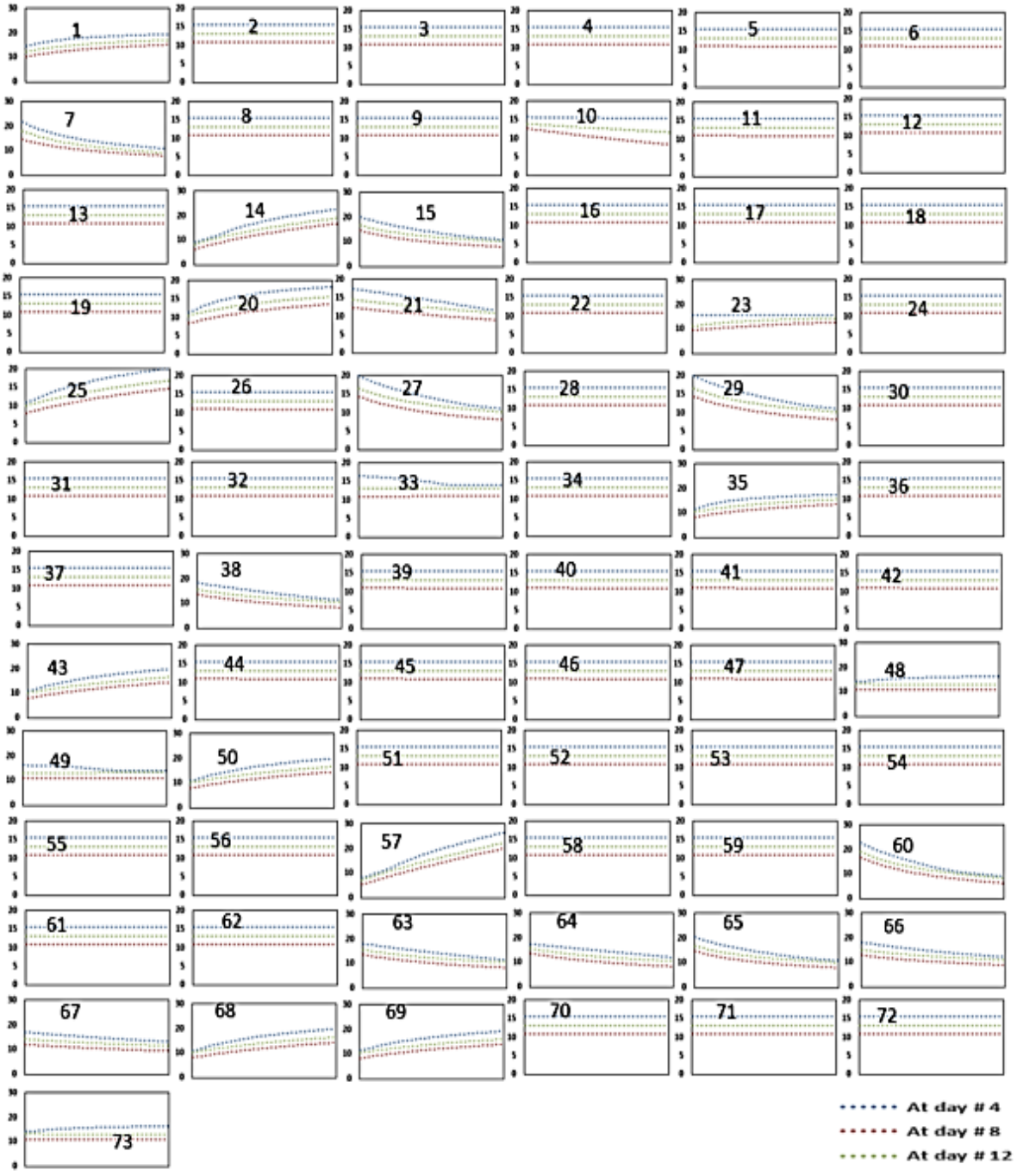

Figure 6.19: Monotonicity plots of all parameters in the LHS matrix for Aβ using ODEs at times t = 4, 8 and 12 (days). Plots show that there is a monotonic relationship between the LHS parameters and Aβ. Numbers shown in the figures correspond to the parameter indexes in Table 5.2.

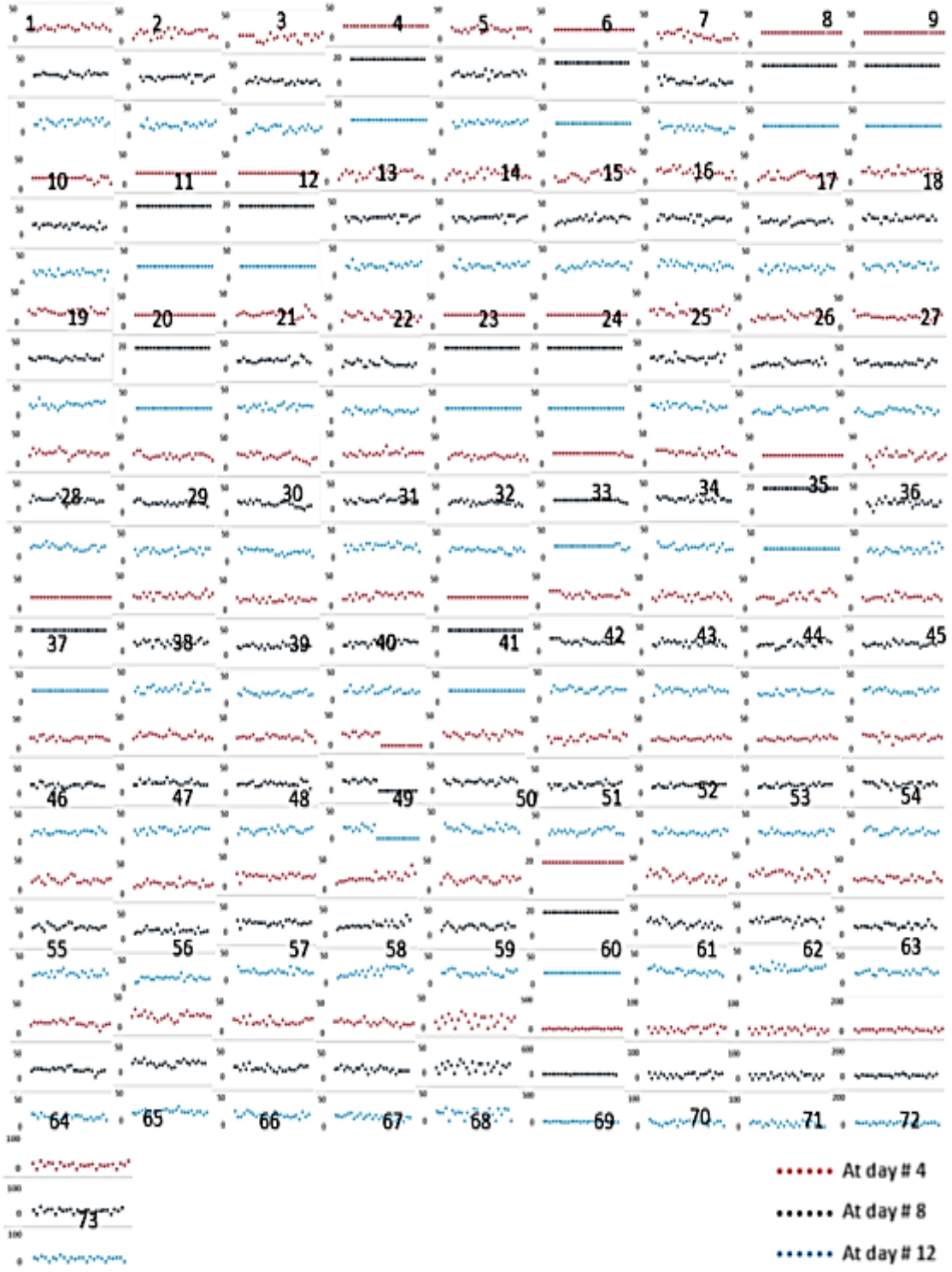

Figure 6.20: Monotonicity plots of all parameters in the LHS matrix for Aβ using MRM/GSSA at times t = 4, 8 and 12 (days). Plots show that there is a monotonic relationship between the LHS parameters and Aβ. Numbers shown in the figures correspond to the parameter indexes in Table 5.2.

PRCC analysis using ODEs and MRM/GSSA shows that KbinMdm2p53 and ksynMdm2 (16 and 66 in Table 5.2) at day #8 are the most important parameters that influence the behaviour of Aβ. Both these parameters have strong correlations with Aβ. Table 6.7 lists the PRCC values and p-values for these parameters using both approaches. Figure 6.21 (A and B) displays the PRCC plots for KbinMdm2p53 and ksynMdm2 using ODEs in A and MRM/GSSA in B.

Table 6.7: Sub-set of parameters for which PRCC>0.5 and p<0.05 against Aβ at day#8 when PRCC uses ODEs and MRM/GSSA

Index	Parameter	ODEs		MRM/GSSA	
		PRCC	p-value	PRCC	p-value
16	KbinMdm2p53	-0.7446	2.48E-05	-0.7006	2.48E-05
66	ksynMdm2	0.7211	3.66E-06	0.7911	8.31E-05

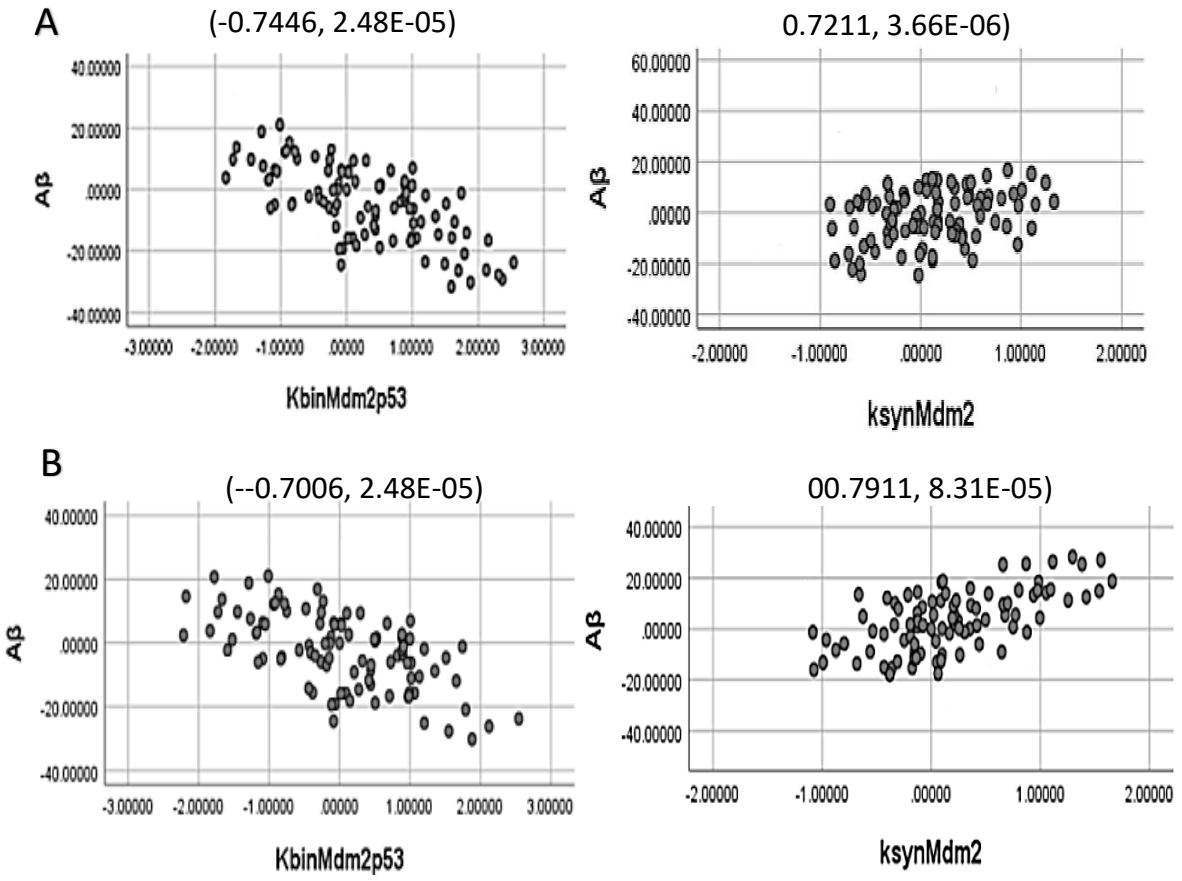

Figure 6.21: PRCC plots for Aβ using ODEs and MRM/GSSA for KbinMdm2p53 and ksynMdm2. The y-axis corresponds to the regression coefficients for Aβ while the x-axis represents the regression coefficients of the parameters. PRCC values and p-values are labelled above the plots and listed in Table 6.7. KbinMdm2p53 and ksynMdm2 are the most important parameters that dramatically change the behaviour of Aβ using ODEs and MRM/GSSA

6.9 Results of LHS/PRCC for plaques

The plots in Figure 6.22 show the behaviour of plaques over 12 days corresponding to the parameter combinations of the LHS scheme using ODEs (A) and MRM/GSSA (B). The vertical lines in A and B indicate the time points we used to calculate the level of uncertainty from the LHS parameters (days #4, #8 and #12). One hundred runs are plotted using ODEs and MRM/GSSA.

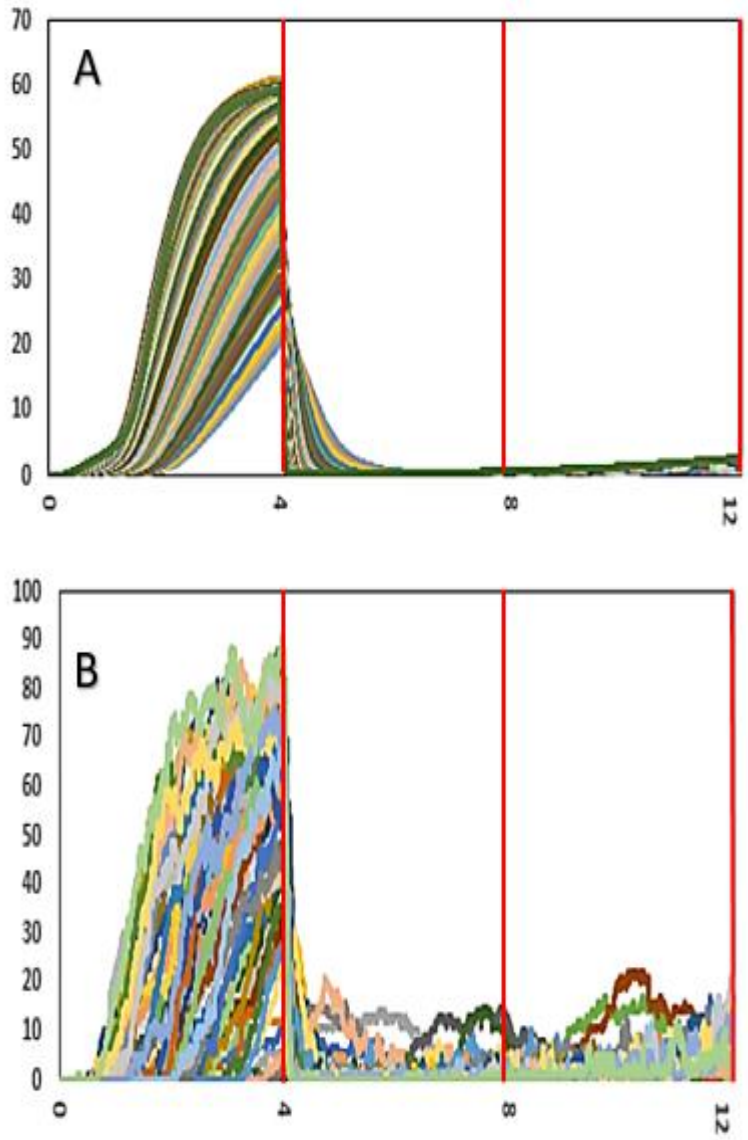

Figure 6.22: Behaviour of plaques over 12 days. A and B show the behaviour of plaques corresponding to the parameter combinations in the LHS scheme using ODEs and MRM/GSSA. Days 4, 8 and 12, indicated by the vertical lines (red lines), are used as time points to compute the level of uncertainty from the LHS parameters on the behaviour of plaques. It can be clearly seen that plaques are more sensitive to the parameter combinations of the LHS scheme in the first four days (from time zero to four (immunization day).

We show in Figures 6.23 and 6.24 that there is a monotonic relationship between the plaques and the parameters in the LHS matrix using ODEs and MRM/GSSA. We then, investigate the parameters in the LHS matrix to classify the most important parameters that have strongest correlation with plaques.

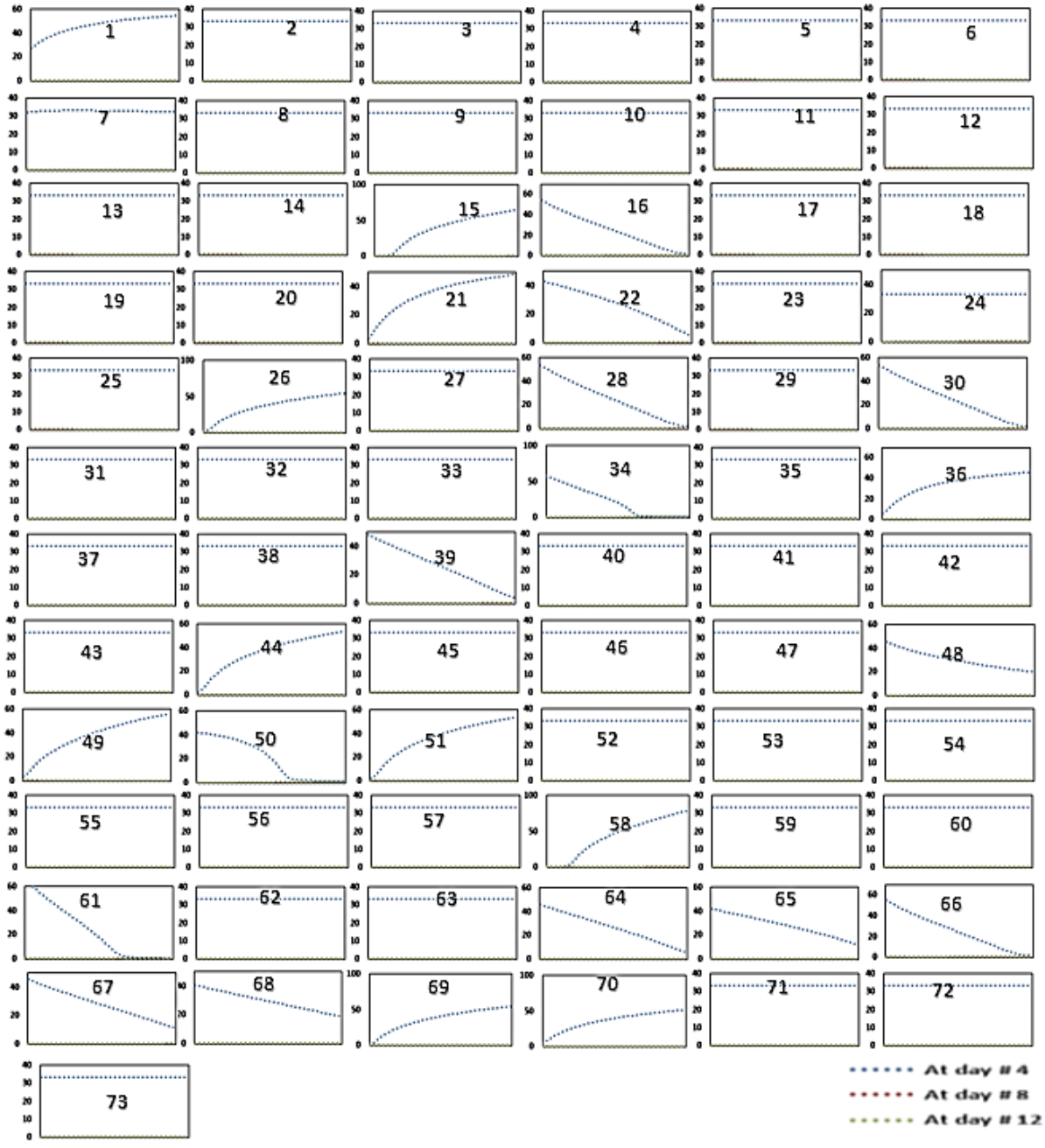

Figure 6.23: Monotonicity plots of all parameters in the LHS matrix for plaques using ODEs at times t = 4, 8 and 12 (days). The plots show that there is a monotonic relationship between the LHS parameters and plaques. Only one line is clearly seen in all plots (day #4) because plaques are only sensitive before immunization. The immunization is totally clear of plaques from the system even when the parameters are perturbed. Numbers shown in the figures correspond to the parameter indexes in Table 5.2.

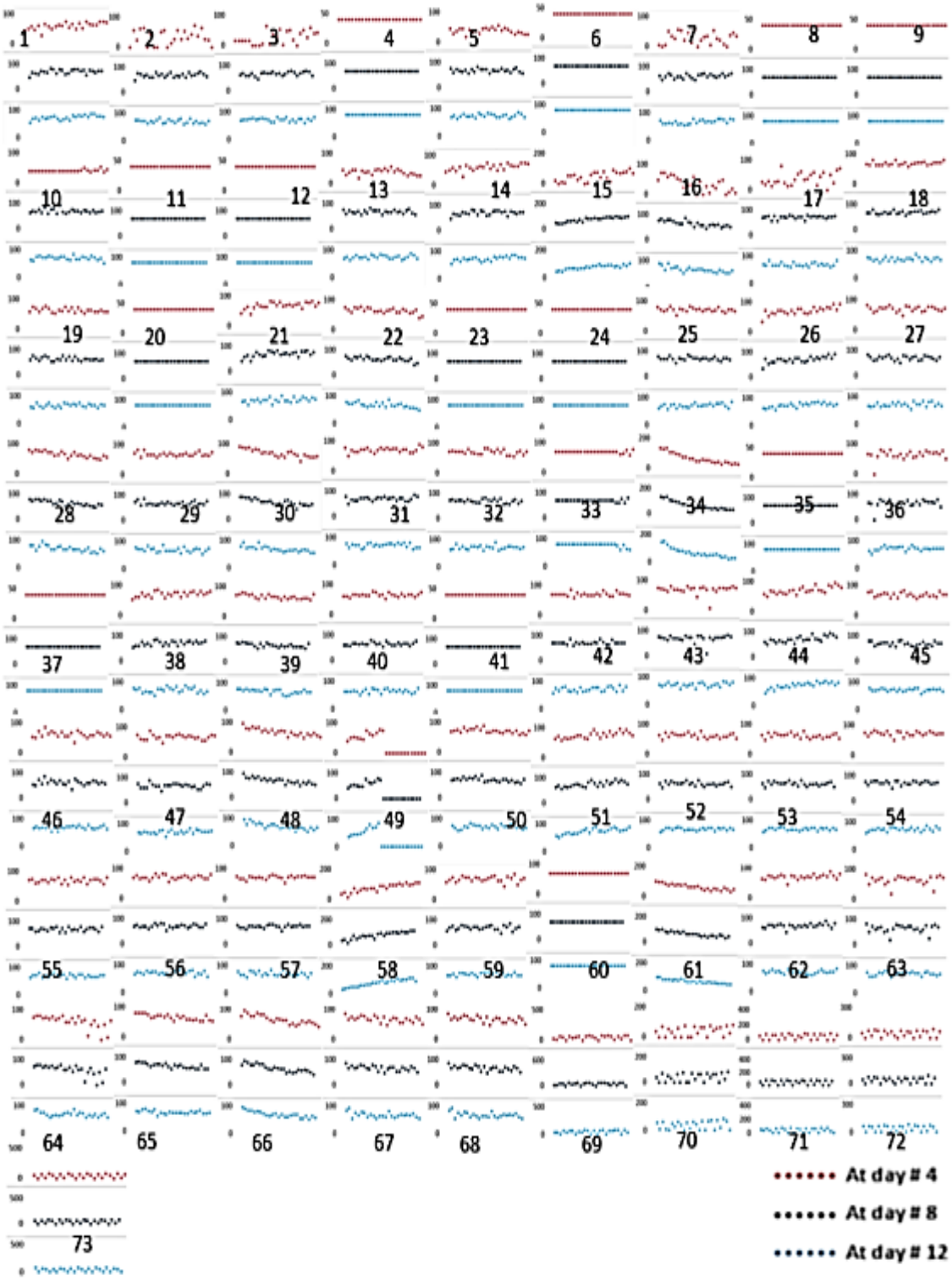

Figure 6.24: Monotonicity plots of all parameters in the LHS matrix for plaques using MRM/GSSA at times t = 4, 8 and 12 (days). The plots show that there is a monotonic relationship between the LHS parameters and the plaques. As shown in Figure 6.22, the plaques show variance after immunization (day #4). The level of plaques reaches around 30 molecules in response to parameter perturbations. Numbers shown in the figures correspond to the parameter indexes in Table 5.2.

PRCC analysis using ODEs shows that kbinMdm2p53 and ksynMdm2 (16 and 66 in Table 5.2) are the most important parameters that have strong correlations with plaques at day #4. Table 6.8 lists the PRCC values and p-values for these parameters. Figure 6.25 displays the PRCC plots of these parameters with plaques. PRCC analysis using MRM/GSSA demonstrates that kdegTau20Sport and kbinMdm2p53 (29 and 16 in Table 5.2) are the most important parameters that have the most influence on the behaviour of the plaques. Table 6.9 lists the PRCC and p-values for kdegTau20Sport and kbinMdm2p53. Figure 6.25 displays the PRCC plots for these parameters. Note, in Figures 6.25 and 6.26, the y-axis corresponds to the regression coefficients for plaques while the x-axis represents regression coefficients parameters

Table 6.8: Sub-set of parameters for which PRCC>0.5 and p<0.05 against plaques at day #8 when PRCC uses ODEs

Index	Parameter	ODEs	
		PRCC	p-value
16	KbinMdm2p53	-0.5786	1.01E-03
66	ksynMdm2	0.6235	4.68E-04

Table 6.9: Sub-set of parameters for which PRCC>0.5 and p<0.05 against plaques at day #8 when PRCC uses MRM/GSSA

Index	Parameter	MRM/GSSA	
		PRCC	p-value
29	kdegTau20Sport	0.501	0.00066
16	kbinMdm2p53	-0.5041	0.0024

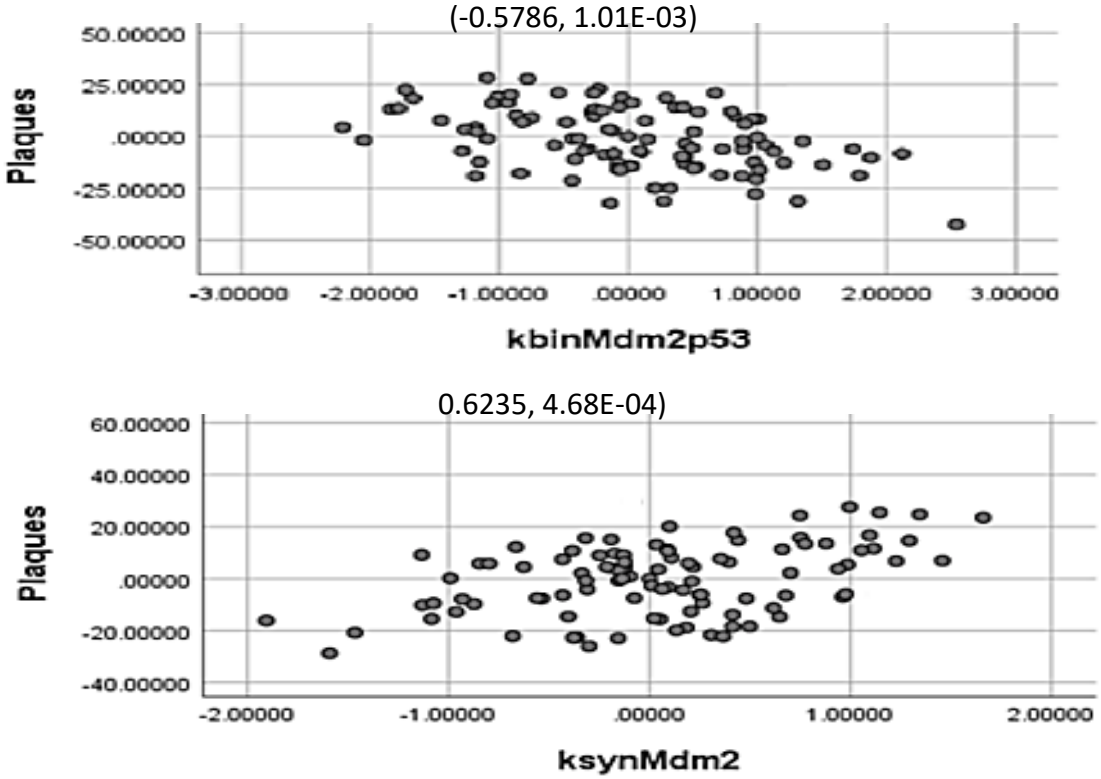

Figure 6.25: PRCC plots for plaques using ODEs. KbinMdm2p53 and ksynMdm2 are the most important parameters that affect the behaviour of plaques. The PRCC and p-values are labelled above plots and listed in Table 6.8; the parameter names are labelled under the plots.

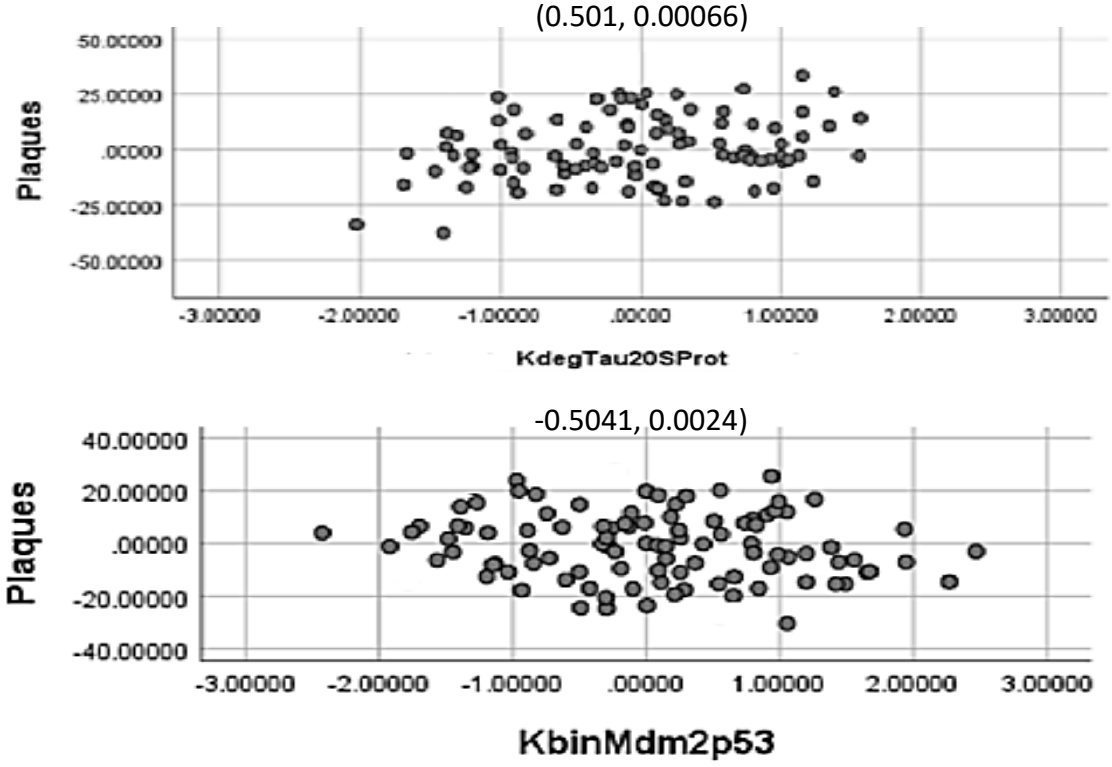

Figure 6.26: PRCC plots for plaques using MRM/GSSA. KdegTau20Sport and KbinMdm2p53 are the most important parameters that affect the behaviour of plaques. PRCC values and p-values are labelled above the plots and listed in Table 6.9 and the parameter names are labelled under the plots.

6.10 Results of LHS/PRCC for tangles

Tangles are important contributors to AD. Therefore, the behaviour of tangles is investigated over the space of the parameters in the system. The plots in Figure 6.27 show the behaviour of tangles over 12 days corresponding to the parameter combinations of the LHS scheme using ODEs (A) and MRM/GSSA (B). The vertical lines in A and B indicate the time points we use to calculate the level of uncertainty of the LHS parameters (days #4, #8 and #12). Figures 6.28 and 6.29 verify the monotonic relationship between the tangles and LHS parameters using ODEs and MRM/GSSA.

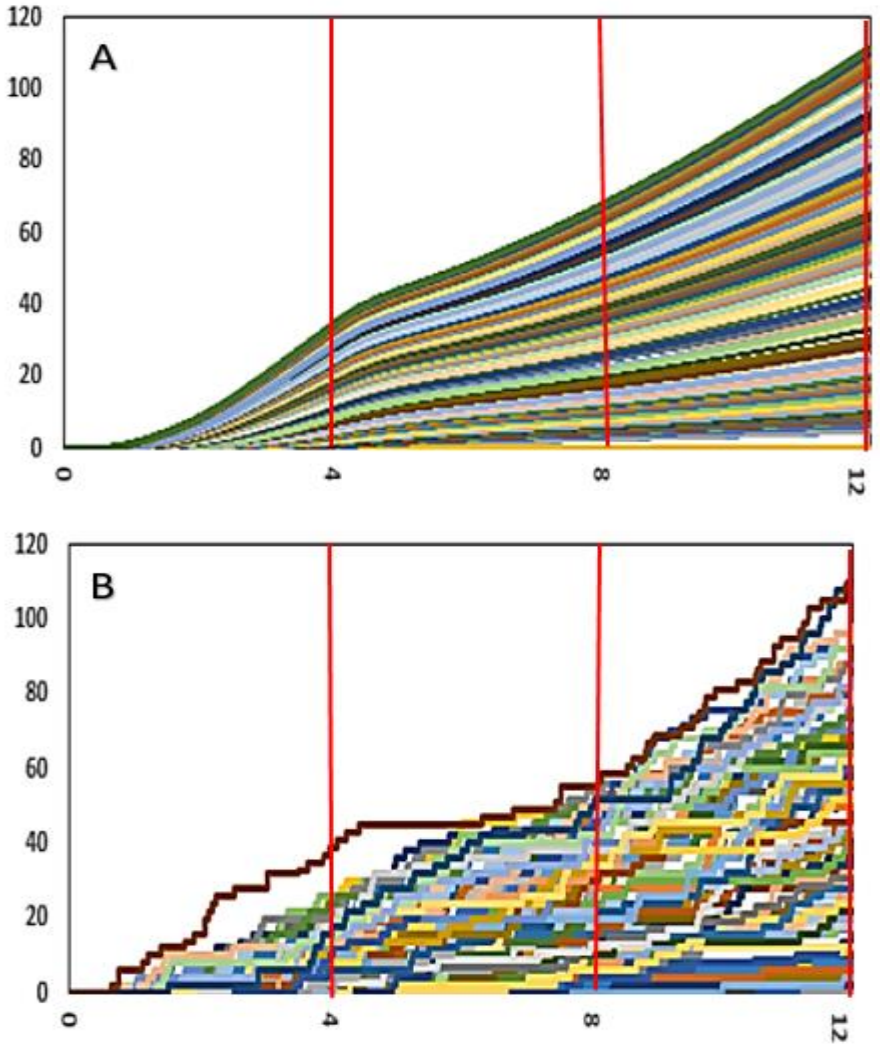

Figure 6.27: Behaviour of the tangles over 12 days. A and B show the behaviour of plaques corresponding to the parameter combinations of the LHS scheme using ODEs and MRM/GSSA. Days 4, 8 and 12, indicated by the vertical lines (red lines), are used as time points to compute the level of uncertainty from LHS parameters on the behaviour of tangles. ODEs and MRM/GSSA nearly have the same results for tangles, as shown in A and B

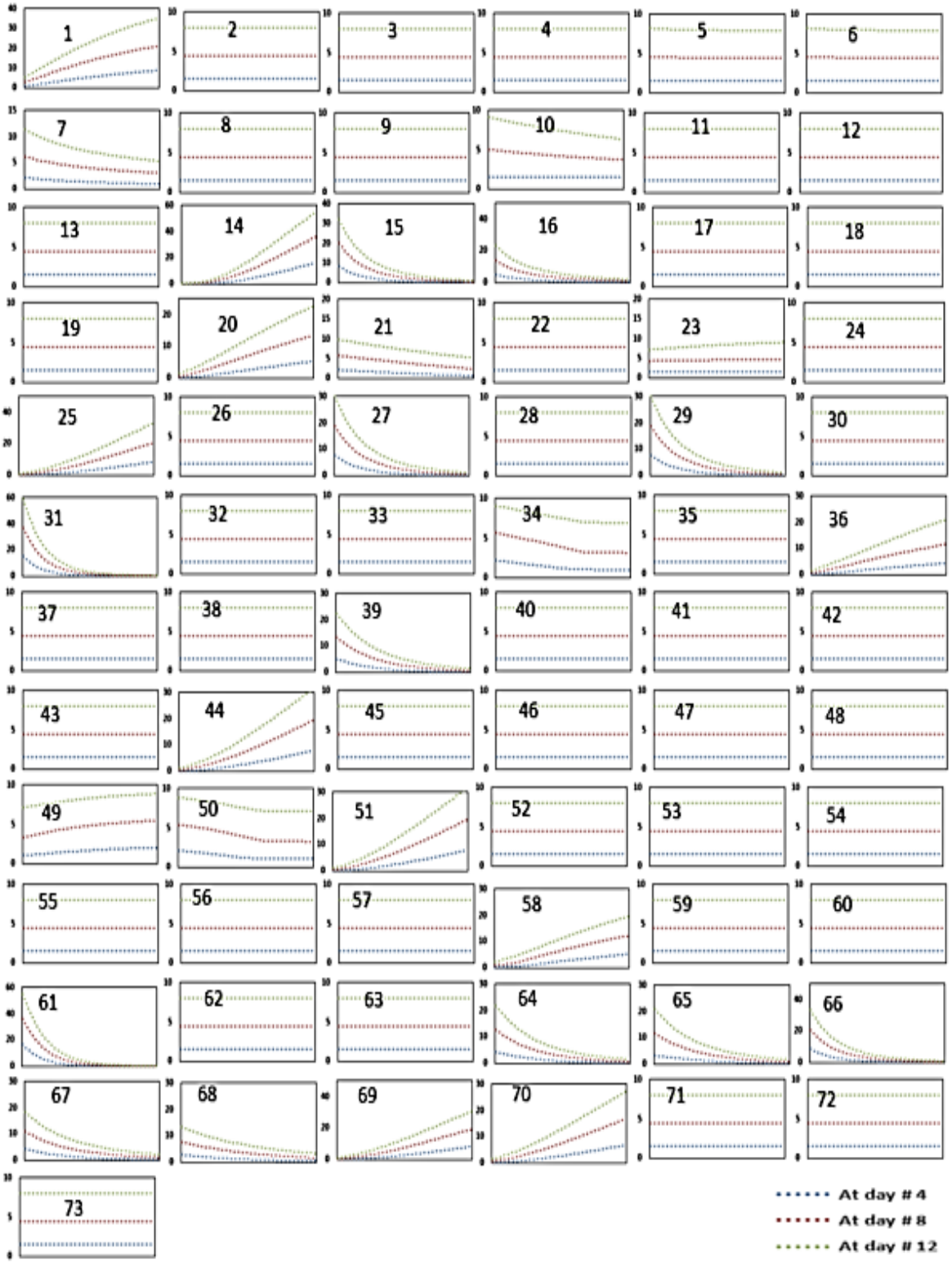

Figure 6.28: Monotonicity plots of all parameters in the LHS matrix for tangles using ODEs at times t = 4, 8 and 12 (days). The plots show that there is a monotonic relationship between the LHS parameters and the plaques. Numbers shown in the figures correspond the parameter indexes in Table 5.2.

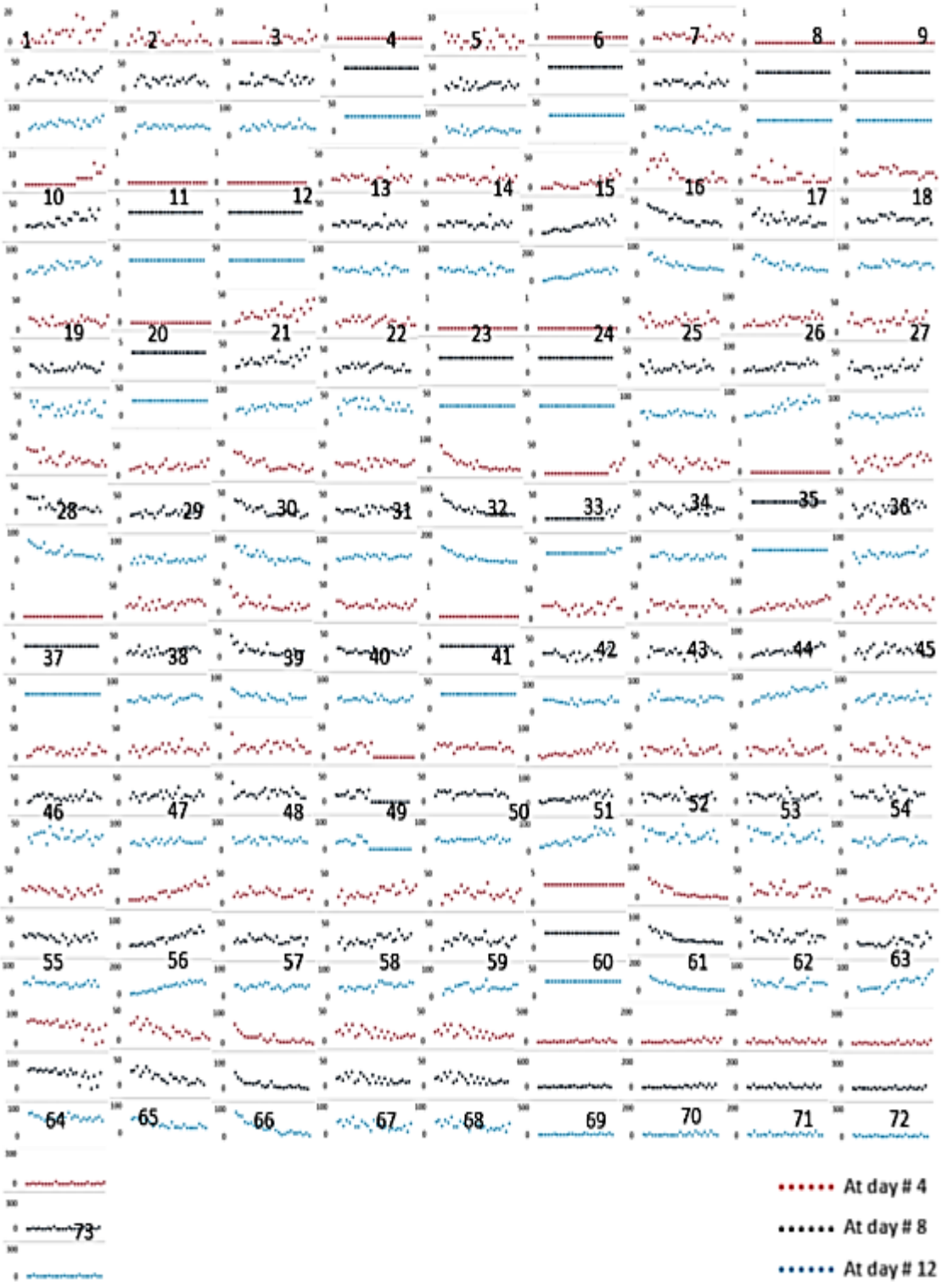

Figure 6.29: Monotonicity plots of all parameters in the LHS matrix for tangles using MRM/GSSA at times t = 4, 8 and 12 (days). The plots show that there is a monotonic relationship between the LHS parameters and plaques. Numbers shown in the figures correspond to the parameter indexes in Table 5.2.

PRCC analysis using ODEs shows that KbinMdm2p53 (16) is the only parameter that has a strong correlation with tangles at day #12. The PRCC value is -0.6102 and the p-value is 2.64E-0.5. The PRCC plot for kbinMdm2p53 is shown in Figure 6.30. PRCC analysis using MRM/GSSA demonstrates that kgenROSGila, ksynMdm2, KbinMdm2p53 and kbinE2UB (37, 66, 16 and 14 in Table 5.2) have strong correlations with tangles. Table 6.9 lists the PRCC values and p-values of these parameters and Figure 6.31 displays the PRCC plots for these parameters.

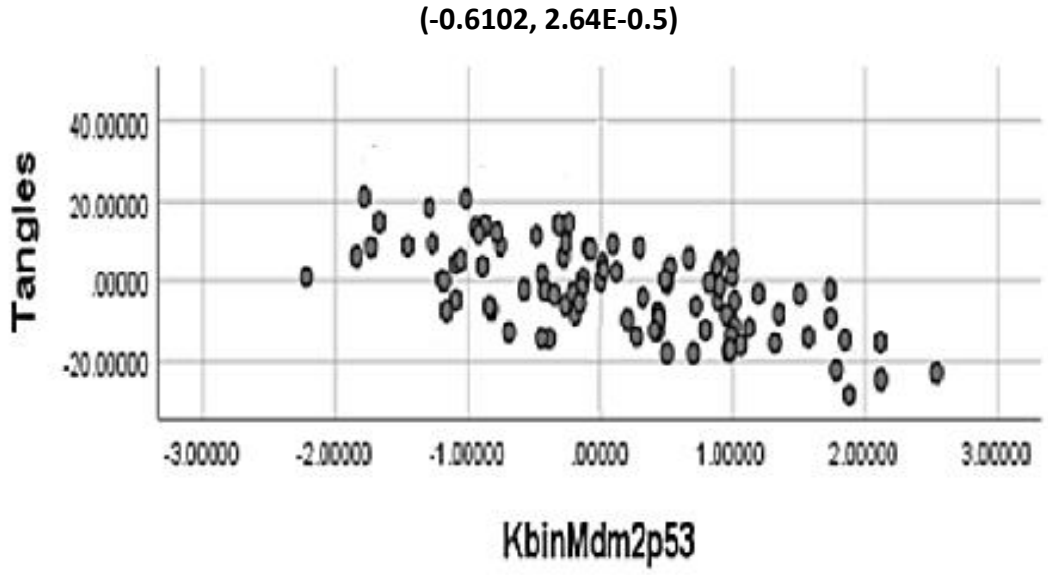

Figure 6.30: PRCC plots for tangles using ODEs. KbinMdm2p53 is the most important parameter that affects the behaviour of the tangles. PRCC and p-values are labelled above the plot.

Table 6.10: Sub-set of parameters for which PRCC>0.5 and p<0.05 against tangles at day #12 when PRCC uses MRM/GSSA

Index	Parameter	MRM/GSSA	
		PRCC	p-value
37	kgenROSGila	-0.6057	0.00033
66	ksynMdm2	0.6073	1.98E-005
16	KbinMdm2p53	0.6493	2.93E-006
14	kbinE2UB	-0.7167	1.3855E-007

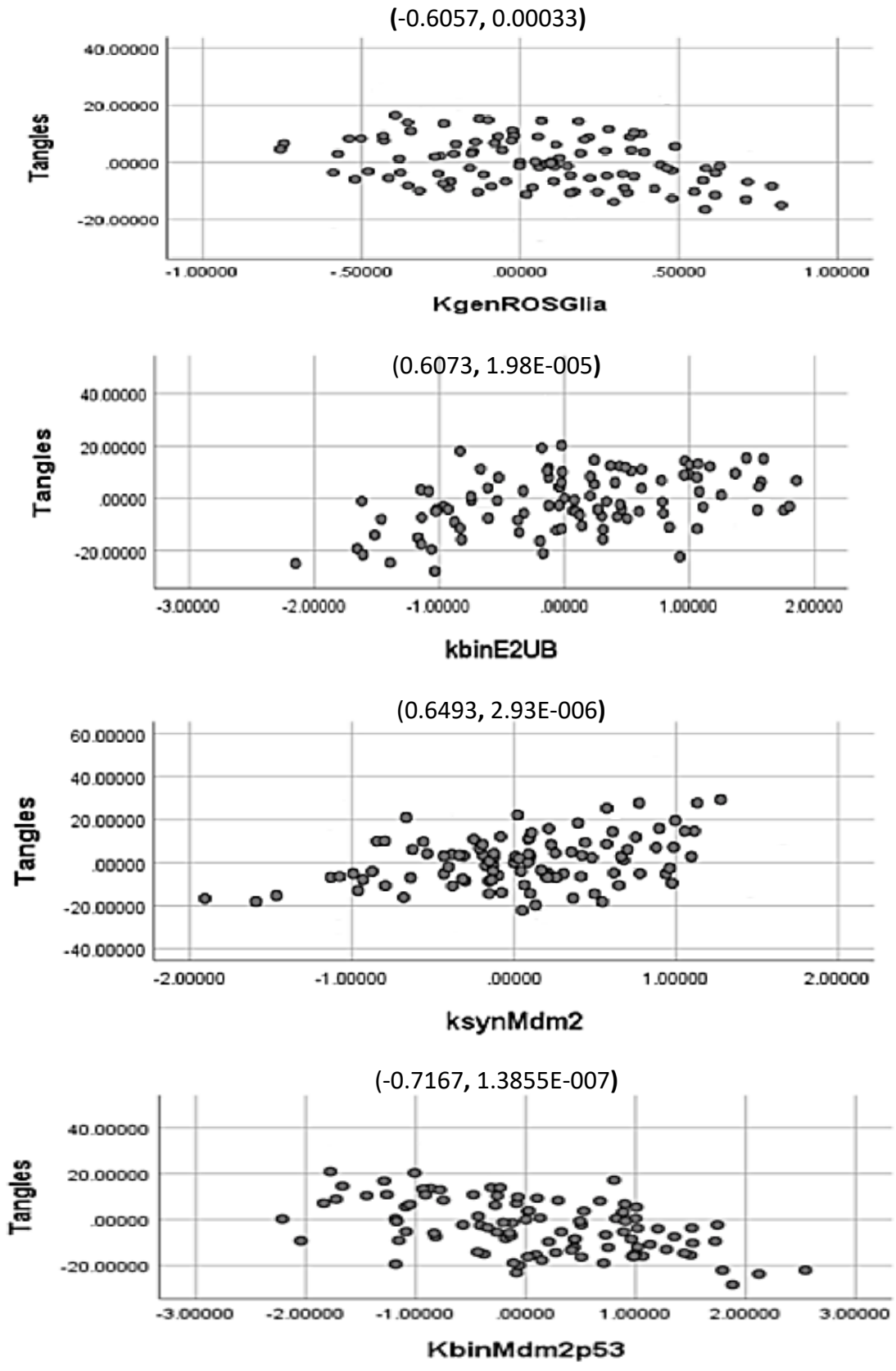

Figure 6.31: PRCC plots for tangles using MRM/GSSA. KgenROSGila, ksynMdm2, KbinMdm2p53 and kbinE2UB are the most important parameters that affect the behaviour of the tangles. The PRCC value and p-values are labelled above the figures and are also listed in Table 6.9. The y-axis corresponds to the regression coefficients for Aβ while the x-axis represents the regression coefficients' parameters.

6.11 Results of LHS/PRCC for GilaA

In Figure 6.32, we show the behaviour of GilaA in response to the parameter combinations of the LHS scheme over 12 days. Part A shows the behaviour of GilaA from ODEs while the results of MRM/GSSA are represented in Part B. Figure 6.32 (A and B) contains vertical lines (red lines); these lines indicate the time points where we calculate the level of uncertainty in the behaviour of GilaA from the LHS parameters.

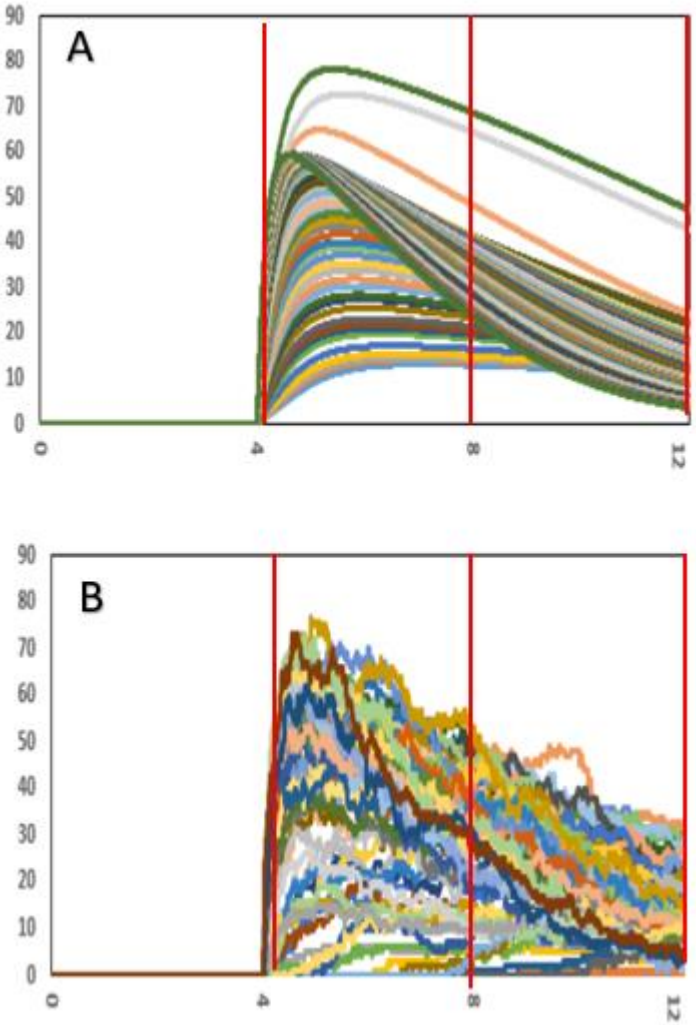

Figure 6.32: Behaviour of GilaA over 12 days. A and B, respectively, show the behaviour of GilaA corresponding to the parameter combinations of the LHS scheme using ODEs and MRM/GSSA. Days 4.2, 8 and 12, indicated by the vertical lines (red lines), are used as time points to compute the level of uncertainty from the LHS parameters on the behaviour of GilaA. For GilaA, we use day #4.2 to calculate the sensitivity because at day #4, the level of GilaA is zero and it starts to increase in response to antibodies that are added to the system at day #4. Therefore, we use the closest point after day #4 to check the behaviour of GilaA over the space of parameters in the system.

Verifying the monotonic relationship between GilaA and the LHS parameters is the first step to be achieved before using PRCC analysis. Figures 6.33 and 6.34 show how the monotonic relationship between GilaA and parameters in the LHS matrix is verified using ODEs and MRM/GSSA, respectively.

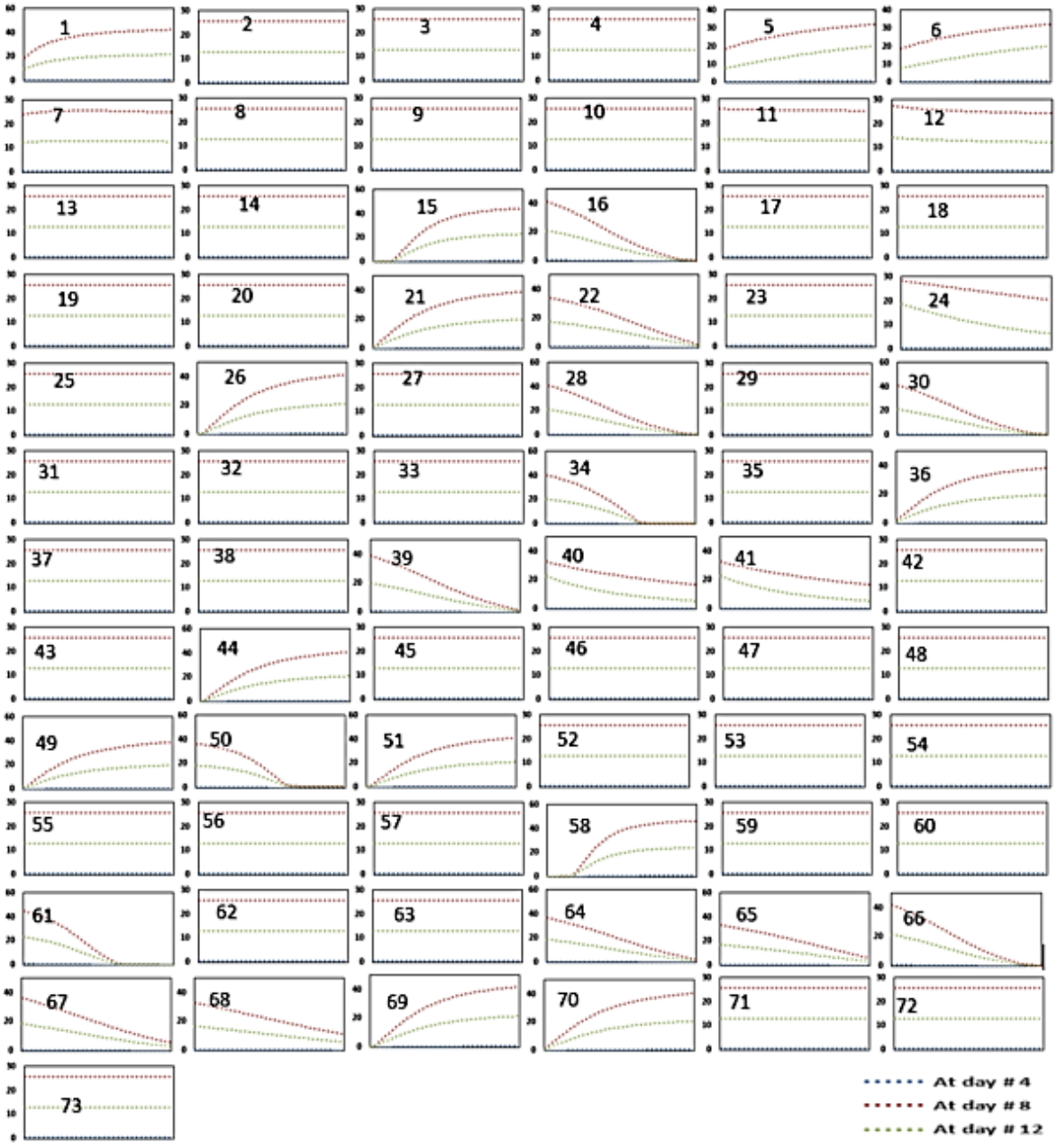

Figure 6.33: Monotonicity plots of all parameters in the LHS matrix for GilaA using ODEs at times t = 4.2, 8 and 12 (days). The plots show that there is a monotonic relationship between the LHS parameters and GilaA. Numbers shown in the figures correspond the parameter indexes in Table 5.2.

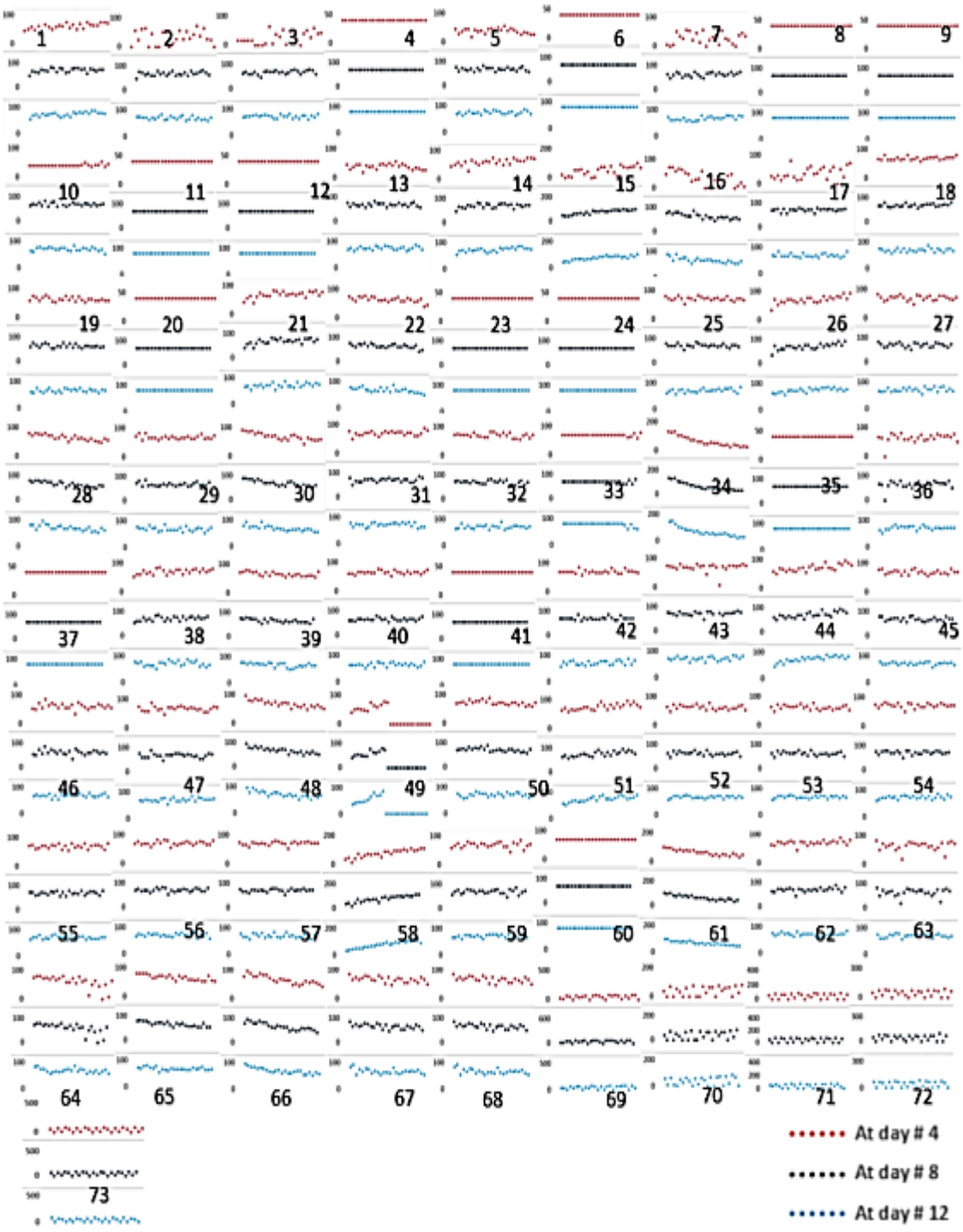

Figure 6.34: Monotonicity plots of all parameters in the LHS matrix for GilaA using ODEs at times t = 4.2, 8 and 12 (days). The plots show that there is a monotonic relationship between the LHS parameters and GilaA. Numbers shown in the figures correspond to the parameter indexes in Table 5.2.

PRCC analysis using ODEs demonstrates that none of the parameters have strong correlations with GliaA while the analysis using MRM/GSSA indicates that there are three parameters that have strong correlations with GilaA at day #4.2. These parameters are KdegAbetaGlia, ksynMdm2 and ktangfor (23, 66 and 73 in Table 5.2). This table lists PRCC values and p-values for these parameters. Figure 6.35 displays the PRCC plots for GilaA in response to these parameters.

Table 6.11: Sub-set of parameters for which PRCC>0.5 and p<0.05 against GilaA at day #4.2 when PRCC uses MRM/GSSA

Index	Parameter	MRM/GSSA	
		PRCC	p-value
23	**KdegAbetaGlia**	**-0.503**	**0.00041**
66	**ksynMdm2**	**0.543**	**0.00023**
73	**ktangfor**	**-0.582**	**0.2E-04**

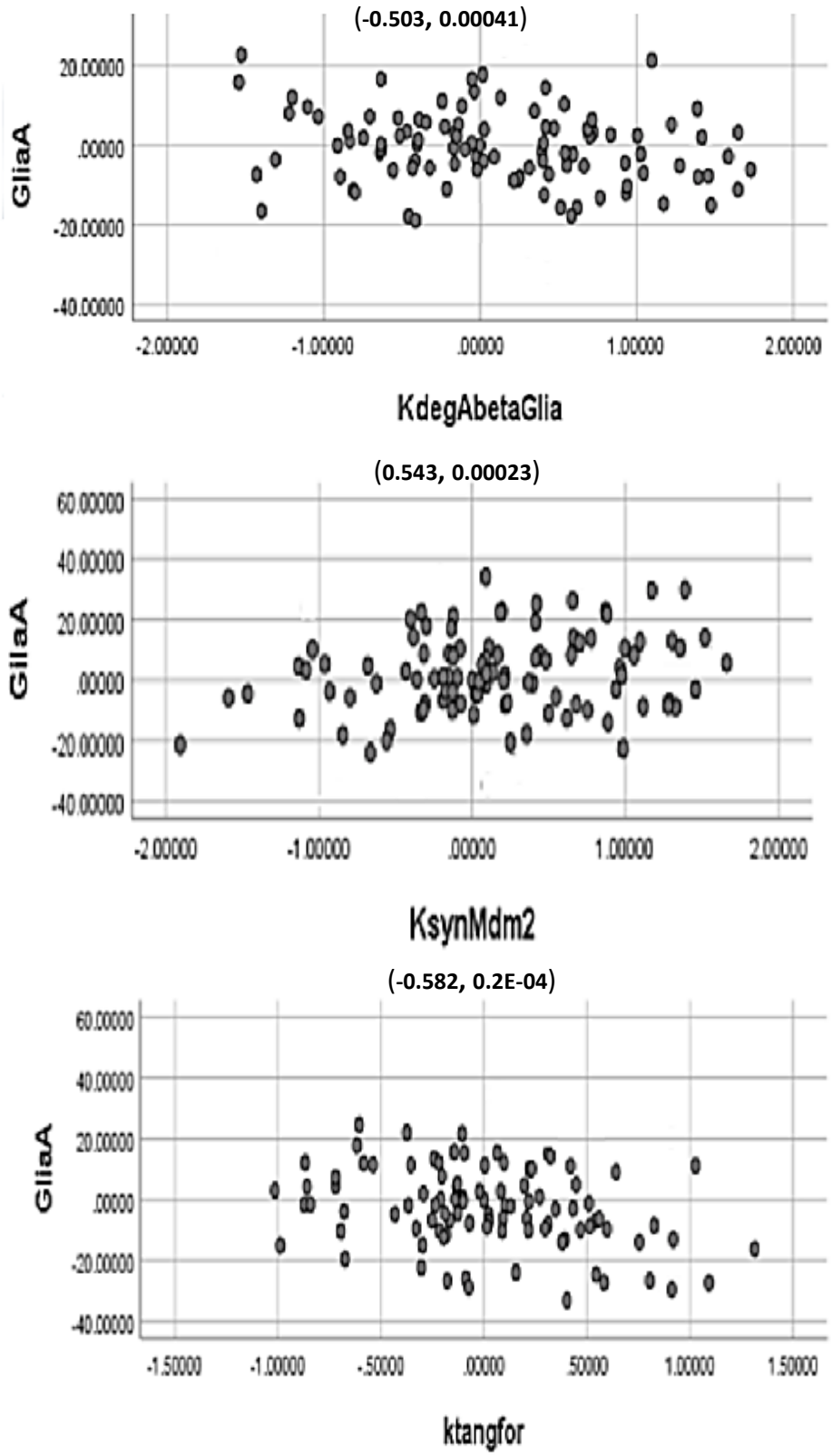

Figure 6.35: PRCC plots for GilaA using MRM/GSSA. KdegAbetaGlia, ksynMdm2, ktangfor are the most important parameters that affect the behaviour of GilaA at day #4.2. The PRCC value and p-values are listed in Table 6.10. The y-axis corresponds to the regression coefficients for Aβ while the x-axis represents the regression coefficients parameters.

6.12 Summary

This chapter discusses the results of LHS/PRCC using ODEs and MRM/GSSA for the selected species in immunization in the AD model. In the first four sections we described, using an example from the system, how to generate the LHS matrix and how to rank the values in this matrix. We also described how the monotonic relationship is verified between the LHS parameters and the outcome measures using an example. It was found that all species selected to be investigated have a monotonic relationship with the LHS parameters using ODEs and MRM/GSSA.

We also show using an example from the system how all steps of PRCC are handled and how PRCC values for a specific parameter are calculated using Pearson correlation coefficient (PCC) for the residuals from the two regression models that representing the ranked parameter in terms of the other ranked parameter values and the ranked outcome measures in terms of the other ranked parameter values.

Then, we discuss LHS/PRCC results for all of the selected species. PRCC demonstrated that:

1- p53 has no strong correlation with the LHS parameters when PRCC uses ODEs and MRM/GSSA.
2- ATMA has a strong correlation with kbinMdm2p53 at all-time points (days #4, #8 and #12) when PRCC uses ODEs, while ATMA has a strong correlation with Ksynp53mRNAAbeta only at day #12 when PRCC uses MRM/GSSA.
3- p53_GSk3β has strong correlation using ODES with kbinMdm2p53, kbinGSK3bp53 and kbinE2Ub at day #4 while only KbinMdm2p53 and ksynMdm2 at day #4 have strong correlation with p53_GSk3β when PRCC uses MRM/GSSA.
4- Aβ is very sensitive after immunization at day #8 in response to kbinMdm2p53 and ksynMdm2 when PRCC uses ODEs and MRM/GSSA.
5- Plaques are only sensitive at day #4 for kbinMdm2p53 and ksynMdm2 when PRCC uses ODEs and kdegTau20Sport and kbinMdm2p53 when it uses MRM/GSSA.

6- Tangles are very sensitive in the last day of the system only to KbinMdm2p53 when ODEs are used, while kgenROSGila, ksynMdm2, KbinMdm2p53 and kbinE2UB have strong correlations with tangles when MRM/GSSA are used in PRCC analysis.
7- GliaA is not sensitive to any of the LHS parameters when ODEs are used while it is very sensitive to KdegAbetaGlia, ksynMdm2 and ktangfor when MRM/GSAA is used.

It was really interesting to find that parameters specific to p53 and Mdm2 (KbinMdm2p53 and ksynMdm2) ranked so highly since these parameters have strong correlations with most of the selected species under study using ODEs and MRM/GSSA. This is because increasing the binding of Mdm2 and p53 and increasing the synthesis of Mdm2 prevents binding of GSK3β to p53 and decrease the activity of GSK3β. It was also interesting to find that parameters specific to p53 regulation pathway (KbinMdm2p53, ksynMdm2, kbinE2UB and Ksynp53mRNAAbeta) are the most important parameters in the system.

Most of the selected species are more sensitive in response to the LHS parameters at day #4. Therefore, immunization day is classified to be the most important day in the system that need to be taken into account to observe the sensitivity of the system in response to parameters perturbation.

Chapter 7
Conclusion and Future Directions

In this thesis, an immunization in AD model is modelled and its behaviour is investigated in response to parameters perturbation, one at a time and over the global space of parameters using LSA and GSA, respectively. This model is deterministically and stochastically modelled using ODEs GSSA, MRM/GSSA and the modified tau-leap method. The finite difference approximation method is used to locally investigate the behaviour of the system in response to parameters perturbation, one at a time, using ODEs and MRM/GSSA. LHS/PRCC is used to assess the behaviour of the system over global parameters space using also ODEs and MRM/GSSA. In this chapter, we give a general overview of our work and conclusions, summarise the major contribution and suggest several future directions that can follow this work.

7.1 Overview of the study and conclusions

The first object of this research is to not only accelerate a single run of GSSA but also include the concurrency feature in order to increase the performance of GSSA (Chapter 4). To accomplish this target, we modified MRM to be suitable to be combined with GSSA. The MRM method is a programming model that uses a parallel distributed algorithms on a cluster to run multiple processes simultaneously. We employ k threads to run k copies of GSSA for the same system. These threads elect k reactions and these k reactions go through a selection step to check their eligibility to be executed, where k is equal to the number of reactions that have propensity function more than zero. The value of k is dynamically changed depending on the status of the system.

The second objective is to validate MRM/GSSA also in Chapter 3 by comparing it with GSSA and the modified tau leap method. Immunization in AD model is modelled using these three approaches to achieve this validation in terms of results (stochasticity), performance (CPU time), reliability and implementation. In term of results, MRM/GSSA is more able to represent the stochasticity feature than the modified tau-leap method. We use all three approaches to produce 200

realizations and display the mean of these 200 runs. We use standard deviation to check how the set of data from these 200 realizations spread around its mean. GSSA shows the largest standard deviation and MRM/GSSA show larger standard deviation than the modified tau-leap method. In term of time, MRM/GSSA shows better performance than GSSA. MRM/GSSA also is comparable with the modified tau leap method. MRM/GSSA needs half time that is required by GSSA and a round 110% of time required by the modified tau leap method. However, MRM/GSSA is more reliable than the modified tau leap method that needs to deal with a critical value (n number of critical reactions). The value of n needs to be carefully determined depending on the status of the system. Therefore, an advance analysis of the system under required prior modelling step. Also, MRM/GSSA is much easier to be implemented than the modified tau leap method.

Conclusion: MRM/GSSA is not only able to include the stochastic feature more than the modified tau-leap method, but also more reliable and much easier to be implemented than the modified tau-leap method.

The third objective is to deterministically and stochastically investigate the critical behaviour of main species in immunization in the AD model. p53, ATMA, p53_GSK3β, Aβ, plaques, tangles and GliaA are selected to be the main species of the system. Investigating the critical behaviour of main species is achieved using LSA and GSA. To perform LSA using ODEs we use a finite difference approximation. To stochastically perform LSA, we use MRM/GSSA in conjunction with common random number (CRN) method. We use LHS/PRCC to analyse the global sensitivities of the parameters of the system and predict the most vulnerable target the main species of the system.

LSA using ODEs and MRM/GSSA shows that the behaviour of p53, ATMA, p53_GSK3β and Aβ are not dramatically changed in response to parameter perturbations. LSA using ODEs shows that only 28 parameters can change the behaviour of p53, ATMA and p53_GSK3β and 24 parameters to change the behaviour of Aβ. LSA using MRM/GSS demonstrates that 66 and 71 parameters adjust the behaviour of p53, ATMA and p53_GSK3β when parameters are

perturbed to 50% and 200% of their basal values, respectively. Aβ is changed in response to 71 parameters when LSA uses MRM/GSSA. Using ODEs to perform the sensitivity analysis show that p53, ATMA, p53_GSK3β and Aβ are more sensitive to their parameters in the early stages of the system. MRM/GSSA to perform the sensitivity analysis shows that p53, ATMA, p53_GSK3β and Aβ are sensitive over the whole period of the system.

Conclusion: performing LSA using ODEs and MRM/GSSA shows that p53, ATMA, p53_GSK3β and Aβ are not highly contributing to the overall behaviour of the system. The only difference between ODEs and MRM/GSSA is that the number of parameters that change the behaviour of these species.

LSA sensitivity analysis using ODEs and MRN/GSSA demonstrates that plaques, tangles and GliaA are very sensitive species in response to parameters perturbation one at a time since they dramatically changed in response to some parameters adjustments. LSA using ODEs and MRM/GSSA shows that there are 28 and 71 parameters adjust the behaviour of tangles, respectively. Conclusion: plaques, tangles and GliaA are highly contributing the overall behaviour of the system and more parameters affected the level of plaques when LSA uses MRM/GSSA.

Plaques level is significantly changed in response to 2 and 8 parameters when parameters are adjusted to 50% using ODEs and MRM/GSSA, respectively. Whereas, 5 and 13 parameters are dramatically changed plaques behaviour when parameters are perturbed to 200% using ODEs and MRM/GSSA. Conclusion: plagues are more sensitive for increasing the rates of parameters using both approaches.

LSA using ODEs shows that tangles are significantly changed in response to 11 parameters using ODEs when parameters are perturbed to 50% of their basal values while only 6 parameters dramatically changed tangles behaviour when parameters are adjusted to 200% of their basal values. Using MRM/GSSA to perform the sensitivity analysis show same parameters (14 parameters) are dramatically changed the behaviour of tangles when parameters are perturbed to

50% and 200% of their basal value. Conclusion: tangles are more sensitive for decreasing parameters rate using ODEs.

The level of GliaA is significantly changed in response to 2 and 6 parameters when parameters are adjusted to 50% using ODEs and MRM/GSSA, respectively. Whereas, 6 and 13 parameters are dramatically changed the behaviour of GliaA when parameters are perturbed to 200% using ODEs and MRM/GSSA. Conclusion: GliaA is more sensitive for increasing the rates of parameters using both approaches.

GSA using LHS/PRCC (Chapter 6) demonstrates that parameters specific to p53 and Mdm2 (KbinMdm2p53 and ksynMdm2) ranked so highly since these parameters affect the behaviour of most of the selected species under study using ODEs and MRM/GSSA. This is because increasing the binding of Mdm2 and p53 and increasing the syntheses of Mdm2 prevent binding of GSK3β to p53 and lower the activity of GSK3β. It was also interesting to find that parameters specific to p53 regulation pathway (KbinMdm2p53, ksynMdm2, kbinE2UB and Ksynp53mRNAAbeta) are the most important parameters in the system. Conclusion: parameters specific to p53 regulation are the most important parameters that highly contribute to the variation.

7.2 Contributions

The major contributions of this thesis are:

1- Developiving MRM/GSSA to accelerate a single run of GSSA.
2- Validating MRM/GSSA by comparing it with not only GSSA itself, but also the modified tau-leap method and verifying that MRM/GSSA needs only half time required by GSSA and it is commparable with the modified tau-leap method. MRM/GSSA is not only more able to represent variance, but also more reliable to be used for any biochemical system than the modified tau-leap method.
3- Using ODEs and MRM/GSSA to perform LSA and GSA to:
    - Determine the maximum and minimum ranges of each parameter in immunization in AD model.

- Classify the most important species in the model
- Classify the most important parameters that contribute to the overall behaviour of the system not only when parameters are perturbed one at a time, but also over the space of parameters.
- Identify pathways that are not dramatically changed when parameters are perturbed.

7.3 Future Directions

We suggest several future direction that can follow the current work:

1. Developing a tool that is based on MRM/GSSA to not only model biochemical system, but also stochastically perform LSA and GSA.

2. Proposing a dynamic way to change the value of n in the modified tau-leap method depending on the dynmaic status of the system.

3. At the level of LSA:
    - Investigate the behaviour of all species in response to parameters pertubation since all species are important in the system while we just investiged the behaviour of seven species in this parameters.
    - For those parameters that dramatically changed the behaviour of the selected species, reducing the ranges of minimum and maximum to determine the exact ranges of these parameters.

4. Investigating the behaviour of more species in response to parameters perturbation over the global space of parameters would be the future direction at the level of GSA.

Appendix A

Alzheimer's disease Models

Table A.1: Mathematical models of AD. Table A.1 lists collection of mathematical models that have been proposed to model different concepts of AD. Table A.1 includes:

1- Title of the publication
2- Reference
3- Study nature
4- Modelling Type
5- Pathways involved
6- Process modelled

Table A. 1: Mathmatical Models of AD

ID	Title of the publication	Reference	Study Nature	Modelling Type	Pathways Involved	Process Modelled
1	Alzheimer's disease: a mathematical model for onset and progression	(Bertsch, Franchi, Marcello, Tesi, & Tosin, 2016)	Modelling	Integro differential equations; PDE	APP breakdown, fibril organization, BBB transport	Transport and diffusion of Aβ along with the random onset of Alzheimer's disease
2	The zinc dyshomeostasis hypothesis of Alzheimer's disease	(Craddock et al., 2012)	Experiment + modelling	Molecular Model, Ordinary Differential Equations	Taupathy, fibril organization, ion homoeostasis	Role of zinc in beta-amyloid aggregation and memory formation
3	A mathematical model of the impact of novel treatments on the A beta burden in the Alzheimer's brain	(Craft, Wein, & Selkoe, 2002)	Modelling	Ordinary Differential Equations	Fibril organization	Kinetics of Aβ levels in the brain, cerebrospinal fluid and plasma
5	The choline-leakage hypothesis for the loss of acetylcholine in Alzheimer's disease	(Ehrenstein, Galdzicki, & Lange, 1997)	Experiment + modelling	Ordinary Differential Equations	Synaptic transmission (acetylcholine), APP breakdown	Two-component positive feedback: Aβ-dependent leakage of choline and ACh-dependent production of Aβ
6	A positive-feedback model for the loss of acetylcholine in Alzheimer's disease	(Ehrenstein, Galdzicki, & Lange, 2000)	Experiment + modelling	Ordinary Differential Equations	Synaptic transmission (acetylcholine), APP breakdown	Two component positive feedback: Aβ-mediated apoptosis decreases ACh and low ACh favours APP processing

7	**Effect of beta-amyloid block of the fast-inactivating K^+ channel on intracellular Ca^{2+} and excitability in a modelled neuron.**	**(Good & Murphy, 1996)**	**Modelling**	**Partial Differential Equations**	**Ion homoeostasis, Synaptic transmission**	**Interplay between Aβ, ion homoeostasis and neuron excitability**
8	**Cerebral amyloid-beta proteostasis is regulated by the membrane transport protein, ABCC1, in mice.**	**(Krohn et al., 2011)**	**Experiment + modelling**	**Ordinary Differential Equations**	**APP breakdown, BBB transport**	**Processes regulating the production and removal of Aβ aggregates**
9	**Mathematical models of alpha-synuclein transport in axons**	**(Kuznetsov & Kuznetsov, 2016)**	**Modelling**	**Ordinary & Partial Differential Equations; Algebraic Equations**	**Taupathy, MT-based transport**	**Dynamics of MT-based-Tau protein transport in degenerating axons**
10	**Of mice and maths: a systems biology model for Alzheimer's disease**	**(Kyrtsos, 2011)**	**Experiment + modelling**	**Ordinary & Partial Differential Equations**	**Energy metabolism, inflammatory response, synaptic ttransmission, fibril organization, APP breakdown, BBB transport**	**Interplay between APP, Aß and cholesterol processing in the brain**
11	**Studying the role of ApoE in Alzheimer's disease pathogenesis using a systems biology model**	**(Kyrtsos & Baras, 2013)**	**Modelling**	**Algebraic Equations**	**Inflammatory response, apoptosis, APP breakdown, fibril organization, intercellular signalling, genetics**	**ApoE allele variation and inflammation**

12	**Modelling the role of the glymphatic pathway and cerebral blood vessel properties in Alzheimer's disease pathogenesis**	**(Kyrtsos & Baras, 2015)**	**Modelling**	**Ordinary & Partial Differential Equations**	**APP breakdown**	**Aβ dynamics regulated by brain vasculature, glymphatic system kinetics and age**
13	**Multi-compartmental modelling of SORLA[1]'s influence on amyloidogenic processing in Alzheimer's disease**	**(Lao, Schmidt, Schmitz, Willnow, & Wolkenhauer, 2012)**	**Experiment + Modelling**	**Ordinary Differential Equations**	**APP breakdown**	**Effects of SORLA on APP processing**
14	**Chemotactic signalling, microglia, and Alzheimer's disease senile plaques: is there a connection?**	**(Luca, Chavez-Ross, Edelstein-Keshet, & Mogilner, 2003)**	**Modelling**	**Partial Differential Equations**	**Inflammatory response**	**Microglia chemotaxis in response to a combination of chemoattractant and chemorepellents**
15	**Mathematical model of Alzheimer's disease and the Apoe gene.**	**(Macdonald & Pritchard, 2000)**	**Modelling**	**Markov Model (differential equations)**	**Genetics**	**AD evolution with respect to ApoE gene variability**
16	**A mathematical model of aging-related and cortisol induced hippocampal dysfunction**	**(McAuley et al., 2009)**	**Modelling**	**Ordinary Differential Equations**	**Synaptic transmission**	**Effects of elevated plasma cortisol on hippocampal activity and atrophy**

[1] ***SORLA*** **is an endocytosis and sorting receptor**

17	**Interplay between alpha-, beta- and gamma-secretases determines biphasic amyloid-beta protein level in the presence of a gamma-secretase inhibitor**	**(Ortega, Stott, Visser, & Bendtsen, 2013)**	**Experiment + Modelling**	**Ordinary Differential Equations**	**APP breakdown**	**Interplay between α-, β-, and γ-secretases on Aβ dynamics in presence of a γ-secretase inhibitor**
18	**A mathematical model of the kinetics of beta-amyloid fibril growth from the denatured state.**	**(Pallitto & Murphy, 2001)**	**Experiment + modelling**	**Algebraic & Ordinary Differential Equations**	**Fibril organization**	**Fibril formation process of Aβ**
19	**GSK3 and p53 — is there a link in Alzheimer's disease?**	**(Proctor & Gray, 2010)**	**Modelling**	**Stochastic Model**	**Taupathy, fibril organization, protein degradation, oxidative stress**	**Role of GSK3 and p53 in Aβ aggregation dynamics**
20	**Aggregation, impaired degradation and immunization targeting of amyloid-beta dimers in Alzheimer's disease: a stochastic modelling approach**	**(Proctor, Pienaar, Elson, & Kirkwood, 2012)**	**Modelling**	**Stochastic Model**	**Fibril organization**	**Aβ turnover and its aggregation kinetics along with the effect of immunization against Aβ dimers**
21	**Investigating interventions in Alzheimer's disease with computer simulation models.**	**(Proctor et al., 2013)**	**Modelling**	**Ordinary Differential Equations**	**Fibril organization, taupathy, oxidative stress, inflammatory response, apoptosis**	**Effectiveness of passive and active immunisation against Aβ in phosphorylated tau, tangles and Aβ plaques**

22	Mathematical modelling for the pathogenesis of Alzheimer's disease.	(Puri & Li, 2010)	Modelling	Ordinary Differential Equations	Intercellular signalling, inflammatory response, apoptosis	Cross-talk among distinct states of microglia, astroglia, and neurons
23	Differences in amyloid-beta clearance across mouse and human blood-brain barrier models: kinetic analysis and mechanistic modelling.	(Qosa et al., 2014)	Experiment + modelling	Ordinary Differential Equations	Fibril organization, BBB transport	Uptake, efflux and degradation of Aβ
24	Computational modelling of the effects of amyloid-beta on release probability at hippocampal synapses.	(Romani et al., 2013)	Experiment + modelling		Synaptic transmission	Role of Aβ on synaptic currents
25	Electrostimulation to reduce synaptic scaling driven progression of Alzheimer's disease.	(Rowan, Neymotin, & Lytton, 2014)	Modelling	Rule-based Model	Synaptic transmission	Effect of electrostimulation on synaptic activity of different neuron populations
26	Multi-compartmental modelling of SORLA's influence on amyloidogenic processing in Alzheimer's disease.	(Lao et al., 2012)	Experiment + modelling	Ordinary Differential Equations	APP breakdown	Effect of SORLA on amyloidogenic processing kinetics

27	**Modulators of gamma-secretase activity can facilitate the toxic side-effects and pathogenesis of Alzheimer's disease.**	**(Svedružić, Popović, & Šendula-Jengić, 2013)**	**Modelling**	**Algebraic Equations**	**APP breakdown**	**Modulation of γ-secretase activity by the biphasic inhibitor, DAPT**
28	**Altered intrinsic excitability of hippocampal CA1 pyramidal neurons in aged PDAPP mice**	**(Tamagnini et al., 2015)**	**Experiment + modelling**	**Ordinary Differential Equations**	**Genetics**	**Effect of altered Aβ levels on action potential of aged neurons**
29	**Modelling of calcium dynamics in brain energy metabolism and Alzheimer's disease**	**(Tiveci, Akın, Çakır, Saybaşılı, & Ülgen, 2005)**	**Experiment + modelling**	**Ordinary Differential Equations**	**Ion homoeostasis, energy metabolism**	**Dynamics of calcium ion in membrane ionic currents, glycolysis, mitochondrial activity and exchanges through the blood-brain barrier**
30	**Are improper kinetic models hampering drug development?**	**(Walsh, 2014)**	**Modelling**	**Algebraic Equations**	**APP breakdown**	**Kinetic model of the drug action of DAPT on gamma-secretase.**
31	**Vulnerabilities in the tau network and the role of ultrasensitive points in tau pathophysiology**	**(Yuraszeck et al., 2010)**	**Modelling**	**Ordinary Differential Equations**	**Taupathy**	**Aggregation process of 3R and 4R isoforms of tau proteins**

Appendix B

System's Description

Appendix B includes four Tables and one Figure.

- Table B.1 lists all reactions of the system (Names, Equations and Kinetic laws)
- Table B. 2 includes the set of ODEs
- Table B. 3 contains all species with their initial values.
- Table B.4 consists of parameters, their description and their initial values.
- Figure B.1 displays p53 regulation and its reaction.
- Table B.5 lists reactions that are included in p53 regulation. Reaction numbers correspond to the numbers in Table 1

Table B. 1: Reactions of the system

#	Reaction name	Reaction Equation	Kinetic law
1	p53_mRNA_Synthesis	$\mathrm{Source} \xrightarrow{\mathrm{ksynp53mRNA}} \mathrm{p53\_mRNA}$	$v1 = \mathrm{ksynp53mRNA} * \mathrm{Source}$
2	p53_mRNA_Degradation	$\mathrm{p53\_mRNA} \xrightarrow{\mathrm{kdegp53mRNA}} \mathrm{sink}$	$v2 = \mathrm{kdegp53mRNA} * \mathrm{p53mRNA}$
3	Mdm2Synthesis	$\mathrm{Mdm2mRNA} \xrightarrow{\mathrm{ksynMdm2}} \mathrm{Mdm2\_mRNA} + \mathrm{Mdm2}$	$v3 = \mathrm{ksynMdm2} * \mathrm{Mdm2\_mRNA}$
4	Mdm2mRNASynthesis1	$\mathrm{p53} \xrightarrow{\mathrm{ksynMdm2mRNA}} \mathrm{p53} + \mathrm{Mdm2\_mRNA}$	$v4 = \mathrm{ksynMdm2mRNA} * \mathrm{p53}$
5	Mdm2mRNASynthesis2	$\mathrm{p53\_P} \xrightarrow{\mathrm{ksynMdm2mRNA}} \mathrm{p53\_P} + \mathrm{Mdm2\_mRNA} + \mathrm{Mdm2\_mRNAsyn}$	$v5 = \mathrm{ksynMdm2mRNA} * \mathrm{p53\_P}$
6	Mdm2mRNASynthesis3	$\mathrm{GSK3b\_p53} \xrightarrow{\mathrm{ksynMdm2mRNAGSK3bp53}} \mathrm{GSK3b\_p53} + \mathrm{Mdm2\_mRNA}$	$v6 = \mathrm{ksynMdm2mRNAGSK3bp53} * \mathrm{GSK3b\_p53}$
7	Mdm2 mRNA Synthesis4	$\mathrm{GSK3b\_p53\_P} \xrightarrow{\mathrm{ksynMdm2mRNAGSK3bp53}} \mathrm{GSK3b\_p53\_P} + \mathrm{Mdm2\_mRNA}$	$v7 = \mathrm{ksynMdm2mRNAGSK3bp53} * \mathrm{GSK3b\_p53\_P}$
8	Mdm2mRNADegradation	$\mathrm{Mdm2\ mRNA} \xrightarrow{\mathrm{kdegMdm2mRNA}} \mathrm{Sink} + \mathrm{Mdm2\_mRNAdeg}$	$v8 = \mathrm{kdegMdm2mRNA} * \mathrm{Mdm2\_mRNA}$
9	p53_Mdm2 Binding	$\mathrm{Mdm2} + \mathrm{p53} \xrightarrow{\mathrm{kbinMdm2p53}} \mathrm{Mdm2\_p53}$	$v9 = \mathrm{kbinMdm2p53} * \mathrm{p53} * \mathrm{Mdm2}$
10	p53_Mdm2 Release	$\mathrm{Mdm2\_p53} \xrightarrow{\mathrm{krelMdm2p53}} \mathrm{Mdm2} + \mathrm{p53}$	$v10 = \mathrm{krelMdm2p53} * \mathrm{p53\ \_Mdm2}$
11	GSK3_p53 Binding	$\mathrm{GSK3b} + \mathrm{p53} \xrightarrow{\mathrm{kbinGSK3bp53}} \mathrm{GSK3b\_p53}$	$v11 = \mathrm{kbinGSK3bp53} * \mathrm{GSK3b} * \mathrm{p53}$
12	GSK3_p53 Release	$\mathrm{GSK3b\_p53} \xrightarrow{\mathrm{krelGSK3bp53}} \mathrm{GSK3b} + \mathrm{p53}$	$v12 = \mathrm{krelGSK3bp53} * \mathrm{GSK3b\_p53}$
13	GSK3_p53_P Binding	$\mathrm{GSK3b} + \mathrm{p53\_P} \xrightarrow{\mathrm{kbinGSK3bp53}} \mathrm{GSK3b\_p53\_P}$	$v13 = \mathrm{kbinGSK3bp53} * \mathrm{GSK3b} * \mathrm{p53\_P}$
14	GSK3_p53_P Release	$\mathrm{GSK3b\_p53\_P} \xrightarrow{\mathrm{kbinGSK3bp53}} \mathrm{GSK3b} + \mathrm{p53\_P}$	$v14 = \mathrm{krelGSK3bp53} * \mathrm{GSK3b\_p53\_P}$
15	E1_Ub Binding	$\mathrm{E1} + \mathrm{Ub} + \mathrm{ATP} \xrightarrow{\mathrm{kbinE1Ub}} \mathrm{E1\_Ub} + \mathrm{AMP}$	$v15 = \frac{\mathrm{kbinE1Ub} * \mathrm{E1} * \mathrm{Ub} * \mathrm{ATP}}{5000 + \mathrm{ATP}}$
16	E2_Ub Binding	$\mathrm{E2} + \mathrm{E1\_Ub} \xrightarrow{\mathrm{kbinE2Ub}} \mathrm{E2\_Ub} + \mathrm{E1}$	$v16 = \mathrm{kbinE2Ub} * \mathrm{E2} * \mathrm{E1\_Ub}$
17	Mdm2_Ubiquitination	$\mathrm{Mdm2} + \mathrm{E2\_Ub} \xrightarrow{\mathrm{kMdm2Ub}} \mathrm{Mdm2\_Ub} + \mathrm{E2}$	$v17 = \mathrm{kMdm2Ub} * \mathrm{Mdm2} * \mathrm{E2\_Ub}$
18	Mdm2 poly Ubiquitination1	$\mathrm{Mdm2\_Ub} + \mathrm{E2\_Ub} \xrightarrow{\mathrm{kMdm2PolyUb}} \mathrm{Mdm2\_Ub2} + \mathrm{E2}$	$v18 = \mathrm{kMdm2PolyUb} * \mathrm{Mdm2\_Ub} * \mathrm{E2\_Ub}$
19	Mdm2 poly Ubiquitination2	$\mathrm{Mdm2\_Ub2} + \mathrm{E2\_Ub} \xrightarrow{\mathrm{kMdm2PolyUb}} \mathrm{Mdm2\_Ub3} + \mathrm{E2}$	$v19 = \mathrm{kMdm2PolyUb} * \mathrm{Mdm2\_Ub2} * \mathrm{E2\_Ub}$
20	Mdm2 poly Ubiquitination3	$\mathrm{Mdm2\_Ub3} + \mathrm{E2\_Ub} \xrightarrow{\mathrm{kMdm2PolyUb}} \mathrm{Mdm2\_Ub4} + \mathrm{E2}$	$v20 = \mathrm{kMdm2PolyUb} * \mathrm{Mdm2\_Ub3} * \mathrm{E2\_Ub}$
21	Mdm2 Deubiquitination4	$\mathrm{Mdm2\_Ub4} + \mathrm{Mdm2DUB} \xrightarrow{\mathrm{kactDUBMdm2}} \mathrm{Mdm2\ Ub3} + \mathrm{Mdm2DUB} + \mathrm{Ub}$	$v21 = \mathrm{kactDUBMdm2} * \mathrm{Mdm2\_Ub4} * \mathrm{Mdm2DUB}$
22	Mdm2 Deubiquitination3	$\mathrm{Mdm2\_Ub3} + \mathrm{Mdm2DUB} \xrightarrow{\mathrm{kactDUBMdm2}} \mathrm{Mdm2\_Ub2} + \mathrm{Mdm2DUB} + \mathrm{Ub}$	$v22 = \mathrm{kactDUBMdm2} * \mathrm{Mdm2\_Ub3} * \mathrm{Mdm2DUB}$
23	Mdm2 Deubiquitination2	$\mathrm{Mdm2\_Ub2} + \mathrm{Mdm2DUB} \xrightarrow{\mathrm{kactDUBMdm2}} \mathrm{Mdm2\_Ub} + \mathrm{Mdm2DUB} + \mathrm{Ub}$	$v23 = \mathrm{kactDUBMdm2} * \mathrm{Mdm2\_Ub2} * \mathrm{Mdm2DUB}$
24	Mdm2 Deubiquitination1	$\mathrm{Mdm2\_Ub} + \mathrm{Mdm2DUB} \xrightarrow{\mathrm{kactDUBMdm2}} \mathrm{Mdm2} + \mathrm{Mdm2DUB} + \mathrm{Ub}$	$v24 = \mathrm{kactDUBMdm2} * \mathrm{Mdm2\_Ub} * \mathrm{Mdm2DUB}$
25	Mdm2_Proteasome Binding1	$\mathrm{Mdm2\_Ub4} + \mathrm{Proteasome} \xrightarrow{\mathrm{kbinProt}} \mathrm{Mdm2\_Ub4\_Proteasome}$	$v25 = \mathrm{kbinProt} * \mathrm{Mdm2\_Ub4} * \mathrm{Proteasome}$
26	Mdm2 Degradation	$\mathrm{Mdm2\_Ub4\_Proteasome} \xrightarrow{\mathrm{kdegMdm2} * \mathrm{kproteff}} \mathrm{Proteasome} + 4\mathrm{Ub}$	$v26 = \mathrm{kdegMdm2} * \mathrm{kproteff} * \mathrm{Mdm2\_Ub4\_Proteasome}$
27	p53 Synthesis	$\mathrm{p53mRNA} \xrightarrow{\mathrm{ksynp53}} \mathrm{p53} + \mathrm{p53mRNA} + \mathrm{p53syn}$	$v27 = \mathrm{ksynp53} * \mathrm{p53mRNA}$
28	p53 Monoubiquitination	$\mathrm{E2\_Ub} + \mathrm{Mdm2\_p53} \xrightarrow{\mathrm{kp53Ub}} \mathrm{Mdm2\ p53\ Ub} + \mathrm{E2}$	$v28 = \mathrm{kp53Ub} * \mathrm{E2\_Ub} * \mathrm{Mdm2\_p53}$
29	p53 Polyubiquitination1	$\mathrm{Mdm2\_p53\_Ub} + \mathrm{E2\_Ub} \xrightarrow{\mathrm{kp53PolyUb}} \mathrm{Mdm2\_p53\_Ub2} + \mathrm{E2}$	$v29 = \mathrm{kp53PolyUb} * \mathrm{Mdm2\_p53\_Ub} * \mathrm{E2\_Ub}$

30	p53 Polyubiquitination2	$Mdm2\_p53\_Ub2 + E2\_Ub \xrightarrow{kp53PolyUb} Mdm2\_p53\_Ub3 + E2$	$v30 = kp53PolyUb * Mdm2\_p53\_Ub2 * E2\_Ub$
31	p53 Polyubiquitination3	$Mdm2\_p53\_Ub3 + E2\_Ub \xrightarrow{kp53PolyUb} Mdm2\_p53\_Ub4 + E2$	$v31 = kp53PolyUb * Mdm2\_p53\_Ub3 * E2\_Ub$
32	p53 Deubiqutination4	$Mdm2\_p53\_Ub4 + p53DUB \xrightarrow{kactDUBp53} Mdm2\_p53\_Ub3 + p53DUB + Ub$	$v32 = kactDUBp53 * Mdm2\_p53\_Ub4 * p53DUB$
33	p53 Deubiquitination3	$Mdm2\_p53\_Ub3 + p53DUB \xrightarrow{kactDUBp53} Mdm2\_p5\_Ub2 + p53DB + Ub$	$v33 = kactDUBp53 * Mdm2\_p53\_Ub3 * p53DUB$
34	p53 Deubiquitination2	$Mdm2\_p53\_Ub2 + p53DUB \xrightarrow{kactDUBp53} Mdm2\_p53\_Ub + p53DUB + Ub$	$v34 = kactDUBp53 * Mdm2\_p53\_Ub2 * p53DUB$
35	p53 Deubiquitination1	$Mdm2\_p53\_Ub + p53DUB \xrightarrow{kactDUBp53} Mdm2\_p53 + p53DUB + Ub$	$v35 = kactDUBp53 * Mdm2\_p53\_Ub * p53DUB$
36	Mdm2_GSK3 phosphorylation1	$Mdm2\_p53\_Ub4 + GSK3b \xrightarrow{kphosMdm2GSK3b} Mdm2\_P1\_p53\_Ub4 + GSK3b$	$v36 = kphosMdm2GSK3b * Mdm2\_p53\_Ub4 * GSK3b$
37	Mdm2 GSK3 phosphorylation2	$Mdm2\_p53\_Ub4 + GSK3b\_p53 \xrightarrow{kphosMdm2GSK3bp53} Mdm2\_P1\_p53\_Ub4 + GSK3b\_p53$	$v37 = kphosMdm2GSK3bp53 * Mdm2\_p53\_Ub4 * GSK3b\_p53$
38	Mdm2 GSK3 phosphorylation3	$Mdm2\_p53\_Ub4 + GSK3b\_p53\_P \xrightarrow{kphosMdm2GSK3bp53} Mdm2\_P1\_p53\_Ub4 + GSK3b\_p53\_p$	$v38 = kphosMdm2GSK3bp53 * Mdm2\_p53\_Ub4 * GSK3b\_p53\_P$
39	p53_Proteasome Binding1	$Mdm2\_P\_p53\_Ub4 + Proteasome \xrightarrow{kbinProt} p53\_Ub4\_Proteasome + Mdm2$	$v39 = kbinProt * Mdm2\_P\_p53\_Ub4 * Proteasome$
40	Degradation p53_Ub4	$p53\_Ub4\_Proteasome + ATP \xrightarrow{kdegp53*kproteff} 4Ub + Proteasome + ADP$	$v40 = \frac{kdegp53 * kproteff * p53\_Ub4\_Proteasome * ATP}{5000 + ATP}$
41	Tau_MT binding	$Tau \xrightarrow{kbinMTTau} MT\_Tau$	$v41 = kbinMTTau * Tau$
42	Tau_MT release	$MT\_Tau \xrightarrow{krelMTTau} Tau$	$v42 = krelMTTau * MT\_Tau$
43	Tau phosphorylation1	$GSK3b\_p53 + Tau \xrightarrow{kphospTauGSK3bp53} GSK3b\_p53 + Tau\_P1$	$v43 = kphospTauGSK3bp53 * GSK3b\_p53 * Tau$
44	Tau phosphorylation2	$GSK3b\_p53 + Tau\_P1 \xrightarrow{kphospTauGSK3bp53} GSK3b\_p53 + Tau\_P2$	$v44 = kphospTauGSK3bp53 * GSK3b\_p53 * Tau\_P$
45	Tau phosphorylation3	$GSK3b\_p53\_P + Tau \xrightarrow{kphospTauGSK3bp53} GSK3b\_p53\_P + Tau\_P1$	$v45 = kphospTauGSK3bp53 * GSK3b\_p53\_P * Tau$
46	Tau phosphorylation4	$GSK3b\_p53\_P + Tau\_P1 \xrightarrow{kphospTauGSK3bp53} GSK3b\_p53\_P + Tau\_P2$	$v46 = kphospTauGSK3bp53 * GSK3b\_p53\_P * Tau\_P1$
47	Tau phosphorylation5	$GSK3b + Tau \xrightarrow{kphospTauGSK3b} GSK3b + Tau\_P1$	$v47 = kphospTauGSK3b * GSK3b * Tau$
48	Tau phosphorylation6	$GSK3b + Tau\_P1 \xrightarrow{kphospTauGSK3b} GSK3b + Tau\_P2$	$v48 = kphospTauGSK3b * GSK3b * Tau\_P1$
49	Tau dephosphorylation1	$Tau\_P2 + PP1 \xrightarrow{kdephospTau} Tau\_P1 + PP1$	$v49 = kdephospTau * PP1 * Tau\_P2$
50	Tau dephosphorylation2	$Tau\_P1 + PP1 \xrightarrow{kdephospTau} Tau + PP1$	$v50 = kdephospTau * PP1 * Tau\_P1$
51	Tau_P1 Aggregation1	$2 * Tau\_P1 \xrightarrow{kaggTauP1} 2 * AggTau$	$v51 = kaggTauP1 * Tau\_P1^{2} * 0.5$
52	Tau_P1 Aggregation2	$Tau\_P1 + AggTau \xrightarrow{kaggTauP1} 2 * AggTau$	$v52 = kaggTauP1 * Tau\_P1 * AggTau$
53	Tau_P2 Aggregation1	$2 * Tau\_P2 \xrightarrow{kaggTauP2} 2 * AggTau$	$v53 = kaggTauP2 * Tau\_P2^{2} * 0.5$
54	Tau_P2 Aggregation2	$Tau\_P2 + AggTau \xrightarrow{kaggTauP2} 2 * AggTau$	$v54 = kaggTauP2 * Tau\_P2^{2} * 0.5$
55	Tau Aggregation1	$2 * Tau \xrightarrow{kaggTau} 2 * AggTau$	$v55 = kaggTau * Tau^{2} * 0.5$
56	Tau Aggregation2	$Tau + AggTau \xrightarrow{kaggTau} 2 * AggTau$	$v56 = kaggTau * Tau * AggTau$
57	Tangle Formation1	$2 * AggTau \xrightarrow{ktangfor} 2 * NFT$	$v57 = ktangfor * AggTau^{2} * 0.5$

58	Tangle Formation2	$NFT + AggTau \xrightarrow{ktangfor} 2 * NFT$	$v58 = ktangfor * AggTau * NFT$
59	Proteasome Inhibition Agg Tau	$Proteasome + AggTau \xrightarrow{kinhibprot} AggTau\_Proteasome$	$v59 = kinhibprot * AggTau * Proteasome$
60	Abeta production1	$Source \xrightarrow{kprodAbeta} Abeta$	$v60 = kprodAbeta * Source$
61	Abeta production2	$GSK3b\_p53 \xrightarrow{kprodAbeta2} Abeta + GSK3b\_p53$	$v61 = kprodAbeta2 * GSK3b\_p53$
62	Abeta production3	$GSK3b\_p53\_P \xrightarrow{kprodAbeta2} Abeta + GSK3b\_p53\_P$	$v62 = kprodAbeta2 * GSK3b\_p53\_P$
63	Proteasome Inhibition Abeta	$AbetaDimer + Proteasome \xrightarrow{kinhibprot} AggAbeta\_Proteasome$	$v63 = kinhibprot * AbetaDimer * Proteasome$
64	Abeta Degradation	$Abeta \xrightarrow{kdegAbeta} Sink$	$v64 = kdegAbeta * Abeta$
65	p53 transcription Via Abeta	$Abeta \xrightarrow{ksynp53mRNAAbeta} p53\_mRNA + Abeta$	$v65 = ksynp53mRNAAbeta * Abeta$
66	DNA damage	$IR \xrightarrow{kdam} IR + damDNA$	$v66 = kdam * IR$
67	DNA repair	$damDNA \xrightarrow{krepair} Sink$	$v67 = krepair * damDNA$
68	ATM activation	$damDNA + ATMI \xrightarrow{kactATM} damDNA + ATMA$	$v68 = kactATM * damDNA * ATMI$
69	p53 phosphorylation	$p53 + ATMA \xrightarrow{kphosp53} p53\_P + ATMA$	$v69 = kphosp53 * p53 * ATMA$
70	p53 dephosphorylation	$p53\_P \xrightarrow{kdephosp53} p53$	$v70 = kdephosp53 * p53\_P$
71	Mdm2 phosphorylation	$Mdm2 + ATMA \xrightarrow{kphosMdm2} Mdm2\_P + ATMA$	$v71 = kphosMdm2 * Mdm2 * ATMA$
72	Mdm2 dephosphorylation	$Mdm2\_P \xrightarrow{kdephosMdm2} Mdm2$	$v72 = kdephosMdm2 * Mdm2\_P$
73	Mdm2_P Ubiquitination	$Mdm2\_P + E2\_Ub \xrightarrow{kMdm2PUb} Mdm2\_P\_Ub + E2$	$v73 = kMdm2PUb * Mdm2\_P * E2\_Ub$
74	Mdm2_P polyUbiquitination1	$Mdm2\_P\_Ub + E2\_Ub \xrightarrow{kMdm2PolyUb} Mdm2\_P\_Ub2 + E2$	$v74 = kMdm2PolyUb * Mdm2\_P\_Ub * E2\_Ub$
75	Mdm2_P polyUbiquitination2	$Mdm2\_P\_Ub2 + E2\_Ub \xrightarrow{kMdm2PolyUb} Mdm2\_P\_Ub3 + E2$	$v75 = kMdm2PolyUb * Mdm2\_P\_Ub2 * E2\_Ub$
76	Mdm2_PpolyUbiquitination3	$Mdm2\_P\_Ub3 + E2\_Ub \xrightarrow{kMdm2PolyUb} Mdm2\_P\_Ub4 + E2$	$v76 = kMdm2PolyUb * Mdm2\_P\_Ub3 * E2\_Ub$
77	Mdm2_P Deubiquitination4	$Mdm2\_P\_Ub4 + Mdm2DUB \xrightarrow{kactDUBMdm2} Mdm2\_P\_Ub3 + Mdm2DUB + Ub$	$v77 = kactDUBMdm2 * Mdm2\_P\_Ub4 * Mdm2DUB$
78	Mdm2_P Deubiquitination3	$Mdm2\_P\_Ub3 + Mdm2DUB \xrightarrow{kactDUBMdm2} Mdm2\_P\_Ub2 + Mdm2DUB + Ub$	$v78 = kactDUBMdm2 * Mdm2\_P\_Ub3 * Mdm2DUB$
79	Mdm2_P Deubiquitination2	$Mdm2\_P\_Ub2 + Mdm2DUB \xrightarrow{kactDUBMdm2} Mdm2\_P\_Ub + Mdm2DUB + Ub$	$v79 = kactDUBMdm2 * Mdm2\_P\_Ub2 * Mdm2DUB$
80	Mdm2_P Deubiquitination1	$Mdm2\_P\_Ub + Mdm2DUB \xrightarrow{kactDUBMdm2} Mdm2\_P + Mdm2DUB + Ub$	$v80 = kactDUBMdm2 * Mdm2\_P\_Ub * Mdm2DUB$
81	Mdm2_P_Proteasome Binding1	$Mdm2\_P\_Ub4 + Proteasome \xrightarrow{kbinProt} Mdm2\_P\_Ub4\_Proteasome$	$v81 = kbinProt * Mdm2\_P\_Ub4 * Proteasome$
82	Mdm2_P Degradation	$Mdm2\_P\_Ub4\_Proteasome \xrightarrow{kdegMdm2*kproteff} Proteasome + 4 * Ub$	$v82 = kdegMdm2 * Mdm2\_P\_Ub\_Proteasome * kproteff$
83	ATM Inactivation	$ATMA \xrightarrow{kinactATM} ATMI$	$v83 = kinactATM * ATMA$
84	Abeta ROS production1	$Abeta \xrightarrow{kgenROSAbeta} Abeta + ROS$	$v84 = kgenROSAbeta * Abeta$
85	Plaque ROS production	$AbetaPlaque \xrightarrow{kgenROSPlaque} AbetaPlaque + ROS$	$v85 = kgenROSPlaque * AbetaPlaque$
86	Agg Abeta ROS production2	$AggAbeta\_Proteasome \xrightarrow{kgenROSAbeta} AggAbeta\_Proteasome + ROS$	$v86 = kgenROSAbeta * AggAbeta\_Proteasome$
87	ROS DNA damage	$ROS \xrightarrow{kdamROS} ROS + damDNA$	$v87 = kdamROS * ROS$

88	Tau Synthesis	$\mathbf{Source} \xrightarrow{\mathbf{ksynTau}} \mathbf{Tau}$	$\mathbf{v88 = ksynTau * Source}$
89	Tau Proteasome Binding	$\mathbf{Tau + Proteasome} \xrightarrow{\mathbf{kbinTauProt}} \mathbf{Tau\_Proteasome}$	$\mathbf{v89 = kbinTauProt * Tau * Proteasome}$
90	Tau 20SProteasome Degradation	$\mathbf{Tau\_Proteasome} \xrightarrow{\mathbf{kdegTau20SProt}} \mathbf{Proteasome}$	$\mathbf{v90 = kdegTau20SProt * Tau\_Proteasome}$
91	Abeta Aggregation1	$\mathbf{2 * Abeta} \xrightarrow{\mathbf{kaggAbeta}} \mathbf{AbetaDimer}$	$\mathbf{v91 = kaggAbeta * Abeta^2 * 0.5}$
92	Abeta Plaque Formation1	$\mathbf{2 * AbetaDimer} \xrightarrow{\mathbf{kpf}} \mathbf{AbetaPlaque}$	$\mathbf{v92 = kpf * AbetaDimer^2 * 0.5}$
93	Abeta Plaque Growth	$\mathbf{AbetaDimer + AbetaPlaque} \xrightarrow{\mathbf{kpf,kpghalf}} \mathbf{2 * AbetaPlaque}$	$\mathbf{v93} = \frac{\mathbf{kpf * AbetaPlaque^2 * AbetaDimer}}{\mathbf{kpghalf^2 + AbetaPlaque^2}}$
94	Abeta Disaggregation1	$\mathbf{AbetaDimer} \xrightarrow{\mathbf{kdisaggAbeta}} \mathbf{2 * Abeta}$	$\mathbf{v94 = kdisaggAbeta * AbetaDimer}$
95	Abeta Disaggregation3	$\mathbf{AbetaPlaque} \xrightarrow{\mathbf{kdisaggAbeta1}} \mathbf{AbetaDimer + disaggPlaque1}$	$\mathbf{v95 = kdisaggAbeta1 * AbetaPlaque}$
96	Abeta Disaggregation4	$\mathbf{AbetaPlaque + antiAb} \xrightarrow{\mathbf{kdisaggAbeta2}} \mathbf{AbetaDimer + antiAb + disaggPlaque2}$	$\mathbf{v96 = kdisaggAbeta2 * AbetaPlaque * antiAb}$
97	Abeta_antiAb Binding	$\mathbf{Abeta + antiAb} \xrightarrow{\mathbf{kbinAbantiAb}} \mathbf{Abeta\_antiAb}$	$\mathbf{v97 = kbinAbantiAb * Abeta * antiAb}$
98	AbetaDimer_antiAb Binding	$\mathbf{AbetaDimer + antiAb} \xrightarrow{\mathbf{kbinAbantiAb}} \mathbf{AbetaDimer\_antiAb}$	$\mathbf{v98 = kbinAbantiAb * AbetaDimer * antiAb}$
99	Abeta_antiAb Degredation	$\mathbf{Abeta\_antiAb} \xrightarrow{\mathbf{kdegAbeta}} \mathbf{antiAb}$	$\mathbf{v99 = 10 * kdegAbeta * Abeta\_antiAb}$
100	AbetaDimer antiAb Degredation	$\mathbf{AbetaDimer\_antiAb} \xrightarrow{\mathbf{kdegAbeta}} \mathbf{antiAb}$	$\mathbf{v100 = 10 * kdegAbeta * AbetaDimer\_antiAb}$
101	Glia Activation Step1	$\mathbf{GliaI + AbetaPlaque} \xrightarrow{\mathbf{kactglia1}} \mathbf{GliaM1 + AbetaPlaque}$	$\mathbf{v101 = kactglia1 * GliaI * AbetaPlaque}$
102	Glia Activation Step2	$\mathbf{GliaM1 + AbetaPlaque} \xrightarrow{\mathbf{kactglia1}} \mathbf{GliaM2 + AbetaPlaque}$	$\mathbf{v102 = kactglia1 * GliaM1 * AbetaPlaque}$
103	Glia Activation Step3	$\mathbf{GliaM2 + antiAb} \xrightarrow{\mathbf{kactglia2}} \mathbf{GliaA + antiAb}$	$\mathbf{v103 = kactglia2 * GliaM2 * antiAb}$
104	Glia Inactivation Step1	$\mathbf{GliaA} \xrightarrow{\mathbf{kactglia2}} \mathbf{GliaM2}$	$\mathbf{v104 = kactglia1 * GliaA}$
105	Glia Inactivation Step2	$\mathbf{GliaM2} \xrightarrow{\mathbf{kactglia2}} \mathbf{GliaM1}$	$\mathbf{v105 = kactglia2 * GliaM2}$
106	Glia Inactivation Step3	$\mathbf{GliaM1} \xrightarrow{\mathbf{kactglia2}} \mathbf{GliaI}$	$\mathbf{v106 = kactglia2 * GliaM1}$
107	Abeta Binding To Glia	$\mathbf{AbetaPlaqu + GliaA} \xrightarrow{\mathbf{kbinAbetaGlia}} \mathbf{AbetaPlaqu\_GliaA}$	$\mathbf{v107 = kbinAbetaGlia * AbetaPlaqu * GliaA}$
108	Abeta Release From Glia	$\mathbf{AbetaPlaqu\_GliaA} \xrightarrow{\mathbf{krelAbetaGlia}} \mathbf{AbetaPlaqu + GliaA}$	$\mathbf{v108 = krelAbetaGlia * AbetaPlaque\_GliaA}$
109	Abeta Plaque Clearance By Glia	$\mathbf{AbetaPlaqu\_GliaA} \xrightarrow{\mathbf{kdegAbetaGlia}} \mathbf{GliaA + degAbetaGlia}$	$\mathbf{v109 = kdegAbetaGlia * AbetaPlaque\_GliaA}$
110	ROS generation By Glia	$\mathbf{betaPlaqu\_GliaA} \xrightarrow{\mathbf{kgenROSGlia}} \mathbf{AbetaPlaqu\_GliaA + ROS}$	$\mathbf{v110 = kgenROSGlia * AbetaPlaque\_GliaA}$
111	antiAb Removal	$\mathbf{antiAb} \xrightarrow{\mathbf{kdegAntiAb}} \mathbf{Sink}$	$\mathbf{v111 = kdegAntiAb * antiAb}$
112	ROS removal	$\mathbf{ROS} \xrightarrow{\mathbf{kremROS}} \mathbf{Sink}$	$\mathbf{v112 = kremROS * ROS}$

Table B.2: ODE Equations

Equations ($\frac{d}{dt}$)	#	Equations ($\frac{d}{dt}$)	#
$Mdm2 = v3 + v10 + v24 + v39 + v72 - v9 - v17 - v71$	1	$p53 = v4 + v10 + v12 + v27 + v70 - v4 - v9 - v11 - v69$	2
$Mdm2\_p53 = v9 + v35 - v10 - v28$	3	$Mdm2\_mRNA = v3 + v4 + v5 + v6 + v7 - v3 - v8$	4
$p53\_mRNA = v1 + v27 + v65 - v2 - v27$	5	$ATMA = v68 + v69 + v71 - v69 - v71 - v83$	6
$ATMI = v83 - v68$	7	$p53\_P = v5 + v14 + v69 - v5 - v13 - v70$	8
$Mdm2\_P = v71 + v80 - v72 - v73$	9	$IR = v66 - v66$	10
$ROS = v84 + v85 + v86 + v87 + v110 - v87 - v112$	11	$damDNA = v66 + v68 + v87 - v67 - v68$	12
$E1 = v16 - v15$	13	$E2 = v17 + v18 + v19 + v20 + v28 + v29 + v30 + v31 + v73 + v74 + v75 + v76 - v16$	14
$E1\_Ub = v15 - v16$	15	$E2\_Ub = v16 - v17 - v18 - v19 - v20 - v28 - v29 - v30 - v31 - v73 - v74 - v75 - v76$	16
$Proteasom = v26 + v40 + v82 + v90 - v25 - v39 - v59 - v63 - v81 - v89$	17	$Ub = v21 + v22 + v23 + v24 + 4 * v26 + v32 + v33 + v34 + v35 + 4 * v40 + v77 + v78 + v79 + v80 + 4 * v82 - v15$	18
$p53DUB = v32 + v33 + v34 + v35 - v32 - v33 - v34 - v35$	19	$Mdm2DUB = v21 + v22 + v23 + v24 + v77 + v78 + v79 + v80 - v21 - v22 - v23 - v24 - v77 - v78 - v79 - v80$	20
$DUB = 0$	21	$Mdm2\_p53\_Ub = v28 + v34 - v29 - v35$	22
$Mdm2\_p53\ Ub = v29 + v33 - v30 - v34$	23	$Mdm2\_p53\_Ub3 = v30 + v32 - v31 - v33$	24
$Mdm2\_p53\_Ub4 = v31 - v32 - v36 - v37 - v38$	25	$Mdm2\_P1\_p53\_Ub4 = v36 + v37 + v38 - v39$	26
$Mdm2\_Ub = v17 + v23 - v18 - v24$	27	$Mdm2\_Ub2 = v18 + v22 - v19 - v23$	28
$Mdm2\_Ub3 = v19 + v21 - v20 - v22$	29	$Mdm2\_Ub4 = v20 - v21 - v25$	30
$Mdm2\_P\_Ub = v73 + v79 - v74 - v80$	31	$Mdm2\_P\_Ub2 = v74 + v78 - v75 - v79$	32
$Mdm2\_P\_Ub3 = v75 + v77 - v76 - v78$	33	$Mdm2\_P\_Ub4 = v76 - v77 - v81$	34
$p53\_Ub4\_Proteasome = v39 - v40$	35	$Mdm2\_Ub4\_Proteasome = v25 - v26$	36
$Mdm2\_P\_Ub4\ Proteasome = v81 - v82$	37	$GSK3b = v12 + v14 + v36 + v47 + v48 - v11 - v13 - v36 - v47 - v48$	38

$GSK3b\_p53 = v6 + v11 + v37 + v43 + v44 + v61 - v6 - v12 - v37 - v43 - v44 - v61$	39	$GSK3b\_p53\_P = v7 + v13 + v38 + v45 + v46 + v62 - v7 - v14 - v38 - v45 - v46 - v62$	40
$Abeta = v60 + v61 + v62 + v65 + v84 + 2 * v94 - v64 - v65 - v84 - 2 * v91 - v97$	41	$AggAbeta\_Proteasome = v63 + v86 - v86$	42
$AbetaPlaq = v85 + v92 + 2 * v93 + v101 + v102 + v108 - v85 - v93 - v95 - v96 - v101 - v102 - v107$	43	$Tau = v42 + v50 + v88 - v41 - v43 - v45 - v47 - 2 * v55 - v56 - v89$	44
$Tau\_P1 = v43 + v45 + v47 + v49 - v44 - v46 - v48 - v50 - 2 * v51 - v52$	45	$Tau\_P2 = v44 + v46 + v48 - v49 - 2 * v53 - v54$	46
$MT\_Tau = v41 - v42$	47	$AggTau = 2 * v51 + 2 * v52 + 2 * v53 + 2 * v54 + 2 * v55 + 2 * v56 - v52 - v54 - v56 - 2 * v57 - v58 - v59$	48
$AggTau\_Proteasome = v59$	49	$Proteasome\_Tau = v89 - v90$	50
$PP1 = v49 + v50 - v49 - v50$	51	$NFT = 2 * v57 + 2 * v58 - v58$	52
$ATP = 0$	53	$ADP = 0$	54
$AMP = 0$	55	$AbetaDimer = v91 + v95 + v96 - v63 - 2 * v92 - v93 - v94 - v98$	56
$AbetaPlaque\_GliaA = v107 + v110 - v108 - v109 - v110$	57	$GliaI = v106 - v101$	58
$GliaM1 = v101 + v105 - v102 - v106$	59	$GliaM2 = v102 + v104 - v103 - v105$	60
$GliaA = v103 + v108 + v109 - v104 - v107$	61	$antiAb = v96 + v99 + v100 + v103 - v96 - v97 - v98 - v103 - v111$	62
$Abeta\_antiAb = v97 - v99$	63	$AbetaDimer\_antiAb = v98 - v100$	64
$degAbetaGlia = v109$	65	$disaggPlaque1 = v95$	66
$disaggPlaque2 = v96$	67	$Source = 0$	68
$Sink = 0$	69		

Table B.3: Species of the system

Name	Initial value	Description	Name	Initial value	Description
Mdm2	5.0	E3 ubiquitin-protein ligase Mdm2 (Unbound Mdm2 protein)	Proteasome	500.0	A large multisubunit complex catalyzes protein degradation
p53	5.0	Cellular tumor antigen p53 (Unbound p53 protein)	Ub	4000.0	Polyubiquitin-B exists either covalently attached to another protein, or free (unanchored).
Mdm2_p53	95.0	Mdm2/p53 complex	p53DUB	200.0	Deubiquitinating enzyme for p53
Mdm2_mRNA	10.0	Mdm2 messenger RNA	Mdm2DUB	200.0	Deubiquitinating enzyme for Mdm2
p53_mRNA	10.0	p53 messenger RNA	DUB	200.0	Ubiquitin carboxyl-terminal hydrolase DUB controls levels of cellular ubiquitin through processing of

					ubiquitin precursors and ubiquitinated proteins. Thiol protease that recognizes and hydrolyzes a peptide bond at the C-terminal glycine of either ubiquitin or RUB1. Preferentially cleaves ubiquitin from peptides and small adducts
ATMA	0.0	Serine-protein kinase ATM (Active ATM)	Mdm2_p53_Ub	0.0	Monoubiquitinated p53
ATMI	200.0	Inactive ATM	Mdm2_p53_Ub2	0.0	Polyubiquitinated p53
p53_P	0.0	Phosphorylated p53	Mdm2_p53_Ub3	0.0	Polyubiquitinated p53
Mdm2_P	0.0	Phosphorylated Mdm2	Mdm2_p53_Ub4	0.0	Polyubiquitinated p53
IR	0.0	IR Ionizing radiation	Mdm2_P1_p53_Ub4	0.0	Phosphorylated Mdm2 bound to p53
ROS	0.0	Reactive Oxygen Species: Molecules or ions formed by the incomplete one-electron reduction of oxygen.	Mdm2_Ub	0.0	Monoubiquitinated Mdm2
damDNA	0.0	Deoxyribonucleic acid	Mdm2_Ub2	0.0	Polyubiquitinated Mdm2
E1	100.0	Ubiquitin/SUMO-activating enzyme E1: alters the function, location or trafficking of a protein	Mdm2_Ub3	0.0	Polyubiquitinated Mdm2
E2	100.0	Ubiquitin-conjugating enzymes: catalyse the covalent attachment of ubiquitin to target proteins	Mdm2_Ub4	0.0	Polyubiquitinated Mdm2
E1_Ub	0.0	E1 bound by Ub	Mdm2_P_Ub	0.0	Monoubiquitinated phospho-Mdm2
E2_Ub	0.0	E2 bound by Ub	Mdm2_P_Ub2	0.0	Polyubiquitinated phospho-Mdm2
Mdm2_P_Ub3	0.0	Polyubiquitinated phospho-Mdm2	Mdm2_Ub4_Proteasome	0.0	Mdm2 bound to proteasome
Mdm2_P_Ub4	0.0	Polyubiquitinated phospho-Mdm2	Mdm2_P_Ub4-Proteasome	0.0	Mdm2 bound to proteasome
p53_Ub4_Proteasome	0.0	p53 bound to proteasome	GSK3b	500.0	Glycogen synthase kinase-3 beta. Constitutively active protein kinase that acts as a negative regulator in the hormonal control of glucose homeostasis.
GSK3β _p53	0.0	GSK3β bound to p53	AMP (constant)	1000.0	Adenosine monophosphate
GSK3β _p53_P	0.0	GSK3β bound to phosphorylated p53	AbetaDimer	0.0	
Abeta	0.0	Amyloid-beta A4 protein	AbetaPlaque_GliaA	0.0	
AggAbeta-Proteasome	0.0	AggAbeta bound to the proteasome	GliaI	100.0	Inactive Glia.
AbetaPlaque	0.0	Aβ plaque	GliaP1	0.0	Partially active Glia 1

Tau	0.0	Microtubule-associated protein Tau	GliaP2	0.0	Partially active Glia 2
Tau_P1	0.0	tau phosphorylated by GSK3β at one site	GliaA	0.0	Glia active
Tau_P2	0.0	tau phosphorylated by GSK3β at two sites	antiAb	0.0	Antibody against amyloid-beta
MT_Tau	100.0	tau bound to the microtubule		50.0	$t \geq 345600$
AggTau	0.0	small aggregate of tau	Abeta_antiAb	0.0	Abeta monomer bound to antibody
AggTau_Proteasome	0.0	AggTau bound to proteasome	AbetaDimer_antiAb	0.0	Abeta dimer bound to antibody
Proteasome_Tau	0.0	Tau bound to proteasome	degAbetaGlia	0.0	
PP1	50.0	Serine/threonine-protein phosphatase PP1-alpha catalytic subunit is essential for cell division.	disaggPlaque1	0.0	
NFT	0.0	tau neurofibrillary tangle	disaggPlaque2	0.0	
ATP (constant)	10000.0	Adenosine triphosphate	Source (constant)	1.0	An empty set: it is often used to represent the source of a creation process.
ADP (constant)	1000.0	Adenosine diphosphate: A purine ribonucleoside 5'-diphosphate having adenine as the nucleobase	Sink (constant)	1.0	An empty set: it is often used to represent the result of a degradation process.

Table B.4: Parameters of the system

Rate constant (k_s)	Description	value	Rate constant (k_s)	Description	value
ksynp53mRNA	p53mRNASynthesis	0.001	kMdm2Ub	Mdm2Ubiquitination	$4.56 * 10^{-6}$
kdegp53mRNA	p53mRNADegradation	10^{-4}	kMdm2PUb	Mdm2PUbiquitination	$6.84 * 10^{-6}$
ksynMdm2mRNA	Mdm2mRNASynthesis1	5.10^{-4}	kMdm2PolyUb	Mdm2polyUbiquitination1	0.005
kdegMdm2mRNA	Mdm2mRNADegradation	5.10^{-4}	kdam	DNAdamage	0.080
ksynMdm2mRNAGSK3bp53	Mdm2mRNASynthesis3	$7 * 10^{-4}$	krepair	DNArepair	$2 * 10^{-5}$
ksynp53	p53Synthesis	0.007	kactATM	ATMactivation	10^{-4}
kdegp53	p53Degradation	0.005	kinactATM	ATMinactivation	$5 * 10^{-4}$
kbinMdm2p53	p53Mdm2Binding	0.001	kphosp53	p53phosphorylation	$2 * 10^{-4}$
krelMdm2p53	p53Mdm2Release	$1.155 * 10^{-5}$	kdephosp53	p53dephosphorylation	0.500
kbinGSK3bp53	GSK3p53Binding	$2 * 10^{-6}$	kphosMdm2	Mdm2phosphorylation	2.000
krelGSK3bp53	GSK3p53Release	0.002	kdephosMdm2	Mdm2dephosphorylation	0.500

ksynMdm2	Mdm2Synthesis	$4.95 * 10^{-4}$	kphosMdm2GSK3b	Mdm2GSK3phosphorylation1	0.005
kdegMdm2	Mdm2Degradation	0.010	kphosMdm2GSK3bp53	Mdm2GSK3phosphorylation2	0.500
kbinE1Ub	E1UbBinding	$2 * 10^{-4}$	kphospTauGSK3bp53	Tauphosphorylation4	0.100
kbinE2Ub	E2UbBinding	0.001	kphospTauGSK3b	Tauphosphorylation6	$2 * 10^{-4}$
kp53Ub	p53Monoubiquitination	$5 * 10^{-5}$	kdephospTau	Taudephosphorylation2	0.010
kp53PolyUb	p53Polyubiquitination	0.010	kbinMTTau	TauMTbinding	0.100
kbinProt	Mdm2ProteasomeBinding1	$2 * 10^{-6}$	krelMTTau	TauMTrelease	10^{-4}
kactDUBp53	p53Deubiquitination3	10^{-7}	ksynTau	TauSynthesis	$8 * 10^{-5}$
kactDUBMdm2	Mdm2PDeubiquitination4	10^{-7}	kbinTauProt	TauProteasomeBinding	$1.925 * 10^{-7}$
kproteff	Extra parameter is used in different degradation reactions	1.000	kdegTau20SProt	Tau20SProteasomeDegradation	0.010
kremROS	ROSremoval	$7 * 10^{-5}$	kaggTau	Tauaggregation1	10^{-8}
kprodAbeta	Abetaproduction1	$1.86 * 10^{-5}$	kaggTauP1	auP1Aggregation1	10^{-8}
kprodAbeta2	Abetaproduction2	$1.86 * 10^{-5}$	kaggTauP2	TauP2Aggregation1	10^{-7}
kdegAbeta	AbetaDegredation	$1.5 * 10^{-5}$	ktangfor	TangleFormation1	0.001
kaggAbeta	Abetaaggregation1	$3 * 10^{-6}$	kinhibprot	ProteasomeInhibitionAggTau	10^{-7}
kdisaggAbeta	AbetaDisaggregation1	10^{-6}	ksynp53mRNAAbeta	p53transcriptionViaAbeta	10^{-7}
kdisaggAbeta1	AbetaDisaggregation3	$2 * 10^{-4}$	kdamROS	ROSDNAdamage	10^{-5}
kdisaggAbeta2	AbetaDisaggregation4	10^{-6}	kgenROSAbeta	AggAbetaROSproduction2	$2 * 10^{-5}$
kdegAbetaGlia	Abeta_antiAbDegredation	0.005	kgenROSPlaque	PlaqueROSproduction	10^{-5}
kpf	AbetaPlaqueFormation	0.200	kgenROSGlia	ROSgenerationByGlia	10^{-5}
kpg	AbetaPlaqueGrowth	0.150	kinactglia2	GliaInactivationStep3	$5 * 10^{-6}$
kpghalf	AbetaPlaqueGrowth1	10.000	kbinAbetaGlia	AbetaBindingToGlia	10^{-5}
kactglia1	GliaActivationStep1	$6 * 10^{-7}$	krelAbetaGlia	AbetaReleaseFromGlia	$5 * 10^{-5}$
kactglia2	GliaActivationStep3	$6 * 10^{-7}$	kdegAntiAb	antiAbRemoval	$2.75 * 10^{-6}$
kinactglia1	GliaInactivationStep1	$5 * 10^{-6}$	kbinAbantiAb	Abeta_antiAbBinding	10^{-6}

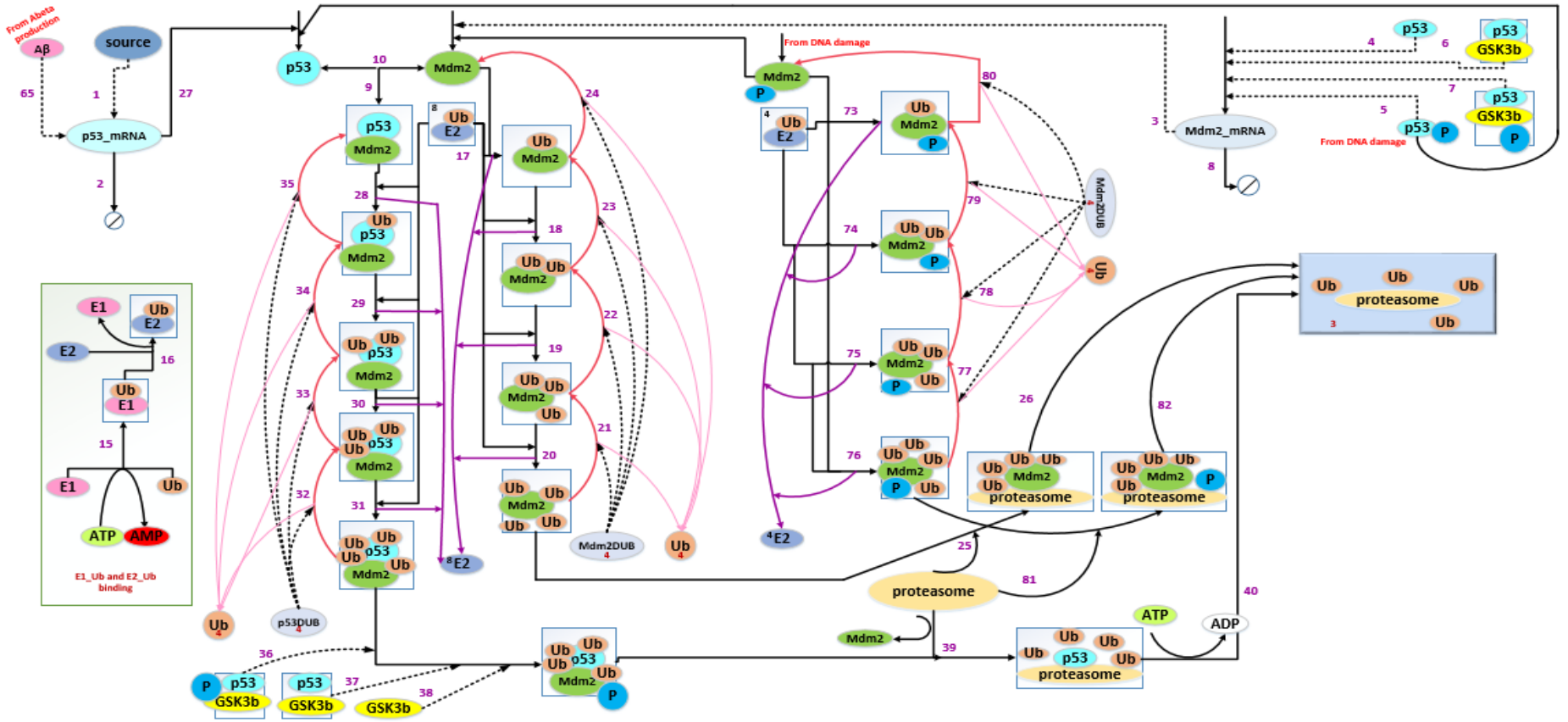

Figure 1: p53 regulation. This graph shows how p53 and Mdm2 are produced and degrade. Both of them are degraded using proteasome system but p53 should bind to Mdm2 to be degraded (middle part of the graph). On the left top side, the graph shows how the species of p53_mRNA produced, degrade and how it is considered as another pathway to increase the unbound p53 in the systems. The species of p53_mRNA is indirectly increased as a result of the DNA damage since Aβ (increased through GSK3b when there is a damage) increases the production of p53_mRNA. On the right top side, the graph shows how p53, p53_P, p53_GSK3b and (p53_GSK3b)_P are used to be a modifier to increase the production of Mdm2_mRNA. On the left bottom side, the graph shows how E1 (Ubiquitin/SUMO-activating enzymes) binds with Ub (Polyubiquitin-B) to E1_Ub and later E1 is replaced by E2 (Ubiquitin-conjugating enzymes) to produce E2_Ub that is used for degradation process as shown in the graph. Dashed lines from a species indicates the species is a modifier of the reaction.

Table B.5: Reactions of p53 regulation. Reaction numbers correspond to the numbers in Table B.1

#	Reaction name	Reaction Equation
1	p53_mRNA_Synthesis	$\text{Source} \xrightarrow{ksynp53mRNA} p53\_mRNA$
2	p53_mRNA_Degradation	$p53\_mRNA \xrightarrow{kdegp53mRNA} sink$
3	Mdm2Synthesis	$Mdm2mRNA \xrightarrow{ksynMdm2} Mdm2\_mRNA + Mdm2$
4	Mdm2mRNASynthesis1	$p53 \xrightarrow{ksynMdm2mRNA} p53 + Mdm2\_mRNA$
5	Mdm2mRNASynthesis2	$p53\_P \xrightarrow{ksynMdm2mRNA} p53\_P + Mdm2\_mRNA + Mdm2\_mRNAsyn$
6	Mdm2mRNASynthesis3	$GSK3b\_p53 \xrightarrow{ksynMdm2mRNAGSK3bp53} GSK3b\_p53 + Mdm2\_mRNA$
7	Mdm2 mRNA Synthesis4	$GSK3b\_p53\_P \xrightarrow{ksynMdm2mRNAGSK3bp53} GSK3b\_p53\_P + Mdm2\_mRNA$
8	Mdm2mRNADegradation	$Mdm2\ mRNA \xrightarrow{kdegMdm2mRNA} Sink + Mdm2\_mRNAdeg$
9	p53_Mdm2 Binding	$Mdm2 + p53 \xrightarrow{kbinMdm2p53} Mdm2\_p53$
10	p53_Mdm2 Release	$Mdm2\_p53 \xrightarrow{krelMdm2p53} Mdm2 + p53$
15	E1_Ub Binding	$E1 + Ub + ATP \xrightarrow{kbinE1Ub} E1\_Ub + AMP$
16	E2_Ub Binding	$E2 + E1\_Ub \xrightarrow{kbinE2Ub} E2\_Ub + E1$
17	Mdm2_Ubiquitination	$Mdm2 + E2\_Ub \xrightarrow{kMdm2Ub} Mdm2\_Ub + E2$
18	Mdm2 poly Ubiquitination1	$Mdm2\_Ub + E2\_Ub \xrightarrow{kMdm2PolyUb} Mdm2\_Ub2 + E2$
19	Mdm2 poly Ubiquitination2	$Mdm2\_Ub2 + E2\_Ub \xrightarrow{kMdm2PolyUb} Mdm2\_Ub3 + E2$
20	Mdm2 poly Ubiquitination3	$Mdm2\_Ub3 + E2\_Ub \xrightarrow{kMdm2PolyUb} Mdm2\_Ub4 + E2$
21	Mdm2 Deubiquitination4	$Mdm2\_Ub4 + Mdm2DUB \xrightarrow{kactDUBMdm2} Mdm2\ Ub3 + Mdm2DUB + Ub$
22	Mdm2 Deubiquitination3	$Mdm2\_Ub3 + Mdm2DUB \xrightarrow{kactDUBMdm2} Mdm2\_Ub2 + Mdm2DUB + Ub$
23	Mdm2 Deubiquitination2	$Mdm2\_Ub2 + Mdm2DUB \xrightarrow{kactDUBMdm2} Mdm2\_Ub + Mdm2DUB + Ub$
24	Mdm2 Deubiquitination1	$Mdm2\_Ub + Mdm2DUB \xrightarrow{kactDUBMdm2} Mdm2 + Mdm2DUB + Ub$
25	Mdm2_Proteasome Binding1	$Mdm2\_Ub4 + Proteasome \xrightarrow{kbinProt} Mdm2\_Ub4\_Proteasome$
26	Mdm2 Degradation	$Mdm2\_Ub4\_Proteasome \xrightarrow{kdegMdm2*kproteff} Proteasome + 4Ub$
27	p53 Synthesis	$p53mRNA \xrightarrow{ksynp53} p53 + p53mRNA + p53syn$
28	p53 Monoubiquitination	$E2\_Ub + Mdm2\_p53 \xrightarrow{kp53Ub} Mdm2\ p53\ Ub + E2$
29	p53 Polyubiquitination1	$Mdm2\_p53\_Ub + E2\_Ub \xrightarrow{kp53PolyUb} Mdm2\_p53\_Ub2 + E2$
30	p53 Polyubiquitination2	$Mdm2\_p53\_Ub2 + E2\_Ub \xrightarrow{kp53PolyUb} Mdm2\_p53\_Ub3 + E2$

#	Reaction name	Reaction Equation
30	p53 Polyubiquitination2	$Mdm2\_p53\_Ub2 + E2\_Ub \xrightarrow{kp53PolyUb} Mdm2\_p53\_Ub3 + E2$
31	p53 Polyubiquitination3	$Mdm2\_p53\_Ub3 + E2\_Ub \xrightarrow{kp53PolyUb} Mdm2\_p53\_Ub4 + E2$
32	p53 Deubiqutination4	$Mdm2\_p53\_Ub4 + p53DUB \xrightarrow{kactDUBp53} Mdm2\_p53\_Ub3 + p53DUB + Ub$
33	p53 Deubiquitination3	$Mdm2\_p53\_Ub3 + p53DUB \xrightarrow{kactDUBp53} Mdm2\_p5\_Ub2 + p53DB + Ub$
34	p53 Deubiquitination2	$Mdm2\_p53\_Ub2 + p53DUB \xrightarrow{kactDUBp53} Mdm2\_p53\_Ub + p53DUB + Ub$
35	p53 Deubiquitination1	$Mdm2\_p53\_Ub + p53DUB \xrightarrow{kactDUBp53} Mdm2\_p53 + p53DUB + Ub$
36	Mdm2_GSK3 phosphorylation1	$Mdm2\_p53\_Ub4 + GSK3b \xrightarrow{kphosMdm2GSK3b} Mdm2\_P1\_p53\_Ub4 + GSK3b$
37	Mdm2 GSK3 phosphorylation2	$Mdm2\_p53\_Ub4 + GSK3b\_p53 \xrightarrow{kphosMdm2GSK3bp53} Mdm2\_P1\_p53\_Ub4 + GSK3b\_p53$
38	Mdm2 GSK3 phosphorylation3	$Mdm2\_p53\_Ub4 + GSK3b\_p53\_P \xrightarrow{kphosMdm2GSK3bp53} Mdm2\_P1\_p53\_Ub4 + GSK3b\_p53\_p$
39	p53_Proteasome Binding1	$Mdm2\_P\_p53\_Ub4 + Proteasome \xrightarrow{kbinProt} p53\_Ub4\_Proteasome + Mdm2$
40	Degradation p53_Ub4	$p53\_Ub4\_Proteasome + ATP \xrightarrow{kdegp53*kproteff} 4Ub + Proteasome + ADP$
74	Mdm2_P polyUbiquitination1	$Mdm2\_P\_Ub + E2\_Ub \xrightarrow{kMdm2PolyUb} Mdm2\_P\_Ub2 + E2$
75	Mdm2_P polyUbiquitination2	$Mdm2\_P\_Ub2 + E2\_Ub \xrightarrow{kMdm2PolyUb} Mdm2\_P\_Ub3 + E2$
76	Mdm2_PpolyUbiquitination3	$Mdm2\_P\_Ub3 + E2\_Ub \xrightarrow{kMdm2PolyUb} Mdm2\_P\_Ub4 + E2$
77	Mdm2_P Deubiquitination4	$Mdm2\_P\_Ub4 + Mdm2DUB \xrightarrow{kactDUBMdm2} Mdm2\_P\_Ub3 + Mdm2DUB + Ub$
78	Mdm2_P Deubiquitination3	$Mdm2\_P\_Ub3 + Mdm2DUB \xrightarrow{kactDUBMdm2} Mdm2\_P\_Ub2 + Mdm2DUB + Ub$
79	Mdm2_P Deubiquitination2	$Mdm2\_P\_Ub2 + Mdm2DUB \xrightarrow{kactDUBMdm2} Mdm2\_P\_Ub + Mdm2DUB + Ub$
80	Mdm2_P Deubiquitination1	$Mdm2\_P\_Ub + Mdm2DUB \xrightarrow{kactDUBMdm2} Mdm2\_P + Mdm2DUB + Ub$
81	Mdm2_P_Proteasome Binding1	$Mdm2\_P\_Ub4 + Proteasome \xrightarrow{kbinProt} Mdm2\ P\ Ub4\ Proteasome$

Appendix C

LSA Results.

Appendix C includes Tables C.1 and C.2. In Table C.1, we list the results of LSA using ODEs while Table C.2 lists LSA results when it uses MRM/GSSA.

TableC.1: LSA results using ODEs

Species		p53		ATMA		GSK3b_p53		Aβ		Plaques		Tangles		GliaA	
Parameters	P.V	50%	200%	50%	200%	50%	200%	50%	200%	50%	200%	50%	200%	50%	200%
1. kactATM	μ	**-34.35**	**31.89**	**-31.26**	**38.59**	**-14.16**	**12.31**	**-2.661**	**2.157**	**-3.207**	**2.86**	**-5.529**	**7.658**	**-11.13**	**3.526**
	σ	**9.085**	**6.747**	**11.72**	**10.48**	**3.50**	**2.58**	**0.622**	**0.515**	**6.820**	**5.19**	**3.982**	**5.258**	**8.789**	**2.768**
	Max	**-47.85**	**41.34**	**-51.84**	**51.67**	**-19.12**	**16.02**	**-3.556**	**3.103**	**-20.29**	**15.08**	**-12.70**	**17.06**	**-23.57**	**7.407**
	Time	**281253**	**177972**	**329193**	**214557**	**272604**	**167652**	**268794**	**101238**	**276054**	**212670**	**1036800**	**1036800**	**444993**	**446820**
2. kactDUBMdm2	μ	**0**	**0**	**0**	**0**	**0**	**0**	**0**	**0**	**0**	**0**	**0**	**0**	**0**	**0**
	σ	**0**	**0**	**0**	**0**	**0**	**0**	**0**	**0**	**0**	**0**	**0**	**0**	**0**	**0**
	Max	**0**	**0**	**0**	**0**	**0**	**0**	**0**	**0**	**0**	**0**	**0**	**0**	**0**	**0**
	Time														
3. kactDUBp53	μ	**0**	**0**	**0**	**0**	**0**	**0**	**0**	**0**	**0**	**0**	**0**	**0**	**0**	**0**
	σ	**0**	**0**	**0**	**0**	**0**	**0**	**0**	**0**	**0**	**0**	**0**	**0**	**0**	**0**
	Max	**0**	**0**	**0**	**0**	**0**	**0**	**0**	**0**	**0**	**0**	**0**	**0**	**0**	**0**
	Time														
4. kactDUBProtp53	μ	**0**	**0**	**0**	**0**	**0**	**0**	**0**	**0**	**0**	**0**	**0**	**0**	**0**	**0**
	σ	**0**	**0**	**0**	**0**	**0**	**0**	**0**	**0**	**0**	**0**	**0**	**0**	**0**	**0**
	Max	**0**	**0**	**0**	**0**	**0**	**0**	**0**	**0**	**0**	**0**	**0**	**0**	**0**	**0**
	Time														
5. kactglia1	μ	**0**	**0**	**0**	**0**	**0**	**0**	**0**	**0**	**0**	**0**	**0**	**0**	**-10.05**	**6.309**
	σ	**0**	**0**	**0**	**0**	**0**	**0**	**0**	**0**	**0**	**0**	**0**	**0**	**7.930**	**4.948**
	Max	**0**	**0**	**0**	**0**	**0**	**0**	**0**	**0**	**0**	**0**	**0**	**0**	**-21.25**	**13.22**
	Time													**445746**	**446370**
6. Kactglia2	μ	**0**	**0**	**0**	**0**	**0**	**0**	**0**	**0**	**0**	**0**	**0**	**0**	**-7.115**	**7.135**
	σ	**0**	**0**	**0**	**0**	**0**	**0**	**0**	**0**	**0**	**0**	**0**	**0**	**5.250**	**5.210**
	Max	**0**	**0**	**0**	**0**	**0**	**0**	**0**	**0**	**0**	**0**	**0**	**0**	**-15.11**	**16.27**
	Time													**394071**	**369540**
7. kaggAbeta		**0**	**0**	**0**	**0**	**0**	**0**	**0**	**0**	**0**	**0**	**0**	**0**	**0**	**0**
		0	**0**	**0**	**0**	**0**	**0**	**0**	**0**	**0**	**0**	**0**	**0**	**0**	**0**
		0	**0**	**0**	**0**	**0**	**0**	**0**	**0**	**0**	**0**	**0**	**0**	**0**	**0**
8. kaggTau	μ	**0**	**0**	**0**	**0**	**0**	**0**	**0**	**0**	**0**	**0**	**0**	**0**	**0**	**0**
	σ	**0**	**0**	**0**	**0**	**0**	**0**	**0**	**0**	**0**	**0**	**0**	**0**	**0**	**0**
	Max	**0**	**0**	**0**	**0**	**0**	**0**	**0**	**0**	**0**	**0**	**0**	**0**	**0**	**0**
	Time														
9. kaggTauP1	μ	**0**	**0**	**0**	**0**	**0**	**0**	**0**	**0**	**0**	**0**	**0**	**0**	**0**	**0**
	σ	**0**	**0**	**0**	**0**	**0**	**0**	**0**	**0**	**0**	**0**	**0**	**0**	**0**	**0**
	Max	**0**	**0**	**0**	**0**	**0**	**0**	**0**	**0**	**0**	**0**	**0**	**0**	**0**	**0**

	Time														
10. kaggTauP2	μ	**0**	**0**	**0**	**0**	**0**	**0**	**0**	**0**	**0**	**0**	**-3.742**	**6.613**	**0**	**0**
	σ	**0**	**0**	**0**	**0**	**0**	**0**	**0**	**0**	**0**	**0**	**2.701**	**4.601**	**0**	**0**
	Max	**0**	**0**	**0**	**0**	**0**	**0**	**0**	**0**	**0**	**0**	**-8.635**	**14.51**	**0**	**0**
	Time											**1036800**	**1036800**		
11. kbinAbantiAb	μ	**3.085**	**-5.54**	**2.847**	**-4.98**	**1.226**	**-2.233**	**1.050**	**-1.694**	**0**	**0**	**0**	**0**	**0**	**0**
	σ	**2.513**	**4.49**	**2.368**	**4.092**	**1.004**	**1.827**	**0.849**	**1.293**	**0**	**0**	**0**	**0**	**0**	**0**
	Max	**6.65**	**-11.65**	**6.149**	**-10.30**	**2.667**	**-4.759**	**2.287**	**-3.194**	**0**	**0**	**0**	**0**	**0**	**0**
	Time	**565974**	**595521**	**567300**	**598410**	**567234**	**595905**	**381069**	**378612**						
12. kbinAbetaGlia	μ	**0**	**0**	**0**	**0**	**0**	**0**	**0**	**0**	**0**	**0**	**0**	**0**	**0**	**0**
	σ	**0**	**0**	**0**	**0**	**0**	**0**	**0**	**0**	**0**	**0**	**0**	**0**	**0**	**0**
	Max	**0**	**0**	**0**	**0**	**0**	**0**	**0**	**0**	**0**	**0**	**0**	**0**	**0**	**0**
	Time														
13. kbinE1Ub	μ	**0**	**0**	**0**	**0**	**0**	**0**	**0**	**0**	**0**	**0**	**0**	**0**	**0**	**0**
	σ	**0**	**0**	**0**	**0**	**0**	**0**	**0**	**0**	**0**	**0**	**0**	**0**	**0**	**0**
	Max	**0**	**0**	**0**	**0**	**0**	**0**	**0**	**0**	**0**	**0**	**0**	**0**	**0**	**0**
	Time														
14. kbinE2Ub	μ	**-5.403**	**2.764**	**-3.158**	**3.095**	**-2.158**	**1.095**	**0**	**0**	**-1.117**	**0.6018**	**0**	**0**	**0**	**0**
	σ	**1.815**	**0.932**	**0.782**	**0.746**	**0.682**	**0.346**	**0**	**0**	**0.793**	**0.4246**	**0**	**0**	**0**	**0**
	Max	**-8.328**	**4.268**	**-2.146**	**8.994**	**-3.146**	**1.594**	**0**	**0**	**-2.502**	**1.337**	**0**	**0**	**0**	**0**
	Time	**347937**	**347487**	**338525**	**339038**	**348525**	**349038**			**1036780**	**1036790**				
15. kbinGSK3bp53	μ	**-14.57**	**2.595**	**-22.15**	**19.25**	**-26.21**	**40.95**	**-5.178**	**6.077**	**-5.407**	**7.059**	**-7.351**	**29.20**	**-22.87**	**5.568**
	σ	**8.848**	**3.866**	**12.18**	**7.145**	**6.957**	**8.858**	**1.179**	**1.137**	**11.96**	**12.22**	**5.383**	**18.26**	**18.08**	**4.325**
	Max	**-34.48**	**12.851**	**-51.43**	**34.36**	**-37.25**	**50.03**	**-7.101**	**7.360**	**-43.77**	**33.69**	**-17.19**	**57.44**	**-48.41**	**11.46**
	Time	**350583**	**180801**	**359379**	**213141**	**349458**	**230649**	**345582**	**200985**	**345600**	**223155**	**1036800**	**1036800**	**448092**	**454383**
16. kbinMdm2p53	μ	**62.95**	**-41.89**	**12.50**	**-13.44**	**23.66**	**-17.42**	**3.710**	**-3.258**	**4.336**	**-3.759**	**16.01**	**-6.223**	**4.606**	**-14.24**
	σ	**15.51**	**11.64**	**4.946**	**7.175**	**5.200**	**4.507**	**0.706**	**0.730**	**7.738**	**8.196**	**10.57**	**4.496**	**3.599**	**11.25**
	Max	**81.53**	**-60.48**	**23.12**	**-29.82**	**29.33**	**-24.17**	**4.561**	**-4.408**	**21.51**	**6.162**	**33.36**	**-14.32**	**9.579**	**-30.18**
	Time	**268470**	**325509**	**223923**	**306858**	**235170**	**311250**	**210189**	**300108**	**231708**	**364842**	**1036800**	**1036800**	**451998**	**444831**
17. kbinMTTau	μ	**0**	**0**	**0**	**0**	**0**	**0**	**0**	**0**	**0**	**0**	**12.19**	**-5.379**	**0**	**0**
	σ	**0**	**0**	**0**	**0**	**0**	**0**	**0**	**0**	**0**	**0**	**8.263**	**3.909**	**0**	**0**
	Max	**0**	**0**	**0**	**0**	**0**	**0**	**0**	**0**	**0**	**0**	**25.79**	**-12.51**	**0**	**0**
	Time											**1036800**	**1036800**		
18. kbinProt	μ	**0**	**0**	**0**	**0**	**0**	**0**	**0**	**0**	**0**	**0**	**0**	**0**	**0**	**0**
	σ	**0**	**0**	**0**	**0**	**0**	**0**	**0**	**0**	**0**	**0**	**0**	**0**	**0**	**0**
	Max	**0**	**0**	**0**	**0**	**0**	**0**	**0**	**0**	**0**	**0**	**0**	**0**	**0**	**0**
	Time														
19. kbinTauProt	μ	**0**	**0**	**0**	**0**	**0**	**0**	**0**	**0**	**0**	**0**	**0**	**0**	**0**	**0**
	σ	**0**	**0**	**0**	**0**	**0**	**0**	**0**	**0**	**0**	**0**	**0**	**0**	**0**	**0**
	Max	**0**	**0**	**0**	**0**	**0**	**0**	**0**	**0**	**0**	**0**	**0**	**0**	**0**	**0**

	Time														
20. kdam	μ	**0**	**0**	**0**	**0**	**0**	**0**	**0**	**0**	**0**	**0**	**0**	**0**	**0**	**0**
	σ	**0**	**0**	**0**	**0**	**0**	**0**	**0**	**0**	**0**	**0**	**0**	**0**	**0**	**0**
	Max	**0**	**0**	**0**	**0**	**0**	**0**	**0**	**0**	**0**	**0**	**0**	**0**	**0**	**0**
	Time														
21. kdamROS	μ	**-34.36**	**31.89**	**-31.26**	**38.59**	**-14.16**	**12.31**	**-2.66**	**2.16**	**-3.21**	**2.86**	**-5.53**	**7.66**	**-11.13**	**3.53**
	σ	**9.086**	**6.747**	**11.72**	**10.48**	**3.503**	**2.579**	**0.622**	**0.515**	**6.820**	**5.195**	**3.982**	**5.258**	**8.789**	**2.768**
	Max	**-47.85**	**41.34**	**-51.84**	**51.67**	**-19.12**	**16.02**	**-3.56**	**3.10**	**-20.29**	**15.08**	**-12.70**	**17.06**	**-23.57**	**7.41**
	Time	**281253**	**177972**	**329265**	**214557**	**272604**	**167652**	**268794**	**101238**	**276150**	**212496**	**1036800**	**1036800**	**445053**	**446820**
22. kdegAbeta	μ	**10.21**	**-10.12**	**9.10**	**-8.92**	**4.01**	**-8.92**	**4.48**	**-3.59**	**0**	**0**	**2.10**	**-1.80**	**0**	**0**
	σ	**3.407**	**3.225**	**3.272**	**3.041**	**1.336**	**3.041**	**1.649**	**1.124**	**0**	**0**	**1.592**	**1.379**	**0**	**0**
	Max	**13.93**	**-13.26**	**12.90**	**-12.05**	**5.44**	**-12.05**	**7.02**	**-5.20**	**0**	**0**	**5.38**	**-4.63**	**0**	**0**
	Time	**1036640**	**1036550**	**1036800**	**1036790**	**1036800**	**1036790**	**345594**	**345582**			**1036800**	**1036790**		
23. kdegAbetaGlia	μ	**0**	**0**	**0**	**0**	**0**	**0**	**0**	**0**	**0**	**0**	**0**	**0**	**0**	**0**
	σ	**0**	**0**	**0**	**0**	**0**	**0**	**0**	**0**	**0**	**0**	**0**	**0**	**0**	**0**
	Max	**0**	**0**	**0**	**0**	**0**	**0**	**0**	**0**	**0**	**0**	**0**	**0**	**0**	**0**
	Time	**0**	**0**	**0**	**0**	**0**	**0**	**0**	**0**	**0**	**0**	**0**	**0**	**0**	**0**
24. kdegAntiAb	μ	**0**	**0**	**0**	**0**	**0**	**0**	**0**	**0**	**0**	**0**	**0**	**0**	**0**	**0**
	σ	**0**	**0**	**0**	**0**	**0**	**0**	**0**	**0**	**0**	**0**	**0**	**0**	**0**	**0**
	Max	**0**	**0**	**0**	**0**	**0**	**0**	**0**	**0**	**0**	**0**	**0**	**0**	**0**	**0**
	Time														
25. kdegMdm2	μ	**0**	**0**	**0**	**0**	**0**	**0**	**0**	**0**	**0**	**0**	**0**	**0**	**0**	**0**
	σ	**0**	**0**	**0**	**0**	**0**	**0**	**0**	**0**	**0**	**0**	**0**	**0**	**0**	**0**
	Max	**0**	**0**	**0**	**0**	**0**	**0**	**0**	**0**	**0**	**0**	**0**	**0**	**0**	**0**
	Time														
26. kdegMdm2mRNA	μ	**-42.82**	**66.23**	**-13.67**	**12.81**	**-17.81**	**24.79**	**-3.33**	**3.85**	**-3.79**	**4.38**	**-6.30**	**16.93**	**-14.42**	**4.66**
	σ	**12.257**	**17.183**	**7.282**	**4.976**	**4.778**	**5.788**	**0.783**	**0.785**	**8.267**	**7.838**	**4.565**	**11.208**	**11.393**	**3.638**
	Max	**-61.97**	**86.49**	**-30.16**	**23.10**	**-24.76**	**30.75**	**-4.52**	**4.72**	**-25.06**	**21.76**	**-14.55**	**35.24**	**-30.55**	**9.68**
	Time	**331983**	**289122**	**309192**	**227061**	**316494**	**247779**	**304401**	**218409**	**292026**	**236790**	**1036800**	**1036800**	**444888**	**451929**
27. kdegp53	μ	**0**	**0**	**0**	**0**	**0**	**0**	**0**	**0**	**0**	**0**	**0**	**0**	**0**	**0**
	σ	**0**	**0**	**0**	**0**	**0**	**0**	**0**	**0**	**0**	**0**	**0**	**0**	**0**	**0**
	Max	**0**	**0**	**0**	**0**	**0**	**0**	**0**	**0**	**0**	**0**	**0**	**0**	**0**	**0**
	Time														
28. kdegp53mRNA	μ	**-42.82**	**66.23**	**-13.67**	**12.81**	**-17.81**	**24.79**	**-3.33**	**3.85**	**-3.79**	**4.38**	**-6.30**	**16.93**	**-14.42**	**4.66**
	σ	**12.257**	**17.183**	**7.282**	**4.976**	**4.778**	**5.788**	**0.783**	**0.785**	**8.267**	**7.838**	**4.565**	**11.208**	**11.393**	**3.638**
	Max	**-61.97**	**86.49**	**-30.16**	**23.10**	**-24.76**	**30.75**	**-4.52**	**4.72**	**-25.06**	**21.76**	**-14.55**	**35.24**	**-30.55**	**9.68**
	Time	**331983**	**289122**	**309192**	**227061**	**316494**	**247779**	**304401**	**218409**	**292026**	**236790**	**1036800**	**1036800**	**444888**	**451929**
29. kdegTau20SProt	μ	**0**	**0**	**0**	**0**	**0**	**0**	**0**	**0**	**0**	**0**	**0**	**0**	**0**	**0**
	σ	**0**	**0**	**0**	**0**	**0**	**0**	**0**	**0**	**0**	**0**	**0**	**0**	**0**	**0**
	Max	**0**	**0**	**0**	**0**	**0**	**0**	**0**	**0**	**0**	**0**	**0**	**0**	**0**	**0**
	Time														

30. kdephosMdm2	μ	61.974	-41.287	12.081	-13.005	23.281	-17.145	3.630	-3.183	4.135	-3.655	15.784	-6.182	4.534	-13.63
	σ	16.226	11.963	4.828	6.998	5.544	4.672	0.782	0.785	7.434	7.920	10.499	4.472	3.542	10.77
	Max	80.603	-59.632	22.037	-28.712	28.904	-23.809	4.476	-4.333	20.686	-23.868	33.070	-14.249	9.426	-28.90
	Time	278106	326274	228534	305481	242070	311115	216123	299103	236964	289572	1036800	1036800	451443	445254
31. kdephosp53	μ	0	0	0	0	0	0	0	0	0	0	0	0	0	0
	σ	0	0	0	0	0	0	0	0	0	0	0	0	0	0
	Max	0	0	0	0	0	0	0	0	0	0	0	0	0	0
	Time														
32. kdephospTau	μ	0	0	0	0	0	0	0	0	0	0	34.404	-7.156	0	0
	σ	0	0	0	0	0	0	0	0	0	0	21.859	5.256	0	0
	Max	0	0	0	0	0	0	0	0	0	0	67.761	-16.870	0	0
	Time											1036800	1036800		
33. kdisaggAbeta	μ	0	0	0	0	0	0	0	0	0	0	0	0	0	0
	σ	0	0	0	0	0	0	0	0	0	0	0	0	0	0
	Max	0	0	0	0	0	0	0	0	0	0	0	0	0	0
	Time														
34. kdisaggAbeta1	μ	4.888	-9.844	4.827	-9.565	1.931	-3.938	1.316	-2.301	1.639	-3.001	1.142	-2.177	2.022	-10.02
	σ	1.756	4.488	2.236	5.634	0.662	1.703	0.301	0.613	3.046	6.342	0.741	1.422	1.547	7.913
	Max	8.840	-20.158	9.709	-22.470	3.445	-7.859	1.741	-3.391	8.582	-18.722	2.304	-4.326	4.091	-21.21
	Time	216906	270186	237822	288456	212193	265518	216075	272304	240267	275985	1036800	1036780	476580	447498
35. kdisaggAbeta2	μ	0	0	0	0	0	0	0	0	0	0	0	0	0	0
	σ	0	0	0	0	0	0	0	0	0	0	0	0	0	0
	Max	0	0	0	0	0	0	0	0	0	0	0	0	0	0
	Time														
36. kgenROSAbeta	μ	-30.627	28.992	-27.988	34.275	-12.608	11.258	-2.378	1.985	-2.969	2.619	-4.836	6.474	-9.784	3.261
	σ	7.588	7.159	9.086	9.412	3.041	2.834	0.602	0.567	6.276	4.778	3.541	4.695	7.730	2.561
	Max	-41.290	37.284	-42.318	42.567	-16.685	14.952	-3.149	3.060	-18.854	14.231	-11.561	15.516	-20.75	6.873
	Time	242751	148149	270192	185523	237501	122079	237288	98832	264465	205047	1036800	1036800	444531	445506
37. kgenROSGlia	μ	0	0	0	0	0	0	0	0	0	0	0	0	0	0
	σ	0	0	0	0	0	0	0	0	0	0	0	0	0	0
	Max	0	0	0	0	0	0	0	0	0	0	0	0	0	0
	Time														
38. kgenROSPlaque	μ	-3.165	4.768	-3.723	5.985	-1.231	1.823	0	0	0	0	0	0	0	0
	σ	4.017	5.526	5.070	7.625	1.534	2.059	0	0	0	0	0	0	0	0
	Max	-12.526	15.871	-16.574	23.115	-4.719	5.789	0	0	0	0	0	0	0	0
	Time	353844	347358	359337	357699	356268	347268								
39. kinactATM	μ	31.34	-34.140	38.06	-31.122	12.088	-14.06	2.108	-2.64	2.680	-3.15	7.537	-5.51	3.415	-10.82
	σ	6.963	9.107	10.65	11.664	2.639	3.518	0.498	0.622	4.893	6.674	5.237	3.971	2.679	8.546
	Max	39.91	-47.23	50.26	-51.28	15.43	-18.87	2.83	-3.51	14.16	-19.83	16.93	-12.67	7.17	-22.92
	Time	183405	280470	219969	329517	173385	271425	115635	268401	217392	275832	1036800	1036800	447441	444993
	μ	0	0	0	0	0	0	0	0	0	0	0	0	6.171	-7.02

40. kinactglia1	σ	0	0	0	0	0	0	0	0	0	0	0	0	5.394	5.591
	Max	0	0	0	0	0	0	0	0	0	0	0	0	13.76	-12.95
	Time													1036760	780846
41. kinactglia2	μ	0	0	0	0	0	0	0	0	0	0	0	0	6.520	-7.98
	σ	0	0	0	0	0	0	0	0	0	0	0	0	4.894	5.929
	Max	0	0	0	0	0	0	0	0	0	0	0	0	11.03	-13.81
	Time													797667	579348
42. kinhibprot	μ	0	0	0	0	0	0	0	0	0	0	0	0	0	0
	σ	0	0	0	0	0	0	0	0	0	0	0	0	0	0
	Max	0	0	0	0	0	0	0	0	0	0	0	0	0	0
	Time														
43. kMdm2PolyUb	μ	0	0	0	0	0	0	0	0	0	0	0	0	0	0
	σ	0	0	0	0	0	0	0	0	0	0	0	0	0	0
	Max	0	0	0	0	0	0	0	0	0	0	0	0	0	0
	Time														
44. kMdm2PUb	μ	-41.118	61.75	-12.871	11.98	-17.069	23.19	-3.162	3.61	-3.608	4.07	-6.169	15.72	-13.373	4.51
	σ	12.031	16.377	6.889	4.768	4.708	5.613	0.793	0.792	7.797	7.334	4.466	10.492	10.566	3.522
	Max	-59.21	80.28	-28.23	21.69	-23.63	28.74	-4.30	4.44	-23.46	20.41	-14.23	33.02	-28.33	9.37
	Time	326907	284235	304800	229758	311487	245631	298704	219036	289533	238710	1036800	1036800	444993	451731
45. kMdm2Ub	μ	0	0	0	0	0	0	0	0	0	0	0	0	0	0
	σ	0	0	0	0	0	0	0	0	0	0	0	0	0	0
	Max	0	0	0	0	0	0	0	0	0	0	0	0	0	0
	Time														
46. kp53PolyUb	μ	0	0	0	0	0	0	0	0	0	0	0	0	0	0
	σ	0	0	0	0	0	0	0	0	0	0	0	0	0	0
	Max	0	0	0	0	0	0	0	0	0	0	0	0	0	0
	Time														
47. kp53Ub	μ	0	0	0	0	0	0	0	0	0	0	0	0	0	0
	σ	0	0	0	0	0	0	0	0	0	0	0	0	0	0
	Max	0	0	0	0	0	0	0	0	0	0	0	0	0	0
	Time														
48. kpf	μ	0	0	0	0	0	0	0	0	1.795	-1.81	0	0	0	0
	σ	0	0	0	0	0	0	0	0	3.772	3.903	0	0	0	0
	Max	0	0	0	0	0	0	0	0	14.77	-13.59	0	0	0	0
	Time									345756	345600				
49. kpg	μ	-3.104	2.30	-3.736	2.92	-1.199	0.88	0	0	-3.435	3.41	-1.122	0.88	-13.679	4.90
	σ	5.482	3.562	6.723	4.633	2.107	1.350	0	0	7.880	7.158	0.702	0.537	10.870	3.889
	Max	-15.46	9.28	-19.98	13.31	-5.85	3.41	0	0	-25.99	29.19	-1.77	1.38	-29.28	10.44
	Time	339624	355254	352941	358794	330063	357303			345600	345831	571725	576147	444378	445506
	μ	1.656	-4.57	1.965	-5.40	0.641	-1.78	0	0	1.870	-4.70	0.574	-1.64	2.537	-21.79

50. kpghalf	σ	2.655	9.023	3.146	10.757	1.029	3.497	0	0	3.455	11.676	0.305	1.060	2.007	17.368
	Max	8.53	-26.93	9.81	-33.75	3.34	-10.32	0	0	10.40	-42.48	0.82	-2.70	5.39	-46.78
	Time	207129	358854	221706	360150	204762	360306			183114	345600	546396	568584	444774	446586
51. kphosMdm2	μ	-41.31	62.11	-13.01	12.10	-17.15	23.33	-3.185	3.64	-3.658	4.14	-6.185	15.82	-13.656	4.54
	σ	11.97	16.258	7.006	4.835	4.676	5.555	0.785	0.784	7.928	7.448	4.474	10.522	10.791	3.545
	Max	-59.68	80.77	-28.74	22.07	-23.83	28.96	-4.34	4.48	-23.89	20.72	-14.26	33.14	-28.94	9.43
	Time	326274	278373	305709	228528	311658	241953	298878	216435	289575	237087	1036800	1036800	445023	451422
52. kphosMdm2GSK3b	μ	0	0	0	0	0	0	0	0	0	0	0	0	0	0
	σ	0	0	0	0	0	0	0	0	0	0	0	0	0	0
	Max	0	0	0	0	0	0	0	0	0	0	0	0	0	0
	Time														
53. kphosMdm2GSK3bp53	μ	0	0	0	0	0	0	0	0	0	0	0	0	0	0
	σ	0	0	0	0	0	0	0	0	0	0	0	0	0	0
	Max	0	0	0	0	0	0	0	0	0	0	0	0	0	0
	Time														
54. kphosp53	μ	0	0	0	0	0	0	0	0	0	0	0	0	0	0
	σ	0	0	0	0	0	0	0	0	0	0	0	0	0	0
	Max	0	0	0	0	0	0	0	0	0	0	0	0	0	0
	Time														
55. kphospTauGSK3b	μ	0	0	0	0	0	0	0	0	0	0	0	0	0	0
	σ	0	0	0	0	0	0	0	0	0	0	0	0	0	0
	Max	0	0	0	0	0	0	0	0	0	0	0	0	0	0
	Time														
56. kphospTauGSK3bp53	μ	0	0	0	0	0	0	0	0	0	0	0	0	0	0
	σ	0	0	0	0	0	0	0	0	0	0	0	0	0	0
	Max	0	0	0	0	0	0	0	0	0	0	0	0	0	0
	Time														
57. kprodAbeta	μ	0	0	0	0	0	0	0	0	0	0	0	0	0	0
	σ	0	0	0	0	0	0	0	0	0	0	0	0	0	0
	Max	0	0	0	0	0	0	0	0	0	0	0	0	0	0
	Time														
58. kprodAbeta2	μ	-28.858	28.30	-26.034	27.86	-11.805	10.97	-6.151	9.66	-5.579	11.00	-5.173	6.98	-23.04	6.32
	σ	10.761	7.386	12.933	9.526	4.163	2.756	1.389	1.837	12.099	18.48	3.632	4.526	18.20	4.859
	Max	-51.04	43.67	-56.20	47.07	-20.01	16.81	-8.28	11.53	-44.51	50.37	-11.10	14.51	-48.72	12.76
	Time	349659	183744	359514	204696	350250	176646	345597	202983	345600	218892	1036800	1036800	448242	460059
59. kproteff	μ	0	0	0	0	0	0	0	0	0	0	0	0	0	0
	σ	0	0	0	0	0	0	0	0	0	0	0	0	0	0
	Max	0	0	0	0	0	0	0	0	0	0	0	0	0	0
	Time														
60. krelAbetaGlia	μ	0	0	0	0	0	0	0	0	0	0	0	0	0	0
	σ	0	0	0	0	0	0	0	0	0	0	0	0	0	0

	Max	0	0	0	0	0	0	0	0	0	0	0	0	0	0
	Time														
61. krelGSK3bp53	μ	2.505	-14.53	19.139	-22.13	40.851	-26.20	6.057	-5.17	6.990	-5.41	29.135	-7.35	5.559	-22.87
	σ	3.757	8.848	7.091	12.180	8.962	6.971	1.151	1.182	12.121	11.957	18.260	5.383	4.318	18.079
	Max	12.56	-34.45	34.03	-51.40	49.89	-37.25	7.33	-7.10	33.42	-43.77	57.40	-17.19	11.44	-48.41
	Time	181275	350583	214329	359379	232335	349644	202716	345597	224340	345600	1036800	1036800	454743	448092
62. krelMdm2p53	μ	0	0	0	0	0	0	0	0	0	0	0	0	0	0
	σ	0	0	0	0	0	0	0	0	0	0	0	0	0	0
	Max	0	0	0	0	0	0	0	0	0	0	0	0	0	0
	Time														
63. krelMTTau	μ	0	0	0	0	0	0	0	0	0	0	0	0	0	0
	σ	0	0	0	0	0	0	0	0	0	0	0	0	0	0
	Max	0	0	0	0	0	0	0	0	0	0	0	0	0	0
	Time														
64. kremROS	μ	29.289	-33.008	35.918	-30.380	11.267	-13.570	1.940	-2.521	1.948	-2.804	6.996	-5.372	2.834	-9.101
	σ	8.013	9.214	11.532	11.322	3.017	3.603	0.509	0.633	3.598	5.840	5.184	3.912	2.217	7.181
	Max	35.161	-43.405	46.275	-47.836	13.511	-17.312	2.280	-3.212	10.324	-17.231	16.415	-12.480	5.918	-19.24
	Time	475563	276084	431373	332922	496650	265425	553347	260556	236898	275760	1036800	1036800	447549	445746
65. krepair	μ	27.018	-31.175	33.279	-28.98	10.38	-12.79	1.771	-2.351	1.179	-2.050	6.240	-5.068	1.960	-5.865
	σ	10.757	10.127	13.912	10.98	4.119	4.098	0.695	0.733	2.166	4.123	5.131	3.799	1.523	4.613
	Max	39.035	-43.773	48.566	-44.64	15.06	-17.90	2.549	-3.141	6.257	-12.124	15.784	-12.077	4.055	-12.32
	Time	522477	434118	491286	403461	530289	441357	551970	467745	264393	281952	1036800	1036800	446370	446451
66. ksynMdm2	μ	66.55	-43.078	12.952	-13.88	24.91	-17.92	3.879	-3.35	4.466	-3.853	17.01	-6.322	4.689	-14.79
	σ	16.95	12.135	5.058	7.436	5.684	4.715	0.770	0.768	7.974	8.443	11.21	4.573	3.662	11.69
	Max	86.89	-62.550	23.571	-30.866	30.95	-25.01	4.764	-4.567	22.131	-25.65	35.31	-14.570	9.742	-31.36
	Time	281985	331008	225297	310458	243270	316686	215322	305361	234120	292248	1036800	1036800	451713	444831
67. ksynMdm2mRNA	μ	32.13	-31.46	7.033	-9.427	12.41	-12.94	2.015	-2.356	2.294	-2.718	7.727	-5.176	3.235	-8.725
	σ	8.611	8.790	2.893	4.730	3.020	3.361	0.426	0.535	4.231	5.639	5.278	3.718	2.536	6.888
	Max	43.16	-44.58	13.02	-19.806	15.84	-17.604	2.525	-3.136	11.82	-16.51	16.66	-11.83	6.765	-18.46
	Time	303597	316701	238794	285615	264360	296766	233442	280677	247236	277563	1036800	1036800	449835	446094
68. ksynMdm2mRNAGSK3bp53	μ	17.35	-22.851	4.100	-6.549	6.807	-9.317	1.133	-1.667	1.323	-1.940	3.929	-4.045	2.144	-5.446
	σ	4.459	6.213	1.763	3.175	1.594	2.344	0.235	0.368	2.475	3.919	2.719	2.889	1.684	4.296
	Max	22.97	-31.693	7.883	-13.472	8.659	-12.43	1.429	-2.185	6.960	-11.32	8.626	-9.194	4.500	-11.50
	Time	275169	299355	241620	273165	248913	280344	227931	264141	246306	268428	1036800	1036800	448497	446325
69. ksynp53	μ	-41.32	60.993	-13.29	13.06	-17.173	23.08	-3.22	3.714	-3.746	4.763	-6.176	15.425	-14.15	4.697
	σ	11.23	12.221	7.121	5.501	4.323	3.932	0.691	0.552	8.164	8.337	4.454	9.937	11.18	3.674
	Max	-59.71	78.827	-29.65	25.79	-23.862	31.55	-4.349	4.862	-24.68	23.261	-14.18	31.61	-30.01	9.790
	Time	322761	234786	305643	210717	309147	2934	299487	72684	288234	2145	1036800	1036800	444597	451167
70. ksynp53mRNA	μ	-36.61	52.03	-11.46	11.00	-15.14	19.80	-2.808	3.175	-3.281	3.878	-5.727	13.022	-11.52	4.312
	σ	9.705	11.59	5.944	4.581	3.712	3.869	0.596	0.543	6.976	6.920	4.124	8.626	9.100	3.374
	Max	-51.22	66.56	-24.90	21.33	-20.40	24.48	-3.692	3.914	-20.74	19.323	-13.11	27.300	-24.40	8.992
	Time	306234	244245	293031	220365	292770	220002	282657	201135	279051	224874	1036800	1036800	445542	450477
	μ	0	0	0	0	0	0	0	0	0	0	0	0	0	0

71. ksynp53mRNAAbeta	σ	**0**	**0**	**0**	**0**	**0**	**0**	**0**	**0**	**0**	**0**	**0**	**0**	**0**	**0**
	Max	**0**	**0**	**0**	**0**	**0**	**0**	**0**	**0**	**0**	**0**	**0**	**0**	**0**	**0**
	Time														
72. ksynTau	μ	**0**	**0**	**0**	**0**	**0**	**0**	**0**	**0**	**0**	**0**	**0**	**0**	**0**	**0**
	σ	**0**	**0**	**0**	**0**	**0**	**0**	**0**	**0**	**0**	**0**	**0**	**0**	**0**	**0**
	Max	**0**	**0**	**0**	**0**	**0**	**0**	**0**	**0**	**0**	**0**	**0**	**0**	**0**	**0**
	Time														
73. ktangfor	μ	**0**	**0**	**0**	**0**	**0**	**0**	**0**	**0**	**0**	**0**	**0**	**0**	**0**	**0**
	σ	**0**	**0**	**0**	**0**	**0**	**0**	**0**	**0**	**0**	**0**	**0**	**0**	**0**	**0**
	Max	**0**	**0**	**0**	**0**	**0**	**0**	**0**	**0**	**0**	**0**	**0**	**0**	**0**	**0**
	Time														

Table C.2: LSA results using MRM/GSSA

Species		p53		ATMA		GSK3b_p53		Aβ		Plaques		Tangles		GliaA	
Parameters	P.V	50%	200%	50%	200%	50%	200%	50%	200%	50%	**200%**	50%	200%	50%	200%
1. kactATM	*μ*	**-21.62**	**31.73**	**-25.22**	**34.34**	**-8.780**	**11.411**	**-1.48**	**2.98**	**0.148**	**1.717**	**-6.228**	**3.948**	**2.738**	**-0.700**
	σ	**47.33**	**58.31**	**31.48**	**35.36**	**20.83**	**24.07**	**4.81**	**5.406**	**2.277**	**4.261**	**4.865**	**3.447**	**3.360**	**3.368**
	Max	**-168**	**281**	**-102**	**151**	**-86**	**112**	**-16**	**24**	**13**	**22**	**-16**	**12**	**13**	**-11**
	Time	**868600**	**937100**	**871500**	**142200**	**869300**	**422200**	**425500**	**426000**	**266100**	**274700**	**922800**	**956100**	**371600**	**356700**
2. kactDUBMdm2	*μ*	**2.42**	**-25.06**	**-2.62**	**-20.68**	**1.303**	**-10.236**	**-0.23**	**-2.43**	**3.235**	**0.990**	**-1.227**	**-5.215**	**0.188**	**2.202**
	σ	**54.83**	**64.52**	**38.74**	**40.73**	**23.56**	**28.18**	**4.880**	**6.454**	**6.019**	**4.052**	**4.524**	**7.713**	**4.420**	**4.531**
	Max	**176**	**-194**	**-111**	**-106**	**87**	**-91**	**-18**	**-18**	**21**	**22**	**-10**	**-20**	**10**	**17**
	Time	**29400**	**968700**	**833100**	**867200**	**28400**	**718200**	**533100**	**741500**	**119200**	**254700**	**1017900**	**1017900**	**743100**	**413500**
3. kactDUBp53	*μ*	**-6.67**	**26.35**	**-3.67**	**-28.19**	**-3.308**	**-14.18**	**-1.15**	**-3.83**	**-3.854**	**-5.734**	**-8.558**	**-6.025**	**-6.616**	**-22.54**
	σ	**63.44**	**55.51**	**49.56**	**49.05**	**26.98**	**30.58**	**5.930**	**6.546**	**7.361**	**16.554**	**6.708**	**5.009**	**7.310**	**19.471**
	Max	**-183**	**218**	**-116**	**-143**	**-84**	**-92**	**-19**	**-25**	**-26**	**-64**	**-22**	**-18**	**-25**	**-55**
	Time	**1003900**	**343100**	**210400**	**340800**	**204300**	**267700**	**118900**	**256600**	**331300**	**345500**	**922800**	**731400**	**642900**	**427800**
4. kactDUBProtp53	*μ*	**0**	**0**	**0**	**0**	**0**	**0**	**0**	**0**	**0**	**0**	**0**	**0**	**0**	**0**
	σ	**0**	**0**	**0**	**0**	**0**	**0**	**0**	**0**	**0**	**0**	**0**	**0**	**0**	**0**
	Max	**0**	**0**	**0**	**0**	**0**	**0**	**0**	**0**	**0**	**0**	**0**	**0**	**0**	**0**
	Time	**0**	**0**	**0**	**0**	**0**	**0**	**0**	**0**	**0**	**0**	**0**	**0**	**0**	**0**
5. kactglia1	*μ*	**36.86**	**23.09**	**0.17**	**-5.02**	**1.145**	**-4.264**	**0.10**	**-1.62**	**0.619**	**0.150**	**3.745**	**-4.845**	**-3.906**	**5.889**
	σ	**67.18**	**84.68**	**28.16**	**27.76**	**20.48**	**19.40**	**4.421**	**5.170**	**3.162**	**3.098**	**2.617**	**4.802**	**3.844**	**5.817**
	Max	**257**	**232**	**106**	**-93**	**70**	**-65**	**14**	**-17**	**18**	**19**	**10**	**-16**	**-16**	**18**
	Time	**328800**	**326700**	**1006700**	**847600**	**937800**	**994700**	**224900**	**810400**	**255700**	**354400**	**488300**	**1017900**	**427800**	**423900**
6. Kactglia2	*μ*	**35.04**	**44.37**	**2.32**	**9.82**	**0.718**	**4.293**	**-0.22**	**-0.46**	**0.474**	**-0.251**	**-1.161**	**-3.570**	**-7.631**	**11.640**
	σ	**65.51**	**65.04**	**30.79**	**36.13**	**17.64**	**21.93**	**4.604**	**4.553**	**2.786**	**1.449**	**3.580**	**4.947**	**9.055**	**9.958**
	Max	**204**	**204**	**117**	**146**	**60**	**100**	**-15**	**-15**	**27**	**-18**	**-8**	**-14**	**-28**	**29**
	Time	**248600**	**248600**	**617200**	**1010400**	**645800**	**936500**	**494000**	**811800**	**358900**	**357400**	**922800**	**761400**	**639400**	**882000**
7. kaggAbeta	*μ*	**6.30**	**-35.67**	**5.07**	**-17.50**	**2.395**	**5.353**	**5.05**	**5.22**	**0.976**	**-3.605**	**3.058**	**-8.261**	**-1.384**	**-11.945**
	σ	**58.08**	**50.15**	**39.56**	**38.77**	**24.61**	**23.37**	**7.361**	**6.051**	**4.574**	**8.933**	**4.694**	**8.119**	**3.120**	**9.977**
	Max	**219**	**-242**	**141**	**-111**	**93**	**93**	**31**	**25**	**21**	**-30**	**12**	**-22**	**-12**	**-29**
	Time	**929100**	**633400**	**521100**	**265200**	**533300**	**1012800**	**971200**	**1012000**	**255700**	**219400**	**488900**	**904700**	**458600**	**463800**
8. kaggTau	*μ*	**-2.03**	**0.46**	**-3.29**	**-4.66**	**-0.946**	**0.067**	**-0.79**	**0.26**	**-0.802**	**-0.650**	**-7.120**	**2.835**	**-3.882**	**-0.650**
	σ	**31.95**	**46.24**	**21.21**	**32.39**	**22.02**	**20.87**	**4.862**	**4.975**	**2.599**	**2.516**	**6.788**	**2.346**	**3.952**	**3.587**
	Max	**-162**	**122**	**-89**	**-94**	**-84**	**66**	**-17**	**17**	**-11**	**-15**	**-18**	**6**	**-16**	**-10**
	Time	**970400**	**924600**	**519600**	**340900**	**510600**	**936500**	**533100**	**107600**	**349500**	**349500**	**761400**	**225800**	**407100**	**872700**
9. kaggTauP1	*μ*	**0**	**9.23**	**0**	**11.47**	**0**	**3.834**	**0**	**2.98**	**0**	**1.717**	**0**	**3.948**	**0**	**-0.700**
	σ	**0**	**36.48**	**0**	**27.10**	**0**	**16.01**	**0**	**5.406**	**0**	**4.261**	**0**	**3.447**	**0**	**3.368**
	Max	**0**	**186**	**0**	**112**	**0**	**86**	**0**	**24**	**0**	**22**	**0**	**12**	**0**	**-11**
	Time	**0**	**936400**	**0**	**572100**	**0**	**936200**	**0**	**940400**	**0**	**274700**	**0**	**956100**	**0**	**356700**
10. kaggTauP2	*μ*	**-2.49**	**0.24**	**-4.29**	**-4.66**	**-0.946**	**0.067**	**-0.79**	**0.26**	**-0.802**	**-0.650**	**-7.120**	**2.835**	**-3.882**	**-0.650**
	σ	**51.95**	**48.24**	**31.21**	**30.39**	**22.02**	**20.87**	**4.862**	**4.975**	**2.599**	**2.516**	**6.788**	**2.346**	**3.952**	**3.587**
	Max	**-162**	**144**	**-89**	**-92**	**-84**	**66**	**-17**	**17**	**-11**	**-15**	**-18**	**6**	**-16**	**-10**
	Time	**970000**	**924600**	**509600**	**340900**	**510600**	**936500**	**533100**	**107600**	**349500**	**349500**	**761400**	**225800**	**407100**	**872700**
11. kbinAbantiAb	*μ*	**-0.71**	**5.15**	**0.84**	**4.58**	**-0.399**	**2.199**	**0.21**	**-1.39**	**0.031**	**-0.127**	**-3.250**	**0.127**	**0.766**	**-0.100**
	σ	**49.91**	**49.26**	**35.34**	**36.48**	**21.82**	**20.71**	**4.817**	**4.979**	**0.947**	**0.844**	**4.545**	**2.491**	**3.304**	**3.117**
	Max	**-179**	**-209**	**107**	**146**	**-79**	**74**	**18**	**-19**	**11**	**-8**	**-12**	**8**	**13**	**10**
	Time	**588900**	**669300**	**937600**	**969600**	**482200**	**970300**	**786900**	**425500**	**353300**	**357700**	**761400**	**572000**	**371500**	**607300**

12. kbinAbetaGlia	μ	12.01	-18.28	12.24	-12.49	5.079	-7.953	0.94	-2.19	0.531	-0.356	-3.906	-4.022	2.547	-5.597
	σ	44.28	55.58	32.34	38.98	18.61	23.82	4.355	4.919	2.427	1.424	6.085	6.410	4.186	4.975
	Max	172	-184	122	130	80	96	21	-18	21	-17	4	-16	17	-16
	Time	971400	837200	936100	1009200	972000	971100	941700	766000	355800	355000	430600	1017900	593200	784600
13. kbinE1Ub	μ	-3.35	-8.06	-0.79	-9.14	-1.464	-3.983	-1.54	-0.55	-3.293	1.927	-0.447	-3.200	-4.537	-4.177
	σ	53.40	55.84	37.87	30.48	23.20	23.57	5.599	6.193	6.728	4.419	4.188	4.886	4.150	4.047
	Max	183	-210	114	-94	82	-100	18	24	-27	17	-8	-14	-14	-14
	Time	970500	669300	1001100	671800	970200	669900	933700	312200	219100	202300	761400	1017900	499100	897200
14. kbinE2Ub	μ	-11.03	-3.13	-0.17	0.29	-4.940	-2.506	-1.65	-1.04	-0.478	-5.122	-3.171	-8.491	-1.059	-22.451
	σ	55.94	81.38	38.42	60.88	23.98	33.91	5.508	7.644	3.620	16.982	4.205	6.388	2.729	18.269
	Max	-200	-199	121	139	-87	100	21	-23	-24	-63	-12	-20	-10	-54
	Time	153900	241600	1008700	935000	154500	937300	943300	256600	345700	339200	922800	922800	669000	468000
15. kbinGSK3bp53	μ	9.94	-1.84	-6.51	18.01	-20.549	36.432	-4.35	4.72	-4.793	3.525	-9.253	23.725	-16.010	2.769
	σ	63.76	49.11	42.66	36.33	22.66	30.89	5.187	6.374	11.646	9.164	8.950	15.107	12.379	4.794
	Max	190	146	-116	118	-85	121	-19	24	-47	35	-25	47	-39	20
	Time	1012600	969200	210400	617000	424800	1012500	496300	197500	339200	255200	1017900	1024300	400000	424800
16. kbinMdm2p53	μ	59.32	-42.20	12.67	-7.77	21.932	-17.710	3.18	-3.30	3.825	-5.669	10.117	-9.955	6.089	-15.791
	σ	78.53	53.83	42.89	48.78	31.40	23.71	6.009	5.907	7.986	11.593	6.102	8.836	5.759	12.766
	Max	306	-204	135	145	128	-91	25	20	32	-39	24	-26	21	-39
	Time	1006300	154000	936700	970400	970600	154500	972900	971200	255900	338400	1014600	1017900	601500	498800
17. kbinMTTau	μ	-10.21	19.13	-2.65	21.85	-5.332	7.164	-1.00	0.91	-4.540	0.470	1.121	-7.206	-11.922	0.416
	σ	71.40	52.70	49.35	26.95	30.12	22.84	7.339	5.242	10.000	2.528	5.284	5.475	9.328	3.721
	Max	-239	236	-124	118	-106	97	-20	21	-33	10	16	-16	-35	14
	Time	425900	1006500	420700	1006100	428700	1009800	256600	783200	324100	248700	1004800	731400	395000	424200
18. kbinProt	μ	12.24	17.08	10.09	-9.56	4.536	-2.115	1.62	-0.49	-0.684	-2.087	-0.055	-0.866	-3.617	-6.090
	σ	55.45	47.96	40.37	38.07	23.40	24.18	5.423	5.135	2.716	4.517	3.755	1.967	4.042	5.417
	Max	246	188	125	-92	108	82	18	-16	-11	-21	-9	-8	-14	-18
	Time	1000200	1000200	967600	847600	1000600	620000	971200	118900	339200	346400	761300	761400	672200	786800
19. kbinTauProt	μ	-3.71	-23.51	-5.86	-22.34	-4.129	-12.091	-0.49	-3.30	-2.577	-5.126	-6.005	-3.947	-2.925	-21.598
	σ	60.99	51.77	53.10	45.37	29.38	28.71	5.906	6.505	5.382	14.773	5.188	4.464	3.954	16.706
	Max	-255	-208	-136	-123	-103	-91	-17	-20	-22	-49	-14	-12	-14	-49
	Time	488700	488700	265400	255200	479600	154500	492700	254800	346100	289300	684900	922800	874400	394900
20. kdam	μ	0	0	0	0	0	0	0	0	0	0	0	0	0	0
	σ	0	0	0	0	0	0	0	0	0	0	0	0	0	0
	Max	0	0	0	0	0	0	0	0	0	0	0	0	0	0
	Time	0	0	0	0	0	0	0	0	0	0	0	0	0	0
21. kdamROS	μ	-50.63	36.46	-44.95	36.75	-23.571	12.09	-4.97	1.76	-5.030	2.651	-9.691	5.586	-19.15	5.352
	σ	63.10	54.44	39.89	24.52	26.66	19.32	6.027	4.924	11.342	5.513	8.036	4.424	14.618	5.669
	Max	-209	201	-140	112	-93	98	-21	20	-50	25	-24	14	-45	24
	Time	918900	170600	328300	1011400	325400	988200	811700	237100	345400	255900	1017900	475900	501000	601500
22. kdegAbeta	μ	-3.30	-35.67	15.49	-17.50	5.353	-8.937	5.22	-4.49	-0.731	-3.605	4.636	-8.261	-4.008	-11.945
	σ	46.71	50.15	32.59	38.77	23.37	25.30	6.051	5.753	3.818	8.933	3.113	8.119	5.359	9.977
	Max	-162	-242	125	-111	93	-72	25	-20	-16	-30	10	-22	-18	-29
	Time	557400	942800	1007800	265200	1012800	134300	1012000	179600	163800	219400	721900	904700	619900	463800
23. kdegAbetaGlia	μ	24.08	19.12	23.56	11.61	7.723	5.700	1.33	0.60	-0.033	-0.089	-0.719	-0.896	-0.802	-0.732
	σ	48.89	51.81	33.45	28.20	19.84	19.67	4.591	4.424	1.046	0.857	3.521	1.413	3.260	3.230
	Max	175	175	152	110	96	85	22	16	-10	-10	-9	-6	-13	-9
	Time	203000	-189	936700	615000	970600	939900	786600	940300	350500	350800	731400	704800	466200	384700

24. kdegAntiAb	μ	12.91	10.27	6.92	6.15	3.171	2.143	-0.07	0.828	-0.107	0.217	-0.921	0.975	1.566	-6.450
	σ	54.67	55.40	33.09	29.85	19.14	20.08	4.600	4.378	0.820	1.235	2.631	2.899	4.079	5.580
	Max	200	192	124	111	92	87	-16	16	-7	16	-10	8	13	-17
	Time	561600	903300	1005100	1009000	1010900	1000000	766100	470000	351900	353300	761400	474700	616900	499000
25. kdegMdm2	μ	-28.79	8.36	-25.20	-0.40	-14.126	0.80	-4.17	-0.25	-6.289	-1.177	-9.387	3.689	-23.610	-0.974
	σ	58.28	60.01	46.84	39.58	29.87	25.8928	6.241	5.280	16.643	3.894	7.400	3.775	18.677	3.975
	Max	-223	183	-142	-98	-95	87	-21	-16	-62	-14	-22	12	-54	-17
	Time	347900	510700	340800	844500	346400	1010500	256600	766000	346400	215200	761400	547400	400600	1034300
26. kdegMdm2mRNA	μ	-59.92	80.74	-38.83	17.76	-27.80	27.82	-6.20	4.650	-6.661	5.214	-9.932	20.057	-24.95	3.672
	σ	54.67	64.33	46.29	37.47	27.24	25.92	5.838	5.773	16.949	9.849	8.801	13.516	20.508	6.263
	Max	-253	318	-138	133	-105	113	-22	27	-65	39	-26	40	-58	25
	Time	488700	561100	265400	943000	426900	1009100	425500	622600	339200	256400	1017900	1013200	499000	436700
27. kdegp53	μ	-0.44	-20.67	2.44	-20.49	-2.429	-10.821	-0.57	-2.46	-3.464	-3.042	-4.843	-1.702	-10.24	-1.837
	σ	51.03	62.21	39.79	47.80	24.48	29.39	5.525	6.118	7.034	6.002	6.947	4.593	7.924	3.670
	Max	-187	-220	139	-123	-88	-104	-18	-20	-23	-26	-18	-13	-23	-15
	Time	604700	488700	971700	420700	154500	424800	531700	271300	201500	339200	922800	761400	410700	467200
28. kdegp53mRNA	μ	80.33	-27.72	25.84	-6.36	27.81	-13.15	4.483	-2.18	6.419	-2.230	4.994	-11.130	5.517	-4.159
	σ	59.16	52.53	35.48	36.95	24.04	20.96	5.217	4.942	11.844	4.755	5.397	9.302	5.251	4.615
	Max	260	-202	127	-109	112	-88	20	-21	46	-27	15	-26	21	-17
	Time	556800	604700	1003600	328300	1010400	423600	470000	425500	270900	346700	1000400	922800	604400	483900
29. kdegTau20SProt	μ	6.59	7.03	-1.60	2.06	0.97	0.96	0.089	0.357	-0.819	-0.635	-3.561	-5.499	-4.858	1.407
	σ	48.74	55.71	39.91	38.82	22.19	24.62	5.614	5.769	2.761	1.958	4.195	6.429	4.458	4.494
	Max	168	171	-98	126	92	85	18	18	-14	-10	-12	-16	-15	15
	Time	172300	310200	847600	1004800	936200	961900	968800	965400	346300	219100	761400	761400	460200	429000
30. kdephosMdm2	μ	55.96	79.15	-0.45	4.47	19.23	-11.260	2.706	-2.02	2.856	-2.298	6.597	-9.090	-5.488	-4.283
	σ	63.64	52.53	37.97	32.60	25.88	20.38	5.854	4.670	5.298	4.603	5.501	8.275	5.305	4.596
	Max	227	243	-81	106	118	-93	30	-17	24	-18	16	-25	-16	-19
	Time	1004300	1028000	682500	941600	1005000	425800	970000	425500	236800	304300	488500	1017900	467200	679300
31. kdephosp53	μ	15.39	17.12	-12.15	-9.41	-5.214	-4.613	-1.28	-1.29	2.456	-2.768	0.784	-0.076	7.257	-6.609
	σ	45.94	59.01	35.75	45.08	24.84	28.22	6.005	7.058	5.394	6.905	4.576	3.386	6.155	6.205
	Max	153	166	-105	-116	-99	-88	-19	-24	25	-31	10	-4	20	-21
	Time	398900	393600	271700	210400	669900	239900	684200	256600	250900	339200	510800	262800	563000	400600
32. kdephospTau	μ	4.69	16.43	-11.65	-10.67	-10.322	-5.065	-2.67	-1.66	-4.461	-5.530	8.439	-11.383	-6.296	-18.746
	σ	57.69	53.01	58.51	47.52	32.14	25.66	6.897	5.918	8.713	13.904	12.491	9.672	5.720	15.345
	Max	155	152	-139	-143	-105	-100	-22	-22	-31	-52	40	-28	-19	-46
	Time	740500	458800	349400	340800	424800	325400	425500	271300	219100	339200	1009900	1017900	394800	400600
33. kdisaggAbeta	μ	34.34	19.41	6.62	-2.68	2.44	-3.611	-0.29	-0.88	-1.794	0.007	-3.363	-5.183	-3.566	-0.926
	σ	45.54	45.59	43.28	24.85	23.66	18.05	5.246	4.120	3.945	1.154	2.416	5.697	4.495	3.455
	Max	184	149	114	-95	80	-81	-16	-20	-18	16	-10	-16	-17	-10
	Time	593200	371000	934600	521100	940600	510600	255300	533100	275000	353100	761400	1017900	414300	389200
34. kdisaggAbeta1	μ	4.39	12.45	-18.06	-11.75	-10.359	-6.844	-2.57	-1.38	-3.289	-6.011	-6.656	-8.325	-4.992	-22.057
	σ	57.97	58.48	35.05	55.79	25.46	31.24	5.736	6.535	6.816	15.584	5.417	6.351	4.914	19.118
	Max	157	206	-119	-143	-87	-99	-18	-22	-24	-60	-18	-18	-17	-56
	Time	399700	1028400	856700	340800	868600	325400	881600	336300	219100	345400	1017900	761400	871000	458300
35. kdisaggAbeta2	μ	41.05	38.50	12.10	12.04	5.27	4.06	0.483	0.417	0.017	0.011	1.575	-1.147	2.220	-2.846
	σ	44.23	41.81	28.71	39.70	19.28	20.89	4.432	4.522	0.846	0.866	3.817	4.007	3.480	4.679
	Max	206	149	105	146	72	88	19	14	6	6	12	-10	14	-14
	Time	426100	348400	937700	1006000	944600	1003600	944300	924500	356600	353300	493900	761400	977900	1035100

36. kgenROSAbeta	μ	-47.26	59.83	-52.52	36.96	-32.79	12.05	-7.73	2.782	-5.501	2.578	-11.35	7.575	-25.533	-3.156
	σ	52.49	40.24	48.01	32.79	32.43	21.81	7.469	4.877	18.209	5.418	9.646	4.061	20.791	4.118
	Max	-171	195	-143	150	-103	86	-24	19	-66	23	-28	14	-58	-15
	Time	779400	367200	340800	941200	428800	984300	256600	325500	345400	270300	922800	500900	499000	875200
37. kgenROSGlia	μ	22.65	41.12	-1.52	10.34	-2.350	5.38	-0.67	1.065	-0.090	0.071	-0.236	1.394	-1.501	-4.185
	σ	48.31	42.19	32.83	24.29	20.02	18.22	4.734	4.509	0.747	0.915	2.634	2.684	2.892	5.695
	Max	157	182	-99	80	-74	75	-19	19	-6	6	-4	6	-10	-17
	Time	398900	426400	750200	658000	753400	962600	767700	940000	357900	366100	684900	429200	871000	871000
38. kgenROSPlaque	μ	24.44	38.36	-5.41	10.22	-1.456	3.93	-0.69	-0.07	-1.085	-2.924	-7.333	-3.167	2.553	-5.829
	σ	41.73	47.95	41.35	41.84	24.02	24.32	5.075	5.205	3.184	6.237	5.415	3.893	3.671	5.153
	Max	196	212	-104	124	-81	89	-19	-18	-18	-24	-16	-14	15	-23
	Time	636100	1028600	420700	999000	424800	999900	271300	534300	339600	345700	761400	761400	370100	400600
39. kinactATM	$\boldsymbol{\mu}$	64.18	0.79	40.90	-24.34	13.69	-11.29	2.515	-2.33	1.805	-2.465	1.582	-11.158	4.297	-7.859
	$\boldsymbol{\sigma}$	44.44	43.69	39.74	35.80	23.45	22.57	5.411	5.703	4.921	5.307	3.502	9.341	5.770	6.614
	Max	211	149	179	-102	122	-82	24	-18	21	-23	13	-26	24	-24
	Time	302500	125800	1008800	252700	1000500	674500	968900	531700	250000	324500	663000	1017900	604000	400600
40. kinactglia1	μ	-3.48	9.22	-28.17	-13.19	-13.708	-8.104	-3.68	-2.48	-3.715	0.087	-8.384	-3.072	4.773	-9.601
	σ	53.97	55.72	50.80	50.75	31.35	30.40	5.980	6.081	7.228	2.274	7.671	6.035	4.605	8.039
	Max	-159	172	-139	-125	-105	-107	-22	-22	-29	10	-22	-14	18	-25
	Time	829200	552600	357900	417700	426900	428700	425500	766000	339200	255700	922800	904700	429000	871000
41. kinactglia2	μ	0	51.39	0	18.56	0	8.88	0	2.544	0	1.057	0	1.621	0	-11.339
	σ	0	42.89	0	33.80	0	20.03	0	4.938	0	1.914	0	2.951	0	9.851
	Max	0	197	0	130	0	86	0	22	0	10	0	10	0	-30
	Time	0	445400	0	931000	0	971600	0	974300	0	352600	0	994700	0	782000
42. kinhibprot	μ	5.03	44.42	-19.85	15.02	-9.822	6.52	-3.05	-0.07	-0.195	-0.710	-3.592	0.125	-1.118	-0.691
	σ	47.83	46.07	29.99	40.63	21.52	22.30	5.520	5.533	2.078	3.419	4.789	2.553	3.136	3.398
	Max	120	227	-121	127	-105	88	-20	-18	-12	-18	-14	8	-14	-14
	Time	287200	497100	426900	1011800	426900	1008000	766000	274700	346700	350500	1017900	1005300	406500	382100
43. kMdm2PolyUb	μ	24.13	25.48	-6.04	1.53	-2.101	-1.327	-0.51	-0.91	-3.469	-3.880	-0.867	-4.042	-10.229	-7.548
	σ	52.24	51.29	46.28	46.37	27.76	26.86	6.052	5.709	7.574	7.922	2.604	3.170	8.225	6.196
	Max	209	169	-111	118	-88	-92	-17	-17	-32	-32	-8	-10	-25	-22
	Time	187300	1023800	360500	929600	154500	384600	430200	248400	346400	345900	704800	575900	458300	394800
44. kMdm2PUb	μ	-4.70	97.93	-2.60	10.28	-13.605	25.62	-2.42	3.300	-1.449	7.956	-7.515	17.198	-2.204	3.946
	σ	38.63	62.57	40.13	36.58	24.14	25.40	5.775	6.097	3.624	15.571	8.182	8.936	4.259	4.875
	Max	-132	290	-113	108	-103	111	-21	22	-21	56	-22	27	-16	21
	Time	518600	191100	463700	943400	479600	972000	531700	106100	350800	202300	922800	472200	404500	424800
45. kMdm2Ub	μ	7.34	7.69	-13.70	-11.26	-9.538	-8.944	-3.34	-2.11	-5.205	-4.918	-3.983	-7.553	-22.143	-23.092
	σ	67.73	59.86	57.01	54.81	33.29	30.66	8.014	6.915	17.663	17.516	3.274	6.006	18.861	18.449
	Max	181	189	-138	-138	-102	-93	-24	-22	-65	-63	-12	-16	-58	-54
	Time	1030800	1013500	265400	265400	478800	267700	256600	256600	345400	339200	1017900	731400	499000	405900
46. kp53PolyUb	μ	19.29	16.97	-6.37	-6.16	-4.185	-4.591	-2.48	-0.68	-5.582	-2.909	-7.664	-7.690	-15.972	-9.812
	σ	59.76	48.08	43.51	29.20	28.55	20.71	6.475	4.921	13.227	6.244	6.582	6.123	12.419	7.520
	Max	183	158	-116	-83	-89	-73	-21	-19	-45	-22	-20	-20	-37	-22
	Time	727400	257900	210400	265700	249100	134300	254800	118900	279100	206400	922800	1017900	400600	391700
47. kp53Ub	μ	7.75	16.95	-18.08	-7.41	-4.591	-5.397	-1.22	-2.01	-2.333	-5.694	-9.896	2.602	-0.573	-19.873
	σ	47.77	67.78	37.63	50.94	20.71	31.71	5.434	7.585	4.838	16.936	7.743	4.253	2.939	16.254
	Max	136	233	-108	-138	-73	-93	-22	-24	-18	-60	-20	10	-7	-55
	Time	907300	551200	360800	265400	134300	267700	533100	256600	346800	338400	704800	665700	390400	405900

48. kpf	μ	32.14	16.79	6.70	-2.94	0.99	-4.715	-0.06	-1.42	-0.149	-2.642	-0.595	-2.151	0.500	-4.137
	σ	49.47	48.06	24.07	40.11	20.85	25.07	5.147	5.715	4.542	5.280	3.242	3.950	4.618	4.143
	Max	190	168	89	-96	66	-99	-19	-19	-19	-20	-6	-12	18	-15
	Time	553000	922700	936900	572300	617400	669900	118900	118900	168200	346500	761400	731400	601500	357000
49. kpg	μ	164.05	177.53	18.30	31.21	47.58	51.67	6.977	7.292	4.453	18.451	29.742	39.358	1.369	5.862
	σ	66.43	76.82	30.29	40.81	27.17	29.33	5.593	6.566	8.672	31.509	13.196	22.390	3.418	8.465
	Max	368	366	116	139	130	144	27	24	32	95	44	74	14	25
	Time	390100	194600	969100	1009700	1000500	1012400	72000	654100	126800	337000	890000	1015100	439500	598900
50. kpghalf	μ	179.02	156.19	29.94	17.14	52.38	44.88	7.834	6.118	11.100	10.453	27.617	24.530	6.780	2.177
	σ	68.60	76.00	32.03	41.29	25.84	34.94	6.318	6.582	18.184	17.113	17.239	14.525	6.328	3.385
	Max	421	357	125	112	130	147	26	33	55	55	61	46	22	15
	Time	390100	550700	928800	940800	968300	969100	974000	300000	255700	315600	1011500	978000	593200	442800
51. kphosMdm2	μ	12.00	162.91	-13.25	16.65	-6.674	47.72	-1.57	6.751	-5.331	11.802	-7.003	29.745	-15.408	1.681
	σ	51.86	63.98	42.36	30.88	27.23	24.96	6.513	6.086	12.247	19.300	5.530	16.208	11.744	4.890
	Max	159	344	-138	117	-95	130	-19	26	-43	60	-16	50	-34	17
	Time	911700	370800	265400	971700	267700	940000	256600	933800	324400	254700	922800	1006400	501500	420700
52. kphosMdm2GSK3b	μ	62.33	92.19	0.99	16.50	12.34	24.23	1.511	4.365	-3.282	5.652	3.490	9.476	-8.015	-0.404
	σ	72.04	51.39	44.09	33.01	31.01	23.58	6.738	5.256	7.641	9.493	4.074	7.326	6.878	6.680
	Max	279	261	117	118	107	110	21	26	-28	33	15	23	-23	-17
	Time	686900	740100	971200	942900	1009300	938000	941200	786300	218900	179700	1010100	861200	400000	871300
53. kphosMdm2GSK3bp53	μ	57.85	47.70	-7.00	-5.30	10.15	5.63	1.629	-0.57	1.277	-5.282	3.000	0.560	1.689	-18.885
	σ	66.47	82.84	38.61	49.79	30.86	36.53	6.487	8.188	4.880	14.876	3.451	3.504	3.455	15.079
	Max	224	252	-110	-138	121	99	26	-23	21	-50	10	8	15	-46
	Time	810900	908400	463700	265400	1003300	939800	976800	271300	274700	298800	433300	485200	424800	502100
54. kphosp53	μ	79.80	85.78	12.01	13.45	19.21	21.40	2.516	3.561	2.532	6.822	6.374	14.045	4.064	2.635
	σ	66.81	48.00	39.88	40.83	28.56	25.60	5.969	5.898	5.903	11.526	5.105	7.688	5.070	5.366
	Max	275	231	145	148	119	104	23	25	26	36	16	26	24	20
	Time	398700	296100	1010000	1008600	999800	932300	965600	938100	254700	248700	416500	982800	429000	441900
55. kphospTauGSK3b	μ	59.83	42.66	-2.46	-12.42	11.57	4.37	1.082	-1.01	0.991	-5.748	7.012	1.095	-1.259	-19.060
	σ	62.02	77.89	40.11	47.11	30.17	34.61	6.129	7.325	3.023	16.514	6.172	3.215	5.084	15.582
	Max	225	231	-96	-138	109	103	21	-19	14	-58	22	8	-14	-50
	Time	1029000	424600	733800	265400	970700	1007300	991800	248400	249200	324100	1010800	861800	1032600	394800
56. kphospTauGSK3bp53	μ	91.50	65.06	15.94	0.70	23.52	13.72	3.731	1.549	5.308	-1.132	-6.712	42.605	-1.286	-3.617
	σ	53.67	62.67	25.51	33.43	21.36	25.33	5.267	5.423	9.538	4.528	6.884	27.180	2.989	4.404
	Max	268	256	90	102	93	93	21	18	32	-19	-18	72	-10	-17
	Time	685800	497600	146500	971600	812400	558600	134700	396500	179700	183100	761400	656000	498300	412400
57. kprodAbeta	μ	62.11	94.05	-4.51	23.01	12.81	24.34	2.595	3.202	4.373	4.041	6.548	15.938	1.605	1.137
	σ	57.47	61.40	38.39	39.34	25.51	27.32	5.470	5.009	8.351	7.738	3.838	8.349	4.453	4.744
	Max	287	298	-99	143	96	122	24	20	30	32	14	35	19	15
	Time	344700	845400	841000	969300	1011300	971300	1036500	357200	211400	254700	500500	1033000	374200	431600
58. kprodAbeta2	μ	26.57	80.32	-36.92	11.54	-4.832	19.25	-6.27	10.907	-2.427	6.062	8.410	11.078	-1.085	5.114
	σ	118.12	69.00	39.75	41.18	46.20	30.71	6.941	9.180	4.196	15.714	7.295	9.690	4.089	5.379
	Max	368	260	82	144	-104	114	-23	33	-17	66	22	36	-13	24
	Time	367100	985100	1020100	937400	479600	936000	533100	787200	280700	311900	412700	1002700	1032400	601500
59. kproteff	μ	92.93	66.81	20.04	-0.20	24.01	14.31	3.675	1.915	3.824	0.429	9.466	-1.581	0.791	-0.875
	σ	49.02	58.10	36.64	38.54	23.33	26.24	5.750	5.917	7.338	3.431	7.933	3.852	5.278	4.069
	Max	240	268	122	-129	119	109	26	26	30	18	25	-11	18	-14
	Time	380800	1030600	937400	844500	939900	969500	944200	941700	212900	230700	990200	761400	601500	923200

60. krelAbetaGlia	μ	62.42	56.59	1.12	-2.10	12.30	9.76	1.190	1.506	-3.232	-3.036	11.089	6.312	-6.493	-6.871
	σ	66.32	70.55	46.15	41.15	30.50	31.14	5.856	6.871	7.274	7.368	9.214	4.368	6.053	5.709
	Max	264	249	136	-118	104	99	18	22	-28	-28	32	14	-21	-19
	Time	947300	396100	941100	274600	932500	971000	933100	971500	219100	219100	993300	454200	406700	499000
61. krelGSK3bp53	μ	46.62	67.35	2.05	-10.58	48.98	-14.370	6.814	-2.91	7.347	-4.334	37.492	-11.379	2.232	-11.229
	σ	56.70	60.10	39.59	38.08	40.95	21.56	7.402	4.815	13.017	8.881	21.424	9.667	4.758	8.745
	Max	202	275	124	-95	174	-92	30	-17	47	-38	70	-28	17	-26
	Time	435900	498300	937800	712700	930300	718200	931800	533600	278600	346500	980300	1017900	376900	540200
62. krelMdm2p53	μ	37.17	70.30	-14.32	6.44	2.13	15.27	0.039	1.923	1.850	3.098	3.391	13.024	0.882	-1.071
	σ	72.16	71.44	38.25	46.62	33.48	31.02	7.204	6.829	5.022	6.102	4.647	9.915	3.549	4.002
	Max	230	286	-97	140	97	120	19	20	25	24	14	28	14	-12
	Time	812000	985100	742500	1002300	1012700	970200	245500	142700	297500	199200	491300	492400	604700	871000
63. krelMTTau	μ	74.74	43.67	2.15	-11.25	17.75	4.38	3.261	-0.76	5.546	-5.202	-7.294	14.325	-5.085	-21.071
	σ	59.77	82.59	39.89	52.33	27.33	36.36	5.840	7.662	9.415	17.148	6.458	17.085	4.959	17.949
	Max	256	248	115	-138	104	97	20	-22	35	-62	-18	43	-18	-55
	Time	1023300	596600	1010700	265400	1007300	937500	1003800	256600	150900	345700	904700	1015400	485100	407200
64. kremROS	μ	104.62	42.97	33.86	-20.63	27.69	5.47	4.089	1.518	2.789	-0.986	12.363	2.768	5.736	4.155
	σ	58.59	58.49	41.76	35.11	25.96	25.39	5.832	5.522	6.451	2.723	9.702	4.541	5.757	5.330
	Max	264	225	162	-127	127	107	25	18	25	-13	40	14	22	23
	Time	1013600	425100	969900	274800	971900	970900	971800	787100	274700	222600	1012000	527000	601700	603400
65. krepair	μ	115.29	37.44	39.89	-19.98	32.18	2.42	4.472	0.020	5.259	1.890	10.852	7.256	-0.161	1.219
	σ	51.41	73.13	31.23	34.30	22.82	32.82	5.095	6.525	8.767	4.010	7.812	5.887	2.738	4.597
	Max	269	268	148	-109	113	95	23	21	36	16	24	18	-11	18
	Time	549700	396400	1004700	477900	1005000	67700	911400	73800	255700	103600	899400	408500	362600	601500
66. ksynMdm2	μ	177.46	-0.58	22.55	-19.78	51.30	-12.008	7.378	-2.52	6.034	1.955	33.946	-8.768	5.423	1.054
	σ	82.50	58.76	31.31	46.55	28.93	28.14	6.258	6.543	11.727	5.971	20.732	7.937	5.521	3.881
	Max	406	-170	119	-129	147	-87	28	-21	44	22	64	-24	21	14
	Time	385300	829200	1010600	844500	986600	837400	971000	861400	254700	254700	939800	1017900	601700	616200
67. ksynMdm2mRNA	μ	86.41	31.46	-8.41	2.06	20.84	1.53	2.713	0.305	7.185	-2.457	8.515	0.645	2.156	-3.264
	σ	85.71	48.84	41.56	41.96	34.90	25.46	7.200	4.972	13.137	5.775	5.556	2.980	4.318	3.944
	Max	305	177	-129	120	122	89	28	17	42	-23	22	-6	19	-14
	Time	1013300	889100	844500	938100	1011900	935300	138100	933100	249000	288700	1022900	761400	598900	394800
68. ksynMdm2mRNAGSK3bp53	μ	103.48	0.40	14.91	-28.57	27.40	-12.016	3.875	-3.44	3.271	-6.087	6.341	-8.697	-0.575	-21.451
	σ	68.41	66.03	35.10	46.44	28.06	30.83	5.419	7.059	8.248	17.268	5.354	6.439	7.452	17.187
	Max	288	182	134	-143	124	-99	23	-24	34	-66	18	-20	-18	-56
	Time	475600	1013600	935300	340800	1006500	325400	556500	274700	254700	345400	1009900	761400	921000	410600
69. ksynp53	μ	6.34	110.76	-10.36	3.74	-9.408	28.98	-3.26	4.098	-5.345	3.660	-4.260	18.353	-21.538	2.214
	σ	59.43	80.55	59.33	39.35	32.45	30.32	7.532	6.347	15.882	8.076	2.850	12.142	17.804	5.730
	Max	136	411	-138	136	-103	133	-23	25	-54	35	-11	42	-50	20
	Time	626900	641100	265400	1011100	424800	980500	254800	981800	339200	256300	922800	984400	405000	601500
70. ksynp53mRNA	μ	0.36	-4.25	-1.29	-40.07	-11.164	-14.754	-1.98	-3.98	-2.787	-5.502	-7.728	-0.266	-2.861	-24.152
	σ	36.07	75.12	43.81	51.52	21.77	36.77	5.433	7.373	5.836	17.590	8.504	4.580	4.649	19.478
	Max	113	-162	-128	-143	-82	-95	-20	-23	-29	-66	-22	-8	-17	-57
	Time	595800	309800	844500	340800	837400	346400	860300	271400	350600	345400	922800	704800	493400	410600
71. ksynp53mRNAAbeta	μ	39.30	5.37	11.49	-22.54	4.29	-10.028	0.702	-2.37	3.086	-5.861	1.429	-9.313	2.274	-19.930
	σ	42.76	63.77	36.90	51.63	22.85	32.60	5.326	7.441	5.968	17.291	2.425	7.543	4.276	18.555
	Max	189	211	134	-143	85	-99	17	-23	24	-66	6	-22	15	-57
	Time	397400	924700	931000	340800	934200	325400	924500	336300	255700	345400	644700	761400	424900	410600

72. ksynTau	μ	**20.04**	**-49.60**	**-4.42**	**-55.48**	**-3.384**	**-33.591**	**-0.05**	**-8.09**	**-0.899**	**-2.146**	**-4.740**	**-8.712**	**2.264**	**-5.666**
	σ	**49.68**	**47.74**	**36.79**	**36.37**	**24.69**	**26.60**	**5.969**	**6.814**	**2.907**	**5.170**	**6.938**	**9.123**	**3.682**	**5.143**
	Max	**173**	**-171**	**-99**	**-143**	**-90**	**-105**	**-17**	**-23**	**-19**	**-25**	**-18**	**-24**	**15**	**-18**
	Time	**370600**	**829200**	**750200**	**340800**	**669900**	**426900**	**271300**	**766000**	**339200**	**345400**	**1017900**	**922800**	**596600**	**871000**
ktangfor	μ	**158.03**	**177.51**	**13.76**	**24.83**	**45.46**	**51.67**	**7.165**	**7.705**	**11.020**	**11.308**	**29.323**	**22.189**	**6.161**	**2.309**
	σ	**75.89**	**69.06**	**32.15**	**30.26**	**25.19**	**26.22**	**5.390**	**6.135**	**19.691**	**18.683**	**16.417**	**11.318**	**5.868**	**4.343**
	Max	**379**	**353**	**93**	**106**	**128**	**128**	**26**	**27**	**62**	**61**	**58**	**42**	**23**	**19**
	Time	**1026600**	**456900**	**137100**	**129700**	**52700**	**52700**	**389700**	**653100**	**239800**	**264000**	**900400**	**1012600**	**605400**	**431600**

Appendix D GSA Results

This appendix includes results of LHS/PRCC for all the selected species in response to all parameters.

- Table D.1 includes LHS/PRCC results for p53 in response to the LHS parameters using ODEs.
- Table D.2 includes LHS/PRCC results for p53 in response to the LHS parameters using MRM/GSSA.
- Table D.3 includes LHS/PRCC results for ATMA in response to the LHS parameters using ODEs.
- Table D.4 includes LHS/PRCC results for ATMA in response to the LHS parameters using MRM/GSSA.
- Table D.5 includes LHS/PRCC results for p53_GSK3β in response to the LHS parameters using ODEs.
- Table D.6 includes LHS/PRCC results for p53_GSK3β in response to the LHS parameters using MRM/GSSA.
- Table D.7 includes LHS/PRCC results for Aβ in response to the LHS parameters using ODEs.
- Table D.8 includes LHS/PRCC results for Aβ in response to the LHS parameters using MRM/GSSA.
- Table D.9 includes LHS/PRCC results for plaques in response to the LHS parameters using ODEs.
- Table D.10 includes LHS/PRCC results for plaques in response to the LHS parameters using MRM/GSSA.
- Table D.11 includes LHS/PRCC results for tangles in response to the LHS parameters using ODEs.
- Table D.12 includes LHS/PRCC results for tangles in response to the LHS parameters using MRM/GSSA.
- Table D.13 includes LHS/PRCC results for GilaA in response to the LHS parameters using ODEs.
- Table D.14 includes LHS/PRCC results for GilaA in response to the LHS parameters using MRM/GSSA.

Table D.1: Output from PRCC Analysis for p53 using ODEs

index	Parameter names	Day #4		Day #8		Day #12		index	Parameter names	Day #4		Day #8		Day #12	
		PRCC	p-value	PRCC	p-value	PRCC	p-value			PRCC	p-value	PRCC	p-value	PRCC	p-value
1	kactATM	0.109	0.276	-0.106	0.290	-0.027	0.785	38	kgenROSPlaque	0.120	0.231	-0.071	0.480	-0.086	0.391
2	kactDUBMdm2	0.004	0.968	0.073	0.463	0.004	0.965	39	kinactATM	0.210	0.034	-0.092	0.356	-0.008	0.939
3	kactDUBp53	-0.066	0.512	0.088	0.377	0.010	0.922	40	kinactglia1	-0.168	0.090	0.210	0.034	-0.094	0.346
4	kactDUBProtp53	-0.099	0.320	-0.169	0.090	0.049	0.623	41	kinactglia2	-0.035	0.725	-0.001	0.993	0.026	0.798
5	kactglia1	0.025	0.805	-0.016	0.869	-0.057	0.569	42	kinhibprot	0.091	0.364	-0.057	0.566	-0.038	0.705
6	Kactglia2	0.028	0.782	-0.020	0.842	-0.118	0.236	43	kMdm2PolyUb	0.069	0.491	-0.244	0.014	0.026	0.799
7	kaggAbeta	-0.047	0.636	0.072	0.471	0.098	0.327	44	kMdm2PUb	0.013	0.895	-0.123	0.220	-0.139	0.163
8	kaggTau	0.064	0.523	0.016	0.870	0.239	0.016	45	kMdm2Ub	0.018	0.858	0.023	0.820	-0.045	0.653
9	kaggTauP1	-0.041	0.679	-0.016	0.870	-0.239	0.016	46	kp53PolyUb	0.027	0.790	0.192	0.053	-0.086	0.388
10	kaggTauP2	0.062	0.537	-0.052	0.605	0.027	0.787	47	kp53Ub	-0.033	0.743	-0.159	0.110	-0.048	0.634
11	kbinAbantiAb	0.088	0.381	-0.161	0.107	0.152	0.127	48	kpf	0.242	0.014	-0.007	0.945	0.048	0.631
12	kbinAbetaGlia	-0.311	0.001	0.024	0.807	-0.069	0.492	49	kpg	-0.136	0.173	-0.048	0.635	0.006	0.953
13	kbinE1Ub	0.146	0.142	-0.080	0.425	-0.070	0.485	50	kpghalf	0.254	0.010	0.021	0.836	0.133	0.181
14	kbinE2Ub	0.089	0.376	-0.052	0.605	0.226	0.023	51	kphosMdm2	-0.173	0.082	-0.051	0.609	0.046	0.647
15	kbinGSK3bp53	0.044	0.661	-0.225	0.023	-0.087	0.385	52	kphosMdm2GSK3b	-0.017	0.866	-0.175	0.079	-0.123	0.218
16	kbinMdm2p53	-0.070	0.483	0.027	0.784	-0.287	0.003	53	kphosMdm2GSK3bp53	0.020	0.842	0.050	0.619	-0.021	0.837
17	kbinMTTau	-0.036	0.718	-0.060	0.548	0.050	0.615	54	kphosp53	-0.058	0.559	0.002	0.983	0.113	0.260
18	kbinProt	-0.045	0.654	0.062	0.537	-0.002	0.981	55	kphospTauGSK3b	-0.002	0.986	0.050	0.618	0.117	0.240
19	kbinTauProt	0.076	0.446	-0.074	0.457	-0.013	0.898	56	kphospTauGSK3bp53	0.043	0.666	0.038	0.704	-0.159	0.110
20	kdam	-0.182	0.067	0.134	0.180	0.045	0.655	57	kprodAbeta	-0.019	0.852	0.045	0.654	-0.029	0.773
21	kdamROS	0.204	0.039	0.170	0.088	0.051	0.609	58	kprodAbeta2	-0.020	0.843	-0.009	0.927	-0.052	0.603
22	kdegAbeta	-0.025	0.806	0.035	0.728	-0.086	0.389	59	kproteff	0.137	0.169	0.005	0.959	-0.019	0.849
23	kdegAbetaGlia	0.011	0.910	-0.053	0.599	-0.031	0.756	60	krelAbetaGlia	-0.137	0.169	-0.128	0.200	0.073	0.467
24	kdegAntiAb	-0.060	0.552	-0.032	0.751	0.108	0.278	61	krelGSK3bp53	0.087	0.386	0.137	0.171	0.120	0.229
25	kdegMdm2	0.069	0.489	0.107	0.284	-0.088	0.378	62	krelMdm2p53	0.038	0.703	-0.046	0.645	-0.014	0.890
26	kdegMdm2mRNA	-0.044	0.660	-0.072	0.474	0.034	0.735	63	krelMTTau	-0.049	0.626	-0.146	0.144	-0.139	0.163
27	kdegp53	-0.028	0.782	0.132	0.186	0.010	0.921	64	kremROS	0.041	0.679	-0.016	0.871	0.108	0.281
28	kdegp53mRNA	-0.127	0.203	-0.178	0.074	-0.095	0.343	65	krepair	0.164	0.099	0.012	0.902	0.028	0.783
29	kdegTau20SProt	-0.186	0.061	0.051	0.609	0.182	0.067	66	ksynMdm2	-0.004	0.967	-0.003	0.977	0.292	0.003
30	kdephosMdm2	-0.045	0.653	-0.008	0.939	0.054	0.588	67	ksynMdm2mRNA	-0.162	0.104	0.133	0.182	-0.156	0.118
31	kdephosp53	-0.058	0.561	-0.059	0.554	-0.019	0.847	68	ksynMdm2mRNAGSK3bp	-0.031	0.758	0.024	0.809	-0.038	0.708
32	kdephospTau	0.001	0.996	0.069	0.489	0.005	0.959	69	ksynp53	0.075	0.453	-0.101	0.311	0.069	0.490
33	kdisaggAbeta	0.049	0.625	-0.005	0.959	-0.072	0.469	70	ksynp53mRNA	-0.043	0.671	-0.009	0.926	0.044	0.658
34	kdisaggAbeta1	0.114	0.254	-0.164	0.099	-0.116	0.247	71	ksynp53mRNAAbeta	0.124	0.216	-0.171	0.085	0.176	0.076
35	kdisaggAbeta2	-0.114	0.254	0.277	0.005	0.119	0.234	72	ksynTau	0.063	0.532	-0.119	0.233	0.095	0.342
36	kgenROSAbeta	-0.051	0.609	0.060	0.548	-0.082	0.413	73	ktangfor	-0.45	0.651	-0.36	0.751	-0.003	0.979
37	kgenROSGlia	-0.118	0.237	-0.083	0.407	0.199	0.045								

Table D.2: Output from PRCC Analysis for p53 using MRM/GSSA

index	Parameter names	Day #4		Day #8		Day #12		index	Parameter names	Day #4		Day #8		Day #12	
		PRCC	p-value	PRCC	p-value	PRCC	p-value			PRCC	p-value	PRCC	p-value	PRCC	p-value
1	kactATM	-0.174	0.081	-0.119	0.234	0.026	0.792	38	kgenROSPlaque	-0.088	0.376	-0.067	0.503	0.068	0.499
2	kactDUBMdm2	-0.011	0.910	0.127	0.202	0.060	0.548	39	kinactATM	-0.003	0.973	-0.095	0.345	0.032	0.753
3	kactDUBp53	0.058	0.566	0.069	0.493	-0.041	0.685	40	kinactglia1	-0.017	0.864	-0.051	0.608	-0.065	0.515
4	kactDUBProtp53	0.020	0.844	0.002	0.982	0.048	0.630	41	kinactglia2	-0.157	0.116	0.035	0.730	0.046	0.644
5	kactglia1	-0.174	0.081	-0.079	0.429	0.089	0.371	42	kinhibprot	0.007	0.945	-0.041	0.686	-0.027	0.785
6	Kactglia2	-0.063	0.531	-0.156	0.117	-0.118	0.237	43	kMdm2PolyUb	0.028	0.778	-0.070	0.485	-0.071	0.476
7	kaggAbeta	-0.037	0.709	-0.028	0.780	0.153	0.124	44	kMdm2PUb	-0.134	0.179	0.023	0.821	-0.092	0.358
8	kaggTau	0.167	0.094	0.081	0.419	0.114	0.253	45	kMdm2Ub	0.066	0.508	0.046	0.649	-0.076	0.447
9	kaggTauP1	-0.167	0.094	-0.081	0.419	-0.114	0.253	46	kp53PolyUb	-0.153	0.124	-0.010	0.923	-0.131	0.188
10	kaggTauP2	-0.047	0.642	-0.154	0.123	0.068	0.499	47	kp53Ub	0.083	0.406	-0.058	0.562	0.130	0.194
11	kbinAbantiAb	0.157	0.114	0.247	0.012	0.059	0.558	48	kpf	-0.120	0.230	-0.004	0.965	-0.156	0.117
12	kbinAbetaGlia	-0.054	0.590	-0.017	0.864	0.063	0.532	49	kpg	0.067	0.501	-0.050	0.619	0.131	0.188
13	kbinE1Ub	-0.023	0.817	-0.064	0.525	-0.014	0.889	50	kpghalf	0.144	0.148	0.141	0.157	0.155	0.120
14	kbinE2Ub	0.168	0.091	0.098	0.329	0.038	0.703	51	kphosMdm2	-0.078	0.436	0.018	0.856	0.010	0.922
15	kbinGSK3bp53	-0.048	0.635	-0.079	0.430	-0.147	0.142	52	kphosMdm2GSK3b	-0.168	0.092	-0.037	0.715	-0.029	0.771
16	kbinMdm2p53	-0.265	0.007	-0.018	0.854	-0.271	0.006	53	kphosMdm2GSK3bp53	-0.045	0.653	-0.054	0.591	0.126	0.206
17	kbinMTTau	-0.003	0.979	0.103	0.303	0.024	0.807	54	kphosp53	-0.022	0.828	0.169	0.089	0.037	0.713
18	kbinProt	-0.024	0.810	0.091	0.361	-0.100	0.318	55	kphospTauGSK3b	-0.007	0.945	-0.039	0.698	0.069	0.488
19	kbinTauProt	0.003	0.979	-0.029	0.769	-0.090	0.366	56	kphospTauGSK3bp53	-0.042	0.677	-0.082	0.413	-0.054	0.588
20	kdam	0.058	0.561	-0.038	0.704	0.075	0.453	57	kprodAbeta	0.023	0.817	0.039	0.697	-0.129	0.195
21	kdamROS	-0.140	0.162	-0.005	0.959	-0.079	0.433	58	kprodAbeta2	0.011	0.912	-0.098	0.328	0.023	0.822
22	kdegAbeta	-0.007	0.942	0.004	0.967	0.060	0.548	59	kproteff	-0.098	0.328	0.092	0.356	-0.080	0.425
23	kdegAbetaGlia	-0.003	0.972	-0.044	0.659	0.039	0.697	60	krelAbetaGlia	-0.027	0.785	0.067	0.506	0.154	0.123
24	kdegAntiAb	0.085	0.395	-0.048	0.630	0.077	0.441	61	krelGSK3bp53	0.134	0.178	0.095	0.341	0.070	0.485
25	kdegMdm2	0.013	0.895	0.005	0.959	0.013	0.899	62	krelMdm2p53	0.161	0.106	0.035	0.730	-0.010	0.924
26	kdegMdm2mRNA	0.086	0.393	-0.035	0.729	-0.022	0.828	63	krelMTTau	-0.051	0.612	-0.083	0.404	-0.079	0.431
27	kdegp53	0.110	0.270	0.000	0.997	0.026	0.794	64	kremROS	0.230	0.020	0.070	0.486	0.051	0.612
28	kdegp53mRNA	-0.024	0.808	0.008	0.935	-0.048	0.629	65	krepair	0.038	0.701	-0.150	0.134	0.050	0.618
29	kdegTau20SProt	0.177	0.074	0.153	0.125	0.165	0.098	66	ksynMdm2	0.298	0.002	0.004	0.969	0.127	0.202
30	kdephosMdm2	0.145	0.145	0.030	0.763	0.004	0.968	67	ksynMdm2mRNA	-0.111	0.265	0.005	0.959	-0.143	0.152
31	kdephosp53	0.034	0.738	0.000	0.998	-0.063	0.529	68	ksynMdm2mRNAGSK3bp	-0.119	0.235	0.168	0.091	0.144	0.149
32	kdephospTau	-0.072	0.475	-0.075	0.454	-0.026	0.799	69	ksynp53	-0.009	0.929	0.041	0.682	-0.062	0.539
33	kdisaggAbeta	-0.055	0.586	0.042	0.676	0.043	0.667	70	ksynp53mRNA	-0.008	0.936	-0.137	0.171	0.063	0.531
34	kdisaggAbeta1	-0.015	0.883	0.109	0.277	-0.095	0.344	71	ksynp53mRNAAbeta	0.080	0.425	0.219	0.027	0.090	0.368
35	kdisaggAbeta2	0.121	0.227	-0.044	0.660	0.109	0.274	72	ksynTau	0.080	0.424	0.097	0.332	-0.082	0.414
36	kgenROSAbeta	-0.043	0.669	-0.109	0.275	-0.247	0.012	73	ktangfor	-0.132	0.184	-0.114	0.253	0.038	0.708
37	kgenROSGlia	0.134	0.178	0.020	0.840	0.088	0.381								

Table D.3: Output from PRCC Analysis for ATMA using ODEs

index	Parameter names	Day #4		Day #8		Day #12		index	Parameter names	Day #4		Day #8		Day #12	
		PRCC	p-valu	PRCC	p-valu	PRCC	p-valu			PRCC	p-valu	PRCC	p-valu	PRCC	p-valu
1	kactATM	-0.005	0.964	-0.040	0.690	-0.041	0.682	38	kgenROSPlaque	-0.081	0.421	-0.096	0.339	-0.090	0.369
2	kactDUBMdm2	0.030	0.768	0.003	0.976	0.005	0.959	39	kinactATM	-0.008	0.938	-0.016	0.873	-0.018	0.859
3	kactDUBp53	0.017	0.864	0.045	0.657	0.045	0.652	40	kinactglia1	-0.093	0.351	-0.065	0.519	-0.066	0.508
4	kactDUBProtp53	0.047	0.640	0.037	0.713	0.040	0.687	41	kinactglia2	0.023	0.819	0.001	0.995	0.003	0.977
5	kactglia1	-0.028	0.781	-0.076	0.447	-0.075	0.452	42	kinhibprot	-0.058	0.560	-0.036	0.720	-0.038	0.707
6	Kactglia2	-0.162	0.103	-0.147	0.140	-0.142	0.155	43	kMdm2PolyUb	0.029	0.770	0.017	0.869	0.016	0.875
7	kaggAbeta	0.097	0.332	0.098	0.328	0.100	0.318	44	kMdm2PUb	-0.131	0.188	-0.123	0.219	-0.124	0.213
8	kaggTau	0.240	0.015	0.223	0.024	0.222	0.025	45	kMdm2Ub	-0.047	0.640	-0.072	0.470	-0.073	0.465
9	kaggTauP1	-0.240	0.015	-0.223	0.024	-0.222	0.025	46	kp53PolyUb	-0.096	0.337	-0.104	0.297	-0.109	0.276
10	kaggTauP2	0.013	0.900	-0.014	0.887	-0.011	0.912	47	kp53Ub	-0.093	0.355	-0.043	0.671	-0.041	0.680
11	kbinAbantiAb	0.167	0.093	0.172	0.084	0.173	0.082	48	kpf	0.056	0.575	0.014	0.888	0.015	0.878
12	kbinAbetaGlia	-0.062	0.538	-0.065	0.517	-0.068	0.499	49	kpg	-0.001	0.988	0.049	0.628	0.050	0.618
13	kbinE1Ub	0.228	0.021	0.218	0.027	0.223	0.025	50	kpghalf	0.133	0.181	0.140	0.160	0.137	0.170
14	kbinE2Ub	-0.060	0.551	-0.074	0.459	-0.070	0.485	51	kphosMdm2	0.046	0.647	0.040	0.687	0.043	0.667
15	kbinGSK3bp53	-0.110	0.270	-0.080	0.424	-0.084	0.401	52	kphosMdm2GSK3b	-0.121	0.227	-0.099	0.320	-0.097	0.334
16	kbinMdm2p53	-0.501	0.002	-0.508	0.009	-0.560	0.008	53	kphosMdm2GSK3bp53	-0.061	0.541	-0.037	0.715	-0.037	0.715
17	kbinMTTau	0.062	0.538	0.019	0.848	0.014	0.886	54	kphosp53	0.080	0.423	0.103	0.302	0.109	0.274
18	kbinProt	0.009	0.929	-0.006	0.954	-0.005	0.960	55	kphospTauGSK3b	0.134	0.180	0.140	0.161	0.138	0.168
19	kbinTauProt	-0.008	0.935	-0.005	0.958	-0.012	0.903	56	kphospTauGSK3bp53	-0.179	0.071	-0.152	0.127	-0.151	0.130
20	kdam	0.074	0.462	0.055	0.581	0.058	0.561	57	kprodAbeta	-0.045	0.655	0.003	0.976	0.003	0.974
21	kdamROS	0.042	0.674	0.040	0.686	0.038	0.703	58	kprodAbeta2	-0.052	0.602	-0.040	0.691	-0.040	0.690
22	kdegAbeta	-0.084	0.404	-0.037	0.711	-0.037	0.715	59	kproteff	0.001	0.993	0.008	0.935	0.014	0.889
23	kdegAbetaGlia	-0.043	0.670	-0.053	0.594	-0.050	0.617	60	krelAbetaGlia	0.097	0.331	0.075	0.453	0.073	0.465
24	kdegAntiAb	0.115	0.251	0.109	0.277	0.115	0.250	61	krelGSK3bp53	0.121	0.226	0.118	0.239	0.117	0.242
25	kdegMdm2	-0.090	0.366	-0.077	0.444	-0.079	0.433	62	krelMdm2p53	0.016	0.870	-0.033	0.743	-0.037	0.711
26	kdegMdm2mRNA	0.054	0.588	0.045	0.651	0.041	0.681	63	krelMTTau	-0.164	0.099	-0.166	0.096	-0.166	0.095
27	kdegp53	0.009	0.925	0.038	0.702	0.037	0.716	64	kremROS	0.139	0.164	0.121	0.225	0.123	0.219
28	kdegp53mRNA	-0.093	0.352	-0.082	0.414	-0.077	0.439	65	krepair	0.063	0.529	0.008	0.932	0.006	0.954
29	kdegTau20SProt	0.199	0.045	0.199	0.045	0.198	0.046	66	ksynMdm2	0.285	0.004	0.269	0.006	0.268	0.006
30	kdephosMdm2	0.086	0.388	0.007	0.945	0.008	0.938	67	ksynMdm2mRNA	-0.134	0.179	-0.152	0.127	-0.147	0.139
31	kdephosp53	-0.044	0.658	0.032	0.753	0.025	0.805	68	ksynMdm2mRNAGSK3bp5	-0.043	0.669	-0.032	0.750	-0.035	0.725
32	kdephospTau	-0.002	0.987	0.004	0.971	0.007	0.944	69	ksynp53	0.079	0.430	0.033	0.744	0.033	0.739
33	kdisaggAbeta	-0.073	0.463	-0.063	0.528	-0.071	0.478	70	ksynp53mRNA	0.047	0.642	0.026	0.796	0.025	0.802
34	kdisaggAbeta1	-0.122	0.222	-0.114	0.255	-0.115	0.248	71	ksynp53mRNAAbeta	0.139	0.163	0.174	0.081	0.175	0.078
35	kdisaggAbeta2	0.105	0.292	0.131	0.190	0.133	0.184	72	ksynTau	0.076	0.449	0.122	0.221	0.112	0.261
36	kgenROSAbeta	-0.116	0.247	-0.072	0.472	-0.069	0.488	73	ktangfor	-0.042	0.672	-0.046	0.649	-0.044	0.660
37	kgenROSGlia	0.222	0.025	0.154	0.123	0.152	0.126								

Table B.4: Output from PRCC Analysis for ATMA using MRM/GSSA

index	Parameter names	Day #4		Day #8		Day #12		index	Parameter names	Day #4		Day #8		Day #12	
		PRCC	p-value	PRCC	p-value	PRCC	p-value			PRCC	p-value	PRCC	p-value	PRCC	p-value
1	kactATM	-0.037	0.709	-0.016	0.871	0.093	0.351	38	kgenROSPlaque	-0.105	0.292	-0.100	0.317	0.011	0.915
2	kactDUBMdm2	0.039	0.700	0.086	0.390	-0.057	0.568	39	kinactATM	-0.124	0.215	-0.126	0.205	0.010	0.918
3	kactDUBp53	-0.038	0.702	0.010	0.917	-0.044	0.663	40	kinactglia1	-0.192	0.053	0.014	0.887	-0.067	0.506
4	kactDUBProtp53	0.068	0.498	-0.072	0.472	0.067	0.503	41	kinactglia2	-0.065	0.517	-0.013	0.894	0.094	0.349
5	kactglia1	-0.231	0.019	-0.032	0.752	0.141	0.156	42	kinhibprot	0.002	0.986	0.142	0.153	0.020	0.839
6	Kactglia2	0.064	0.526	-0.148	0.137	-0.148	0.139	43	kMdm2PolyUb	-0.008	0.937	0.032	0.747	0.012	0.906
7	kaggAbeta	0.030	0.767	-0.169	0.089	0.023	0.818	44	kMdm2PUb	-0.028	0.777	0.084	0.401	-0.086	0.388
8	kaggTau	0.173	0.081	0.064	0.521	0.143	0.151	45	kMdm2Ub	-0.021	0.837	-0.293	0.014	-0.034	0.734
9	kaggTauP1	-0.173	0.081	-0.064	0.521	-0.143	0.151	46	kp53PolyUb	-0.132	0.185	-0.059	0.556	-0.180	0.070
10	kaggTauP2	-0.023	0.822	-0.070	0.482	0.133	0.181	47	kp53Ub	-0.107	0.286	-0.012	0.905	0.045	0.653
11	kbinAbantiAb	0.106	0.287	0.050	0.616	0.123	0.217	48	kpf	-0.024	0.812	-0.067	0.503	-0.079	0.433
12	kbinAbetaGlia	0.056	0.577	-0.111	0.265	-0.022	0.824	49	kpg	0.045	0.654	0.179	0.072	0.064	0.523
13	kbinE1Ub	-0.071	0.481	-0.162	0.103	-0.076	0.446	50	kpghalf	0.150	0.132	0.137	0.169	0.128	0.199
14	kbinE2Ub	0.094	0.347	0.002	0.986	0.117	0.241	51	kphosMdm2	-0.157	0.115	0.078	0.439	0.081	0.420
15	kbinGSK3bp53	-0.113	0.258	-0.093	0.351	-0.172	0.083	52	kphosMdm2GSK3b	-0.137	0.169	0.003	0.974	-0.137	0.169
16	kbinMdm2p53	-0.139	0.165	-0.034	0.737	-0.069	0.490	53	kphosMdm2GSK3bp53	0.036	0.717	0.168	0.091	0.030	0.768
17	kbinMTTau	0.025	0.802	-0.094	0.346	-0.030	0.765	54	kphosp53	0.050	0.619	-0.036	0.716	0.025	0.801
18	kbinProt	0.069	0.493	0.065	0.518	-0.004	0.969	55	kphospTauGSK3b	0.032	0.746	0.023	0.818	0.106	0.290
19	kbinTauProt	0.021	0.838	-0.199	0.044	-0.052	0.603	56	kphospTauGSK3bp53	-0.120	0.228	-0.035	0.728	-0.128	0.201
20	kdam	0.063	0.532	-0.044	0.660	0.197	0.047	57	kprodAbeta	0.143	0.151	0.109	0.275	-0.098	0.328
21	kdamROS	-0.063	0.531	-0.119	0.233	-0.015	0.879	58	kprodAbeta2	-0.027	0.786	-0.190	0.056	-0.070	0.482
22	kdegAbeta	-0.059	0.558	0.012	0.906	0.056	0.575	59	kproteff	0.023	0.820	-0.069	0.488	-0.071	0.475
23	kdegAbetaGlia	0.076	0.450	-0.006	0.955	-0.111	0.269	60	krelAbetaGlia	0.002	0.983	-0.046	0.644	0.156	0.118
24	kdegAntiAb	0.093	0.354	0.055	0.583	0.087	0.387	61	krelGSK3bp53	0.089	0.374	0.192	0.054	0.148	0.136
25	kdegMdm2	-0.011	0.915	0.072	0.475	-0.006	0.953	62	krelMdm2p53	0.109	0.274	0.032	0.749	0.045	0.654
26	kdegMdm2mRNA	0.030	0.768	-0.008	0.939	-0.083	0.407	63	krelMTTau	-0.032	0.749	0.039	0.696	-0.006	0.952
27	kdegp53	0.091	0.361	-0.038	0.707	0.067	0.507	64	kremROS	0.174	0.079	-0.091	0.364	-0.058	0.562
28	kdegp53mRNA	-0.168	0.091	0.024	0.814	-0.216	0.029	65	krepair	0.074	0.459	-0.209	0.035	-0.067	0.504
29	kdegTau20SProt	0.221	0.025	-0.046	0.644	0.199	0.045	66	ksynMdm2	0.265	0.007	-0.034	0.737	0.071	0.478
30	kdephosMdm2	0.073	0.465	-0.058	0.564	-0.092	0.356	67	ksynMdm2mRNA	-0.069	0.489	0.108	0.278	-0.083	0.408
31	kdephosp53	-0.065	0.518	-0.005	0.962	0.116	0.246	68	ksynMdm2mRNAGSK3b	0.013	0.899	0.094	0.350	0.171	0.086
32	kdephospTau	-0.068	0.494	-0.066	0.512	0.021	0.832	69	ksynp53	-0.077	0.442	0.072	0.474	0.048	0.632
33	kdisaggAbeta	-0.073	0.464	0.178	0.073	0.025	0.802	70	ksynp53mRNA	0.002	0.988	-0.141	0.158	-0.172	0.084
34	kdisaggAbeta1	-0.004	0.969	0.162	0.104	-0.011	0.914	71	ksynp53mRNAAbeta	0.009	0.926	0.178	0.073	0.220	0.026
35	kdisaggAbeta2	0.077	0.445	-0.054	0.591	-0.033	0.739	72	ksynTau	0.080	0.423	0.210	0.034	0.061	0.543
36	kgenROSAbeta	-0.088	0.380	0.065	0.515	-0.123	0.220	73	ktangfor	-0.013	0.896	0.008	0.932	-0.060	0.552
37	kgenROSGlia	0.140	0.161	0.034	0.735	0.015	0.884								

Table B.5: Output from PRCC Analysis for p53_GSK3β using ODEs

index	Parameter names	Day #4		Day #8		Day #12		index	Parameter names	Day #4		Day #8		Day #12	
		PRCC	p-value	PRCC	p-value	PRCC	p-value			PRCC	p-value	PRCC	p-value	PRCC	p-value
1	kactATM	-0.019	0.852	-0.047	0.642	-0.047	0.642	38	kgenROSPlaque	-0.094	0.350	-0.099	0.321	-0.100	0.320
2	kactDUBMdm2	0.013	0.893	0.000	0.999	0.004	0.971	39	kinactATM	-0.003	0.980	-0.015	0.884	-0.016	0.871
3	kactDUBp53	0.010	0.924	0.043	0.670	0.042	0.674	40	kinactglia1	-0.093	0.350	-0.076	0.448	-0.076	0.445
4	kactDUBProtp53	0.045	0.655	0.048	0.633	0.048	0.630	41	kinactglia2	0.025	0.802	0.015	0.884	0.014	0.892
5	kactglia1	-0.056	0.577	-0.081	0.419	-0.082	0.414	42	kinhibprot	-0.045	0.656	-0.038	0.703	-0.040	0.687
6	Kactglia2	-0.129	0.197	-0.135	0.177	-0.134	0.179	43	kMdm2PolyUb	0.030	0.763	0.020	0.842	0.019	0.846
7	kaggAbeta	0.100	0.315	0.101	0.310	0.101	0.310	44	kMdm2PUb	-0.132	0.186	-0.125	0.211	-0.120	0.228
8	kaggTau	0.231	0.020	0.228	0.021	0.229	0.021	45	kMdm2Ub	-0.045	0.651	-0.069	0.492	-0.069	0.493
9	kaggTauP1	-0.231	0.020	-0.228	0.021	-0.229	0.021	46	kp53PolyUb	-0.083	0.406	-0.107	0.286	-0.109	0.274
10	kaggTauP2	0.023	0.820	-0.005	0.962	-0.005	0.960	47	kp53Ub	-0.065	0.518	-0.041	0.680	-0.041	0.684
11	kbinAbantiAb	0.159	0.111	0.162	0.104	0.162	0.103	48	kpf	0.045	0.657	0.017	0.865	0.017	0.867
12	kbinAbetaGlia	-0.066	0.507	-0.071	0.476	-0.072	0.469	49	kpg	0.007	0.942	0.044	0.663	0.044	0.660
13	kbinE1Ub	-0.070	0.486	-0.075	0.451	-0.075	0.455	50	kpghalf	0.133	0.181	0.137	0.170	0.137	0.170
14	kbinE2Ub	0.620	0.002	0.232	0.019	0.232	0.019	51	kphosMdm2	0.050	0.617	0.046	0.647	0.046	0.647
15	kbinGSK3bp53	0.671	4.2E-	-0.077	0.439	-0.077	0.444	52	kphosMdm2GSK3b	-0.120	0.231	-0.106	0.287	-0.104	0.297
16	kbinMdm2p53	-0.592	0.0016	-0.262	0.008	-0.262	0.008	53	kphosMdm2GSK3bp53	-0.024	0.809	-0.030	0.763	-0.030	0.766
17	kbinMTTau	0.057	0.572	0.026	0.798	0.024	0.811	54	kphosp53	0.104	0.300	0.110	0.270	0.111	0.269
18	kbinProt	0.006	0.954	-0.007	0.948	-0.011	0.914	55	kphospTauGSK3b	0.128	0.199	0.138	0.166	0.139	0.163
19	kbinTauProt	-0.010	0.921	-0.009	0.930	-0.010	0.922	56	kphospTauGSK3bp53	-0.160	0.109	-0.157	0.116	-0.155	0.121
20	kdam	0.046	0.650	0.056	0.576	0.056	0.576	57	kprodAbeta	-0.025	0.805	0.000	1.000	0.001	0.994
21	kdamROS	0.047	0.642	0.045	0.653	0.044	0.657	58	kprodAbeta2	-0.054	0.588	-0.039	0.701	-0.039	0.701
22	kdegAbeta	-0.086	0.393	-0.051	0.613	-0.051	0.613	59	kproteff	-0.016	0.870	0.003	0.976	0.006	0.956
23	kdegAbetaGlia	-0.040	0.686	-0.052	0.602	-0.053	0.599	60	krelAbetaGlia	0.088	0.381	0.082	0.415	0.084	0.400
24	kdegAntiAb	0.105	0.295	0.106	0.288	0.108	0.280	61	krelGSK3bp53	0.113	0.258	0.112	0.261	0.112	0.261
25	kdegMdm2	-0.088	0.380	-0.078	0.434	-0.076	0.446	62	krelMdm2p53	-0.004	0.965	-0.029	0.776	-0.028	0.782
26	kdegMdm2mRNA	0.042	0.676	0.041	0.685	0.043	0.666	63	krelMTTau	-0.148	0.137	-0.167	0.094	-0.168	0.091
27	kdegp53	0.013	0.894	0.040	0.688	0.039	0.695	64	kremROS	0.111	0.265	0.117	0.240	0.114	0.252
28	kdegp53mRNA	-0.094	0.348	-0.085	0.397	-0.086	0.390	65	krepair	0.032	0.751	0.007	0.945	0.005	0.962
29	kdegTau20SProt	0.184	0.064	0.198	0.046	0.197	0.047	66	ksynMdm2	0.288	0.003	0.264	0.007	0.264	0.007
30	kdephosMdm2	0.042	0.674	0.009	0.928	0.008	0.938	67	ksynMdm2mRNA	-0.159	0.111	-0.149	0.135	-0.151	0.131
31	kdephosp53	-0.011	0.911	0.026	0.796	0.025	0.805	68	ksynMdm2mRNAGSK3bp	-0.033	0.741	-0.035	0.731	-0.036	0.718
32	kdephospTau	0.003	0.973	0.003	0.974	0.005	0.961	69	ksynp53	0.064	0.520	0.042	0.673	0.042	0.678
33	kdisaggAbeta	-0.067	0.504	-0.066	0.507	-0.065	0.517	70	ksynp53mRNA	0.042	0.676	0.029	0.769	0.031	0.755
34	kdisaggAbeta1	-0.113	0.256	-0.109	0.277	-0.107	0.284	71	ksynp53mRNAAbeta	0.173	0.082	0.179	0.071	0.180	0.071
35	kdisaggAbeta2	0.111	0.265	0.136	0.174	0.136	0.173	72	ksynTau	0.095	0.344	0.115	0.249	0.116	0.248
36	kgenROSAbeta	-0.091	0.361	-0.066	0.508	-0.066	0.507	73	ktangfor	-0.044	0.662	-0.052	0.607	-0.052	0.607
37	kgenROSGlia	0.200	0.044	0.153	0.125	0.151	0.129								

Table B.6: Output from PRCC Analysis for p53_GSK3β using MRM/GSSA

index	Parameter names	Day #4		Day #8		Day #12		index	Parameter names	Day #4		Day #8		Day #12	
		PRCC	p-value	PRCC	p-value	PRCC	p-value			PRCC	p-value	PRCC	p-value	PRCC	p-value
1	kactATM	-0.116	0.244	-0.134	0.179	0.091	0.361	38	kgenROSPlaque	-0.155	0.119	-0.014	0.890	0.035	0.730
2	kactDUBMdm2	-0.031	0.756	0.080	0.422	0.141	0.158	39	kinactATM	-0.060	0.548	-0.180	0.070	-0.001	0.991
3	kactDUBp53	-0.004	0.972	0.137	0.168	-0.061	0.546	40	kinactglia1	0.031	0.761	-0.090	0.368	0.055	0.581
4	kactDUBProtp53	0.046	0.645	0.007	0.944	0.039	0.696	41	kinactglia2	-0.155	0.119	0.022	0.824	0.033	0.742
5	kactglia1	-0.186	0.061	0.008	0.938	0.086	0.391	42	kinhibprot	0.052	0.601	-0.045	0.655	-0.094	0.349
6	Kactglia2	-0.073	0.464	-0.206	0.038	-0.133	0.182	43	kMdm2PolyUb	-0.010	0.924	-0.058	0.565	-0.138	0.167
7	kaggAbeta	-0.034	0.732	-0.103	0.305	0.048	0.631	44	kMdm2PUb	-0.108	0.278	0.004	0.972	-0.057	0.570
8	kaggTau	0.246	0.013	0.100	0.316	0.110	0.273	45	kMdm2Ub	0.098	0.326	0.038	0.706	-0.080	0.424
9	kaggTauP1	-0.246	0.013	-0.100	0.316	-0.110	0.273	46	kp53PolyUb	-0.095	0.341	-0.091	0.363	-0.146	0.142
10	kaggTauP2	-0.014	0.892	-0.136	0.173	0.026	0.794	47	kp53Ub	0.146	0.143	-0.070	0.483	0.151	0.131
11	kbinAbantiAb	0.196	0.048	0.156	0.118	0.064	0.520	48	kpf	-0.104	0.297	0.019	0.847	-0.164	0.099
12	kbinAbetaGlia	-0.117	0.240	0.033	0.739	0.022	0.824	49	kpg	0.128	0.198	-0.030	0.763	0.164	0.100
13	kbinE1Ub	-0.103	0.304	-0.084	0.403	-0.057	0.567	50	kpghalf	0.159	0.110	0.152	0.126	0.156	0.116
14	kbinE2Ub	0.180	0.070	0.043	0.671	0.080	0.422	51	kphosMdm2	-0.093	0.350	0.032	0.746	0.003	0.979
15	kbinGSK3bp53	-0.151	0.129	-0.004	0.969	-0.041	0.684	52	kphosMdm2GSK3b	-0.131	0.189	-0.010	0.922	0.035	0.728
16	kbinMdm2p53	-0.173	0.081	-0.012	0.905	-0.240	0.015	53	kphosMdm2GSK3bp53	-0.011	0.916	0.042	0.673	0.126	0.205
17	kbinMTTau	0.005	0.963	0.065	0.519	0.015	0.882	54	kphosp53	0.004	0.969	0.107	0.284	0.068	0.494
18	kbinProt	-0.029	0.776	0.090	0.366	-0.150	0.132	55	kphospTauGSK3b	-0.043	0.669	0.024	0.813	0.067	0.503
19	kbinTauProt	-0.001	0.995	-0.075	0.451	-0.046	0.649	56	kphospTauGSK3bp53	-0.082	0.410	-0.133	0.184	-0.060	0.547
20	kdam	0.013	0.896	0.048	0.631	0.047	0.641	57	kprodAbeta	0.078	0.434	0.036	0.722	-0.155	0.120
21	kdamROS	-0.217	0.028	-0.055	0.586	-0.052	0.602	58	kprodAbeta2	0.005	0.960	-0.082	0.411	0.063	0.528
22	kdegAbeta	0.046	0.643	-0.015	0.883	0.032	0.749	59	kproteff	-0.122	0.221	0.047	0.637	-0.089	0.373
23	kdegAbetaGlia	0.042	0.676	0.000	1.000	0.016	0.874	60	krelAbetaGlia	-0.027	0.787	0.077	0.444	0.142	0.155
24	kdegAntiAb	0.102	0.310	0.103	0.304	0.043	0.669	61	krelGSK3bp53	0.043	0.664	0.171	0.086	0.030	0.768
25	kdegMdm2	-0.080	0.426	0.019	0.852	0.005	0.956	62	krelMdm2p53	0.115	0.251	0.044	0.658	-0.009	0.930
26	kdegMdm2mRNA	0.006	0.956	-0.035	0.725	0.075	0.451	63	krelMTTau	-0.079	0.432	-0.094	0.348	-0.102	0.308
27	kdegp53	0.111	0.265	-0.024	0.811	0.025	0.803	64	kremROS	0.160	0.107	0.105	0.294	0.073	0.468
28	kdegp53mRNA	-0.063	0.530	0.025	0.804	-0.125	0.210	65	krepair	-0.002	0.983	-0.159	0.110	0.066	0.508
29	kdegTau20SProt	0.191	0.055	0.082	0.411	0.193	0.052	66	ksynMdm2	0.349	3.180E-	0.117	0.243	0.132	0.187
30	kdephosMdm2	0.103	0.302	-0.017	0.865	-0.011	0.911	67	ksynMdm2mRNA	-0.083	0.406	-0.033	0.745	-0.170	0.087
31	kdephosp53	0.058	0.565	-0.028	0.777	-0.026	0.799	68	ksynMdm2mRNAGSK3bp	-0.106	0.290	0.148	0.138	0.168	0.091
32	kdephospTau	-0.026	0.792	-0.069	0.491	0.025	0.806	69	ksynp53	-0.051	0.612	0.089	0.371	-0.096	0.338
33	kdisaggAbeta	0.036	0.717	0.000	0.998	0.035	0.728	70	ksynp53mRNA	0.034	0.734	-0.134	0.179	0.057	0.569
34	kdisaggAbeta1	-0.026	0.792	0.105	0.291	-0.135	0.176	71	ksynp53mRNAAbeta	0.174	0.081	0.214	0.031	0.086	0.391
35	kdisaggAbeta2	0.107	0.286	-0.036	0.720	0.164	0.100	72	ksynTau	0.116	0.244	0.137	0.170	-0.062	0.534
36	kgenROSAbeta	0.009	0.931	-0.136	0.173	-0.211	0.033	73	ktangfor	0.075	0.454	-0.097	0.334	-0.017	0.867
37	kgenROSGlia	0.104	0.296	0.022	0.829	0.019	0.851								

Table B.7: Output from PRCC Analysis for Aβ using ODEs

index	Parameter names	Day #4		Day #8		Day #12		index	Parameter names	Day #4		Day #8		Day #12	
		PRCC	p-value	PRCC	p-value	PRCC	p-value			PRCC	p-value	PRCC	p-value	PRCC	p-value
1	kactATM	-0.029	0.774	-0.047	0.638	-0.050	0.617	38	kgenROSPlaque	-0.084	0.401	-0.100	0.318	-0.097	0.334
2	kactDUBMdm2	0.010	0.920	-0.003	0.977	-0.002	0.987	39	kinactATM	-0.001	0.990	-0.014	0.888	-0.017	0.867
3	kactDUBp53	0.010	0.924	0.038	0.702	0.041	0.685	40	kinactglia1	-0.100	0.319	-0.079	0.428	-0.078	0.435
4	kactDUBProtp53	0.053	0.599	0.051	0.609	0.053	0.599	41	kinactglia2	0.025	0.804	0.015	0.878	0.014	0.891
5	kactglia1	-0.062	0.533	-0.082	0.412	-0.081	0.416	42	kinhibprot	-0.047	0.637	-0.040	0.691	-0.039	0.697
6	Kactglia2	-0.120	0.229	-0.126	0.206	-0.129	0.195	43	kMdm2PolyUb	0.026	0.793	0.019	0.850	0.017	0.868
7	kaggAbeta	0.103	0.302	0.095	0.343	0.096	0.336	44	kMdm2PUb	-0.142	0.155	-0.128	0.200	-0.126	0.207
8	kaggTau	0.234	0.018	0.231	0.019	0.232	0.019	45	kMdm2Ub	-0.047	0.639	-0.061	0.540	-0.066	0.513
9	kaggTauP1	-0.234	0.018	-0.231	0.019	-0.232	0.019	46	kp53PolyUb	-0.085	0.397	-0.110	0.270	-0.116	0.247
10	kaggTauP2	0.033	0.742	0.005	0.958	0.003	0.979	47	kp53Ub	-0.052	0.602	-0.033	0.746	-0.031	0.759
11	kbinAbantiAb	0.151	0.131	0.154	0.121	0.156	0.117	48	kpf	0.044	0.663	0.020	0.841	0.020	0.839
12	kbinAbetaGlia	-0.067	0.505	-0.075	0.452	-0.074	0.458	49	kpg	0.010	0.917	0.050	0.616	0.051	0.614
13	kbinE1Ub	-0.068	0.497	-0.077	0.442	-0.076	0.450	50	kpghalf	0.137	0.170	0.137	0.170	0.133	0.181
14	kbinE2Ub	0.224	0.023	0.237	0.017	0.238	0.016	51	kphosMdm2	0.047	0.637	0.046	0.647	0.045	0.657
15	kbinGSK3bp53	-0.087	0.384	-0.070	0.486	-0.071	0.477	52	kphosMdm2GSK3b	-0.119	0.234	-0.104	0.297	-0.100	0.318
16	kbinMdm2p53	-0.389	0.003	-0.744	2E-05	-0.467	0.007	53	kphosMdm2GSK3bp53	-0.017	0.867	-0.021	0.831	-0.023	0.820
17	kbinMTTau	0.046	0.643	0.019	0.852	0.014	0.890	54	kphosp53	0.110	0.271	0.116	0.246	0.113	0.258
18	kbinProt	0.000	0.997	-0.010	0.924	-0.013	0.899	55	kphospTauGSK3b	0.123	0.220	0.135	0.176	0.137	0.171
19	kbinTauProt	-0.016	0.873	-0.010	0.917	-0.013	0.898	56	kphospTauGSK3bp53	-0.157	0.115	-0.156	0.118	-0.155	0.120
20	kdam	0.047	0.637	0.053	0.599	0.057	0.569	57	kprodAbeta	-0.027	0.786	-0.005	0.958	-0.004	0.970
21	kdamROS	0.050	0.620	0.045	0.650	0.042	0.671	58	kprodAbeta2	-0.056	0.579	-0.037	0.713	-0.036	0.718
22	kdegAbeta	-0.088	0.380	-0.055	0.586	-0.051	0.608	59	kproteff	-0.014	0.886	0.002	0.983	0.006	0.950
23	kdegAbetaGlia	-0.031	0.759	-0.051	0.614	-0.048	0.634	60	krelAbetaGlia	0.080	0.423	0.077	0.441	0.075	0.453
24	kdegAntiAb	0.112	0.262	0.113	0.257	0.118	0.239	61	krelGSK3bp53	0.111	0.268	0.116	0.247	0.112	0.263
25	kdegMdm2	-0.087	0.384	-0.075	0.455	-0.077	0.443	62	krelMdm2p53	-0.006	0.951	-0.029	0.771	-0.031	0.761
26	kdegMdm2mRNA	0.036	0.716	0.040	0.690	0.041	0.686	63	krelMTTau	-0.143	0.151	-0.166	0.095	-0.167	0.094
27	kdegp53	0.010	0.923	0.037	0.716	0.036	0.722	64	kremROS	0.110	0.273	0.108	0.280	0.112	0.261
28	kdegp53mRNA	-0.094	0.349	-0.088	0.382	-0.086	0.389	65	krepair	0.025	0.807	0.004	0.968	-0.001	0.994
29	kdegTau20SProt	0.181	0.069	0.192	0.054	0.192	0.053	66	ksynMdm2	0.388	0.003	0.7911	3.66E-06	0.365	0.007
30	kdephosMdm2	0.052	0.605	0.007	0.940	0.008	0.938	67	ksynMdm2mRNA	-0.159	0.110	-0.160	0.107	-0.157	0.115
31	kdephosp53	-0.024	0.812	0.020	0.845	0.018	0.857	68	ksynMdm2mRNAGSK3bp	-0.036	0.720	-0.038	0.702	-0.039	0.699
32	kdephospTau	0.003	0.975	0.005	0.963	0.007	0.944	69	ksynp53	0.067	0.507	0.046	0.643	0.047	0.639
33	kdisaggAbeta	-0.072	0.473	-0.072	0.475	-0.072	0.469	70	ksynp53mRNA	0.051	0.609	0.039	0.695	0.037	0.713
34	kdisaggAbeta1	-0.118	0.236	-0.105	0.294	-0.104	0.299	71	ksynp53mRNAAbeta	0.174	0.080	0.181	0.069	0.182	0.067
35	kdisaggAbeta2	0.122	0.221	0.139	0.164	0.141	0.158	72	ksynTau	0.092	0.360	0.116	0.247	0.112	0.261
36	kgenROSAbeta	-0.084	0.402	-0.058	0.561	-0.058	0.565	73	ktangfor	-0.038	0.708	-0.048	0.630	-0.047	0.639
37	kgenROSGlia	0.201	0.043	0.157	0.115	0.154	0.122								

Table D.8: Output from PRCC Analysis for Aβ using MRM/GSSA

index	Parameter names	Day #4		Day #8		Day #12		index	Parameter names	Day #4		Day #8		Day #12	
		PRCC	p-value	PRCC	p-value	PRCC	p-value			PRCC	p-value	PRCC	p-value	PRCC	p-value
1	kactATM	-0.209	0.035	0.008	0.938	0.053	0.599	38	kgenROSPlaque	-0.093	0.354	-0.072	0.472	0.004	0.967
2	kactDUBMdm2	0.069	0.490	0.025	0.799	-0.027	0.785	39	kinactATM	0.004	0.972	-0.093	0.351	-0.156	0.117
3	kactDUBp53	-0.006	0.955	-0.106	0.288	-0.015	0.880	40	kinactglia1	-0.136	0.174	-0.086	0.390	-0.008	0.933
4	kactDUBProtp53	0.129	0.197	-0.018	0.861	0.034	0.732	41	kinactglia2	-0.047	0.642	0.193	0.052	0.013	0.897
5	kactglia1	-0.082	0.415	-0.023	0.816	-0.058	0.563	42	kinhibprot	-0.018	0.857	-0.005	0.963	0.082	0.411
6	Kactglia2	-0.039	0.695	0.014	0.893	0.042	0.675	43	kMdm2PolyUb	-0.002	0.981	-0.064	0.524	-3.7E-04	0.997
7	kaggAbeta	0.094	0.347	0.044	0.659	-0.054	0.592	44	kMdm2PUb	0.142	0.154	-0.017	0.868	0.054	0.588
8	kaggTau	0.088	0.378	0.106	0.289	0.080	0.421	45	kMdm2Ub	0.012	0.902	-0.029	0.773	0.036	0.717
9	kaggTauP1	-0.088	0.378	-0.106	0.289	-0.080	0.421	46	kp53PolyUb	-0.146	0.144	0.015	0.878	-0.279	0.004
10	kaggTauP2	0.047	0.637	0.131	0.190	-0.052	0.605	47	kp53Ub	-0.061	0.543	-0.008	0.934	0.094	0.345
11	kbinAbantiAb	0.123	0.218	-0.040	0.687	-0.039	0.700	48	kpf	-0.006	0.952	0.071	0.476	-0.033	0.745
12	kbinAbetaGlia	0.082	0.413	0.042	0.674	-0.151	0.130	49	kpg	0.087	0.384	0.005	0.960	0.079	0.428
13	kbinE1Ub	-0.091	0.363	-0.132	0.186	0.057	0.571	50	kpghalf	0.175	0.079	0.154	0.121	0.161	0.107
14	kbinE2Ub	0.131	0.188	-0.009	0.928	0.099	0.324	51	kphosMdm2	0.003	0.976	0.028	0.782	-0.008	0.939
15	kbinGSK3bp53	-0.127	0.202	-0.070	0.483	-0.066	0.509	52	kphosMdm2GSK3b	-0.176	0.076	-0.030	0.764	-0.050	0.620
16	kbinMdm2p53	-0.430	0.020	-0.70	2.48E-	-0.385	0.003	53	kphosMdm2GSK3bp53	0.045	0.650	0.119	0.234	0.095	0.344
17	kbinMTTau	-0.034	0.735	-0.014	0.886	-0.018	0.859	54	kphosp53	-0.115	0.250	0.120	0.231	-0.006	0.949
18	kbinProt	-0.085	0.394	0.030	0.764	-0.196	0.049	55	kphospTauGSK3b	0.111	0.267	0.009	0.931	-0.103	0.304
19	kbinTauProt	-0.105	0.293	-0.069	0.491	0.015	0.885	56	kphospTauGSK3bp53	-0.046	0.646	-0.202	0.042	-0.095	0.345
20	kdam	0.050	0.615	0.131	0.190	0.141	0.156	57	kprodAbeta	0.052	0.601	-0.065	0.513	-0.026	0.794
21	kdamROS	-0.180	0.070	-0.010	0.923	0.048	0.635	58	kprodAbeta2	-0.010	0.921	-0.030	0.768	0.040	0.689
22	kdegAbeta	-0.140	0.160	-0.139	0.163	0.019	0.846	59	kproteff	-0.115	0.251	-0.039	0.695	-0.116	0.244
23	kdegAbetaGlia	0.164	0.100	0.130	0.194	-0.047	0.639	60	krelAbetaGlia	0.188	0.059	0.168	0.091	0.194	0.051
24	kdegAntiAb	-0.023	0.816	-0.068	0.495	0.135	0.177	61	krelGSK3bp53	0.070	0.484	0.109	0.275	-0.121	0.226
25	kdegMdm2	-0.130	0.193	0.010	0.921	0.013	0.897	62	krelMdm2p53	0.221	0.025	-0.050	0.616	0.135	0.175
26	kdegMdm2mRNA	0.164	0.099	0.147	0.139	0.031	0.754	63	krelMTTau	0.046	0.649	0.052	0.605	-0.062	0.534
27	kdegp53	0.030	0.763	-0.047	0.637	0.131	0.188	64	kremROS	0.153	0.124	-0.084	0.404	0.061	0.542
28	kdegp53mRNA	-0.054	0.591	-0.133	0.183	-0.184	0.064	65	krepair	-0.004	0.972	-0.114	0.253	0.022	0.830
29	kdegTau20SProt	0.158	0.112	-0.114	0.255	0.145	0.146	66	ksynMdm2	0.209	0.035	0.791	8.31E-	0.253	0.010
30	kdephosMdm2	-0.055	0.583	-0.002	0.983	-0.075	0.452	67	ksynMdm2mRNA	-0.075	0.455	-0.092	0.360	-0.059	0.556
31	kdephosp53	0.042	0.672	-0.047	0.638	0.023	0.818	68	ksynMdm2mRNAGSK3bp	-0.107	0.283	0.144	0.149	-0.123	0.219
32	kdephospTau	-0.040	0.689	0.026	0.797	0.087	0.385	69	ksynp53	0.111	0.265	0.046	0.646	-0.061	0.545
33	kdisaggAbeta	-0.052	0.601	0.171	0.086	0.170	0.088	70	ksynp53mRNA	0.065	0.515	-0.050	0.619	0.184	0.064
34	kdisaggAbeta1	0.013	0.895	-0.053	0.595	-0.013	0.897	71	ksynp53mRNAAbeta	0.036	0.718	0.153	0.126	-0.093	0.351
35	kdisaggAbeta2	0.106	0.288	-0.005	0.958	0.105	0.293	72	ksynTau	-0.031	0.757	0.103	0.304	0.081	0.420
36	kgenROSAbeta	-0.143	0.153	0.002	0.983	-0.182	0.067	73	ktangfor	-0.117	0.243	-0.204	0.040	0.055	0.580
37	kgenROSGlia	0.136	0.172	0.153	0.126	-0.028	0.782								

Table D.9: Output from PRCC Analysis for plaques using ODEs

index	Parameter names	Day #4		Day #8		Day #12		index	Parameter names	Day #4		Day #8		Day #12	
		PRCC	p-value	PRCC	p-value	PRCC	p-value			PRCC	p-value	PRCC	p-value	PRCC	p-value
1	kactATM	-0.079	0.427	0.034	0.736	0.005	0.959	38	kgenROSPlaque	0.030	0.762	-0.077	0.440	-0.071	0.480
2	kactDUBMdm2	-0.014	0.892	-0.047	0.638	-0.015	0.882	39	kinactATM	0.017	0.864	0.033	0.739	-0.001	0.991
3	kactDUBp53	-0.028	0.778	-0.016	0.870	-0.014	0.890	40	kinactglia1	-0.186	0.061	-0.060	0.549	-0.072	0.473
4	kactDUBProtp53	0.049	0.625	-0.022	0.830	-0.013	0.899	41	kinactglia2	0.009	0.927	0.106	0.287	0.089	0.373
5	kactglia1	-0.025	0.806	-0.166	0.095	-0.131	0.189	42	kinhibprot	-0.023	0.818	-0.026	0.794	-0.028	0.777
6	Kactglia2	-0.187	0.059	-0.031	0.755	-0.070	0.482	43	kMdm2PolyUb	0.076	0.446	0.061	0.544	0.042	0.679
7	kaggAbeta	0.082	0.415	0.049	0.622	0.060	0.552	44	kMdm2PUb	-0.065	0.513	-0.048	0.629	-0.078	0.439
8	kaggTau	0.190	0.056	0.171	0.085	0.232	0.019	45	kMdm2Ub	-0.018	0.854	-0.094	0.349	-0.096	0.335
9	kaggTauP1	-0.190	0.056	-0.171	0.085	-0.232	0.019	46	kp53PolyUb	-0.106	0.291	-0.090	0.369	-0.117	0.244
10	kaggTauP2	0.063	0.529	-0.004	0.966	-0.008	0.936	47	kp53Ub	-0.087	0.387	-0.029	0.773	-0.026	0.795
11	kbinAbantiAb	0.133	0.182	0.090	0.369	0.147	0.142	48	kpf	0.032	0.748	0.020	0.839	0.018	0.858
12	kbinAbetaGlia	0.024	0.807	-0.077	0.444	-0.069	0.492	49	kpg	-0.021	0.831	0.097	0.332	0.097	0.331
13	kbinE1Ub	-0.054	0.591	-0.092	0.357	-0.088	0.378	50	kpghalf	0.133	0.181	0.069	0.489	0.120	0.230
14	kbinE2Ub	0.095	0.344	0.214	0.031	0.233	0.018	51	kphosMdm2	0.029	0.771	0.024	0.813	0.018	0.857
15	kbinGSK3bp53	-0.134	0.179	-0.058	0.565	-0.100	0.316	52	kphosMdm2GSK3b	-0.086	0.391	-0.202	0.041	-0.161	0.106
16	kbinMdm2p53	-0.5786	1.1E-03	-0.208	0.036	-0.243	0.014	53	kphosMdm2GSK3bp53	0.005	0.956	0.016	0.870	0.001	0.990
17	kbinMTTau	0.012	0.902	-0.106	0.288	-0.060	0.552	54	kphosp53	0.043	0.667	0.144	0.150	0.146	0.144
18	kbinProt	0.030	0.762	-0.022	0.829	0.004	0.967	55	kphospTauGSK3b	0.042	0.673	0.044	0.663	0.088	0.378
19	kbinTauProt	-0.007	0.947	0.114	0.256	0.071	0.478	56	kphospTauGSK3bp53	-0.094	0.347	-0.054	0.589	-0.123	0.217
20	kdam	0.067	0.507	0.042	0.672	0.067	0.504	57	kprodAbeta	-0.031	0.756	0.068	0.497	0.063	0.528
21	kdamROS	0.005	0.964	-0.018	0.855	-0.017	0.868	58	kprodAbeta2	-0.068	0.497	0.087	0.382	0.047	0.641
22	kdegAbeta	-0.128	0.199	-0.122	0.224	-0.109	0.273	59	kproteff	0.047	0.639	-0.061	0.546	-0.043	0.667
23	kdegAbetaGlia	0.031	0.759	-0.048	0.635	-0.032	0.753	60	krelAbetaGlia	0.119	0.233	-0.076	0.450	-0.034	0.732
24	kdegAntiAb	0.113	0.257	0.157	0.116	0.159	0.111	61	krelGSK3bp53	0.045	0.656	0.102	0.306	0.091	0.360
25	kdegMdm2	-0.100	0.317	-0.053	0.594	-0.079	0.429	62	krelMdm2p53	0.017	0.868	-0.161	0.106	-0.124	0.214
26	kdegMdm2mRNA	0.053	0.594	0.028	0.777	0.045	0.655	63	krelMTTau	-0.070	0.486	-0.100	0.316	-0.131	0.189
27	kdegp53	0.019	0.846	0.020	0.841	0.008	0.940	64	kremROS	0.146	0.142	0.130	0.193	0.155	0.120
28	kdegp53mRNA	-0.087	0.387	-0.109	0.277	-0.125	0.211	65	krepair	0.025	0.802	0.053	0.599	0.032	0.751
29	kdegTau20SProt	0.138	0.166	0.201	0.043	0.230	0.020	66	ksynMdm2	0.6235	4.68E-04	0.196	0.048	0.253	0.010
30	kdephosMdm2	0.130	0.194	0.023	0.818	0.025	0.801	67	ksynMdm2mRNA	-0.034	0.731	-0.135	0.175	-0.135	0.176
31	kdephosp53	-0.160	0.108	0.010	0.919	0.014	0.892	68	ksynMdm2mRNAGSK3bp	0.009	0.930	-0.161	0.106	-0.132	0.185
32	kdephospTau	-0.026	0.794	0.031	0.755	0.030	0.762	69	ksynp53	0.038	0.704	0.031	0.758	0.030	0.764
33	kdisaggAbeta	-0.019	0.853	-0.059	0.556	-0.071	0.477	70	ksynp53mRNA	0.069	0.490	0.018	0.859	0.039	0.698
34	kdisaggAbeta1	-0.093	0.354	-0.105	0.295	-0.110	0.270	71	ksynp53mRNAAbeta	0.201	0.042	0.071	0.481	0.112	0.263
35	kdisaggAbeta2	0.130	0.191	0.133	0.182	0.124	0.213	72	ksynTau	0.032	0.750	0.176	0.077	0.145	0.145
36	kgenROSAbeta	-0.214	0.031	0.030	0.765	-0.015	0.884	73	ktangfor	-0.023	0.819	0.089	0.371	0.049	0.626
37	kgenROSGlia	0.175	0.078	0.142	0.155	0.161	0.106								

Table D.10: Output from PRCC Analysis for plaques using MRM/GSSA

index	Parameter names	Day #4		Day #8		Day #12		index	Parameter names	Day #4		Day #8		Day #12	
		PRCC	p-value	PRCC	p-value	PRCC	p-value			PRCC	p-value	PRCC	p-value	PRCC	p-value
1	kactATM	-0.087	0.387	0.016	0.873	0.122	0.221	38	kgenROSPlaque	-0.099	0.324	-0.014	0.891	-0.110	0.270
2	kactDUBMdm2	0.082	0.412	0.023	0.817	-0.118	0.236	39	kinactATM	0.144	0.147	-0.057	0.568	-0.041	0.680
3	kactDUBp53	-0.025	0.802	-0.005	0.960	0.041	0.681	40	kinactglia1	-0.087	0.384	0.053	0.594	-0.050	0.619
4	kactDUBProtp53	0.052	0.605	0.103	0.303	0.012	0.905	41	kinactglia2	-0.203	0.041	0.127	0.203	0.021	0.837
5	kactglia1	-0.179	0.072	0.030	0.764	-0.009	0.925	42	kinhibprot	-0.111	0.268	-0.021	0.833	0.112	0.264
6	Kactglia2	-0.026	0.793	0.070	0.487	0.009	0.928	43	kMdm2PolyUb	0.039	0.697	0.126	0.208	0.055	0.584
7	kaggAbeta	0.070	0.485	-0.066	0.511	0.105	0.292	44	kMdm2PUb	-0.024	0.813	0.111	0.267	0.045	0.651
8	kaggTau	0.167	0.094	0.079	0.431	0.142	0.154	45	kMdm2Ub	-0.063	0.526	0.033	0.745	0.014	0.892
9	kaggTauP1	-0.167	0.094	-0.079	0.431	-0.142	0.154	46	kp53PolyUb	-0.082	0.415	-0.224	0.024	-0.151	0.129
10	kaggTauP2	0.037	0.715	-0.030	0.761	0.029	0.771	47	kp53Ub	-0.158	0.114	0.085	0.395	-0.039	0.699
11	kbinAbantiAb	0.121	0.227	-0.023	0.816	-0.026	0.792	48	kpf	-0.076	0.447	-0.045	0.650	-0.073	0.468
12	kbinAbetaGlia	0.065	0.516	-0.002	0.983	-0.059	0.558	49	kpg	-0.046	0.648	0.219	0.027	0.152	0.128
13	kbinE1Ub	-0.085	0.395	-0.025	0.801	-0.110	0.272	50	kpghalf	0.162	0.104	0.084	0.403	0.145	0.145
14	kbinE2Ub	0.070	0.482	0.018	0.857	0.209	0.035	51	kphosMdm2	-0.116	0.247	0.078	0.437	-0.077	0.443
15	kbinGSK3bp53	-0.060	0.547	0.069	0.494	-0.092	0.358	52	kphosMdm2GSK3b	-0.147	0.141	0.268	0.006	-0.202	0.042
16	kbinMdm2p53	-0.5041	0.0024	-0.026	0.798	-0.300	0.002	53	kphosMdm2GSK3bp53	-0.053	0.598	-0.027	0.787	0.111	0.266
17	kbinMTTau	0.067	0.501	0.024	0.814	-0.024	0.810	54	kphosp53	0.120	0.231	0.010	0.921	-0.019	0.853
18	kbinProt	0.113	0.257	-0.084	0.403	-0.047	0.640	55	kphospTauGSK3b	0.082	0.411	-0.144	0.147	0.072	0.475
19	kbinTauProt	0.028	0.780	0.013	0.895	-0.074	0.461	56	kphospTauGSK3bp53	-0.038	0.702	-0.147	0.139	-0.096	0.335
20	kdam	0.051	0.612	-0.074	0.458	0.058	0.563	57	kprodAbeta	0.089	0.376	0.065	0.514	0.041	0.684
21	kdamROS	-0.060	0.550	-0.095	0.340	-0.001	0.994	58	kprodAbeta2	-0.032	0.752	-0.029	0.771	-0.081	0.416
22	kdegAbeta	-0.053	0.600	0.038	0.703	0.077	0.443	59	kproteff	0.043	0.671	-0.104	0.299	-0.160	0.109
23	kdegAbetaGlia	0.086	0.392	0.022	0.828	-0.154	0.122	60	krelAbetaGlia	0.112	0.264	-0.022	0.829	0.047	0.637
24	kdegAntiAb	0.059	0.555	-0.066	0.510	0.070	0.483	61	krelGSK3bp53	0.019	0.849	0.032	0.751	0.160	0.107
25	kdegMdm2	-0.103	0.304	-0.070	0.482	0.051	0.608	62	krelMdm2p53	0.042	0.675	-0.203	0.040	0.042	0.676
26	kdegMdm2mRNA	0.032	0.751	0.073	0.465	0.026	0.792	63	krelMTTau	-0.130	0.193	0.017	0.864	-0.160	0.108
27	kdegp53	-0.003	0.974	-0.233	0.018	0.123	0.216	64	kremROS	0.205	0.039	-0.040	0.693	0.059	0.555
28	kdegp53mRNA	-0.113	0.257	-0.130	0.192	-0.075	0.455	65	krepair	-0.008	0.940	-0.006	0.949	0.044	0.658
29	kdegTau20SProt	0.501	0.0006	-0.068	0.497	0.047	0.640	66	ksynMdm2	0.324	0.001	0.123	0.217	0.087	0.383
30	kdephosMdm2	0.204	0.040	-0.040	0.691	-0.070	0.486	67	ksynMdm2mRNA	-0.122	0.224	-0.088	0.377	-0.096	0.338
31	kdephosp53	-0.113	0.257	0.131	0.188	0.096	0.336	68	ksynMdm2mRNAGSK3bp	-0.027	0.788	0.074	0.459	-0.044	0.661
32	kdephospTau	-0.068	0.497	0.131	0.191	0.071	0.478	69	ksynp53	-0.004	0.964	0.003	0.979	0.089	0.372
33	kdisaggAbeta	-0.080	0.422	0.022	0.825	-0.023	0.821	70	ksynp53mRNA	0.028	0.778	0.078	0.434	0.024	0.810
34	kdisaggAbeta1	-0.136	0.173	0.049	0.628	0.050	0.616	71	ksynp53mRNAAbeta	0.173	0.081	0.046	0.649	0.109	0.276
35	kdisaggAbeta2	0.095	0.341	0.020	0.839	0.117	0.243	72	ksynTau	0.091	0.364	0.042	0.678	0.142	0.155
36	kgenROSAbeta	-0.137	0.170	0.090	0.369	-0.179	0.072	73	ktangfor	-0.001	0.992	-0.096	0.336	0.042	0.677
37	kgenROSGlia	0.163	0.101	-0.099	0.322	-0.007	0.944								

Table D.11: Output from PRCC Analysis for plaques using ODEs

index	Parameter names	Day #4		Day #8		Day #12		index	Parameter names	Day #4		Day #8		Day #12	
		PRCC	p-value	PRCC	p-value	PRCC	p-value			PRCC	p-value	PRCC	p-value	PRCC	p-value
1	kactATM	-0.018	0.861	-0.018	0.861	-0.026	0.793	38	kgenROSPlaque	-0.090	0.371	-0.090	0.371	-0.092	0.358
2	kactDUBMdm2	-0.007	0.946	-0.007	0.946	-0.011	0.916	39	kinactATM	-0.002	0.983	-0.002	0.983	-0.008	0.936
3	kactDUBp53	0.013	0.898	0.013	0.898	0.022	0.830	40	kinactglia1	-0.094	0.349	-0.094	0.349	-0.084	0.400
4	kactDUBProtp53	0.045	0.652	0.045	0.652	0.041	0.680	41	kinactglia2	0.024	0.811	0.024	0.811	0.019	0.847
5	kactglia1	-0.072	0.471	-0.072	0.471	-0.076	0.449	42	kinhibprot	-0.039	0.701	-0.039	0.701	-0.034	0.732
6	Kactglia2	-0.121	0.227	-0.121	0.227	-0.121	0.225	43	kMdm2PolyUb	0.028	0.777	0.028	0.777	0.027	0.784
7	kaggAbeta	0.102	0.308	0.102	0.308	0.097	0.333	44	kMdm2PUb	-0.137	0.171	-0.137	0.171	-0.131	0.191
8	kaggTau	0.224	0.024	0.224	0.024	0.227	0.022	45	kMdm2Ub	-0.035	0.723	-0.035	0.723	-0.042	0.674
9	kaggTauP1	-0.224	0.024	-0.224	0.024	-0.227	0.022	46	kp53PolyUb	-0.078	0.435	-0.078	0.435	-0.088	0.379
10	kaggTauP2	0.030	0.764	0.030	0.764	0.022	0.825	47	kp53Ub	-0.048	0.630	-0.048	0.630	-0.043	0.669
11	kbinAbantiAb	0.160	0.108	0.160	0.108	0.156	0.118	48	kpf	0.036	0.719	0.036	0.719	0.031	0.757
12	kbinAbetaGlia	-0.075	0.451	-0.075	0.451	-0.077	0.440	49	kpg	0.033	0.744	0.033	0.744	0.042	0.676
13	kbinE1Ub	-0.077	0.440	-0.077	0.440	-0.073	0.467	50	kpghalf	0.133	0.181	0.133	0.181	0.133	0.181
14	kbinE2Ub	0.222	0.025	0.222	0.025	0.226	0.022	51	kphosMdm2	0.042	0.677	0.042	0.677	0.043	0.667
15	kbinGSK3bp53	-0.094	0.349	-0.094	0.349	-0.085	0.396	52	kphosMdm2GSK3b	-0.117	0.241	-0.117	0.241	-0.114	0.253
16	kbinMdm2p53	-0.275	0.005	-0.275	0.005	-0.6102	2.64E-	53	kphosMdm2GSK3bp53	-0.017	0.862	-0.017	0.862	-0.016	0.873
17	kbinMTTau	0.036	0.717	0.036	0.717	0.031	0.754	54	kphosp53	0.118	0.238	0.118	0.238	0.113	0.257
18	kbinProt	0.007	0.948	0.007	0.948	0.003	0.979	55	kphospTauGSK3b	0.122	0.220	0.122	0.220	0.126	0.206
19	kbinTauProt	-0.005	0.964	-0.005	0.964	-0.005	0.957	56	kphospTauGSK3bp53	-0.150	0.131	-0.150	0.131	-0.154	0.122
20	kdam	0.032	0.750	0.032	0.750	0.036	0.722	57	kprodAbeta	-0.019	0.853	-0.019	0.853	-0.013	0.895
21	kdamROS	0.039	0.695	0.039	0.695	0.036	0.719	58	kprodAbeta2	-0.049	0.625	-0.049	0.625	-0.043	0.671
22	kdegAbeta	-0.067	0.506	-0.067	0.506	-0.061	0.545	59	kproteff	-0.002	0.983	-0.002	0.983	-0.007	0.946
23	kdegAbetaGlia	-0.038	0.701	-0.038	0.701	-0.041	0.682	60	krelAbetaGlia	0.073	0.465	0.073	0.465	0.070	0.487
24	kdegAntiAb	0.104	0.297	0.104	0.297	0.105	0.295	61	krelGSK3bp53	0.120	0.230	0.120	0.230	0.124	0.215
25	kdegMdm2	-0.085	0.397	-0.085	0.397	-0.085	0.396	62	krelMdm2p53	-0.023	0.822	-0.023	0.822	-0.027	0.786
26	kdegMdm2mRNA	0.025	0.803	0.025	0.803	0.032	0.750	63	krelMTTau	-0.136	0.174	-0.136	0.174	-0.145	0.147
27	kdegp53	0.019	0.846	0.019	0.846	0.025	0.801	64	kremROS	0.099	0.320	0.099	0.320	0.104	0.297
28	kdegp53mRNA	-0.104	0.299	-0.104	0.299	-0.096	0.338	65	krepair	0.022	0.826	0.022	0.826	0.018	0.857
29	kdegTau20SProt	0.176	0.077	0.176	0.077	0.180	0.071	66	ksynMdm2	0.293	0.003	0.293	0.003	0.288	0.003
30	kdephosMdm2	0.023	0.820	0.023	0.820	0.018	0.854	67	ksynMdm2mRNA	-0.169	0.089	-0.169	0.089	-0.164	0.099
31	kdephosp53	-0.001	0.990	-0.001	0.990	0.007	0.945	68	ksynMdm2mRNAGSK3bp	-0.021	0.832	-0.021	0.832	-0.031	0.760
32	kdephospTau	0.003	0.977	0.003	0.977	0.005	0.959	69	ksynp53	0.052	0.600	0.052	0.600	0.051	0.608
33	kdisaggAbeta	-0.063	0.531	-0.063	0.531	-0.067	0.503	70	ksynp53mRNA	0.039	0.699	0.039	0.699	0.037	0.709
34	kdisaggAbeta1	-0.116	0.246	-0.116	0.246	-0.115	0.249	71	ksynp53mRNAAbeta	0.174	0.081	0.174	0.081	0.176	0.077
35	kdisaggAbeta2	0.115	0.249	0.115	0.249	0.125	0.211	72	ksynTau	0.104	0.299	0.104	0.299	0.111	0.267
36	kgenROSAbeta	-0.072	0.474	-0.072	0.474	-0.070	0.485	73	ktangfor	-0.039	0.697	-0.039	0.697	-0.042	0.674
37	kgenROSGlia	0.186	0.062	0.186	0.062	0.177	0.075								

Table D.12: Output from PRCC Analysis for plaques using MRM/GSSA

index	Parameter names	Day #4		Day #8		Day #12		index	Parameter names	Day #4		Day #8		Day #12	
		PRCC	p-value	PRCC	p-value	PRCC	p-value			PRCC	p-value	PRCC	p-value	PRCC	p-value
1	kactATM	-0.071	0.476	-0.054	0.589	0.002	0.982	38	kgenROSPlaque	-0.119	0.234	-0.155	0.119	-0.094	0.348
2	kactDUBMdm2	-0.007	0.944	-0.023	0.817	-0.023	0.816	39	kinactATM	0.086	0.389	0.023	0.818	-0.025	0.800
3	kactDUBp53	0.043	0.670	-0.024	0.810	-0.017	0.868	40	kinactglia1	-0.086	0.391	-0.130	0.194	-0.109	0.274
4	kactDUBProtp53	0.042	0.676	0.045	0.650	0.027	0.787	41	kinactglia2	-0.118	0.237	-0.049	0.625	-0.006	0.952
5	kactglia1	-0.124	0.215	-0.154	0.122	-0.114	0.255	42	kinhibprot	-0.001	0.991	0.023	0.817	0.017	0.869
6	Kactglia2	-0.085	0.397	-0.047	0.641	-0.129	0.198	43	kMdm2PolyUb	0.049	0.625	0.042	0.675	0.028	0.779
7	kaggAbeta	0.078	0.437	0.061	0.539	0.088	0.380	44	kMdm2PUb	-0.041	0.684	-0.073	0.469	-0.113	0.258
8	kaggTau	0.129	0.198	0.217	0.028	0.224	0.024	45	kMdm2Ub	0.058	0.563	0.068	0.498	0.050	0.620
9	kaggTauP1	-0.129	0.198	-0.217	0.028	-0.224	0.024	46	kp53PolyUb	-0.028	0.779	-0.029	0.771	-0.033	0.744
10	kaggTauP2	-0.048	0.630	0.020	0.845	-0.005	0.959	47	kp53Ub	-0.060	0.550	-0.066	0.511	-0.041	0.680
11	kbinAbantiAb	0.226	0.022	0.177	0.075	0.150	0.133	48	kpf	0.000	0.998	-0.025	0.806	-0.023	0.817
12	kbinAbetaGlia	-0.101	0.314	-0.097	0.334	-0.076	0.445	49	kpg	-0.024	0.814	0.035	0.729	0.076	0.446
13	kbinE1Ub	-0.098	0.328	-0.092	0.358	-0.076	0.446	50	kpghalf	0.127	0.202	0.157	0.115	0.166	0.095
14	kbinE2Ub	0.137	0.171	0.191	0.054	-0.7167	1.3E-007	51	kphosMdm2	-0.041	0.683	0.021	0.837	0.006	0.953
15	kbinGSK3bp53	-0.123	0.219	-0.097	0.333	-0.081	0.417	52	kphosMdm2GSK3b	-0.141	0.158	-0.109	0.277	-0.092	0.356
16	kbinMdm2p53	-0.264	0.007	-0.295	0.003	0.64	2.93E-006	53	kphosMdm2GSK3bp53	0.016	0.871	0.067	0.503	0.040	0.690
17	kbinMTTau	0.006	0.953	0.029	0.769	0.017	0.868	54	kphosp53	0.116	0.247	0.164	0.100	0.115	0.248
18	kbinProt	-0.013	0.896	-0.023	0.816	-0.037	0.711	55	kphospTauGSK3b	0.154	0.122	0.091	0.364	0.090	0.370
19	kbinTauProt	0.017	0.864	0.012	0.909	0.037	0.716	56	kphospTauGSK3bp53	-0.040	0.693	-0.079	0.429	-0.118	0.238
20	kdam	0.023	0.819	0.010	0.917	0.019	0.852	57	kprodAbeta	0.041	0.681	0.046	0.649	-0.015	0.877
21	kdamROS	-0.041	0.681	0.027	0.789	0.028	0.782	58	kprodAbeta2	-0.049	0.625	-0.069	0.492	-0.051	0.610
22	kdegAbeta	-0.041	0.679	-0.093	0.355	-0.053	0.600	59	kproteff	-0.003	0.980	-0.063	0.530	-0.045	0.656
23	kdegAbetaGlia	0.019	0.850	-0.006	0.954	-0.025	0.801	60	krelAbetaGlia	0.019	0.847	0.033	0.744	0.044	0.662
24	kdegAntiAb	0.074	0.462	0.070	0.482	0.088	0.379	61	krelGSK3bp53	0.044	0.663	0.096	0.339	0.137	0.170
25	kdegMdm2	-0.118	0.236	-0.074	0.459	-0.065	0.519	62	krelMdm2p53	-0.031	0.759	-0.013	0.894	-0.032	0.752
26	kdegMdm2mRNA	0.056	0.575	0.024	0.809	0.041	0.680	63	krelMTTau	-0.093	0.352	-0.104	0.297	-0.106	0.288
27	kdegp53	0.007	0.941	0.024	0.809	0.010	0.922	64	kremROS	0.105	0.295	0.074	0.461	0.083	0.405
28	kdegp53mRNA	-0.127	0.204	-0.102	0.309	-0.134	0.180	65	krepair	0.018	0.855	0.074	0.461	0.076	0.450
29	kdegTau20SProt	0.205	0.039	0.185	0.062	0.155	0.119	66	ksynMdm2	0.256	0.010	0.293	0.00	0.60	1.98E-005
30	kdephosMdm2	0.028	0.782	0.024	0.807	0.046	0.645	67	ksynMdm2mRNA	-0.185	0.063	-0.169	0.090	-0.181	0.068
31	kdephosp53	0.000	1.000	-0.018	0.860	-0.022	0.829	68	ksynMdm2mRNAGSK3bp	-0.017	0.865	-0.004	0.967	0.023	0.818
32	kdephospTau	-0.039	0.695	-0.063	0.526	-0.027	0.790	69	ksynp53	0.034	0.734	0.013	0.894	0.015	0.883
33	kdisaggAbeta	-0.007	0.941	-0.039	0.694	-0.042	0.674	70	ksynp53mRNA	0.060	0.550	0.061	0.540	0.049	0.624
34	kdisaggAbeta1	-0.190	0.056	-0.167	0.094	-0.143	0.152	71	ksynp53mRNAAbeta	0.149	0.134	0.165	0.098	0.117	0.240
35	kdisaggAbeta2	0.052	0.607	0.102	0.308	0.157	0.115	72	ksynTau	0.177	0.075	0.185	0.062	0.163	0.101
36	kgenROSAbeta	-0.032	0.750	-0.106	0.288	-0.102	0.309	73	ktangfor	0.017	0.865	-0.018	0.858	-0.016	0.872
37	kgenROSGlia	0.246	0.013	0.265	0.007	-0.6057	0.00033								

Table D.13: Output from PRCC Analysis for GilaA using ODEs

index	Parameter names	Day #4		Day #8		Day #12		index	Parameter names	Day #4		Day #8		Day #12	
		PRCC	p-value	PRCC	p-value	PRCC	p-value			PRCC	p-value	PRCC	p-value	PRCC	p-value
1	kactATM	-0.026	0.799	-0.158	0.113	-0.080	0.425	38	kgenROSPlaque	-0.094	0.347	0.047	0.637	0.060	0.548
2	kactDUBMdm2	-0.010	0.920	0.087	0.387	0.073	0.468	39	kinactATM	0.000	0.997	-0.147	0.141	-0.065	0.516
3	kactDUBp53	0.016	0.876	0.047	0.643	0.075	0.455	40	kinactglia1	-0.086	0.389	0.000	0.997	0.075	0.455
4	kactDUBProtp53	0.038	0.708	0.021	0.835	0.036	0.721	41	kinactglia2	0.018	0.859	-0.123	0.219	-0.099	0.322
5	kactglia1	-0.074	0.458	0.119	0.232	0.167	0.094	42	kinhibprot	-0.033	0.740	0.029	0.769	0.001	0.993
6	Kactglia2	-0.127	0.205	-0.122	0.220	0.002	0.985	43	kMdm2PolyUb	0.036	0.721	-0.102	0.306	-0.091	0.364
7	kaggAbeta	0.096	0.336	-0.027	0.787	-0.063	0.533	44	kMdm2PUb	-0.125	0.211	-0.018	0.861	0.069	0.489
8	kaggTau	0.219	0.027	0.061	0.541	-0.130	0.193	45	kMdm2Ub	-0.032	0.751	0.004	0.970	0.027	0.787
9	kaggTauP1	-0.219	0.027	-0.061	0.541	0.130	0.193	46	kp53PolyUb	-0.077	0.443	-0.074	0.461	-0.001	0.996
10	kaggTauP2	0.021	0.833	-0.060	0.547	-0.055	0.580	47	kp53Ub	-0.050	0.619	0.049	0.623	0.054	0.591
11	kbinAbantiAb	0.157	0.116	0.110	0.269	-0.075	0.451	48	kpf	0.036	0.719	-0.077	0.442	-0.028	0.782
12	kbinAbetaGlia	-0.079	0.430	0.083	0.409	0.098	0.328	49	kpg	0.026	0.796	-0.016	0.873	-0.075	0.454
13	kbinE1Ub	-0.063	0.529	0.041	0.682	0.076	0.445	50	kpghalf	0.133	0.181	0.103	0.303	-0.059	0.555
14	kbinE2Ub	0.227	0.022	-0.070	0.484	-0.186	0.061	51	kphosMdm2	0.046	0.647	-0.063	0.532	-0.021	0.835
15	kbinGSK3bp53	-0.088	0.377	-0.028	0.779	0.096	0.336	52	kphosMdm2GSK3b	-0.120	0.228	0.216	0.029	0.208	0.036
16	kbinMdm2p53	-0.280	0.004	0.086	0.389	0.217	0.029	53	kphosMdm2GSK3bp53	-0.027	0.790	-0.049	0.626	-0.014	0.889
17	kbinMTTau	0.044	0.658	0.124	0.216	0.070	0.483	54	kphosp53	0.109	0.277	-0.070	0.484	-0.145	0.146
18	kbinProt	0.009	0.927	0.047	0.636	-0.015	0.882	55	kphospTauGSK3b	0.119	0.233	0.101	0.315	-0.004	0.965
19	kbinTauProt	0.005	0.962	-0.133	0.181	-0.116	0.247	56	kphospTauGSK3bp53	-0.148	0.137	-0.137	0.169	0.024	0.807
20	kdam	0.027	0.787	0.095	0.340	0.024	0.813	57	kprodAbeta	-0.025	0.805	-0.033	0.741	-0.061	0.545
21	kdamROS	0.039	0.694	0.030	0.765	0.032	0.748	58	kprodAbeta2	-0.047	0.636	-0.110	0.270	-0.054	0.592
22	kdegAbeta	-0.061	0.542	0.113	0.259	0.109	0.276	59	kproteff	-0.006	0.956	0.081	0.417	0.050	0.615
23	kdegAbetaGlia	-0.042	0.673	-0.076	0.447	-0.028	0.779	60	krelAbetaGlia	0.078	0.438	0.176	0.076	0.081	0.419
24	kdegAntiAb	0.094	0.349	-0.062	0.536	-0.119	0.234	61	krelGSK3bp53	0.117	0.240	-0.103	0.302	-0.093	0.350
25	kdegMdm2	-0.086	0.392	0.013	0.896	0.079	0.428	62	krelMdm2p53	-0.022	0.828	0.175	0.079	0.140	0.162
26	kdegMdm2mRNA	0.029	0.770	0.074	0.459	0.009	0.929	63	krelMTTau	-0.140	0.160	-0.066	0.510	0.023	0.815
27	kdegp53	0.024	0.813	-0.010	0.923	-0.006	0.951	64	kremROS	0.102	0.309	0.016	0.874	-0.104	0.296
28	kdegp53mRNA	-0.097	0.334	0.022	0.825	0.132	0.185	65	krepair	0.025	0.802	-0.117	0.240	-0.069	0.490
29	kdegTau20SProt	0.180	0.070	0.010	0.921	-0.142	0.155	66	ksynMdm2	0.294	0.003	0.016	0.877	-0.251	0.011
30	kdephosMdm2	0.023	0.815	0.024	0.808	-0.029	0.774	67	ksynMdm2mRNA	-0.169	0.089	0.113	0.256	0.154	0.122
31	kdephosp53	0.008	0.938	0.005	0.962	0.001	0.995	68	ksynMdm2mRNAGSK3bp	-0.026	0.797	0.146	0.143	0.115	0.251
32	kdephospTau	-0.003	0.979	-0.052	0.604	-0.013	0.895	69	ksynp53	0.052	0.604	-0.052	0.604	-0.026	0.799
33	kdisaggAbeta	-0.063	0.529	0.006	0.950	0.021	0.838	70	ksynp53mRNA	0.042	0.672	0.012	0.905	-0.013	0.897
34	kdisaggAbeta1	-0.117	0.241	0.073	0.467	0.135	0.175	71	ksynp53mRNAAbeta	0.169	0.090	0.066	0.508	-0.069	0.490
35	kdisaggAbeta2	0.117	0.241	-0.059	0.555	-0.104	0.297	72	ksynTau	0.112	0.263	-0.156	0.118	-0.166	0.096
36	kgenROSAbeta	-0.074	0.457	-0.136	0.171	0.005	0.957	73	ktangfor	-0.094	0.347	-0.167	0.094	-0.097	0.335
37	kgenROSGlia	0.190	0.056	-0.060	0.549	-0.176	0.077								

Table D.14: Output from PRCC Analysis for GilaA using MRM/GSSA

index	Parameter names	Day #4		Day #8		Day #12		index	Parameter names	Day #4		Day #8		Day #12	
		PRCC	p-value	PRCC	p-value	PRCC	p-value			PRCC	p-value	PRCC	p-value	PRCC	p-value
1	kactATM	-0.054	0.589	-0.108	0.280	-0.120	0.230	38	kgenROSPlaque	-0.145	0.146	-0.061	0.545	0.076	0.446
2	kactDUBMdm2	-0.040	0.688	-0.011	0.915	0.074	0.461	39	kinactATM	0.043	0.669	-0.039	0.695	-0.089	0.373
3	kactDUBp53	0.122	0.220	-0.061	0.540	0.028	0.782	40	kinactglia1	-0.047	0.637	-0.001	0.989	0.018	0.856
4	kactDUBProtp53	0.109	0.273	0.071	0.479	0.025	0.803	41	kinactglia2	-0.115	0.250	-0.047	0.638	-0.159	0.110
5	kactglia1	-0.173	0.083	-0.003	0.974	0.043	0.666	42	kinhibprot	-0.117	0.243	-0.118	0.238	-0.079	0.431
6	Kactglia2	-0.060	0.551	0.026	0.795	-0.058	0.561	43	kMdm2PolyUb	0.173	0.082	0.076	0.446	-0.153	0.124
7	kaggAbeta	-0.094	0.348	-0.023	0.816	-0.022	0.823	44	kMdm2PUb	0.159	0.111	-0.002	0.983	0.035	0.729
8	kaggTau	0.046	0.643	0.073	0.467	-0.173	0.082	45	kMdm2Ub	-0.040	0.687	-0.079	0.427	-0.017	0.861
9	kaggTauP1	-0.046	0.643	-0.073	0.467	0.173	0.082	46	kp53PolyUb	-0.040	0.689	0.018	0.858	0.038	0.704
10	kaggTauP2	0.120	0.228	0.192	0.053	0.044	0.657	47	kp53Ub	-0.173	0.083	-0.021	0.835	-0.108	0.281
11	kbinAbantiAb	0.025	0.805	0.031	0.759	0.036	0.721	48	kpf	-0.017	0.863	0.068	0.497	-0.041	0.682
12	kbinAbetaGlia	-0.085	0.398	0.028	0.779	0.176	0.077	49	kpg	0.133	0.181	-0.079	0.430	-0.039	0.698
13	kbinE1Ub	-0.037	0.712	-0.115	0.249	0.024	0.814	50	kpghalf	0.102	0.309	-0.108	0.281	0.177	0.075
14	kbinE2Ub	0.173	0.083	0.212	0.032	-0.128	0.199	51	kphosMdm2	-0.007	0.947	-0.007	0.947	-0.039	0.694
15	kbinGSK3bp53	0.167	0.093	0.078	0.438	-0.017	0.864	52	kphosMdm2GSK3b	-0.003	0.978	0.167	0.093	0.059	0.554
16	kbinMdm2p53	-0.246	0.013	-0.169	0.090	0.212	0.032	53	kphosMdm2GSK3bp53	-0.079	0.429	-0.073	0.469	0.010	0.922
17	kbinMTTau	-0.022	0.825	0.170	0.088	0.044	0.661	54	kphosp53	-0.061	0.545	0.126	0.209	-0.011	0.913
18	kbinProt	0.085	0.398	0.121	0.225	0.059	0.555	55	kphospTauGSK3b	0.115	0.248	0.084	0.399	-0.084	0.401
19	kbinTauProt	-0.102	0.306	-0.017	0.869	-0.061	0.546	56	kphospTauGSK3bp53	-0.200	0.044	-0.280	0.004	-0.115	0.249
20	kdam	0.093	0.350	0.154	0.122	0.136	0.172	57	kprodAbeta	-0.071	0.479	-0.124	0.215	-0.037	0.709
21	kdamROS	0.134	0.181	0.041	0.680	0.010	0.924	58	kprodAbeta2	-0.117	0.241	-0.038	0.703	-0.037	0.709
22	kdegAbeta	0.135	0.177	-0.063	0.530	-0.008	0.936	59	kproteff	-0.033	0.740	0.048	0.632	0.026	0.798
23	kdegAbetaGlia	-0.503	0.0004	0.001	0.991	0.066	0.507	60	krelAbetaGlia	0.107	0.284	0.121	0.228	0.038	0.707
24	kdegAntiAb	-0.011	0.910	-0.109	0.277	-0.122	0.224	61	krelGSK3bp53	0.072	0.472	-0.089	0.376	-0.046	0.645
25	kdegMdm2	-0.042	0.672	-0.084	0.400	-0.038	0.706	62	krelMdm2p53	0.080	0.422	0.156	0.118	0.065	0.514
26	kdegMdm2mRNA	0.060	0.548	0.111	0.267	0.134	0.180	63	krelMTTau	-0.170	0.087	-0.208	0.036	-0.005	0.960
27	kdegp53	0.194	0.050	-0.006	0.954	0.195	0.050	64	kremROS	0.049	0.624	0.252	0.011	0.066	0.511
28	kdegp53mRNA	-0.035	0.729	-0.060	0.546	0.176	0.076	65	krepair	-0.013	0.898	0.031	0.761	-0.102	0.310
29	kdegTau20SProt	-0.068	0.497	-0.052	0.606	0.048	0.634	66	ksynMdm2	0.543	0.00023	0.255	0.010	-0.013	0.900
30	kdephosMdm2	0.163	0.101	0.063	0.530	0.009	0.925	67	ksynMdm2mRNA	-0.059	0.559	-0.078	0.438	0.006	0.950
31	kdephosp53	-0.028	0.779	-0.017	0.863	0.009	0.930	68	ksynMdm2mRNAGSK3bp	0.027	0.791	0.064	0.524	0.177	0.075
32	kdephospTau	0.051	0.613	-0.004	0.972	-0.110	0.271	69	ksynp53	-0.057	0.571	-0.082	0.413	-0.054	0.591
33	kdisaggAbeta	-0.066	0.508	0.071	0.478	-0.067	0.503	70	ksynp53mRNA	-0.045	0.654	-0.036	0.720	-0.105	0.294
34	kdisaggAbeta1	0.091	0.365	0.002	0.984	0.077	0.442	71	ksynp53mRNAAbeta	0.156	0.117	0.135	0.177	0.007	0.946
35	kdisaggAbeta2	0.112	0.262	-0.085	0.395	-0.048	0.634	72	ksynTau	0.056	0.575	-0.139	0.164	-0.121	0.226
36	kgenROSAbeta	-0.112	0.261	-0.080	0.425	-0.012	0.904	73	ktangfor	-0.582	0.2E-04	-0.109	0.274	-0.247	0.012
37	kgenROSGlia	-0.042	0.676	-0.003	0.978	0.059	0.556								

References

Abreu, R., Stich, D., & Morales, J. (2013). On the generalization of the complex step method. *Journal of Computational and Applied Mathematics, 241*, 84-102.

Akrivis, G., Crouzeix, M., & Makridakis, C. (1999). Implicit-explicit multistep methods for quasilinear parabolic equations. *Numerische Mathematik, 82*(4), 521-541.

Anderson, D. F. (2012). An efficient finite difference method for parameter sensitivities of continuous time Markov chains. *SIAM Journal on Numerical Analysis, 50*(5), 2237-2258.

Barroso, L. A., Dean, J., & Holzle, U. (2003). Web search for a planet: The Google cluster architecture. *IEEE micro, 23*(2), 22-28.

Bayer, A. J., Bullock, R., Jones, R. W., Wilkinson, D., Paterson, K., Jenkins, L., . . . Donoghue, S. (2005). Evaluation of the safety and immunogenicity of synthetic Aβ42 (AN1792) in patients with AD. *Neurology, 64*(1), 94-101.

Bent, J., Thain, D., Arpaci-Dusseau, A. C., Arpaci-Dusseau, R. H., & Livny, M. (2004). Explicit Control in the Batch-Aware Distributed File System Symposium conducted at the meeting of the NSDI

Benton, N., Cardelli, L., & Fournet, C. (2002). Modern concurrency abstractions for C#*Springer.* Symposium conducted at the meeting of the ECOOP

Bertsch, M., Franchi, B., Marcello, N., Tesi, M. C., & Tosin, A. (2016). Alzheimer's disease: a mathematical model for onset and progression. *Mathematical medicine and biology: a journal of the IMA, 34*(2), 193-214.

Bluman, G. W., & Anco, S. C. (2002). Ordinary Differential Equations (ODEs). *Symmetry and Integration Methods for Differential Equations*, 101-295.

Boche, D., Denham, N., Holmes, C., & Nicoll, J. A. (2010). Neuropathology after active Aβ42 immunotherapy: implications for Alzheimer's disease pathogenesis. *Acta neuropathologica, 120*(3), 369-384.

Bowers, K. J., Dror, R. O., & Shaw, D. E. (2006). The midpoint method for parallelization of particle simulations. *The Journal of chemical physics, 124*(18), 184109.

Bulirsch, R., & Stoer, J. (1966). Numerical treatment of ordinary differential equations by extrapolation methods. *Numerische Mathematik, 8*(1), 1-13.

Burrage, K., Burrage, P., Leier, A., & Marquez-Lago, T. (2017). A review of stochastic and delay simulation approaches in both time and space in Computational Cell Biology. In *Stochastic Processes, Multiscale Modeling, and Numerical Methods for Computational Cellular Biology* (pp. 241-261): Springer.

Cao, Y., Gillespie, D. T., & Petzold, L. R. (2005). Avoiding negative populations in explicit Poisson tau-leaping. *The Journal of chemical physics, 123*(5), 054104.

Cao, Y., Gillespie, D. T., & Petzold, L. R. (2006). Efficient step size selection for the tau-leaping simulation method. *The Journal of chemical physics, 124*(4), 044109.

Cao, Y., Li, H., & Petzold, L. (2004). Efficient formulation of the stochastic simulation algorithm for chemically reacting systems. *The journal of chemical physics, 121*(9), 4059-4067.

Cao, Y., & Samuels, D. C. (2009). Discrete stochastic simulation methods for chemically reacting systems. *Methods in enzymology, 454*, 115-140.

Castillo, E., Hadi, A. S., Conejo, A., & Fernández-Canteli, A. (2004). A general method for local sensitivity analysis with application to regression models and other optimization problems. *Technometrics, 46*(4), 430-444.

Cazzaniga, P., Pescini, D., Besozzi, D., & Mauri, G. (2006). Tau leaping stochastic simulation method in p systems*Springer.* Symposium conducted at the meeting of the International Workshop on Membrane Computing

Češka, M., Šafránek, D., Dražan, S., & Brim, L. (2014). Robustness analysis of stochastic biochemical systems. *PloS one, 9*(4), e94553.

Chambers, J. E., Quintana, E. V., Duncan, M. J., & Lissauer, J. J. (2002). Symplectic integrator algorithms for modeling planetary accretion in binary star systems. *The Astronomical Journal, 123*(5), 2884.

Cloez, B., Dessalles, R., Genadot, A., Malrieu, F., Marguet, A., & Yvinec, R. (2017). Probabilistic and Piecewise Deterministic models in Biology. *ESAIM: Proceedings and Surveys, 60*, 225-245.
Craddock, T. J., Tuszynski, J. A., Chopra, D., Casey, N., Goldstein, L. E., Hameroff, S. R., & Tanzi, R. E. (2012). The zinc dyshomeostasis hypothesis of Alzheimer's disease. *PLoS One, 7*(3), e33552.
Craft, D. L., Wein, L. M., & Selkoe, D. J. (2002). A mathematical model of the impact of novel treatments on the Aβ burden in the Alzheimer's brain, CSF and plasma. *Bulletin of mathematical biology, 64*(5), 1011-1031.
Cropp, R. A., & Braddock, R. D. (2002). The new Morris method: an efficient second-order screening method. *Reliability Engineering & System Safety, 78*(1), 77-83.
Cukier, R., Levine, H., & Shuler, K. (1978). Nonlinear sensitivity analysis of multiparameter model systems. *Journal of computational physics, 26*(1), 1-42.
De La Fuente, A., Bing, N., Hoeschele, I., & Mendes, P. (2004). Discovery of meaningful associations in genomic data using partial correlation coefficients. *Bioinformatics, 20*(18), 3565-3574.
De Pauw, D. J., & Vanrolleghem, P. A. (2003). Practical aspects of sensitivity analysis for dynamic models Symposium conducted at the meeting of the Proceedings of the 4th IMACS Symposium on Mathematical Modelling (MATHMOD). Vienna, Austria
Dean, J., & Ghemawat, S. (2008). MapReduce: simplified data processing on large clusters. *Communications of the ACM, 51*(1), 107-113.
Dean, J., & Ghemawat, S. (2010). MapReduce: a flexible data processing tool. *Communications of the ACM, 53*(1), 72-77.
Deuflhard, P., Hairer, E., & Zugck, J. (1987). One-step and extrapolation methods for differential-algebraic systems. *Numerische Mathematik, 51*(5), 501-516.
Dubois, B., Feldman, H. H., Jacova, C., Cummings, J. L., DeKosky, S. T., Barberger-Gateau, P., . . . Galasko, D. (2010). Revising the definition of Alzheimer's disease: a new lexicon. *The Lancet Neurology, 9*(11), 1118-1127.
Ehrenstein, G., Galdzicki, Z., & Lange, G. D. (1997). The choline-leakage hypothesis for the loss of acetylcholine in Alzheimer's disease. *Biophysical journal, 73*(3), 1276-1280.
Ehrenstein, G., Galdzicki, Z., & Lange, G. D. (2000). A positive-feedback model for the loss of acetylcholine in Alzheimer's disease. *Annals of the New York Academy of Sciences, 899*(1), 283-291.
Ethier, S., & Kurtz, T., &. *Markov Processes: Characterization and Convergence, 1986*: John Wiley and Sons.
Fang, J., Margot, J.-L., Brozovic, M., Nolan, M. C., Benner, L. A., & Taylor, P. A. (2011). Orbits of near-earth asteroid triples 2001 SN263 and 1994 CC: properties, origin, and evolution. *The Astronomical Journal, 141*(5), 154.
Ferreira Cordeiro, R. L., Traina Junior, C., Machado Traina, A. J., López, J., Kang, U., & Faloutsos, C. (2011). Clustering very large multi-dimensional datasets with mapreduce*ACM.* Symposium conducted at the meeting of the Proceedings of the 17th ACM SIGKDD international conference on Knowledge discovery and data mining
Fisher, J., & Henzinger, T. A. (2007). Executable cell biology. *Nature biotechnology, 25*(11), 1239-1249.
Fuβ, H., Dubitzky, W., Downes, C. S., & Kurth, M. J. (2005). Mathematical models of cell cycle regulation. *Briefings in bioinformatics, 6*(2), 163-177.
Gibson, M. A., & Bruck, J. (2000). Efficient exact stochastic simulation of chemical systems with many species and many channels. *The journal of physical chemistry A, 104*(9), 1876-1889.
Gillespie, D. T. (1976). A general method for numerically simulating the stochastic time evolution of coupled chemical reactions. *Journal of computational physics, 22*(4), 403-434.
Gillespie, D. T. (1977). Exact stochastic simulation of coupled chemical reactions. *The journal of physical chemistry, 81*(25), 2340-2361.
Gillespie, D. T. (1992). A rigorous derivation of the chemical master equation. *Physica A: Statistical Mechanics and its Applications, 188*(1), 404-425.
Gillespie, D. T. (2001). Approximate accelerated stochastic simulation of chemically reacting systems. *The Journal of Chemical Physics, 115*(4), 1716-1733.
Gillespie, D. T. (2007). Stochastic simulation of chemical kinetics. *Annu. Rev. Phys. Chem., 58*, 35-55.

Glynn, P. W., & Iglehart, D. L. (1988). Simulation methods for queues: An overview. *Queueing Systems, 3*(3), 221-255.
Goedert, M., & Spillantini, M. G. (2006). A century of Alzheimer's disease. *science, 314*(5800), 777-781.
Good, T. A., & Murphy, R. M. (1996). Effect of β-amyloid block of the fast-inactivating K+ channel on intracellular Ca2+ and excitability in a modeled neuron. *Proceedings of the National Academy of Sciences, 93*(26), 15130-15135.
Gragg, W. B. (1965). On extrapolation algorithms for ordinary initial value problems. *Journal of the Society for Industrial and Applied Mathematics, Series B: Numerical Analysis, 2*(3), 384-403.
Groot, S., & Kitsuregawa, M. (2010). Jumbo: Beyond mapreduce for workload balancing Symposium conducted at the meeting of the 36th International Conference on Very Large Data Bases, Singapore
Gunawan, R., Cao, Y., Petzold, L., & Doyle, F. J. (2005). Sensitivity analysis of discrete stochastic systems. *Biophysical journal, 88*(4), 2530-2540.
Guzev, V. (2008). Parallel C#: The Usage of Chords and Higher-order Functions in the Design of Parallel Programming Languages Symposium conducted at the meeting of the PDPTA
Hairer, E., Lubich, C., & Roche, M. (2006). *The numerical solution of differential-algebraic systems by Runge-Kutta methods* (Vol. 1409): Springer.
Hamby, D. (1994). A review of techniques for parameter sensitivity analysis of environmental models. *Environmental monitoring and assessment, 32*(2), 135-154.
Haugh, M. (2004). Generating random variables and stochastic processes. *Monte Carlo Simulation: IEOR EA703*.
Heath, A. P., & Kavraki, L. E. (2009). Computational challenges in systems biology. *Computer Science Review, 3*(1), 1-17.
Helton, J. C., & Davis, F. J. (2000). Sampling-based methods. *Sensitivity analysis*, 101-153.
Herajy, M., Liu, F., Rohr, C., & Heiner, M. (2017). Snoopy's hybrid simulator: a tool to construct and simulate hybrid biological models. *BMC systems biology, 11*(1), 71.
Hock, C., Konietzko, U., Streffer, J. R., Tracy, J., Signorell, A., Müller-Tillmanns, B., . . . Garcia, E. (2003). Antibodies against β-amyloid slow cognitive decline in Alzheimer's disease. *Neuron, 38*(4), 547-554.
Hu, F., Hussaini, M. Y., & Manthey, J. (1996). Low-dissipation and low-dispersion Runge–Kutta schemes for computational acoustics. *Journal of computational physics, 124*(1), 177-191.
Humphries, A., & Stuart, A., &. (1998). *Dynamical systems and numerical analysis*: Cambridge University Press, Cambridge.
Ihekwaba, A., Broomhead, D., Grimley, R., Benson, N., White, M., & Kell, D. (2005). Synergistic control of oscillations in the NF-κB signalling pathway. *IEE Proceedings-Systems Biology, 152*(3), 153-160.
Ittner, L. M., Ke, Y. D., Delerue, F., Bi, M., Gladbach, A., van Eersel, J., . . . Napier, I. A. (2010). Dendritic function of tau mediates amyloid-β toxicity in Alzheimer's disease mouse models. *Cell, 142*(3), 387-397.
Jack Jr, C. R., Albert, M. S., Knopman, D. S., McKhann, G. M., Sperling, R. A., Carrillo, M. C., . . . Phelps, C. H. (2011). Introduction to the recommendations from the National Institute on Aging-Alzheimer's Association workgroups on diagnostic guidelines for Alzheimer's disease. *Alzheimer's & Dementia, 7*(3), 257-262.
Jin, Y., Peng, X., Liang, Y., & Ma, J. (2008). Uniform design-based sensitivity analysis of circadian rhythm model in Neurospora. *Computers & Chemical Engineering, 32*(8), 1956-1962.
Jucker, M. (2010). The benefits and limitations of animal models for translational research in neurodegenerative diseases. *Nature medicine, 16*(11), 1210-1214.
Khachaturian, Z. S., & Radebaugh, T. S. (1996). *Alzheimer's disease: cause (s), diagnosis, treatment, and care*: CRC Press.
Kiparissides, A., Kucherenko, S., Mantalaris, A., & Pistikopoulos, E. (2009). Global sensitivity analysis challenges in biological systems modeling. *Industrial & Engineering Chemistry Research, 48*(15), 7168-7180.
Kitano, H. (2002). Systems biology: a brief overview. *Science, 295*(5560), 1662-1664.

Klipp, E., Liebermeister, W., Wierling, C., Kowald, A., & Herwig, R. (2016). *Systems biology: a textbook*: John Wiley & Sons.

Krohn, M., Lange, C., Hofrichter, J., Scheffler, K., Stenzel, J., Steffen, J., . . . Alfen, F. (2011). Cerebral amyloid-β proteostasis is regulated by the membrane transport protein ABCC1 in mice. *The Journal of clinical investigation, 121*(10), 3924.

Kulasiri, D., Liang, J., He, Y., & Samarasinghe, S. (2017). Global sensitivity analysis of a model related to memory formation in synapses: Model reduction based on epistemic parameter uncertainties and related issues. *Journal of theoretical biology, 419*, 116-136.

Kuznetsov, I., & Kuznetsov, A. (2016). Mathematical models of α-synuclein transport in axons. *Computer methods in biomechanics and biomedical engineering, 19*(5), 515-526.

Kyrtsos, C. R. (2011). *Of mice and math: A systems biology model for Alzheimer's disease*: University of Maryland, College Park.

Kyrtsos, C. R., & Baras, J. S. (2013). Studying the role of APOE in Alzheimer's disease pathogenesis using a systems biology model. *Journal of bioinformatics and computational biology, 11*(05), 1342003.

Kyrtsos, C. R., & Baras, J. S. (2015). Modeling the role of the glymphatic pathway and cerebral blood vessel properties in Alzheimer's disease pathogenesis. *PloS one, 10*(10), e0139574.

Lämmel, R. (2008). Google's MapReduce programming model—Revisited. *Science of computer programming, 70*(1), 1-30.

Lannfelt, L., Blennow, K., Zetterberg, H., Batsman, S., Ames, D., Harrison, J., . . . Murdoch, R. (2008). Safety, efficacy, and biomarker findings of PBT2 in targeting Aβ as a modifying therapy for Alzheimer's disease: a phase IIa, double-blind, randomised, placebo-controlled trial. *The Lancet Neurology, 7*(9), 779-786.

Lao, A., Schmidt, V., Schmitz, Y., Willnow, T. E., & Wolkenhauer, O. (2012). Multi-compartmental modeling of SORLA's influence on amyloidogenic processing in Alzheimer's disease. *BMC systems biology, 6*(1), 74.

Lattanzi, S., Moseley, B., Suri, S., & Vassilvitskii, S. (2011). Filtering: a method for solving graph problems in mapreduce*ACM.* Symposium conducted at the meeting of the Proceedings of the twenty-third annual ACM symposium on Parallelism in algorithms and architectures

Lee, Y.-S., Liu, O. Z., Hwang, H. S., Knollmann, B. C., & Sobie, E. A. (2013). Parameter sensitivity analysis of stochastic models provides insights into cardiac calcium sparks. *Biophysical journal, 104*(5), 1142-1150.

Lloret-Villas, A., Varusai, T., Juty, N., Laibe, C., Le NovÈre, N., Hermjakob, H., & Chelliah, V. (2017). The impact of mathematical modeling in understanding the mechanisms underlying neurodegeneration: Evolving dimensions and future directions. *CPT: pharmacometrics & systems pharmacology*.

Loidl, H.-W. (2012). Parallel Programming in C#. *Heriot-Watt University, Edinburgh*.

Luca, M., Chavez-Ross, A., Edelstein-Keshet, L., & Mogilner, A. (2003). Chemotactic signaling, microglia, and Alzheimer's disease senile plaques: Is there a connection? *Bulletin of mathematical biology, 65*(4), 693-730.

Lv, Z., Hu, Y., Zhong, H., Wu, J., Li, B., & Zhao, H. (2010). Parallel k-means clustering of remote sensing images based on mapreduce. *Web Information Systems and Mining*, 162-170.

Maarouf, C. L., Daugs, I. D., Kokjohn, T. A., Kalback, W. M., Patton, R. L., Luehrs, D. C., . . . Beach, T. G. (2010). The biochemical aftermath of anti-amyloid immunotherapy. *Molecular neurodegeneration, 5*(1), 39.

Macdonald, A., & Pritchard, D. (2000). A mathematical model of Alzheimer's Disease and the Apoe gene. *ASTIN Bulletin: The Journal of the IAA, 30*(1), 69-110.

Madani, R., Poirier, R., Wolfer, D. P., Welzl, H., Groscurth, P., Lipp, H. P., . . . Nitsch, R. M. (2006). Lack of neprilysin suffices to generate murine amyloid-like deposits in the brain and behavioral deficit in vivo. *Journal of neuroscience research, 84*(8), 1871-1878.

Mangialasche, F., Solomon, A., Winblad, B., Mecocci, P., & Kivipelto, M. (2010). Alzheimer's disease: clinical trials and drug development. *The Lancet Neurology, 9*(7), 702-716.

Mann, B. E., Trasatti, P. J., Carlozzi, M. D., Ywoskus, J. A., & McGrath, E. J., &. (2003). *Loosely coupled mass storage computer cluster*: Google Patents.

Marino, S., Hogue, I. B., Ray, C. J., & Kirschner, D. E. (2008). A methodology for performing global uncertainty and sensitivity analysis in systems biology. *Journal of theoretical biology, 254*(1), 178-196.

Martins, J. R., Sturdza, P., & Alonso, J. J. (2003). The complex-step derivative approximation. *ACM Transactions on Mathematical Software (TOMS), 29*(3), 245-262.

Mattson, M. P. (2004). Pathways towards and away from Alzheimer's disease. *Nature, 430*(7000), 631.

McAdams, H. H., & Arkin, A. (1999). It'sa noisy business! Genetic regulation at the nanomolar scale. *Trends in genetics, 15*(2), 65-69.

McAuley, M. T., Kenny, R. A., Kirkwood, T. B., Wilkinson, D. J., Jones, J. J., & Miller, V. M. (2009). A mathematical model of aging-related and cortisol induced hippocampal dysfunction. *BMC neuroscience, 10*(1), 26.

McCarter, J. F. (2014). *Dynamics of amyloid plaque formation in Alzheimer's Disease*. lmu.

McCollum, J. M., Peterson, G. D., Cox, C. D., Simpson, M. L., & Samatova, N. F. (2006). The sorting direct method for stochastic simulation of biochemical systems with varying reaction execution behavior. *Computational biology and chemistry, 30*(1), 39-49.

McKay, M. D., Beckman, R. J., & Conover, W. J. (1979). Comparison of three methods for selecting values of input variables in the analysis of output from a computer code. *Technometrics, 21*(2), 239-245.

McKenna, A., Hanna, M., Banks, E., Sivachenko, A., Cibulskis, K., Kernytsky, A., . . . Daly, M. (2010). The Genome Analysis Toolkit: a MapReduce framework for analyzing next-generation DNA sequencing data. *Genome research, 20*(9), 1297-1303.

Mellman, I., & Misteli, T. (2003). Computational cell biology. *The Journal of cell biology, 161*(3), 463-464.

Mizuno, S., Iijima, R., Ogishima, S., Kikuchi, M., Matsuoka, Y., Ghosh, S., . . . Tanaka, H. (2012). AlzPathway: a comprehensive map of signaling pathways of Alzheimer's disease. *BMC systems biology, 6*(1), 52.

Monroe, J. L. (2002). Extrapolation and the Bulirsch-Stoer algorithm. *Physical Review E, 65*(6), 066116.

Munthe-Kaas, H. (1999). High order Runge-Kutta methods on manifolds. *Applied Numerical Mathematics, 29*(1), 115-127.

Nestorov, I. A. (1999). Sensitivity analysis of pharmacokinetic and pharmacodynamic systems: I. A structural approach to sensitivity analysis of physiologically based pharmacokinetic models. *Journal of Pharmacokinetics and Pharmacodynamics, 27*(6), 577-596.

Nicoll, J. A., Barton, E., Boche, D., Neal, J. W., Ferrer, I., Thompson, P., . . . Games, D. (2006). Aβ species removal after Aβ42 immunization. *Journal of Neuropathology & Experimental Neurology, 65*(11), 1040-1048.

Nicoll, J. A., Wilkinson, D., Holmes, C., Steart, P., Markham, H., & Weller, R. O. (2003). Neuropathology of human Alzheimer disease after immunization with amyloid-β peptide: a case report. *Nature medicine, 9*(4), 448-452.

Ortega, F., Stott, J., Visser, S. A., & Bendtsen, C. (2013). Interplay between α-, β-, and γ-secretases determines biphasic amyloid-β protein level in the presence of a γ-secretase inhibitor. *Journal of Biological Chemistry, 288*(2), 785-792.

Pallitto, M. M., & Murphy, R. M. (2001). A mathematical model of the kinetics of β-amyloid fibril growth from the denatured state. *Biophysical journal, 81*(3), 1805-1822.

Pischel, D., Sundmacher, K., & Flassig, R. J. (2017). Efficient simulation of intrinsic, extrinsic and external noise in biochemical systems. *Bioinformatics, 33*(14), i319-i324.

Possin, K. L., Feigenbaum, D., Rankin, K. P., Smith, G. E., Boxer, A. L., Wood, K., . . . Kramer, J. H. (2013). Dissociable executive functions in behavioral variant frontotemporal and Alzheimer dementias. *Neurology, 80*(24), 2180-2185.

Press, W. H. (2007). *Numerical recipes 3rd edition: The art of scientific computing*: Cambridge university press.

Proctor, C. J., Boche, D., Gray, D. A., & Nicoll, J. A. (2013). Investigating interventions in Alzheimer's disease with computer simulation models. *PloS one, 8*(9), e73631.

Proctor, C. J., & Gray, D. A. (2008). Explaining oscillations and variability in the p53-Mdm2 system. *BMC systems biology, 2*(1), 75.
Proctor, C. J., & Gray, D. A. (2010). GSK3 and p53-is there a link in Alzheimer's disease? *Molecular neurodegeneration, 5*(1), 7.
Proctor, C. J., Pienaar, I. S., Elson, J. L., & Kirkwood, T. B. (2012). Aggregation, impaired degradation and immunization targeting of amyloid-beta dimers in Alzheimer's disease: a stochastic modelling approach. *Molecular neurodegeneration, 7*(1), 32.
Puri, I. K., & Li, L. (2010). Mathematical modeling for the pathogenesis of Alzheimer's disease. *PLoS One, 5*(12), e15176.
Qosa, H., Abuasal, B. S., Romero, I. A., Weksler, B., Couraud, P.-O., Keller, J. N., & Kaddoumi, A. (2014). Differences in amyloid-β clearance across mouse and human blood–brain barrier models: kinetic analysis and mechanistic modeling. *Neuropharmacology, 79*, 668-678.
Rapoport, M., Dawson, H. N., Binder, L. I., Vitek, M. P., & Ferreira, A. (2002). Tau is essential to β-amyloid-induced neurotoxicity. *Proceedings of the National Academy of Sciences, 99*(9), 6364-6369.
Raser, J. M., & O'shea, E. K. (2005). Noise in gene expression: origins, consequences, and control. *Science, 309*(5743), 2010-2013.
Rathinam, M., Sheppard, P. W., & Khammash, M. (2010). Efficient computation of parameter sensitivities of discrete stochastic chemical reaction networks. *The Journal of chemical physics, 132*(3), 034103.
Rinne, J. O., Brooks, D. J., Rossor, M. N., Fox, N. C., Bullock, R., Klunk, W. E., . . . Okello, A. A. (2010). 11 C-PiB PET assessment of change in fibrillar amyloid-β load in patients with Alzheimer's disease treated with bapineuzumab: a phase 2, double-blind, placebo-controlled, ascending-dose study. *The Lancet Neurology, 9*(4), 363-372.
Roberson, E. D., Scearce-Levie, K., Palop, J. J., Yan, F., Cheng, I. H., Wu, T., . . . Mucke, L. (2007). Reducing endogenous tau ameliorates amyloid ß-induced deficits in an Alzheimer's disease mouse model. *Science, 316*(5825), 750-754.
Romani, A., Marchetti, C., Bianchi, D., Leinekugel, X., Poirazi, P., Migliore, M., & Marie, H. (2013). Computational modeling of the effects of amyloid-beta on release probability at hippocampal synapses. *Frontiers in computational neuroscience, 7*.
Rowan, M. S., Neymotin, S. A., & Lytton, W. W. (2014). Electrostimulation to reduce synaptic scaling driven progression of Alzheimer's disease. *Frontiers in computational neuroscience, 8*.
Saltelli, A., Chan, K., & Scott, E. M. (2000). *Sensitivity analysis* (Vol. 1): Wiley New York.
Saltelli, A., Ratto, M., Andres, T., Campolongo, F., Cariboni, J., Gatelli, D., . . . Tarantola, S. (2008). *Global sensitivity analysis: the primer*: John Wiley & Sons.
Saltelli, A., Ratto, M., Tarantola, S., & Campolongo, F. (2005). Sensitivity analysis for chemical models. *Chemical reviews, 105*(7), 2811-2828.
Saltelli, A., Tarantola, S., Campolongo, F., & Ratto, M. (2004). *Sensitivity analysis in practice: a guide to assessing scientific models*: John Wiley & Sons.
Saltelli, A., Tarantola, S., & Chan, K.-S. (1999). A quantitative model-independent method for global sensitivity analysis of model output. *Technometrics, 41*(1), 39-56.
Sauer, T. (2012). Numerical solution of stochastic differential equations in finance. In *Handbook of computational finance* (pp. 529-550): Springer.
Schenk, D., Barbour, R., Dunn, W., & Gordon, G. (1999). Immunization with amyloid-beta attenuates Alzheimer-disease-like pathology in the PDAPP mouse. *Nature, 400*(6740), 173.
Schwartz, A. L. (1996). *Theory and implementation of numerical methods based on Runge-Kutta integration for solving optimal control problems*. University of California at Berkeley.
Segovia-Juarez, J. L., Ganguli, S., & Kirschner, D. (2004). Identifying control mechanisms of granuloma formation during M. tuberculosis infection using an agent-based model. *Journal of theoretical biology, 231*(3), 357-376.
Shampine, L. F., & Watts, H. (1969). Block implicit one-step methods. *Mathematics of Computation, 23*(108), 731-740.
Small, S. A., & Duff, K. (2008). Linking Aβ and tau in late-onset Alzheimer's disease: a dual pathway hypothesis. *Neuron, 60*(4), 534-542.

Sturm, O. (2011). *Functional Programming in C#: Classic Programming Techniques for Modern Projects*: John Wiley & Sons.
Sumner, T. (2010). *Sensitivity analysis in systems biology modelling and its application to a multi-scale model of blood glucose homeostasis*. UCL (University College London).
Svedružić, Ž. M., Popović, K., & Šendula-Jengić, V. (2013). Modulators of γ-secretase activity can facilitate the toxic side-effects and pathogenesis of Alzheimer's disease. *PloS one, 8*(1), e50759.
Szallasi, Z., Stelling, J., & Periwal, V. (2006). System modeling in cellular biology. *From Concepts to*.
Székely, T. (2014). *Stochastic modelling and simulation in cell biology*. University of Oxford.
Tamagnini, F., Novelia, J., Kerrigan, T. L., Brown, J. T., Tsaneva-Atanasova, K., & Randall, A. D. (2015). Altered intrinsic excitability of hippocampal CA1 pyramidal neurons in aged PDAPP mice. *Frontiers in cellular neuroscience, 9*.
Theofilas, P., Ehrenberg, A. J., Nguy, A., Thackrey, J. M., Dunlop, S., Mejia, M. B., . . . Suemoto, C. K. (2018). Probing the correlation of neuronal loss, neurofibrillary tangles, and cell death markers across the Alzheimer's disease Braak stages: a quantitative study in humans. *Neurobiology of aging, 61*, 1-12.
Thieme, H. R. (2018). *Mathematics in population biology*: Princeton University Press.
Tian, T., & Burrage, K. (2004). Binomial leap methods for simulating stochastic chemical kinetics. *The Journal of chemical physics, 121*(21), 10356-10364.
Tiveci, S., Akın, A., Çakır, T., Saybaşılı, H., & Ülgen, K. (2005). Modelling of calcium dynamics in brain energy metabolism and Alzheimer's disease. *Computational biology and chemistry, 29*(2), 151-162.
Toh, M. C., & Allen-Vercoe, E. (2015). The human gut microbiota with reference to autism spectrum disorder: considering the whole as more than a sum of its parts. *Microbial ecology in health and disease, 26*(1), 26309.
Trewavas, A. (2006). A Brief History of Systems Biology "Every object that biology studies is a system of systems." Francois Jacob (1974). *The Plant Cell, 18*(10), 2420-2430.
Tyson, J. J., Novak, B., Odell, G. M., Chen, K., & Thron, C. D. (1996). Chemical kinetic theory: understanding cell-cycle regulation. *Trends in biochemical sciences, 21*(3), 89-96.
Ullah, M., Schmidt, H., Cho, K.-H., & Wolkenhauer, O. (2006). Deterministic modelling and stochastic simulation of biochemical pathways using MATLAB. *IEE Proceedings-Systems Biology, 153*(2), 53-60.
Van Griensven, A., Meixner, T., Grunwald, S., Bishop, T., Diluzio, M., & Srinivasan, R. (2006). A global sensitivity analysis tool for the parameters of multi-variable catchment models. *Journal of hydrology, 324*(1), 10-23.
Van Kampen, N. G. (1992). *Stochastic processes in physics and chemistry* (Vol. 1): Elsevier.
van Riel, N. A. (2006). Dynamic modelling and analysis of biochemical networks: mechanism-based models and model-based experiments. *Briefings in bioinformatics, 7*(4), 364-374.
Veliz-Cuba, A., Jarrah, A. S., & Laubenbacher, R. (2010). Polynomial algebra of discrete models in systems biology. *Bioinformatics, 26*(13), 1637-1643.
Walsh, R. (2014). Are improper kinetic models hampering drug development? *PeerJ, 2*, e649.
Wattis, J. A. (2006). An introduction to mathematical models of coagulation–fragmentation processes: a discrete deterministic mean-field approach. *Physica D: Nonlinear Phenomena, 222*(1-2), 1-20.
Wilkinson, D. J. (2009). Stochastic modelling for quantitative description of heterogeneous biological systems. *Nature Reviews Genetics, 10*(2), 122-133.
Xing, T., & Stern, F. (2010). Factors of safety for Richardson extrapolation. *Journal of Fluids Engineering, 132*(6), 061403.
Yang, Y., Mufson, E. J., & Herrup, K. (2003). Neuronal cell death is preceded by cell cycle events at all stages of Alzheimer's disease. *Journal of Neuroscience, 23*(7), 2557-2563.
Yue, H., Brown, M., He, F., Jia, J., & Kell, D. B. (2008). Sensitivity analysis and robust experimental design of a signal transduction pathway system. *International Journal of Chemical Kinetics, 40*(11), 730-741.

Yue, H., Brown, M., Knowles, J., Wang, H., Broomhead, D. S., & Kell, D. B. (2006). Insights into the behaviour of systems biology models from dynamic sensitivity and identifiability analysis: a case study of an NF-κB signalling pathway. *Molecular BioSystems, 2*(12), 640-649.

Yuraszeck, T. M., Neveu, P., Rodriguez-Fernandez, M., Robinson, A., Kosik, K. S., & Doyle III, F. J. (2010). Vulnerabilities in the tau network and the role of ultrasensitive points in tau pathophysiology. *PLoS computational biology, 6*(11), e1000997.

Zi, Z. (2011). Sensitivity analysis approaches applied to systems biology models. *IET systems biology, 5*(6), 336-346.

Zielinski, D. C., Jamshidi, N., Corbett, A. J., Bordbar, A., Thomas, A., & Palsson, B. O. (2017). Systems biology analysis of drivers underlying hallmarks of cancer cell metabolism. *Scientific reports, 7*, 41241.

Zotova, E., Holmes, C., Johnston, D., Neal, J. W., Nicoll, J. A., & Boche, D. (2011). Microglial alterations in human Alzheimer's disease following Aβ42 immunization. *Neuropathology and applied neurobiology, 37*(5), 513-524.